CONTRACT REPORT NO. 2-136

FEASIBILITY STUDY FOR A SURGE-ACTION MODEL OF MONTEREY HARBOR, CALIFORNIA

by

B. W. Wilson

J. A. Hendrickson

R. E. Kilmer

October 1965

Sponsored by

U. S. Army Engineer District

San Francisco

Prepared for

U. S. Army Engineer Waterways Experiment Station

CORPS OF ENGINEERS

Vicksburg, Mississippi

Under

Contract No. DA-22-079-civeng-65-10

by

Science Engineering Associates

San Marino, California

ARMY-MRC VICKSBURG, MISS.

PREFACE

This report is the outcome of the labor of many people who have found fascination in one or more facets of the subject it embraces. It has made use of old, tried and tested methods of analysis and interpretation as well as new techniques, specially developed and refined for the tasks. We venture to think that some of the numerical methods developed for probing the oscillating characteristics of bays, harbors and enclosed bodies of water represent a major technical advance in coastal engineering, hitherto unattained in this field.

The writer for his part has considered this study, for all its arduousness, to be a labor of love and learning because of his long association and interest in problems of this kind. He believes that the main features of the surging problem in Monterey Harbor have been uncovered in these pages even in the face of a great paucity of information of one kind and another. The recommendations for methods of modelling the harbor and its environment are the best that can be adduced from our understanding of the problems involved.

The writer wishes to acknowledge here the very valuable contributions of Drs. James Hendrickson and Robert Kilmer who were mainly responsible for advancing the state of the art in the numerical analysis of the oscillating characteristics of semi-enclosed basins. These developments, which have been elaborated in two appendices to the report, involved many pitfalls and difficult obstacles which had to be surmounted. That they were successfully overcome is a tribute to their talents and team work. Dr. Hendrickson was mainly responsible for elaborating the theory of the appendices and Dr. Kilmer for programming the complicated calculations.

The excellent work of Messrs. Takashi Umehara and George Zwior in the laborious preparation of wave-refraction diagrams and illustrations for the report deserves special mention. Miss Jeanne Reitz, with the

assistance of Mrs. Betty St. George and Mrs. Chris Letterman, has been responsible for the typing of the manuscript. Others who worked on the contract at different times were Mr. Helge Norstrud, Research Engineer, and Miss Dorothy Foster, who assisted in drafting.

Basil W. Wilson
Program Manager
and Principal Investigator

San Marino, California
October, 1965

TABLE OF CONTENTS

TABLE OF CONTENTS (Cont'd.)

TABLE OF CONTENTS (Cont'd.)

TABLE OF CONTENTS (Cont'd.)

LIST OF FIGURES

LIST OF FIGURES (Cont'd.)

LIST OF FIGURES (Cont'd.)

LIST OF FIGURES (Cont'd.)

LIST OF FIGURES (Cont'd.)

LIST OF FIGURES (Cont'd.)

LIST OF FIGURES (Cont'd.)

LIST OF TABLES

SUMMARY

This report attempts to answer basic questions regarding the feasibility of reproducing in an engineering model the surge phenomenon that at various times occurs in Monterey Harbor, California. To this end, a fairly extensive discussion is devoted to the wind and wave climate prevailing in and near Monterey Bay. Sea and swell data are summarized for the deep-water vicinity-area and for Monterey Bay itself, with particular reference to the southern portion, for the coast of which the distribution of refraction coefficient values is given for ordinary waves. Monterey Harbor tends to be quite well protected from the longer-period swells.

Statistical data for the occurrence of long-period waves at three sensor positions in Monterey Harbor are examined and compared with similar-type data for Santa Cruz Harbor, at the northern extremity of Monterey Bay, and for Half Moon Bay Harbor (some 60 miles north of Monterey). Seasonal peculiarities are in evidence. Energy spectra for the long wave data are compared with earlier studies of the Corps of Engineers (1949) and with the results of Residuation analyses made in this report.

The oscillating characteristics of Monterey Bay are examined from several points of view. First, known analytic modes of oscillation of the water body in various semi-enclosed basins of simple geometrical shape are discussed. Application is made to Monterey Bay by likening it to the quadrant of a circular basin of either uniform depth or paraboloidal bottom slope. For greater exactitude numerical methods of calculating the oscillating properties of the bay are pursued. These start from the premise that a nodal condition tends to prevail across the mouth of the bay between Pinos and Santa Cruz Points. An improved Defant-Raichlen numerical "talweg" procedure gives the expected two-dimensional (vertical plane) modes of oscillation, while an improved Stoker numerical procedure yields the expected three-dimensional modes of oscillation of the bay. The computer programs for performing these calculations have been checked by

applying them to special cases for which the analytic solutions are known. The three-dimensional modes for the bay reveal that the deep Monterey canyon has a profound effect on the oscillating regime. The submerged canyon causes the bay to function virtually as two independent halves about the canyon centerline with only weak coupling between the two sections. The three-dimensional numerical analysis, however, is considered to be reliable only for the lowest modes of oscillation because of the considerable uncertainty that the node-condition at the bay-mouth can be sustained for higher modes of oscillation of the bay. Because of this deficiency, the two-dimensional numerical procedure was applied to the Monterey bight (east of the Monterey Peninsula), and the modes of oscillation found for this smaller bay are expected to be more representative of the area enveloping the harbor.

A detailed study is made of the manner of propagation of long period waves into Monterey Bay. Wave refraction diagrams are drawn for incident long waves from three directions encompassing the angular window of approach to Monterey Bay. Unlike ordinary short waves, the long waves reach Monterey Harbor with practically no difference in direction, though there are strong differences of energy content. Refraction diagrams are developed for the primary long wave reflections in the neighborhood of the harbor and these are combined with the incident waves to determine the primary standing wave formations likely to develop in the harbor area. By suitably taking into account the distribution of refraction coefficient values for incident and reflected long waves, as also the shoaling coefficient values, the resulting standing wave amplitudes can be normalized to unit value of long wave height in deep water (10,000 ft.). Graphical synthesis is made of standing wave formations, for four periods found to be important in the wave records for Monterey Harbor. The node positions for these oscillations, found graphically, agree fairly well with the node positions suggested by the two-dimensional, numeral "talweg" analysis for the Monterey bight.

Considerable attention is given to the question whether the surge phenomenon in Monterey Harbor is the consequence of surf-beats or of genuine long-period waves. It is concluded that the latter are most prob-

ably the cause, and their relationship to cyclonic storms is indicated. An attempt is then made to interpret and correlate the results of all the field measurements with those of the theoretical and graphical analyses. Reasonable agreement is found and explanations are given for some of the prominences in the wave energy spectra found at the three sensor locations in the harbor.

The final section of the report discusses the feasibility of a model to reproduce the surge phenomenon and draws upon all the information gained in the preceding parts of the report for this purpose. It is concluded that the conditions can be modelled with reasonable chance of success, and suggestions are made for the calibration of the model and for the analysis and interpretation of the results it may yield.

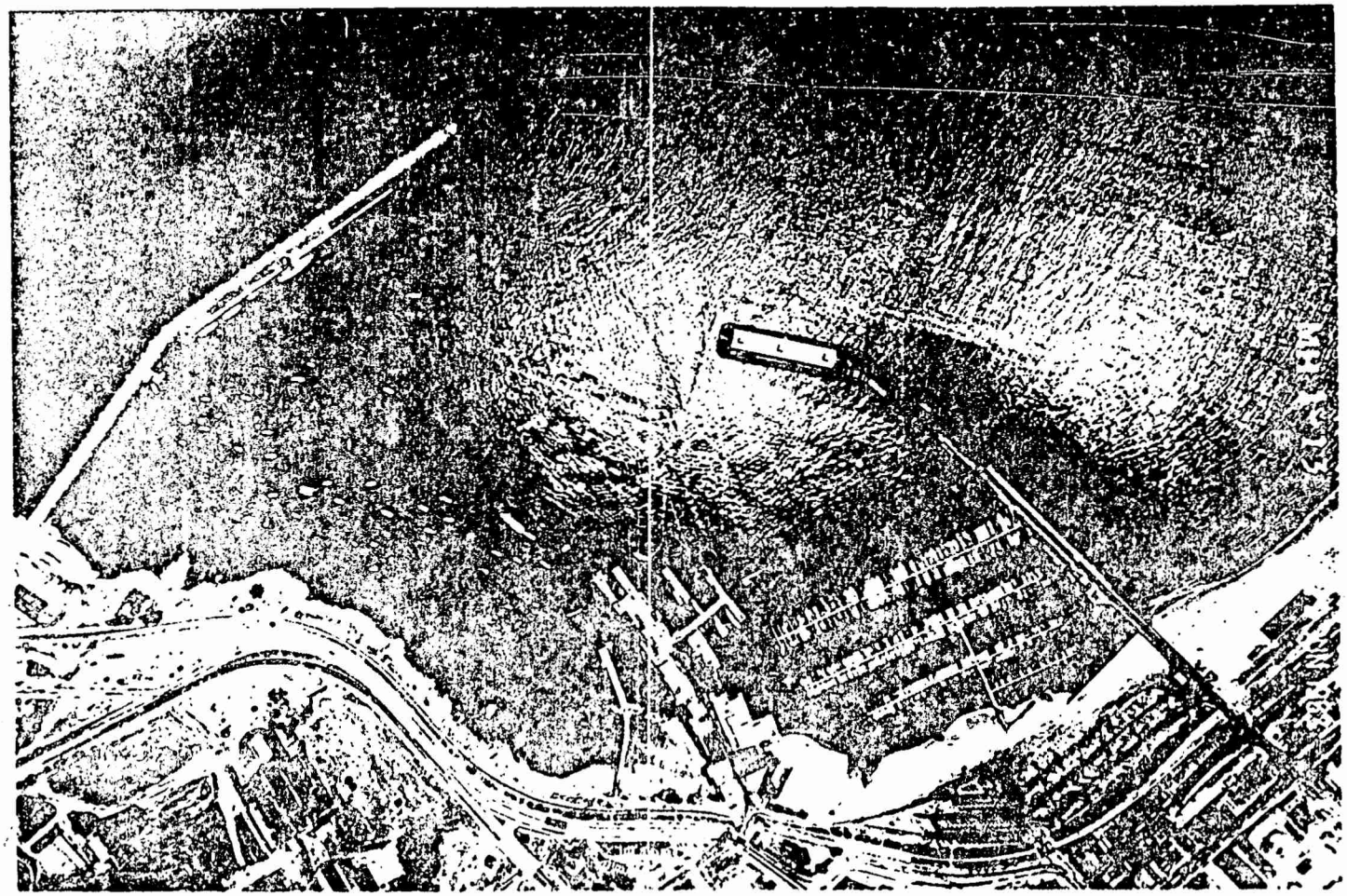

MONTEREY HARBOR, CALIFORNIA
(Photo, U. S. Army Engineer District, San Francisco)

I. INTRODUCTION

The development of Monterey Harbor has been the subject of mature consideration by the Army Corps of Engineers for a large number of years. By 1946 it had become evident that the rubble-mound breakwater was unable to provide sufficient mooring area within its lee for the increasingly large number of fishing boats and small craft using the harbor and that protection from waves and long-period surges was also inadequate. The area had been traditionally subject to the phenomenon of long-period surges which caused violent movements of small craft within the sheltered area and very little was really known at that time, both as regards the origin of these disturbances and their general behavior within the harbor area.

A wave and surge-action model study of the problem was authorized by the Chief of Engineers, U. S. Army, on March 7, 1946, and led to model experiments performed at the Waterways Experiment Station of the Army Corps of Engineers at Vicksburg in the period November 1946 to April 1948 (Hudson, 1949). Various proposals for development of the harbor were tested out in the Vicksburg model, but although these plans showed that adequate protection could be secured for short-period and intermediate-period wave action, the control of long-period wave action of relatively large amplitude remained unsatisfactory.

In the intervening years since, Monterey Harbor has developed mainly as a marina with the construction of a frontal wall and trestle from the center of Municipal Wharf No. 2 and the provision of an array of small craft floating docks within the marina. A plan for the extension of the breakwater towards the opposite shore and a large increase of the shelter area, although authorized for construction, has not yet been put into effect.

The increasing attention focused on long-period wave phenomena in harbors in the last 25 years (since World War II) and the rapidly developing sciences of long-period wave and surge-action modelling and measurement have influenced the Corps of Engineers meanwhile to

reconsider the possibility of attaining a solution of the problem. The present study represents one facet of this program of further investigation, and may be said to have been a consequence of the Monterey Harbor Model Conference held in Pasadena on July 3, 1963. Attendees at this conference included:

Mr. William J. Herron, Jr.
Los Angeles District Office
Corps of Engineers

Mr. John G. Housley
Waterways Experiment Station
Corps of Engineers

Mr. Robert Y. Hudson
Waterways Experiment Station
Corps of Engineers

Mr. Charles E. Lee
Chief Engineer's Office
Corps of Engineers

Dr. Bernard Lé Mehauté
National Engineering Science Company

Mr. Orville T. McGoon
San Francisco District Office
Corps of Engineers

Dr. Lars Skjelbreia
Science Engineering Associates

Mr. Olin F. Weymouth
San Francisco District Office
Corps of Engineers

Dr. Basil W. Wilson
Science Engineering Associates

At this conference Messrs. McGoon and Hudson enlarged on the subjects raised in preliminary correspondence with Wilson regarding possibilities of an analytical study being made for the whole of Monterey Bay, with wave refraction diagrams, etc., that would yield modes of oscillation and throw light on the means whereby Monterey Harbor could be modelled with some chance of reproducing accurately the effects of long-period waves. It was intimated that Monterey Harbor was much subject to oscillations in the period range from 20 secs. to 15 mins. with ranges of height from 2-1/2 to 3 feet for the longer periods to about 6 ins. for the shorter periods. On the other hand, the harbor was apparently well protected from normal wind waves and swell. As noted already, the problems of surging in Monterey Harbor had been investigated in an early model by Hudson (1949), (see also Wilson, 1957), but it was felt by Mr. Hudson himself that the results were not wholly reliable because techniques of modelling long-period waves at that time were not too well refined.

Discussion ensued on surge-action models in general and the methods used in activating seiche or surge action from long-period waves. It was recognized that the possibility existed that surge activity was related to surf beats from groups of high waves in normally-incident storm swell and that this type of activation in models had succeeded in reproducing such effects (cf. Reid and Wade, 1963). On the other hand conventional generation of long-period waves of regular type also produced the appropriate effects (cf. Knapp and Vanoni, 1945; Knapp, 1949; Carr, 1953; Wilson, 1957, 1959).

The parallel was drawn between Monterey Bay, California, and Table Bay, Cape Town, South Africa, and the strong similarities that existed both as regards shape of the bay, location of the harbor and frontage on ocean tracts over which cyclonic storms always tend to approach the coast, were emphasized. Attention was drawn to the fact that, in Table Bay, long-period seiches which caused violent surging in the harbor entrances had been proven incontrovertibly to be linked to barometric fluctuations from long-period air waves moving in from the sea

(Wilson, 1953) and that there seemed good reason to suspect that a similar phenomenon would exist for Monterey Bay. On the other hand, long waves of shorter period, say in the range from 20 secs. to 12 mins. were almost always ground-swells accompanying storm waves (or swells) from travelling cyclones of the open ocean (Wilson, 1951, 1957, 1959).

Demonstration was given of the wave-refraction diagram technique of examining the oscillating characteristics of the region in the manner used for Table Bay (Wilson, 1953). The thought was that the same system could be used for Monterey Bay.

Dr. Lé Mehauté drew attention to the fact that if surging was the outcome of surf-beats, then the orthogonals or wave rays of incident waves would differ from those of incident long waves, although the reflected surges would obey the refraction laws for long waves. It was felt, however, that the differences would be slight and that refraction analysis based on the wave velocity law $c = \sqrt{gh}$ (g = acceleration due to gravity; h = water depth) would be justified in all cases.

Messrs. McGoon and Hudson pointed out that though Monterey was the principal object of study at the present time, there was the possibility that with developments in the Santa Cruz area at the northern end of Monterey Bay similar problems would arise. The writer felt that, ideally, the modelling of Monterey Bay and its harbors should incorporate the whole of Monterey Bay and some of the continental shelf outside the bay, but that such a large model might not be economically justifiable and, in any case, would require supplementation with another model for Monterey Harbor, for more detailed results.

It was pointed out that the problems were highly intricate (cf. Biesel and Lé Mehauté, 1955) because modelling of a fraction of the bay required the introduction of artificial boundaries which could be of considerable importance to the reproduction of realistic conditions. Nevertheless it was felt that it would only be rational to base a model design on a thorough examination of the probable oscillating characteristics of the area.

Messrs. McGoon, Weymouth and Hudson sought advice as to the most advantageous positions for locating long-wave recorders in and near Monterey Harbor. The writer, while endorsing the interior locations favored by the Corps of Engineers, advocated particularly a gage location outside the Municipal Wharf No. 2, near the shore, since this would be an area that would always be antinodal for whatever oscillations tended to occur at the southern extremity of Monterey Bay. Two other positions recommended were on the northern side of the breakwater near the shore where oscillations will also tend to be antinodal and off the end of the municipal wharf at the entrance to the harbor.

Messrs. McGoon and Weymouth indicated that the field program of installing long-period wave recorders and securing spectrum analyses of the results would involve some little time for its implementation, but they felt that the study should include interpretation of the field experiments in the light of theoretical analysis. The writer's feeling on this score was that the wave-refraction diagram analysis could beneficially be started ahead of the field program on the basis of, say, a year's effort, so that at the end of perhaps six months, when wave spectra and other field data became available, the studies could be integrated and conclusions drawn.

The meeting concluded with the following general query epitomized by Mr. Hudson:

On the basis of wave refraction and/or other analyses for Monterey Bay,

1. What type of model or models could best take account of the known surging in Monterey Harbor?

2. How should the model(s) be designed to accomplish this purpose?

3. How could the field spectrum data be used in formulating a test program?

4. What type of analysis should be applied to the model results?

Such, then, is the background to this study and such are the questions which this report attempts to answer.

II. WIND AND WAVE CLIMATE FOR MONTEREY BAY AND VICINITY: INTERPRETATION OF FIELD MEASUREMENTS

1. Location and Characteristics of Monterey Bay with Respect to the Pacific Ocean

Monterey on the west coast of the United States, about 60 n. miles south of San Francisco (Fig. 1) lies at the southern extremity of a large semi-elliptical bay (Monterey Bay) which has topographical features of rather special interest. It is evident from Fig. 1 that the deep trough of the North Pacific basin south of the Mendocino seascarp, approaches closer to the coastline at Monterey than at any other point along the North American coastline. This trough is bounded on the southern side by the Murray seascarp (Fig. 1) and is therefore something of a deep-walled channel running in a west-east direction up to the comparatively narrow continental shelf off San Francisco and Monterey. The significance of this for Monterey Bay is that long-wave energy that may happen to be propagated across the North Pacific Ocean along this direction suffers a degree of containment which may not be wholly offset by the tendency for the energy to spill over the seascarp, as a result of refraction.

A peculiarity of the depth contours nearer to the bay, shown in Figs. 1 and 2, is their convexity, seaward, up to about 10,000 ft. depth, and their concavity, seaward, at lesser depths. The concavity rapidly becomes acute and leads to a deep submarine canyon that penetrates almost to the head of the bay at Moss Landing. The continental shelf within the bay, running out to about the 600 ft. depth contour, is seen in Fig. 2 to be split by this submerged canyon, a fork of which protrudes in the direction of Santa Cruz. This deep canyon will be shown to exert a very important influence on the oscillating characteristics of the region.

A feature of Monterey, which is worth noting, is its strong similarity to Table Bay, Cape Town, South Africa (shown inset in Fig. 2), both as regards shape, outlook, and latitudinal position in the respective hemispheres. Table Bay is considerably smaller and shallower than Monterey Bay and has no canyon cleavage, but it is significant that both

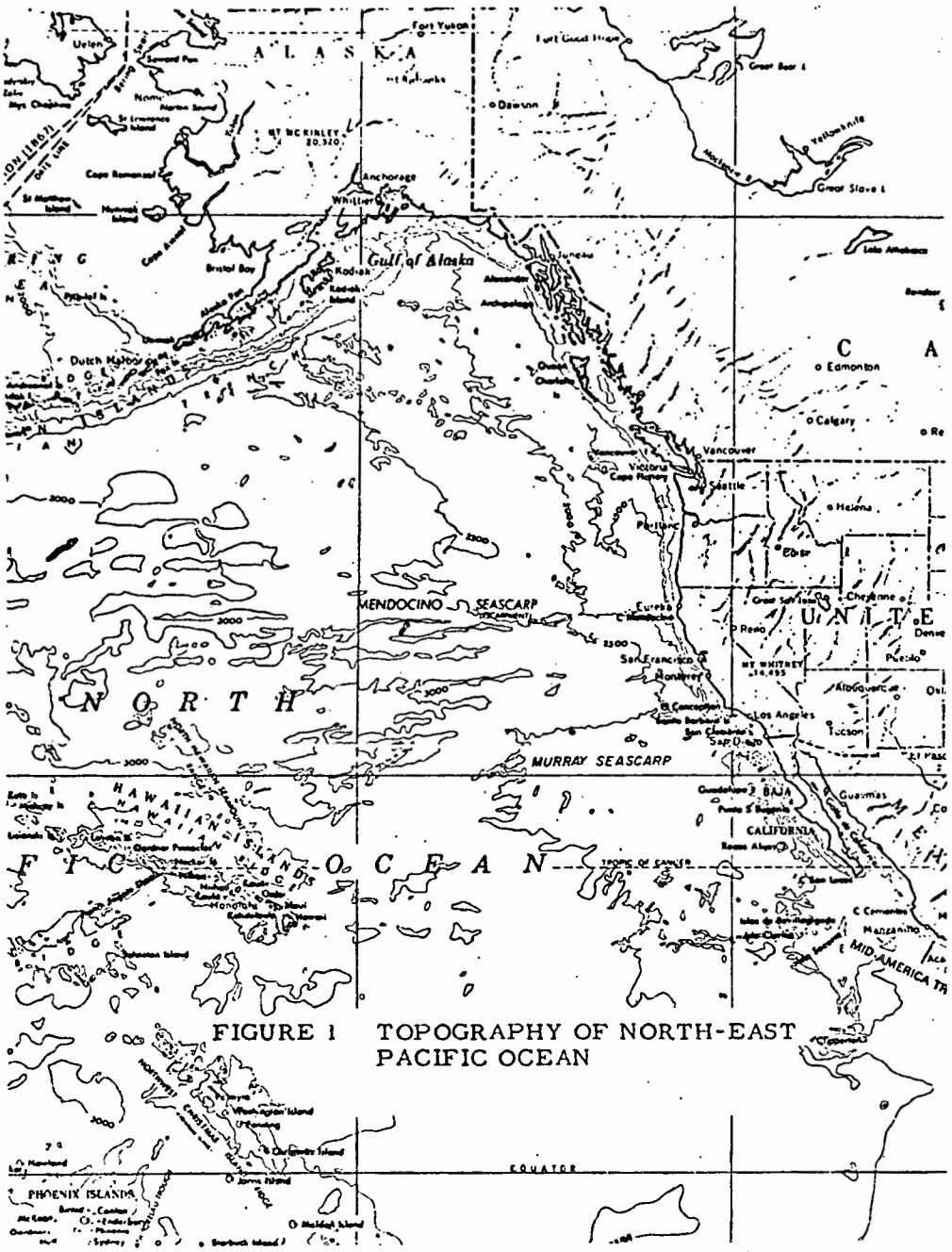

FIGURE 1 TOPOGRAPHY OF NORTH-EAST PACIFIC OCEAN

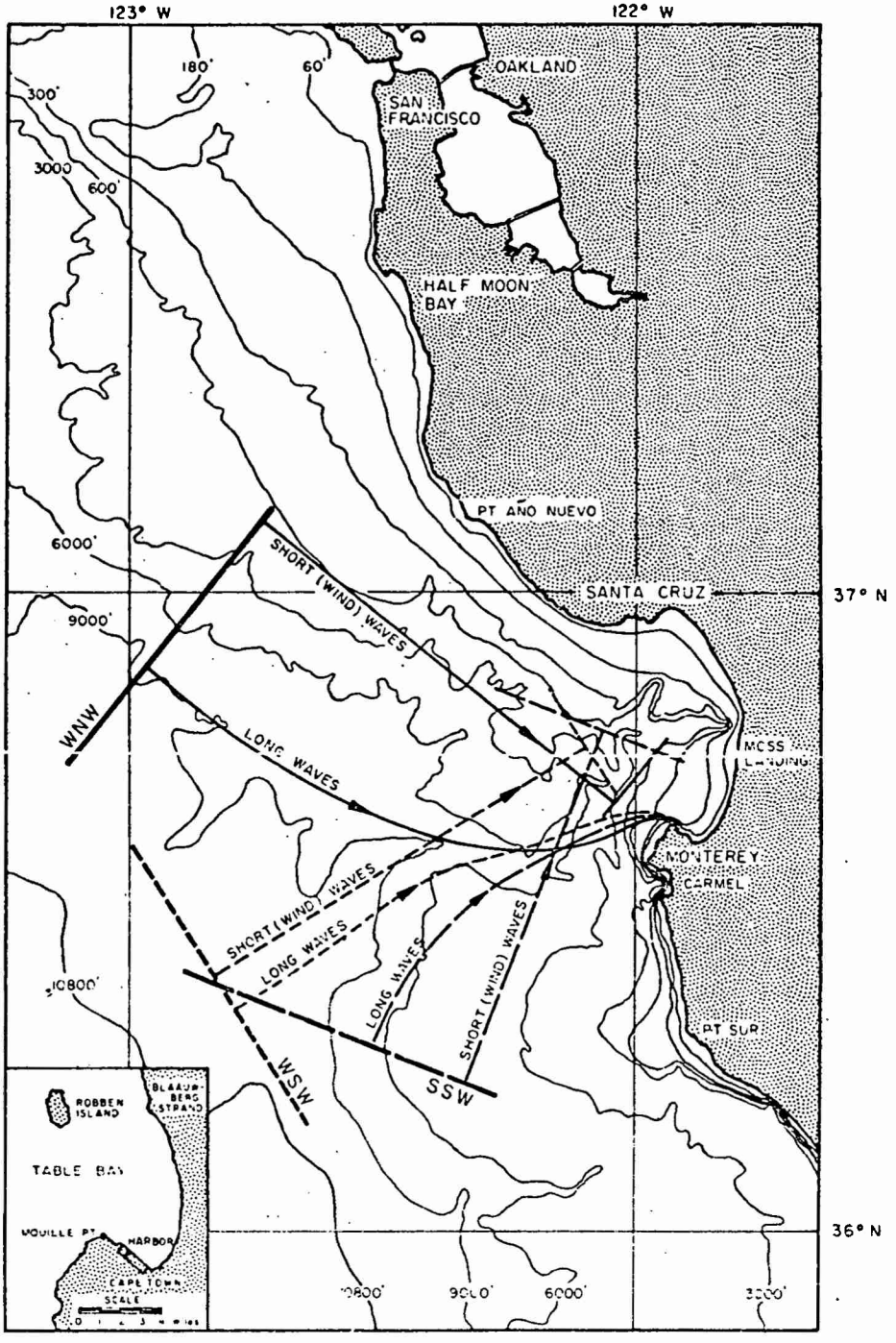

FIGURE 2 LOCATION OF MONTEREY BAY, CALIF., SHOWING APPROACH DIRECTIONS OF WAVES (INSET, TABLE BAY, CAPE TOWN, SOUTH AFRICA)

bays have about the same position in their respective hemispheres with respect to the great oceans and the weather systems that move across them, and both bays are considerably affected by long-period surging phenomena.

2. Prevailing Winds and Storms Affecting Monterey Bay

The similarity, just referred to, may be enlarged upon with the aid of Fig. 3, which shows the dominant atmospheric pressure systems prevailing over the North Pacific Ocean in January and July, respectively representative of winter and summer conditions.

A permanent high-pressure zone is shown to persist in the eastern Pacific and forms, in fact, a belt across the ocean in an east-west direction between latitudes 30° and 40° N. Similar high-pressure belts extend across the oceans in the southern hemisphere in about the same latitudinal positions.

During summer (July) in the northern hemisphere the high-pressure belt moves northward and centers mainly at about latitude 37° N. In winter (January) the high-pressure moves southward and reaches a latitude of about 32° N. This retreat of high-pressure in winter towards the equator is also a feature of the southern hemisphere but occurs, of course, at a time which is seasonally out of phase with the movement in the northern hemisphere. Taken collectively, the high-pressure belts of both hemispheres move in unison to a northern limit in summer (northern hemisphere) and southern limit in winter (northern hemisphere).

The effect of the migration of the high-pressure belt equatorward is shown in Fig. 3a by the development of a well-defined low-pressure center in the North Pacific basin. The dominant path of the low-pressure centers of extra-tropical cyclonic storms (of importance to the west coast of North America), which peal off the high-pressure belt (heavy arrows in Fig. 3) suffers a seasonal shift corresponding to that of the high-pressure belt. In winter therefore these storms are much more proximate to the California coastline than in summer and bring the west coast most of its rain.

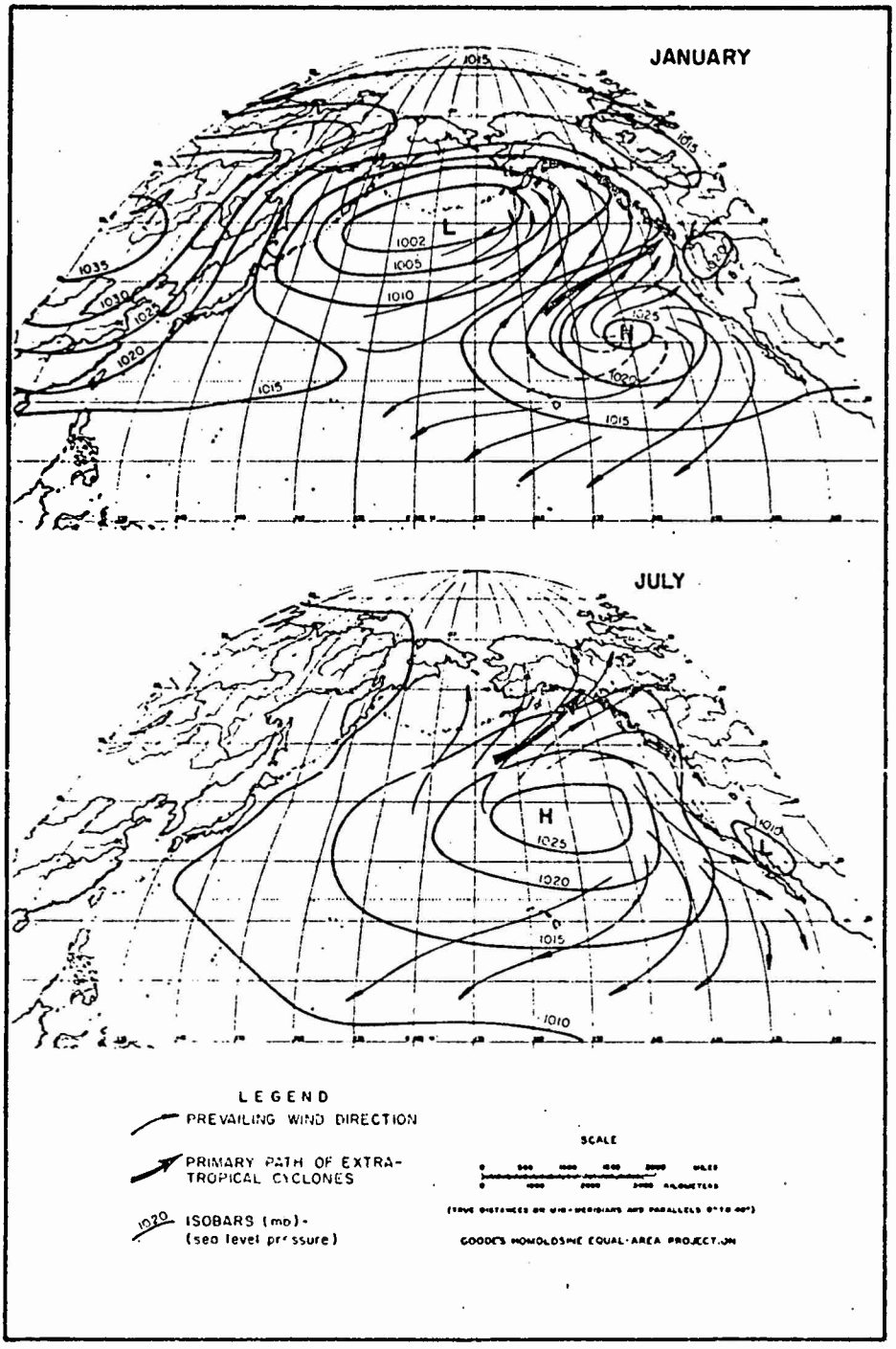

FIGURE 3 SEASONAL MEAN SURFACE PRESSURE AND WIND DISTRIBUTION OVER THE NORTH-EAST PACIFIC OCEAN

Apart from the occasional (transient) infusions of these storms, (which, for short periods, strongly dictate the wind directions), the prevailing flow of air, and therefore direction of wind, is governed by the pressure gradients of the more slowly changing high-pressure belts. This flow of air is indicated by line arrows in Fig. 3.

In greater detail than can be interpreted from charts of the type of Fig. 3, Fig. 4 shows how the prevailing wind directions, which bear upon the California, Oregon and Washington coastlines, change from month to month, as also the dominant atmospheric pressure pattern. It is evident from Fig. 4 that the prevailing winds bearing on Monterey Bay are from W or WNW. Through June, July and August there is a progressive shift of wind direction to NW and NNW and in September and October a reverse trend towards WNW and W, which is largely maintained through November and December.

Since infiltration of storms are few in summer months, the winds of June, July and August largely determine the directions of waves reaching Monterey Bay. In summer therefore wave approach is likely to be predominantly from NW and NNW. In winter time wave directions are more likely to be from W, WNW and NW. The crossing over Monterey Bay of an extra-tropical frontal storm will bring winds from SSW, ahead of the warm front, followed by stronger winds from WSW and finally, from behind the cold front, the strongest winds from WNW and NW.

3. Deep-Water Wave Statistics in Vicinity Exterior to Monterey Bay

At a typical deep-water station off the California coast, in the neighborhood of Monterey Bay and San Francisco, the annual wave conditions may be interpreted in the form shown in Fig. 5. This shows the percentage frequency of occurrence of 'sea' and swell from the NW, W and SW directions at a location 37.5° N. latitude, 123.6° W. longitude, indicated as Station 3 in Fig. 4.

The source of data for Fig. 5 is the U. S. Navy's atlas of sea and swell conditions in the North-East Pacific Ocean (Hydrographic Office,

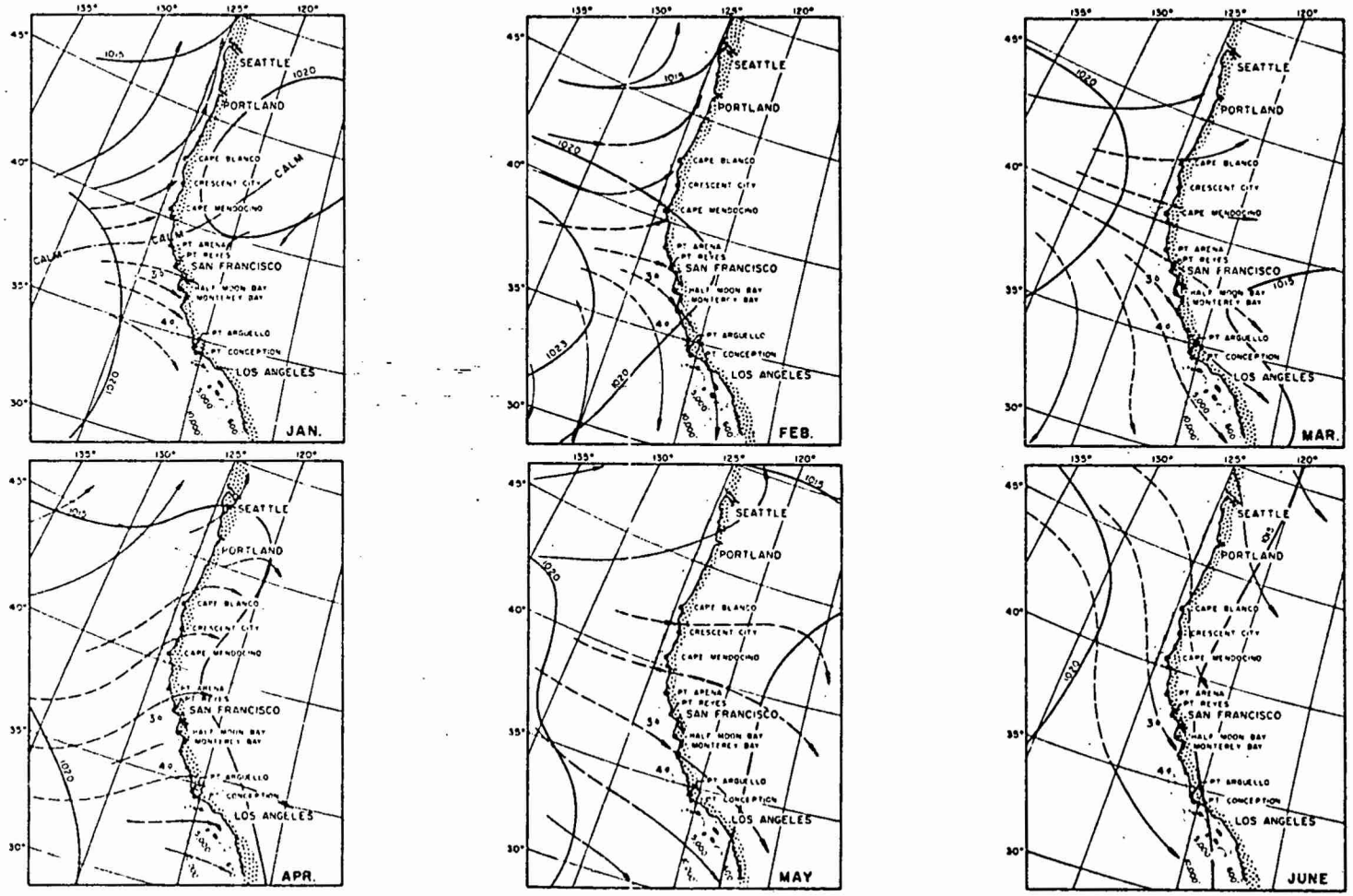

FIGURE 4 MONTHLY MEAN SURFACE PRESSURE AND WIND PATTERNS OFF THE WEST COAST OF THE UNITED STATES

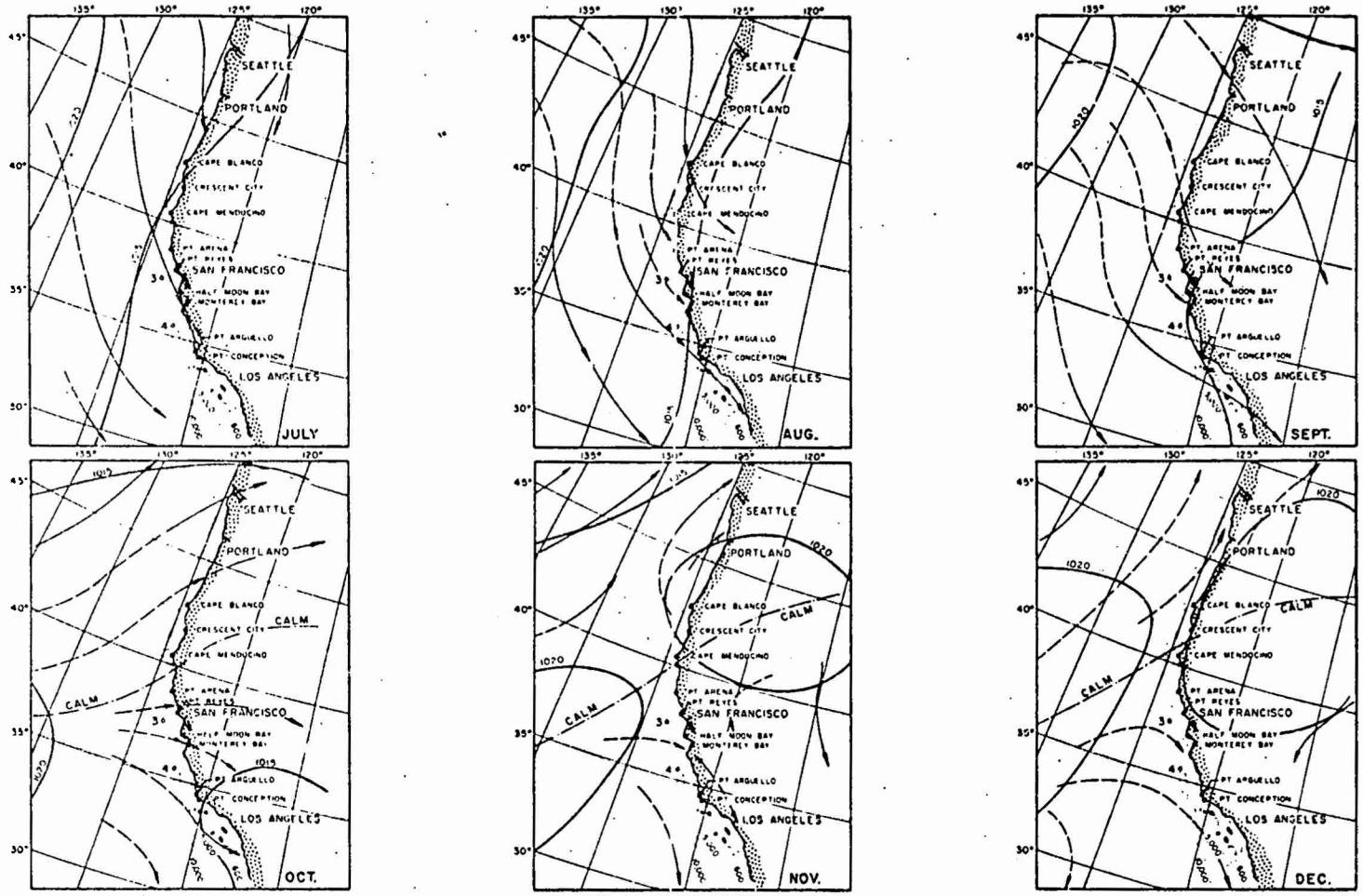

FIGURE 4 (Cont.) MONTHLY MEAN SURFACE PRESSURE AND WIND PATTERNS OFF THE WEST COAST OF THE UNITED STATES

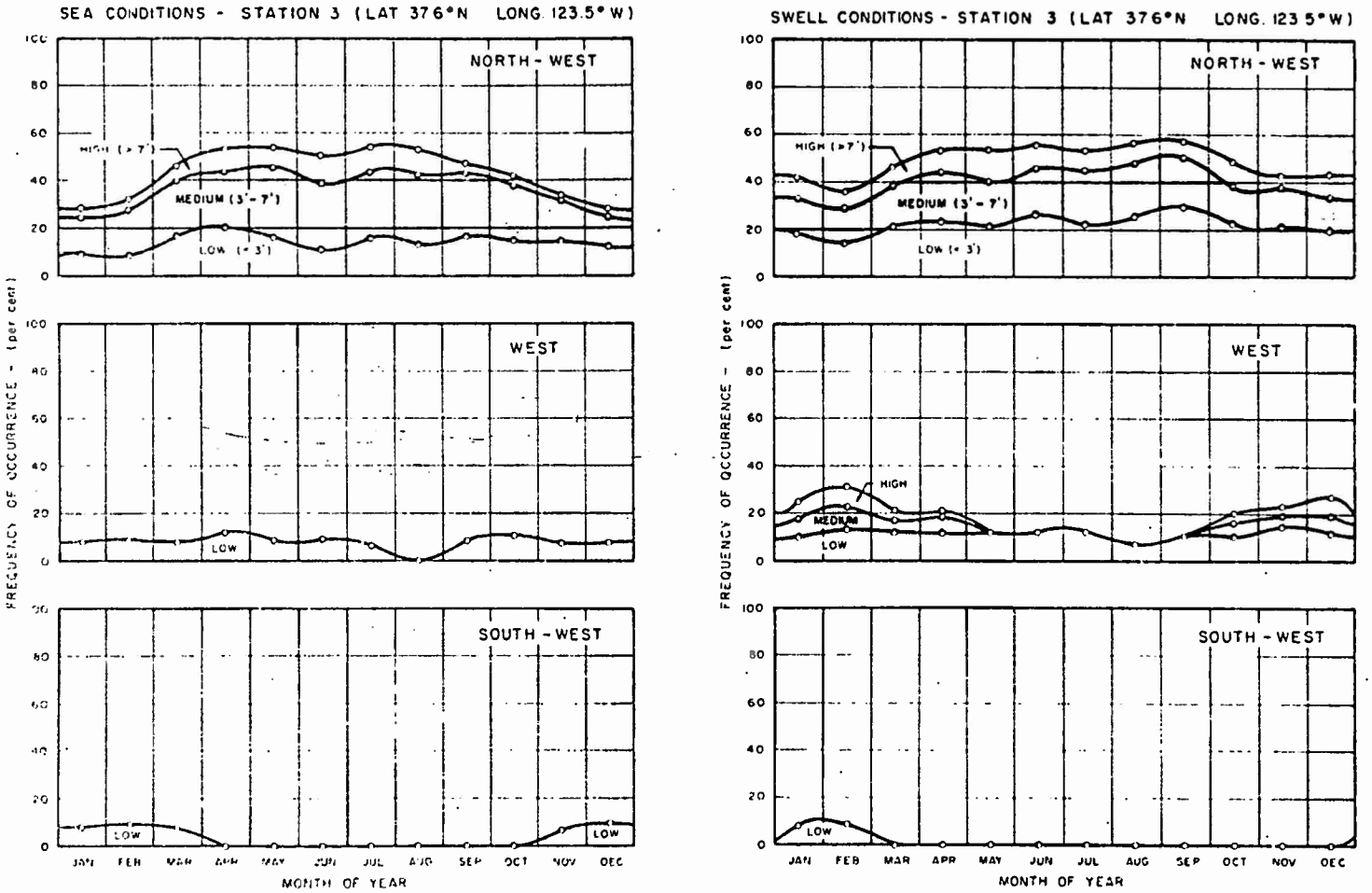

FIGURE 5 ANNUAL VARIATION OF SEA AND SWELL CONDITIONS AT DEEP-WATER STATION 3, OFF COAST OF CENTRAL CALIFORNIA (U.S. NAVY HYDROGRAPHIC OFFICE DATA)

1964). The band-widths marked LOW, MEDIUM and HIGH are the actual percentages of the frequency of occurence of waves in these height categories.

An independent source of data for the same station is to be found in a hindcast study performed for the U.S. Army Corps of Engineers (National Marine Consultants, 1960). These data yield band-width frequencies of occurrence of low, medium and high sea and swell conditions over the year in accordance with Fig. 6.

Generally speaking, there is a similarity between the results of Fig. 5 and Fig. 6. Fig. 6, however, shows a much higher frequency of occurrence of sea and swell from the NW in the summer months than does Fig. 5, but this may be ascribed perhaps to the fact that the Hydrographic Office (HO) data for 1944 showed a fair amount of wave activity from the north compared to very little at all from north in National Marine Consultants (NMC) data. One may suppose that a proportion of this wave activity from north in HO's data could be added to that from the NW to bring Figs. 5 and 6 into closer agreement.

NMC's data in Fig. 6 which are based on hindcasts covering a period of three years (1956-1958), must be considered more reliable than HO's data of 1944, if for no other reason than that they are more detailed and that wave hindcasting techniques have been considerably improved in the intervening decade and a half. Both Figs. 5 and 6, however, agree in showing that sea conditions are low and infrequent throughout the year from all primary directions other than NW. From that direction in July the relative frequencies of occurrence of low waves (height < 3 ft.), medium waves (height, 3 to 7 ft.) and high waves (height > 7 ft.) are respectively 20, 42 and 15 percent. In July low swells from the NW dominate, as shown in Fig. 6. In the winter months, however, medium and high swells from due west tend to become more prominent.

In interpreting Figs. 5 and 6, it should be clear that the frequency of occurrence of sea or swell of any kind is given by the cumulative band-width or maximum ordinate-value of the uppermost curves. Thus in July

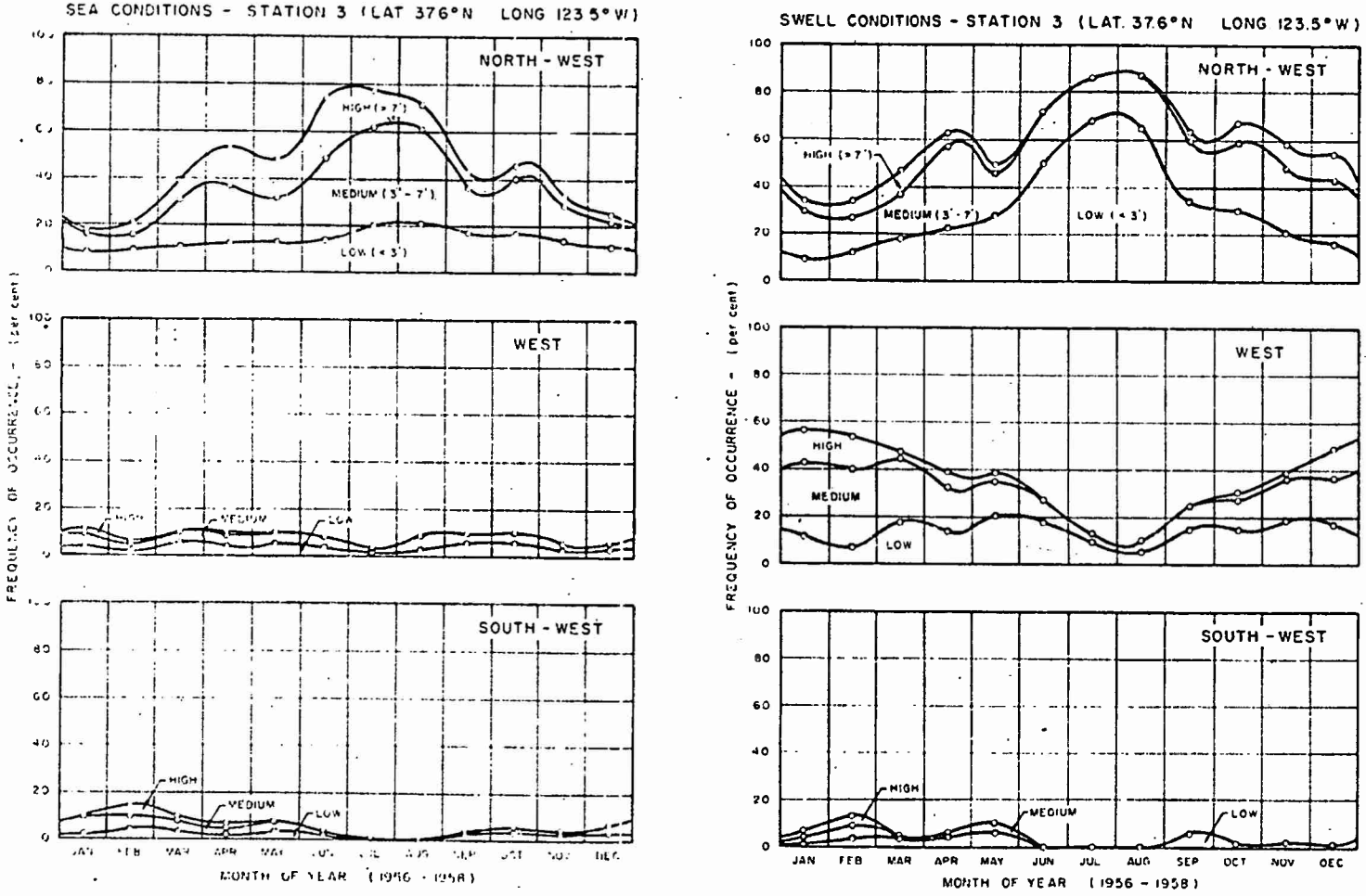

FIGURE 6 ANNUAL VARIATION OF SEA AND SWELL CONDITIONS AT DEEP-WATER STATION 3, OFF COAST OF CENTRAL CALIFORNIA (National Marine Consultants' Data)

there is an 86 percent chance of occurrence of swells of low or medium heights approaching from the NW direction as against a 14 percent chance that they will come from the west.

Typical average annual sea and swell roses for Station 3 are reproduced from NMC data in Figs. 7a and 7b. Corresponding data for the deep-water Station 4 at latitude 35.5° N, longitude 122.0° W (see Fig. 4) are also included in Figs. 7c and 7d. The wave roses give histograms of percentage of occurrence along primary and secondary directions averaged over a year. The usefulness of the annual averaging is open to question in the light of Figs. 5 and 6, but the roses display very prominently the fact that waves approaching the California coast in the neighborhood of Monterey Bay are predominantly from the northwest. The low degree of activity from the southerly directions is also very striking.

4. Approach of Waves to Monterey Bay

It will be apparent from Figs. 1, 2 and 4 that the avenues of approach of waves to Monterey Bay are restricted to about one quadrant of angle, between WNW and SSW. Short wind-waves, which refract only in depths of water less than say 600 feet, may obviously reach the bay from any direction within this quadrant. Long waves, on the other hand, subject to refraction at much greater depths, are apt to have their angular window of approach considerably reduced by the time they are near the mouth of the bay. This is made evident by the orthogonal propagation lines shown in Fig. 2 and will be further illustrated at a later stage in the report, when we come to consider details of long-period wave refraction.

5. Results of Available Studies on Refraction of Ordinary Wind Waves in Monterey Bay

It seems appropriate here to consider such information as may be available on the penetration and refraction of ordinary wind waves and swells into Monterey Bay. The refraction of waves of this kind in Monterey Bay has long been an exercise for engineering and oceanography

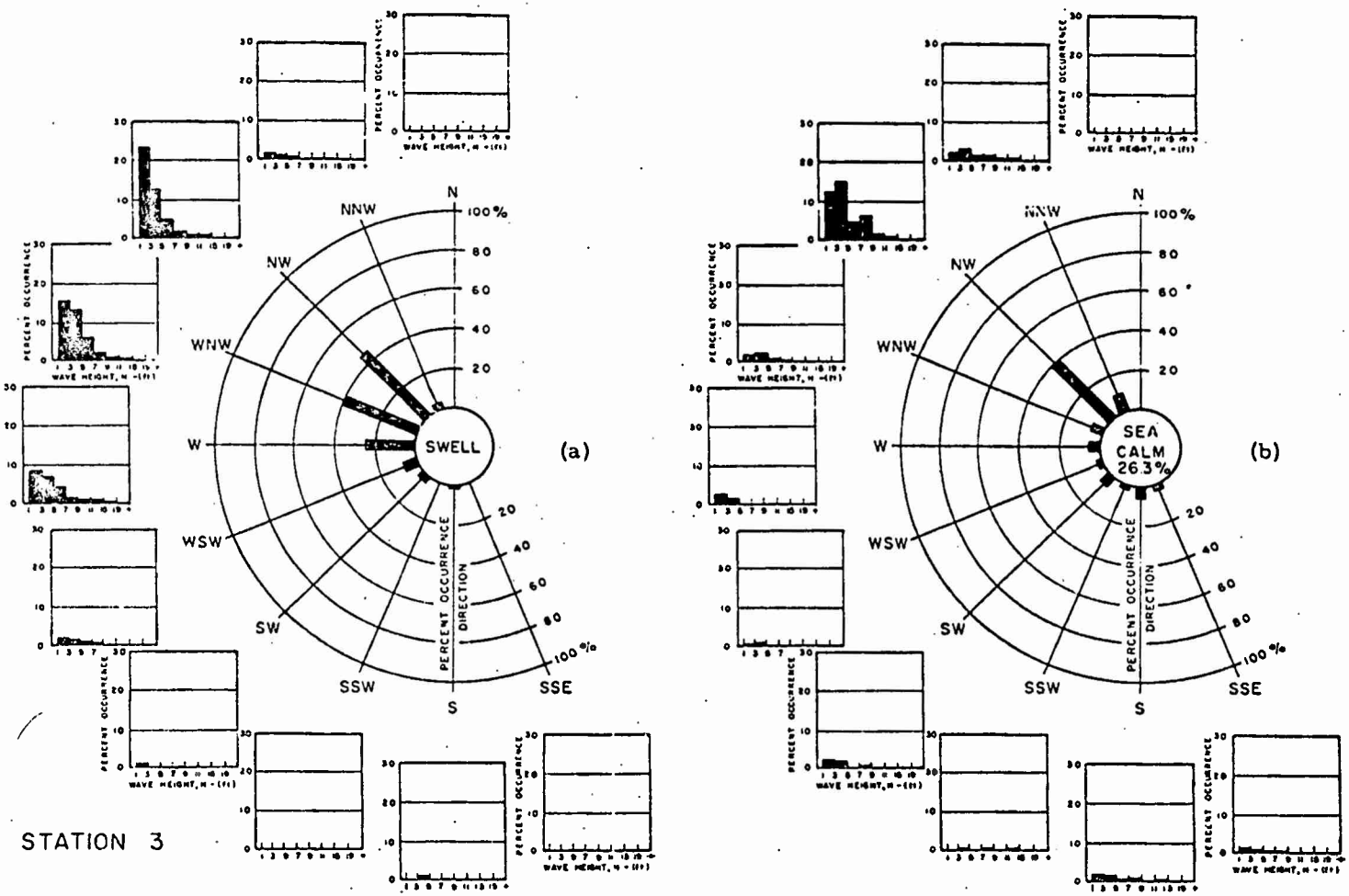

FIGURE 7 AVERAGE ANNUAL SEA AND SWELL ROSES FOR STATION 3, OFF COAST OF CENTRAL CALIFORNIA (NATIONAL MARINE CONSULTANTS' DATA)

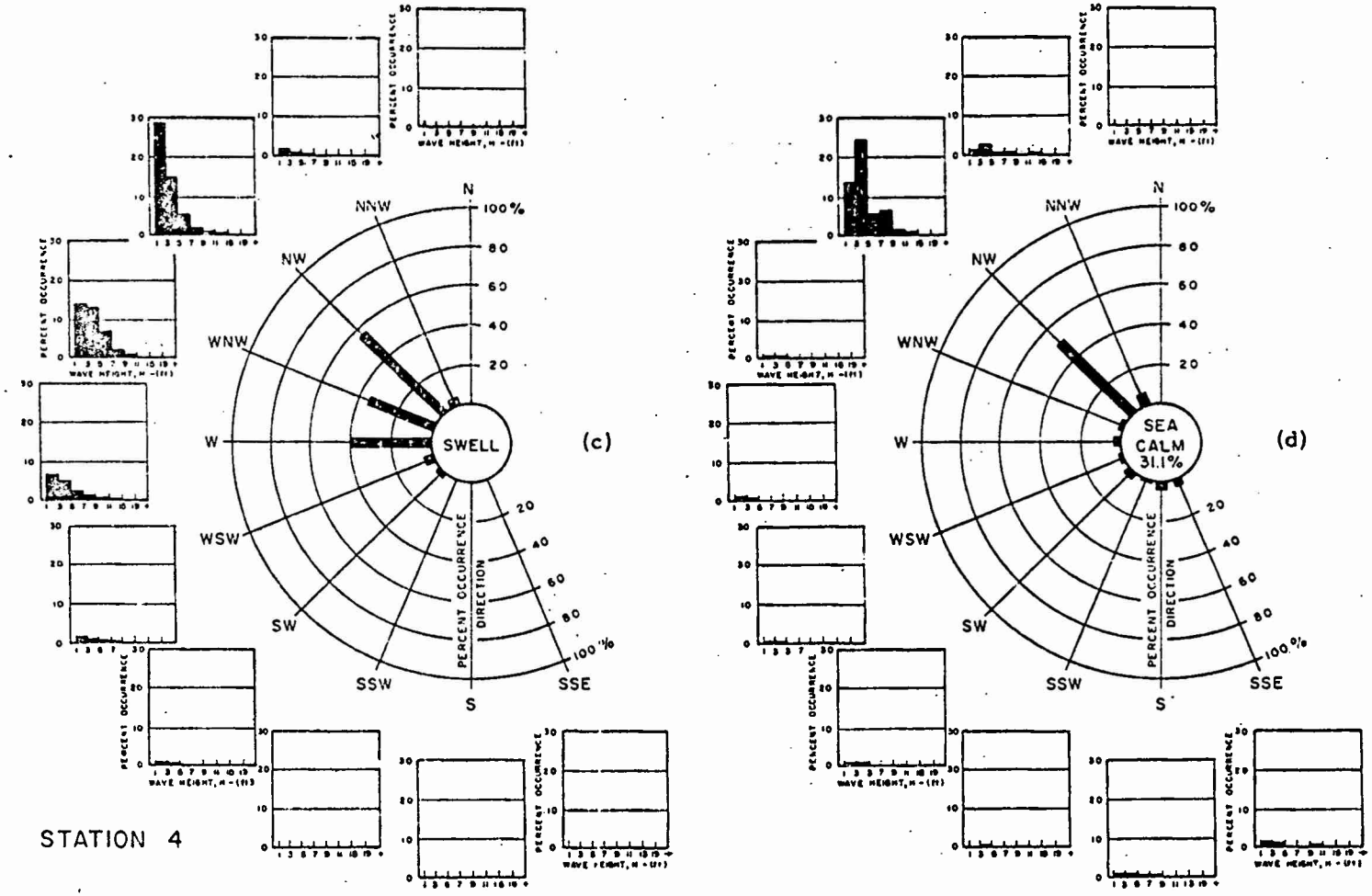

FIGURE 7 (cont.) AVERAGE ANNUAL SEA AND SWELL ROSES FOR STATION 3, OFF COAST OF CENTRAL CALIFORNIA (NATIONAL MARINE CONSULTANTS' DATA)

students at the University of California, Berkeley, and the Naval Postgraduate School in Monterey. The work at Berkeley has been effectively summarized by Johnson (1953) and Wiegel (1964). In Fig. 8 which is borrowed from Wiegel, the refraction patterns of typical 12 sec. waves are shown, approaching Monterey Bay from NW, W and SW directions. Corresponding wave refraction diagrams for Half Moon Bay are also shown in Fig. 8. Half Moon Bay, situated only about 50 n. miles to the north of Monterey is of interest because of long wave measurements that have been made there and will be referred to later. It is evident from Fig. 8 that by the time the waves from all three directions have reached Monterey there is no great difference in their lines of advance in the neighborhood of the harbor. The frontal patterns are, in fact, in good accordance with aerial photographs such as that of Fig. 9.

Fig. 10 (from Johnson, 1963) gives values of refraction coefficients along the coastline of Monterey Bay. Since the refraction coefficients here are measures of the ratios of wave height at the coast to wave height in deep water, it is seen from Fig. 10 c that 8 sec. waves from WNW reach the coast between Monterey and Moss Landing with very little change from their deep-water height. Longer waves of 14 secs. period appear to experience quite a reduction of wave height towards Moss Landing as a consequence of the deep submarine canyon, already noted in Fig. 2. The effects of this canyon are not very evident in Wiegel's diagrams (Fig. 8) which probably are more symbolical than accurate.

By way of checking the Berkeley results, selections were made of some of the best-students' efforts in wave-refraction diagram construction at the Department of Oceanography, Naval Postgraduate School, Monterey. From these the refraction coefficients K_r according to the equation

$$\frac{H}{H_o} = K_r = \sqrt{\frac{b_o}{b}} \qquad (1)$$

were determined. Here H and b are respectively the significant wave height and the breadth between wave rays (or orthogonals to the wave

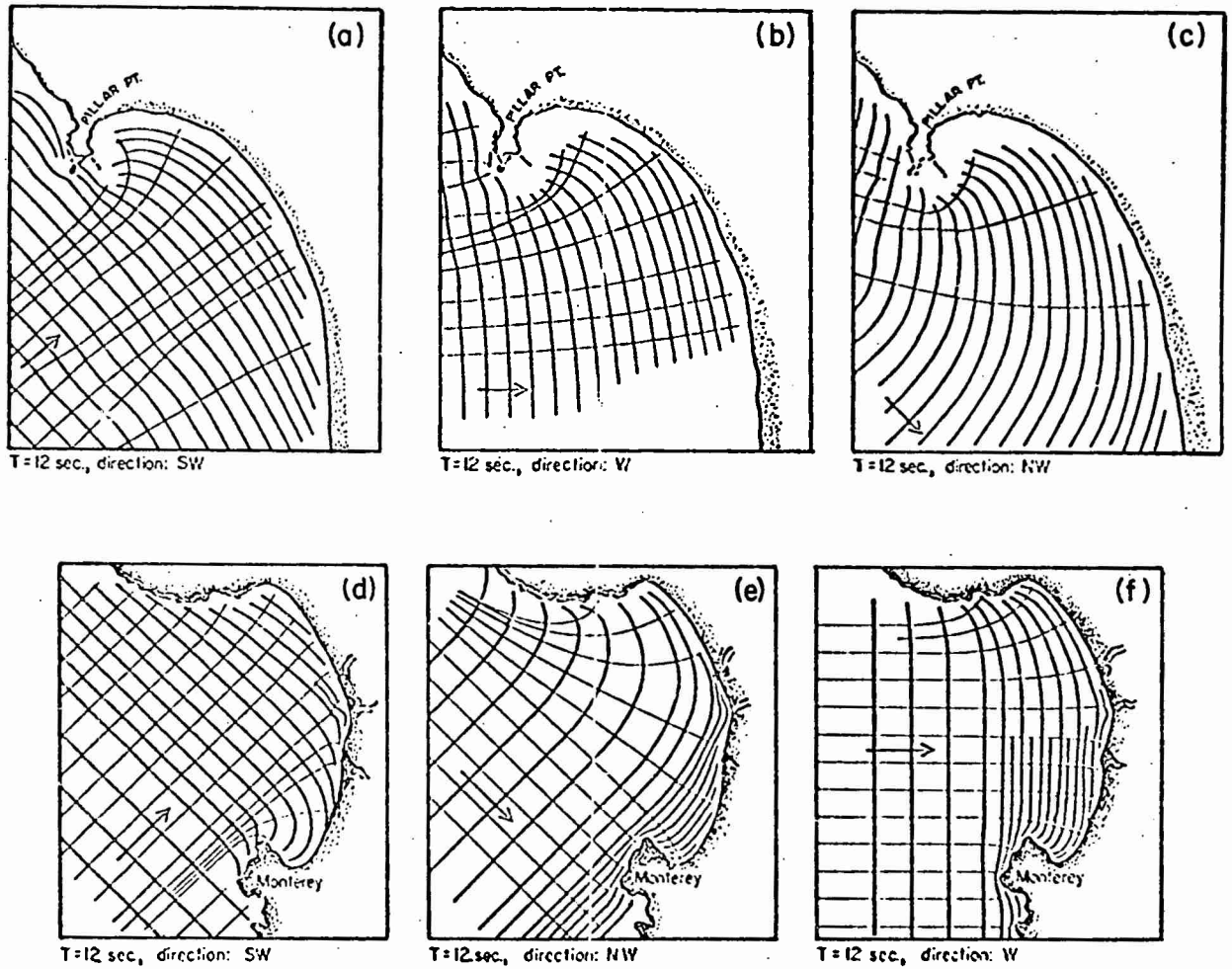

FIGURE 8 WAVE REFRACTION DIAGRAMS; (a, b, c) HALF MOON BAY: (d, e, f) MONTEREY BAY, CALIFORNIA (from Wiegel, 1964)

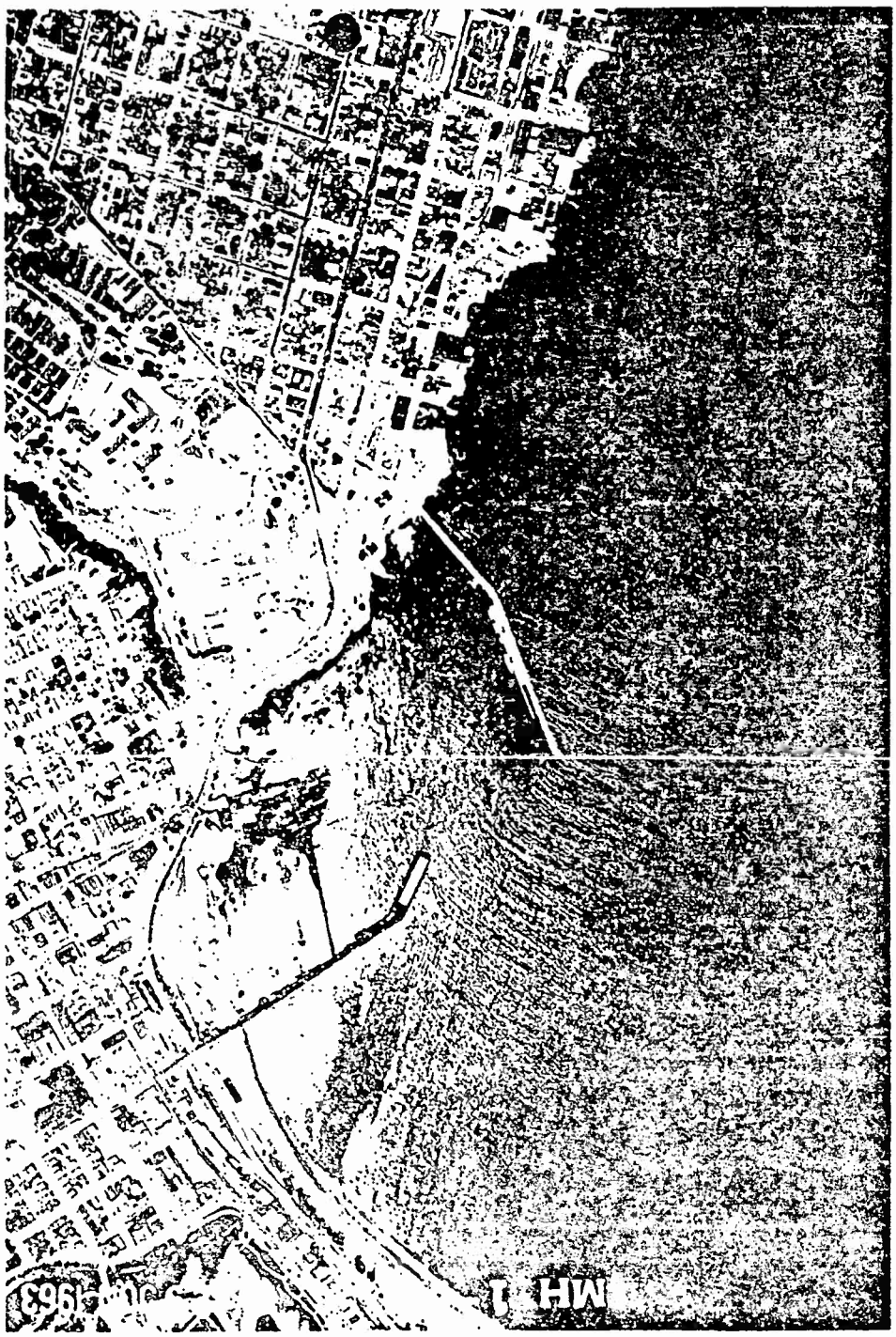

FIGURE 9 AERIAL PHOTOGRAPH OF MONTEREY HARBOR, CALIF. SHOWING INCIDENT WAVES AND SWELLS
(Photo, U. S. Army Engineer District, San Francisco)

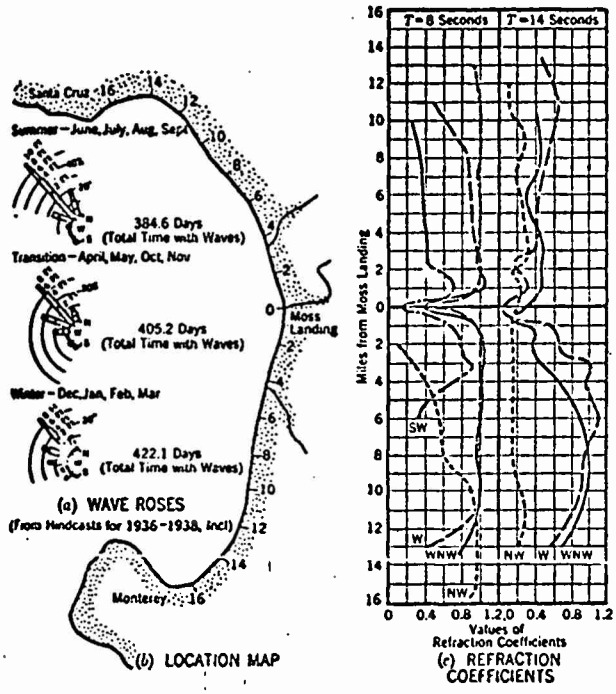

FIGURE 10 SEASONAL WAVE ROSES AND REFRACTION COEFFICIENTS ALONG COASTLINE OF MONTEREY BAY, CALIFORNIA (from Johnson, 1953)

fronts), and the zero subscripts refer to the values of H and b at the deep-water limit where the incoming waves have not yet felt the influence of depth.

The results of these determinations are plotted in Fig. 11 for a variety of wave periods from 8 to 20 secs. and a number of different approach directions from SSW to WNW. In Fig. 11 the coastline has been marked in n. miles, measured from an arbitrary zero near Monterey. One notices from this figure that for all wave directions between WNW and W, bearing on the southern half of Monterey Bay, the refraction coefficient (K_r)-values are close to unity over the portion of the coast (close to Fort Ord) between 5 and 11 n. miles from the origin. As wave direction veers from W to WSW, SW and SSW, so more protection is gained from Monterey Peninsula and the K_r-values near unity are pushed to greater distances (eventually 10 to 11 n. miles from Monterey) where high concentrations of wave energy can occur and K_r-values exceed 2.0. Higher frequency waves, such as the 8 secs. period and lesser periods, are not affected in this respect because of their ability to travel closer inshore before suffering sensible refraction.

We may reach the conclusion then from both Figs. 10 and 11 that Monterey Harbor (near the origin in Fig. 10) is well protected from the worst effects of waves and swells (periods 12 to 20 secs.) but is still susceptible to the influences of waves in the period band 3 to 10 secs., say.

6. Wind-Wave and Long-Period Wave Statistics for Monterey Harbor (Marine Advisers' Data)

Monterey Harbor is shown in detail in Fig. 12, as also in the aerial photographs, Fig. 9 and Frontipiece. Under contract to the U. S. Army Engineer Corps' District, San Francisco, Marine Advisers (1964a) installed and operated a group of three wave sensors positioned at locations 1, 2 and 3 (Fig. 12). Sensors 1 and 2 were arranged to filter sea-swell and tides from the records and therefore functioned as long-period wave

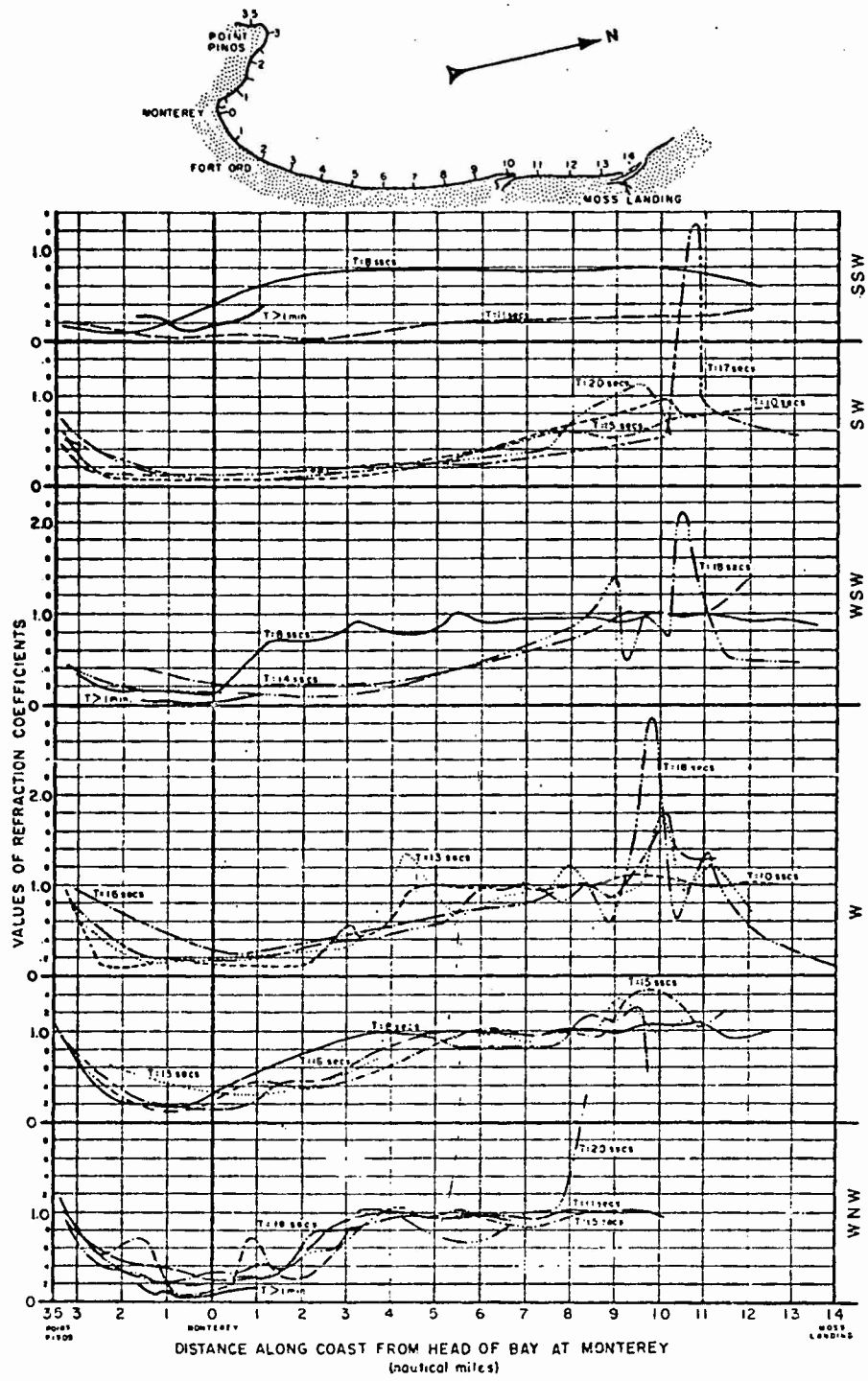

FIGURE 11. REFRACTION COEFFICIENTS FOR SHORT-PERIOD WAVES, MONTEREY TO MOSS LANDING, MONTEREY BAY

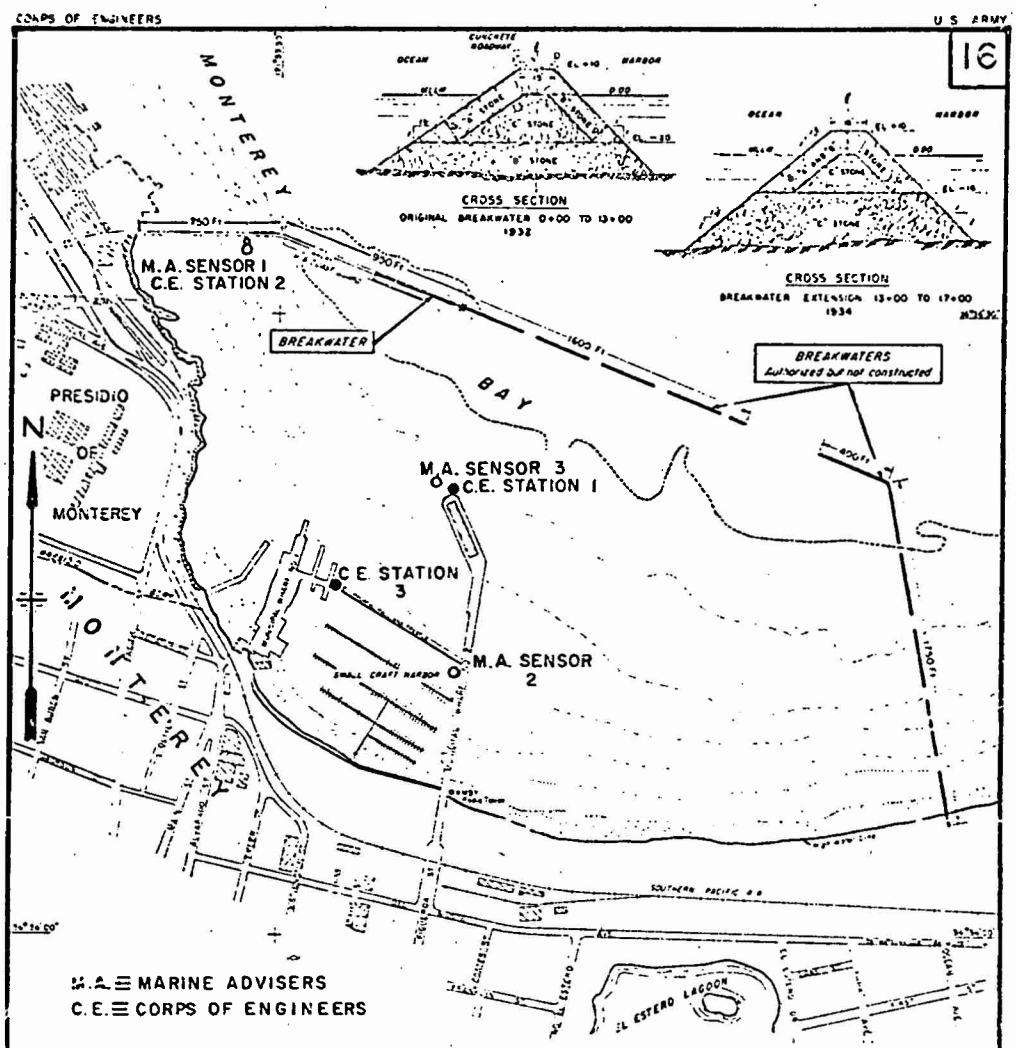

FIGURE 12 LOCATIONS OF LONG WAVE SENSORS (MA) AND WAVE GAUGES (CE) IN MONTEREY HARBOR

recorders. Sensor 3, off the end of Municipal Wharf No. 2, was used to record sea and swell reaching the harbor.

The results of Marine Advisers' tabulated data (1964a) are conveniently summarized in plots such as Fig. 13. The data cover a 6-month period from October to April and plot percentage frequency of occurrence of waves of different heights and periods against time. The band-widths between adjacent isolines define the frequency of occurrence of a particular range of significant wave periods or of significant wave heights. As an example of interpretation, consider the time at the end of February or the beginning of March. According to Fig. 13a, then, of waves and swells occurring at Sensor 3 position, 7 percent would be of 8-10 secs. period, 16 percent of 10-12 secs., 36 percent of 12-14 secs., 33 percent of 14-16 secs., 7 percent of 16-18 secs., and 1 percent of 18-20 secs. From Fig. 13b we find for the same time that 23 percent of the waves would have a significant wave height less than 0.5 ft., 68 percent a height in the range 0.5 to 1.0 ft. and 9 percent of 1.0 to 1.5 ft.

This type of time-plot of the data shows us certain interesting trends of change. It appears that in the period December - January - February there is a marked increase in the longer period waves in the wind-wave spectrum and a corresponding increase in waves of larger height. On comparing this with Fig. 6, a rough correlation can be established for the swell conditions at the deep-water Station 3 for the case of Westerly swells which predominate at this time of year.

Referring now to the long-wave sensor data shown in Figs. 13c to 13f, we find a somewhat corresponding trend at Sensor 1, near the breakwater, the tendency being for the shorter periods to be suppressed in favor of the longer, and the lesser heights in favor of the larger.

There is, however, an important out-of-phasing which merits attention. The tendency to highest long-period waves at Sensor 1 occurs towards the end of January, whereas the highest swells on Sensor 3 are found at the end of December and early January. Periodwise, the strongest trend to long periods at Sensor 1 occurs in December, whereas it is in

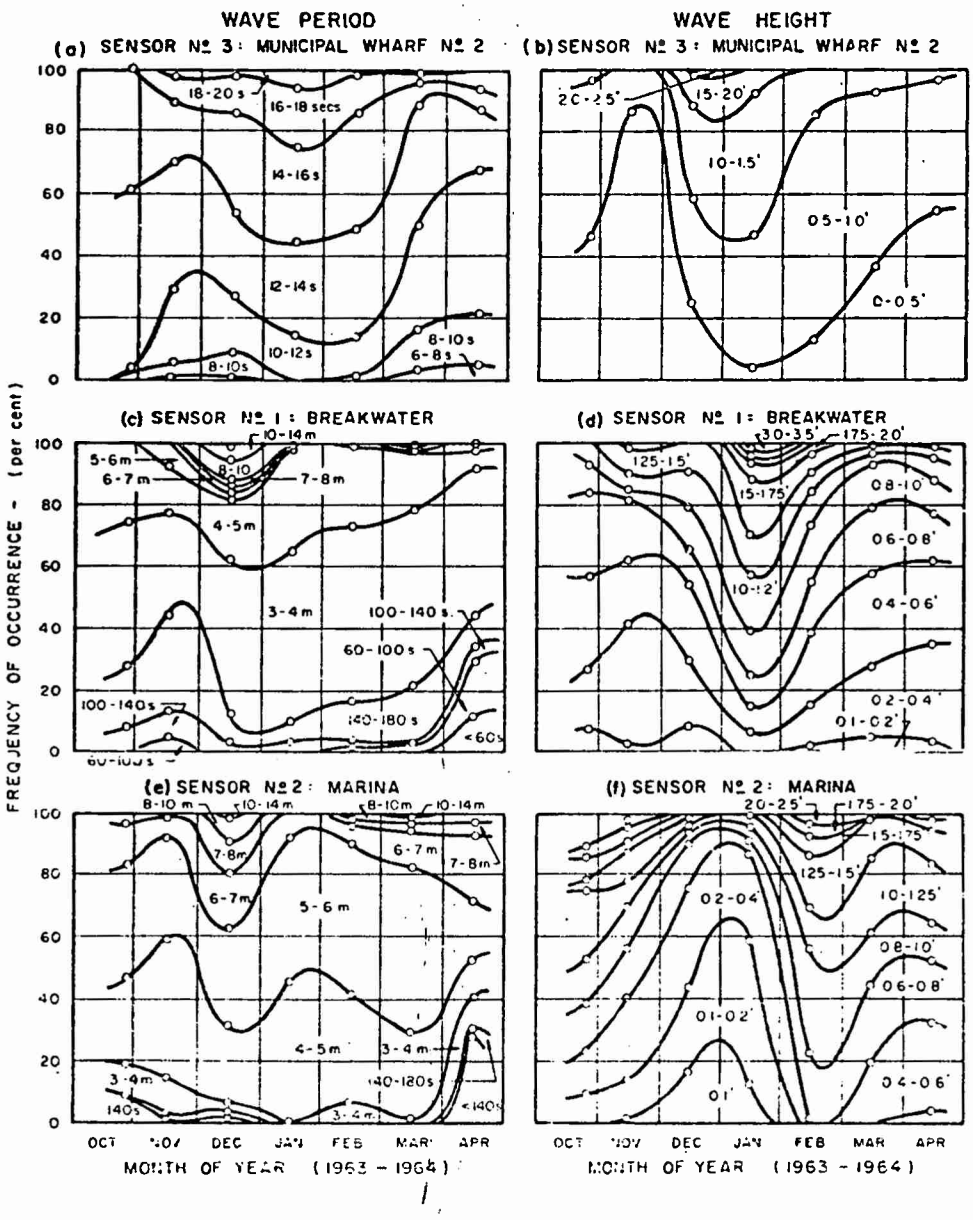

FIGURE 13 SEASONAL VARIATION OF SIGNIFICANT WAVE HEIGHT AND PERIOD AT MA SENSORS, MONTEREY HARBOR

January at Sensor 3. Within the marina at Sensor 2 (Fig. 13e) there is a growth towards longer periods in December similar to that at Sensor 1, near the breakwater.

One further important out-of-phase difference may be remarked between Sensor 3 (Fig. 13b) and Sensor 2 (Fig. 13f). At the same time (December-January), that ordinary swells are increasing strongly in height, long-period wave effects in the marina are diminishing to low heights.

Curiously the effects in terms of height at the long-wave Sensors 1 and 2 (Figs. 13d and 13f) are also largely out-of-phase. The strong tendency for development of large amplitude disturbances in the marina in February is accompanied by a lessening of amplitudes at the breakwater. This could be accounted for perhaps by a progressive directional change with time of the long waves reaching Monterey Harbor, resulting in a secular change in the regime of oscillation and the movement of its nodes.

For the present the evidence seems to favor the view that the occurrence of long waves in Monterey Harbor is not the direct consequence of the occurrence of high swells. There appears to be no inseparable link.

In passing we note that at Sensor 1, near the breakwater, 140-180 secs., 3-4 and 4-5 min. oscillations are particularly prevalent. Within the marina at Sensor 2 it is 4-5, 5-6 and 6-7 min. oscillations that predominate. We shall have occasion to refer to this again.

7. Wind-Wave and Long-Period Wave Statistics for Santa Cruz Harbor (Marine Advisers' Data)

Santa Cruz Harbor (Fig. 14) is located at the northern extremity of Monterey Bay (cf. Fig. 2) and would thus appear to secure some degree of shelter from the northwesterly waves and swells that most frequently assail Monterey Bay. Wave recordings for Santa Cruz, similar to Monterey Bay, were made by Marine Advisers (1964b). A sensor, recording ordinary sea and swell, was established seaward of the west jetty. A second sensor, capable of recording long period waves, was positioned

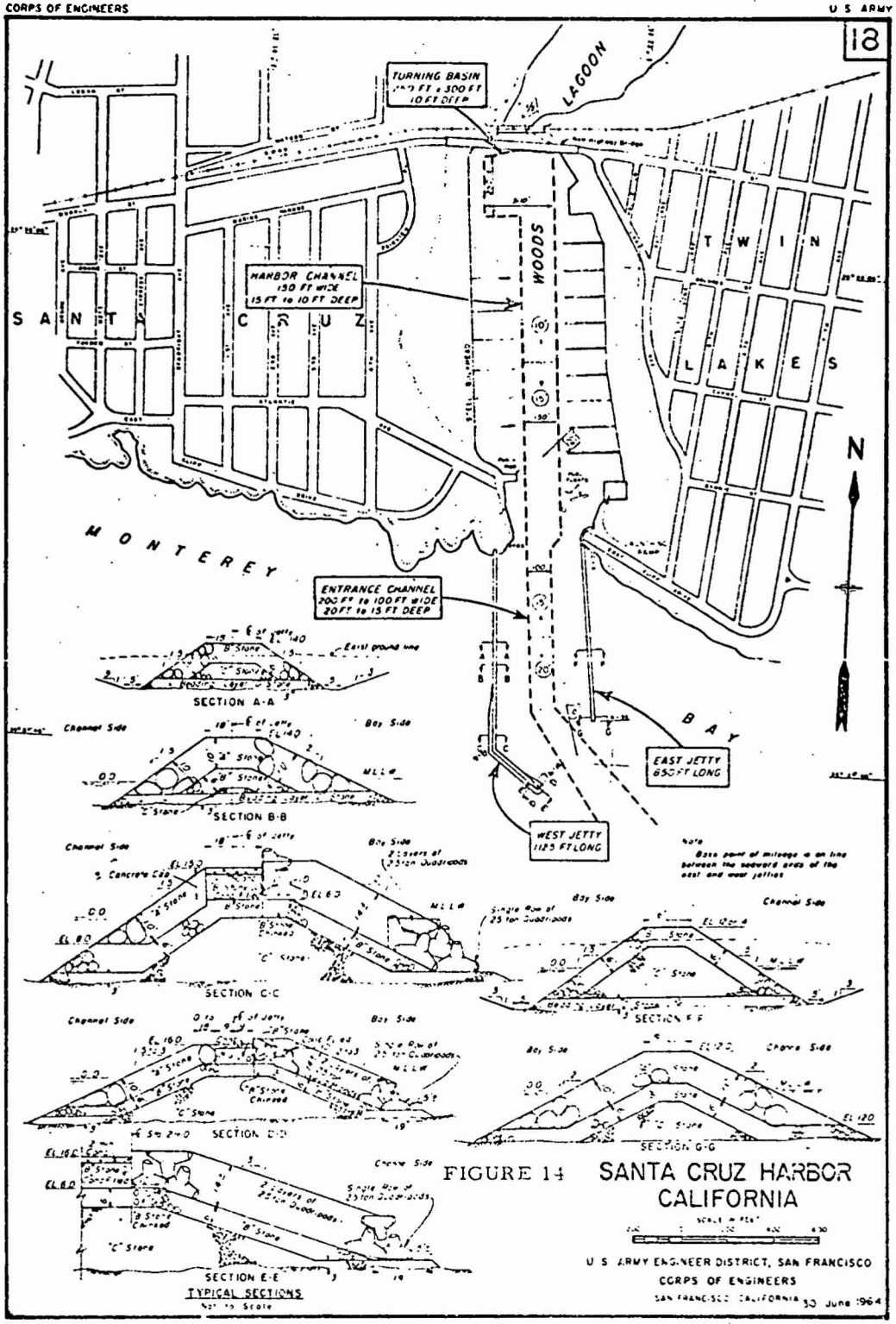
CORPS OF ENGINEERS
U S ARMY
18
TURNING BASIN
LAGOON
HARBOR CHANNEL
150 FT WIDE
15 FT to 10 FT DEEP
WOODS
T W I N
L A K E S
S A N T A C R U Z
N
M O N T E R E Y
ENTRANCE CHANNEL
200 FT to 100 FT WIDE
20 FT to 15 FT DEEP
B A Y
EAST JETTY
650 FT LONG
WEST JETTY
1125 FT LONG
SECTION A-A
SECTION B-B
SECTION C-C
SECTION F-F
SECTION D-D
SECTION G-G
SECTION E-E
TYPICAL SECTIONS
Not to Scale
SANTA CRUZ HARBOR
CALIFORNIA
U S ARMY ENGINEER DISTRICT, SAN FRANCISCO
CORPS OF ENGINEERS
SAN FRANCISCO CALIFORNIA 30 June 1964

FIGURE 14

inside the harbor; exact locations have not been ascertained.

The tabular data (Marine Advisers, 1964 b) has been plotted in Fig. 15 in a manner similar to that of Fig. 13. Unfortunately the sea-swell data are restricted to only three consecutive months and that of the long-wave sensor to only five months. Nevertheless rather interesting parallels are found between Figs. 13 c and 13 d for Monterey Harbor and Figs. 15 c and 15 d for Santa Cruz Harbor. The same suppression of shorter periods in favor of longer is found in the period December-January and the same proclivity for greatest amplitudes occurs in January. In Santa Cruz Harbor the predominant periods are 140-180 secs., 3-4 mins. and 10-14 mins.

The records from the sea-swell sensor (Figs. 15 a and 15 b) are too limited in length of time to be able to establish any very obvious trends of change. The evidence, such as it is, supports decreasing sea-swell periods at the same time that long wave periods are increasing -- again supporting the view that there is independence between these phenomena. On the other hand, the height data of Figs. 15 b and 15 d do show correlation in that long-period wave heights were on the increase (in January) at the same time as sea and swell, exterior to the harbor.

8. Long-Period Wave Statistics for Half Moon Bay (Marine Advisers' Data)

Although not specifically within the range of study of this report, the long-wave activity in Half Moon Bay is nevertheless of interest because of the proximity of this bay to Monterey Bay and its susceptibility to the same basic forms of excitement that stimulate the long-period surging in Monterey Bay.

The location of Half Moon Bay with respect to Monterey Bay and the deep-water Stations 3 and 4 is shown in Figs. 2 and 4, and the shape of the bay is well illustrated in Fig. 8. The long wave sensor installed and operated by Marine Advisers (1964 c) in this case was located within the lee of the west breakwater of the harbor, near Pillar Point (Fig. 8).

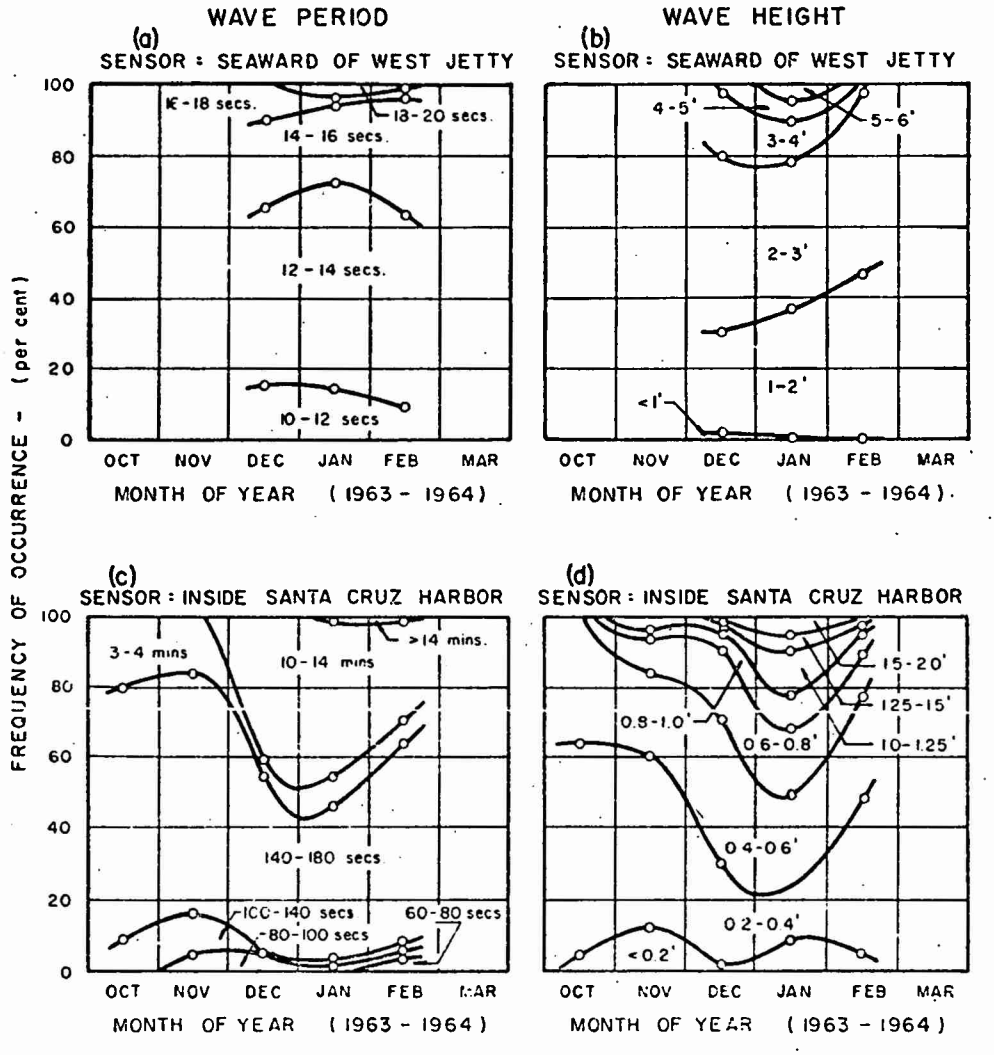

FIGURE 15 SEASONAL VARIATION OF SIGNIFICANT WAVE HEIGHT AND PERIOD AT MA SENSORS, SANTA CRUZ HARBOR

In Fig. 16 we plot the frequency of occurrence data for wave period and wave height on a time-base as before. The data in this case span a full year and may be compared conveniently with the open-sea swell data of Fig. 6 at approximately the same latitude.

It will be noticed that the increase of long-period wave heights over the months from October to March, manifest in Fig. 16 b, is supported by the corresponding increase in swell activity from the westerly approach over those months, shown in Fig. 6. This suggests again, as already deduced in Section 6, that westerly swells and long waves in the fall and winter months are mainly responsible for the surge phenomena in bays on the west coast. Indirectly this supports the viewpoint that long-period waves are associated with the greater proximity during these months (than at other times) of the extra-tropical storms which pare off the high pressure belt in the East Pacific Ocean. Precisely the same conclusion was arrived at in respect to the occurrence of surging in Table Bay Harbor, Cape Town (Wilson, 1951, 1959).

Comparison of Figs. 13 and 16 shows a general correlation between increase of long-period wave activity at Half Moon Bay Harbor and Monterey Harbor. It is noted, however, that heights of disturbances are very much smaller at Half Moon Bay and periods are generally lower, most of the agitation occurring in the period ranges 60-80 and 80-100 secs.

9. Corps of Engineers' Data for Monterey, Moss Landing and Santa Cruz Harbors

Four sheets of drawings (Nos. 6/17/19 of June 1964) supplied to this project by the U. S. Army Engineer District, San Francisco, comprise running time-plots of principal sensor wave periods and heights at both Santa Cruz and Monterey Harbors together, with estimated wind velocity and direction and predicted incidence of swell. These have been closely examined with a view to reaching conclusions that could shed light on the relationship of the surge phenomenon in Monterey Harbor to the measured long-wave characteristics recorded on Monterey Sensors 1, 2 and 3, and Santa Cruz sensors (No. 143 and No. H 142a) as well as local wind and swell.

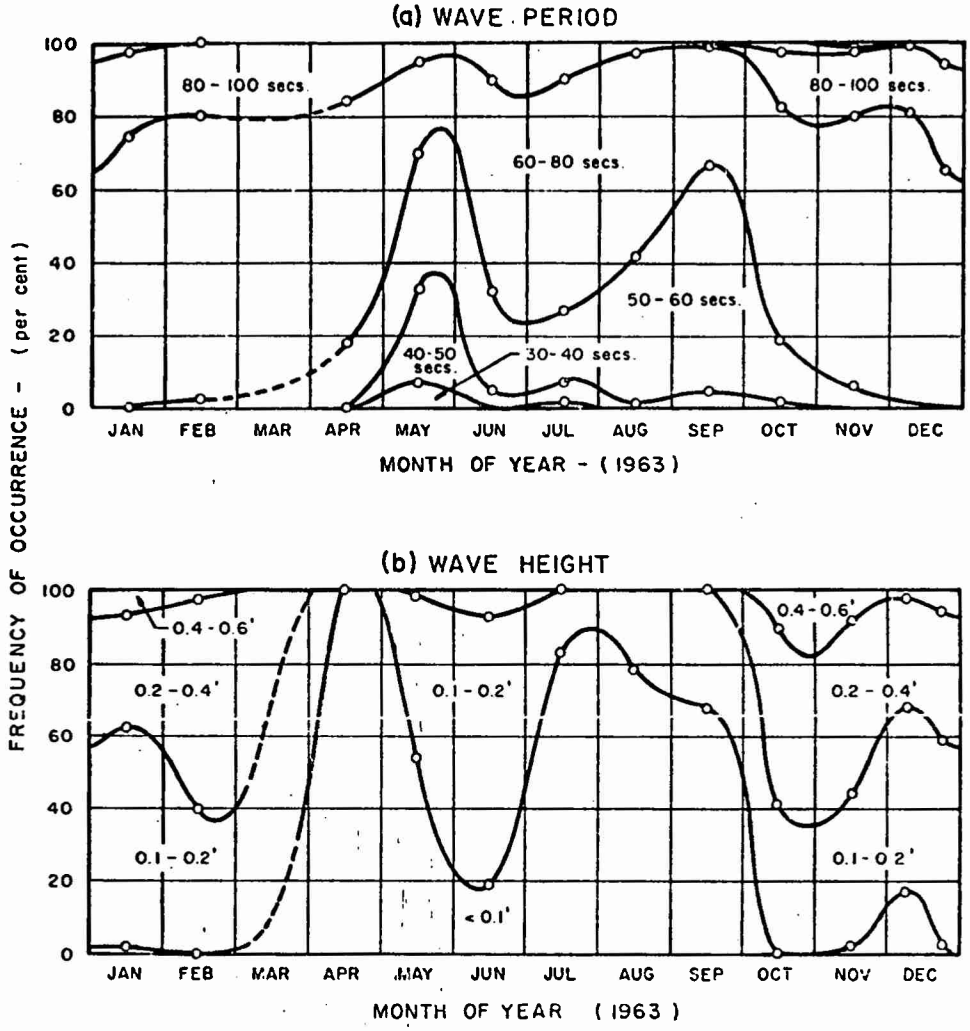

FIGURE 16 ANNUAL VARIATION OF SIGNIFICANT (LONG) WAVE HEIGHT AND PERIOD AT HALF MOON BAY HARBOR

The following observations seem to be pertinent:

a. Occasions of troublesome current in the marina entrance at Monterey Harbor are apparently linked to moderate to strong winds from NW, W and SW, when by qualitative estimate, the wind velocity exceeds about 12 knots.

Comment: This could mean that the presence of local wind results in stimulation of oscillations of the whole bay with periods long enough to pump the harbor and cause strong currents in the entrances. Local strong wind could generate short period waves that could activate the boats at their moorings. It is suspected that small boats will respond adversely to high-amplitude wind waves and swell that manage to penetrate the basins. An exception to conclusion (a) must be noted. On January 15-16, 1964, the wind was almost negligible and sensor activity was low ($H < 1$ ft. in general, except for Sensor 3) yet current activity was reported over this entire period. It is suspected that this was a period of bay seiches induced by barometric oscillations under fine weather conditions. Direct air-water coupling of this kind is a cause of seiches in lakes and bays (cf. Wilson, 1953a).

b. Occasions of troublesome current in the marina entrance are apparently not dependent on large amplitudes of long waves in the period band from 160-400 secs. (average 4 mins.), with Monterey Sensors 1 and 2 registering heights $H > 1$ ft.

Comment: The record for April 1964, for instance, shows no trouble in the interval April 10-17. The sensor at Santa Cruz at this time was showing waves of 12 to 18.5 secs. period with $H \simeq 2.75$ ft. Winds at this time were generally low-rated (less than 10 knots) except on April 11 and 16-17.

On January 27-28, 1964, there was exceptionally high activity

on Sensor 1 (T = 240 secs., H ≃ 3 ft.) but current activity was not reported for 4 hours from 10:00 to 16:00 on January 28. Santa Cruz had only moderate activity (outside jetty H ≃ 3 ft., T = 15 secs.).

c. Occasions of troublesome current in the marina entrance are apparently not dependent on high swell conditions (based on predictions of the Fleet Numerical Weather Facility at Monterey).

Comment: High swell conditions, for instance, predicted for March 14-16, 1964, caused no out-of-the-ordinary sensor activity in Monterey, nor any reported trouble. Winds were low.

Generally, the writer finds the same sort of elusiveness and intangibility in correlating the data of Drawings 6/17/9 as he experienced when attempting similar qualitative correlations to define the causes of surging in Table Bay Harbor, Cape Town (Wilson, 1951). Fig. 17 is an example of the kind of data that were maintained over the years 1942-1947 for Table Bay Harbor (see inset, Fig. 2). The evidence of surging trouble at Cape Town was generally manifest in the magnitude of the oscillations of period less than 5 mins. in the large rectangular Duncan Basin. A typical example (Fig. 17) is the occasion of May 2-3, 1946 when 5 and 9-inch amplitude oscillations of periods 1.8 and 5.5 mins. respectively occurred in the Duncan Basin. Row e shows that a cyclonic storm (low pressure) passed over Cape Town and high winds (row a) of mean velocity 18-24 mph (min 0, max 46 mph) prevailed. Apart from an undoubted correlation between storms and the occurrence of surge at Cape Town, there were many exceptions which often made the causes indefinable. In the case of the Cape Town data there was serious need of ordinary swell recorders, which were unavailable at the time. In the case of the Monterey data of Drawings 6/17/9 it is felt that there is great need for precise wind and barometric pressure data to define the vital links for understanding the cause of surge excitation. It is strongly recommended that anemometer

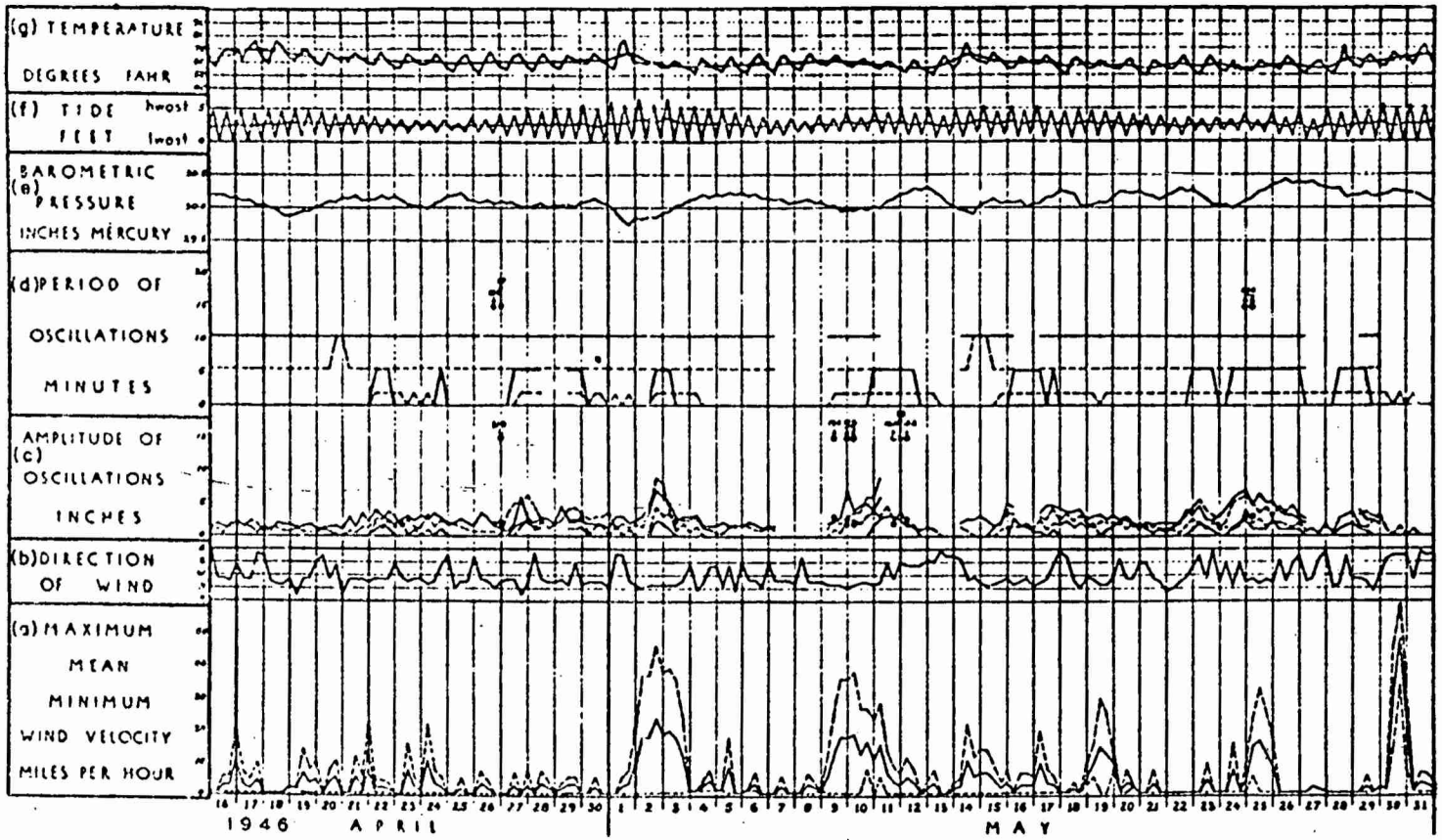

FIGURE 17 CONTINUOUS WEATHER AND WAVE CHART FOR TABLE BAY HARBOR, CAPE TOWN, SOUTH AFRICA, APRIL-MAY, 1946

and barometer equipment be installed and routinely maintained at Monterey Harbor, Moss Landing and Santa Cruz.

It may be noted that essentially the same conclusions as have been arrived at in paragraphs a, b and c above were drawn by Marine Advisers in their report of July, 1964 (p. 19). It may be said too from the writer's experience at Cape Town that conditions that would cause the strongest currents in the basin entrances would always be seiches of periods long enough to pump the basin areas. This requires an external excitation of a period long enough to cause a general rise and fall of water over the entire basin area.

The Corps of Engineers' data in Drawings Nos. 6/17/19 would seem to indicate that at Marine Advisers' (MA) Sensor 1 in the NE corner of the marina at Monterey Harbor, preponderant periods through January 1964 were from 160 to 280 secs. While it is realized that registration of the heights of these period waves is merely an index of long-period agitation, it would appear, on reference to Fig. 13e, that a more satisfactory register for Sensor 1 would have been oscillations in the period range from 4 to 6 mins. For Santa Cruz Harbor the registration of periods in Drawings Nos. 6/17/19 is more in accord with the indications of Fig. 15c.

It seems appropriate to consider here the results of measurements and analyses made by the Army Engineer District, San Francisco, and the Waterways Experiment Station, Vicksburg of wave conditions obtaining in Monterey Harbor in 1946-47. Wave gage locations at that time were at the three positions 1, 2 and 3 marked "C.E. Station" in Fig. 12. Typical samples of traces obtained at that time are reproduced in Fig. 18 (cf. Hudson, 1949) though locations of the records are not identified.

By an analysis procedure, indicated in Fig. 18, for estimation of wave heights and periods, results were reduced to the form shown in Fig. 19 (Hudson, 1949). The graphs here cover three bands of wave frequencies, short-period, intermediate-period and long-period. These data serve to match periods with heights in a manner that cannot be construed from the information presented in Fig. 15. It is evident that among short

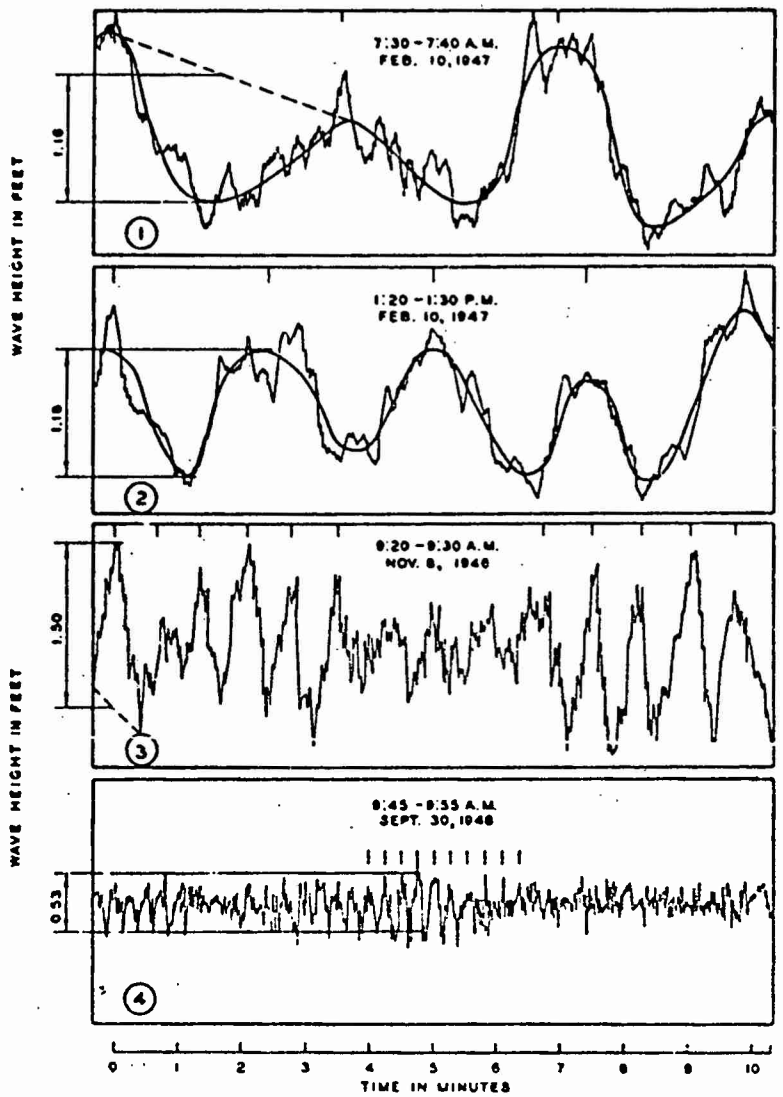

FIGURE 18 FACSIMILES OF LONG WAVE RECORDS FOR MONTEREY HARBOR, SHOWING METHOD OF ANALYZING WAVES (from Hudson, 1949)

METHOD OF ANALYZING PROTOTYPE WAVES

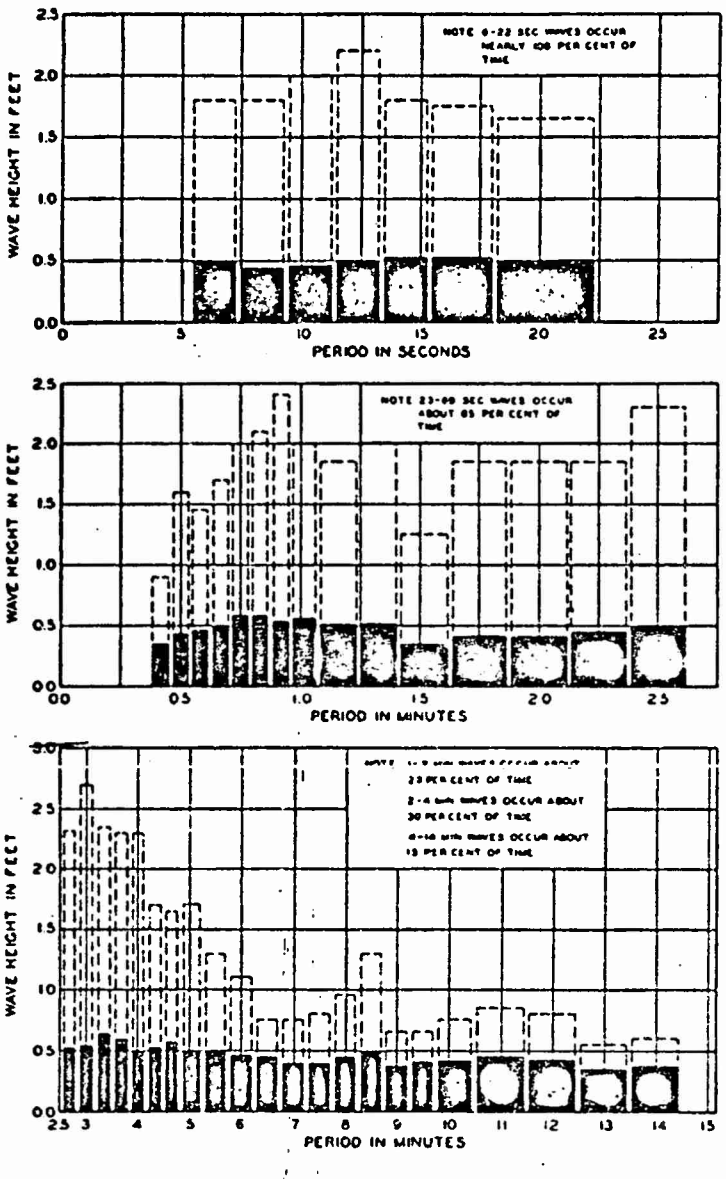

FIGURE 19

PROTOTYPE WAVE INVESTIGATION
WAVE HEIGHTS AND PERIODS
Oct. 1946-Apr. 1947 (from Hudson, 1949)

period waves 12-sec. periodicities tend to predominate in height. In the intermediate range outstanding peaks occur at about 55 secs. and 2.5 mins., while in the long-period range the prominences are found at 3 mins., 5 mins., 8.5 mins., and 11 to 12 mins. Unfortunately no indication is given as to the specific locations for which these results were applicable though it must be inferred that they reflect the wave conditions in the harbor as a whole.

10. Chrystal's Method of Residuation Applied to Typical Field Data (SEA-Analysis).

By way of securing an independent evaluation of the surge conditions in Monterey Bay, a method of analysis found to be of great value in the studies of surge action in Table Bay Harbor, Cape Town, was applied to typical samples of wave records obtained from MA sensors, CE wave gages and Coast and Geodetic Survey tide gages. This method, due originally to Chrystal (1906), successively 'residuates' a given wave record by extracting from it an apparently obvious periodicity.

The fact that amplitudes of oscillations in a record are highly variable does not affect the generality of the method. The occurrence of a beat oscillation, for example, resulting from two wave frequencies of similar value, would tend to show amplitudes varying with time, but the Method of Residuation will extract the entire beat oscillation if the correct combined wave frequency within the beat is used. It would equally well eliminate the beat if two residuations were performed to extract the two component frequencies separately, provided these could be identified. Invariably the removal by residuation of one wave frequency from the record will reveal another that may have been obscured and will permit the residuation process to be repeated until only a relatively smooth trace remains.

The process by which this graphical residuation analysis was accomplished is illustrated in Figs. 20 to 25, which show successive residuations performed on typical wave records and the suspected periods extracted at each step.

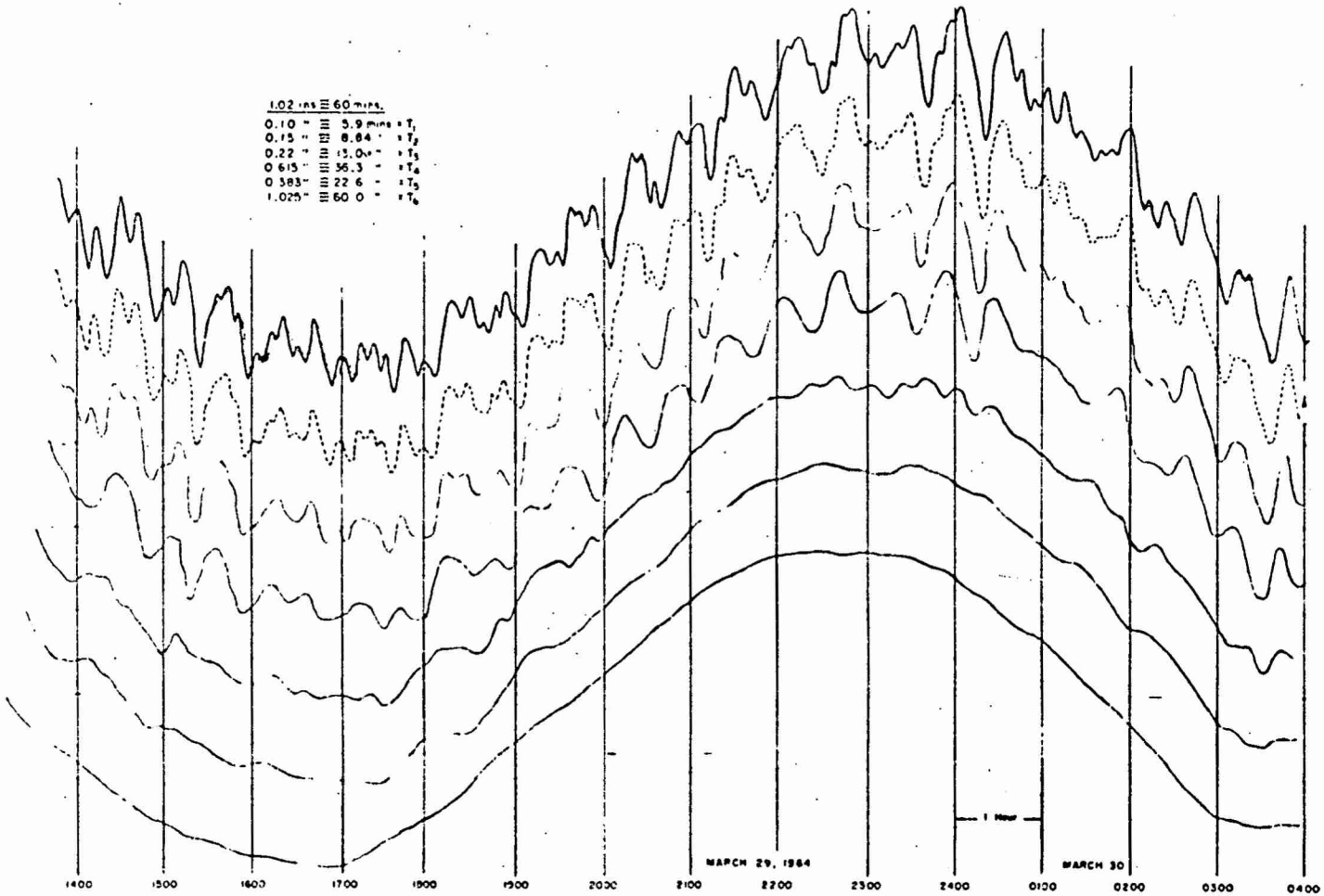

FIGURE 20 SUCCESSIVE RESIDUATIONS OF TIDE GAUGE RECORD FOR MONTEREY HARBOR, FEATURING THE TSUNAMI DISTURBANCE FROM THE ALASKAN EARTHQUAKE, MARCH 20, 1964

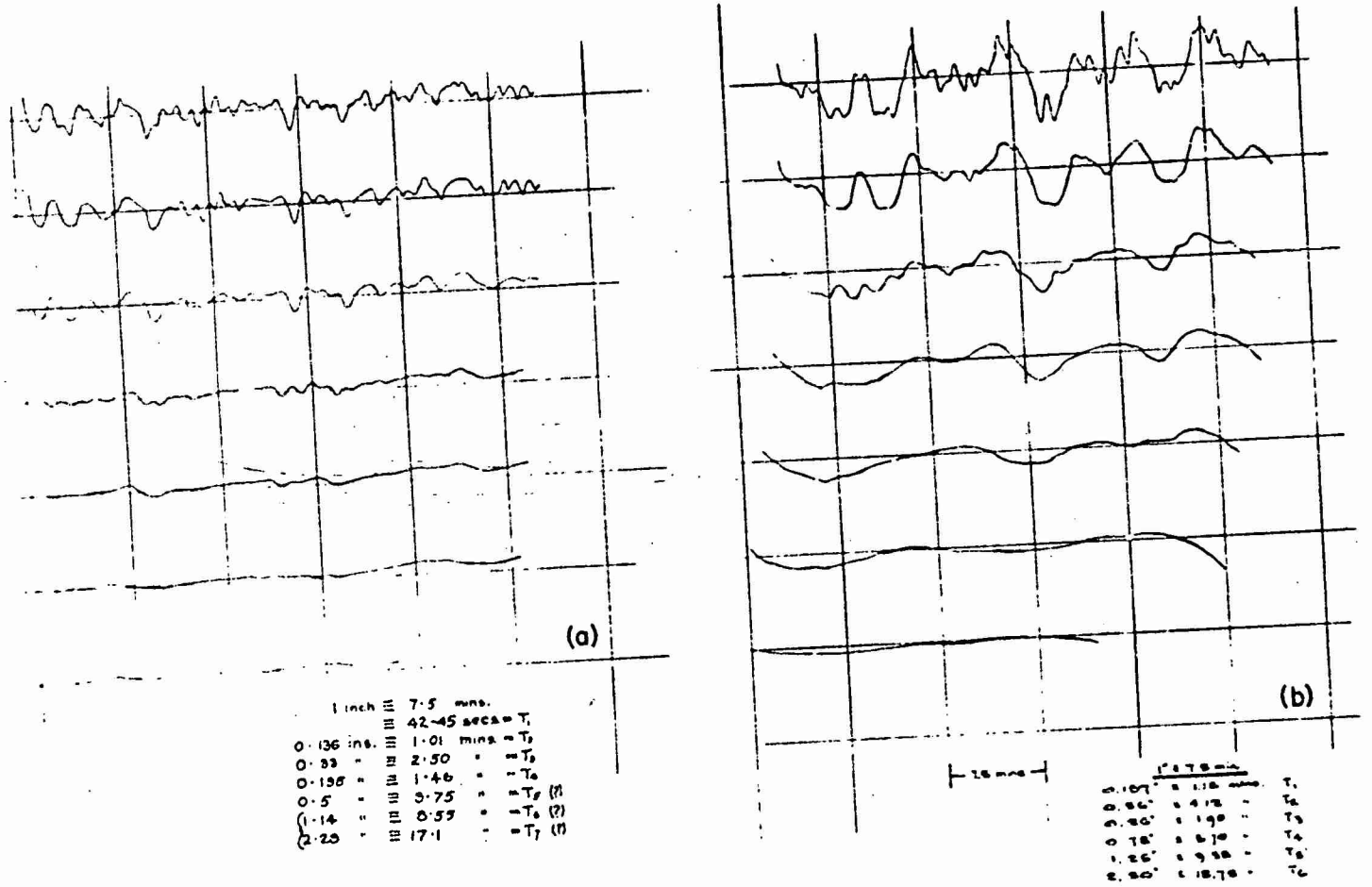

FIGURE 21 SUCCESSIVE RESIDUATIONS OF LONG WAVE RECORDS: (a) SENSOR 1, MONTEREY HARBOR FEB. 10, 1964; (b) SENSOR 2, MONTEREY HARBOR, FEB. 10, 1964

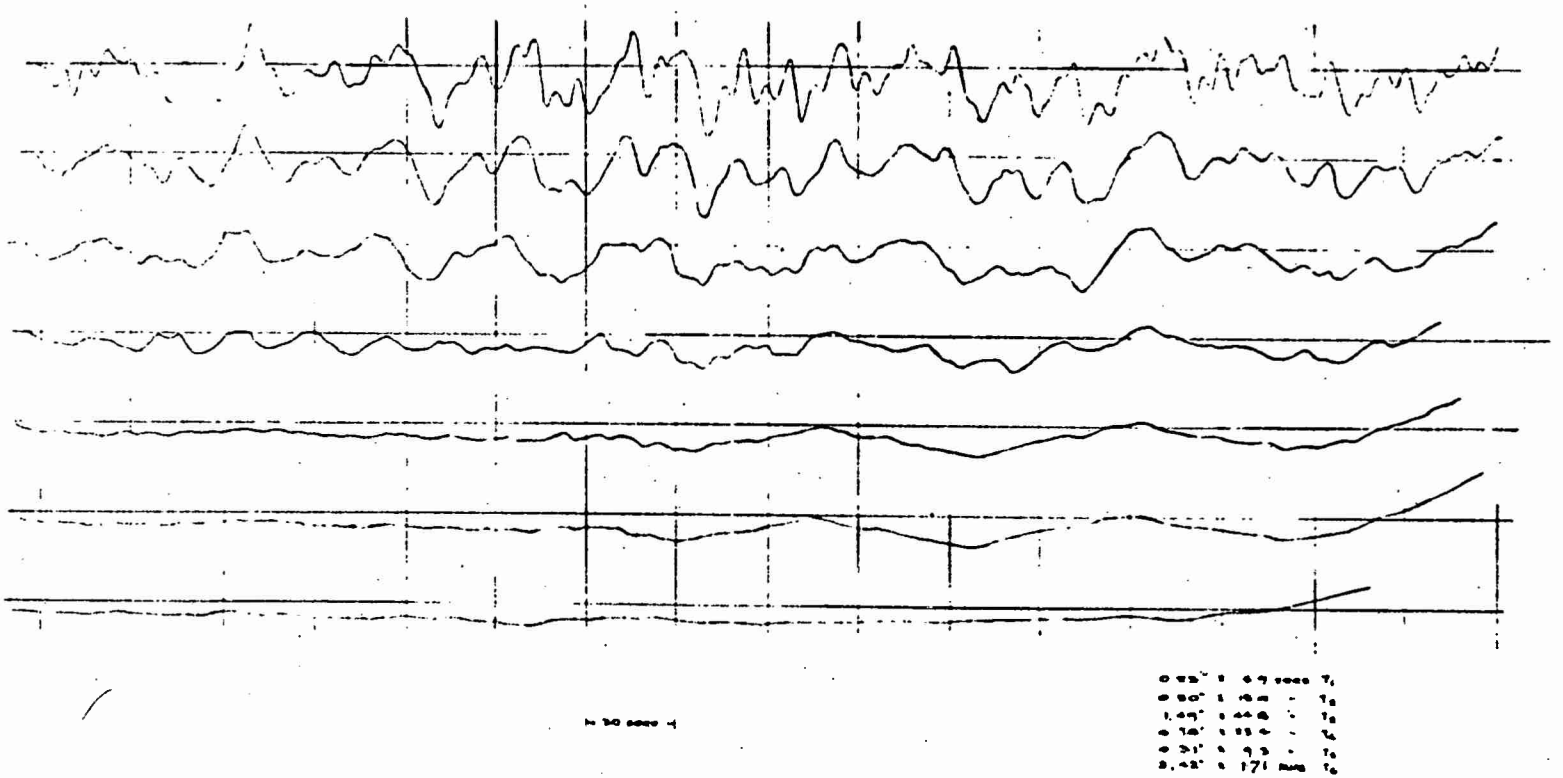

FIGURE 22 SUCCESSIVE RESIDUATIONS OF LONG WAVE SENSOR 3 RECORD, MONTEREY HARBOR, FEB. 10, 1964

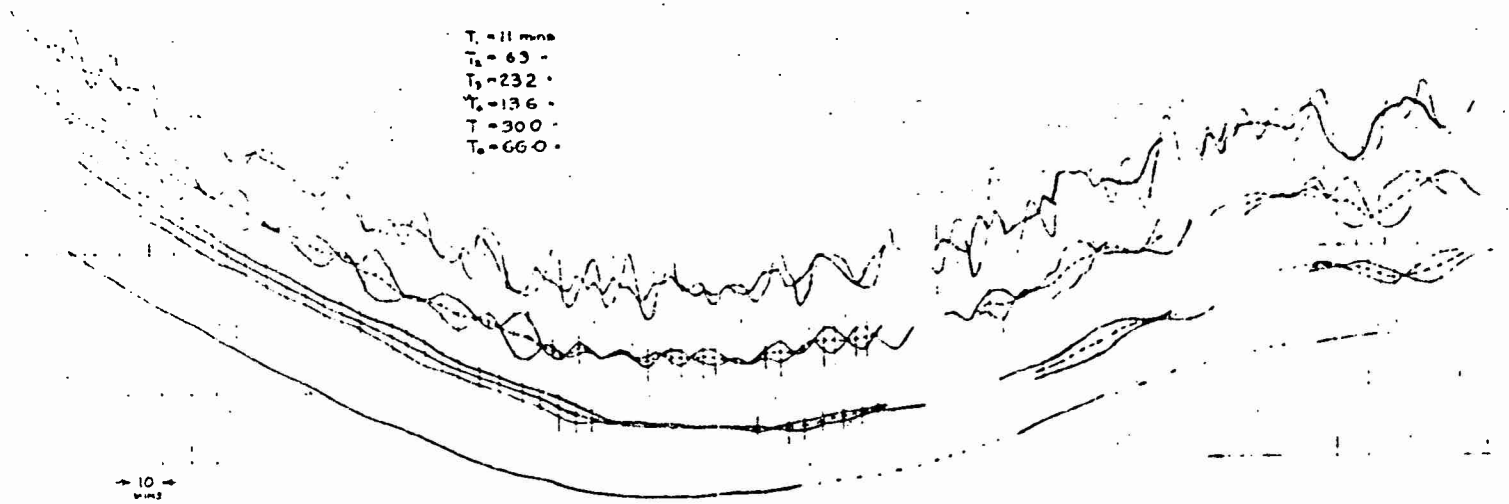

FIGURE 23 SUCCESSIVE RESIDUATIONS OF TIDE GAUGE RECORD FOR SANTA CRUZ HARBOR, NOV. 24, 1964

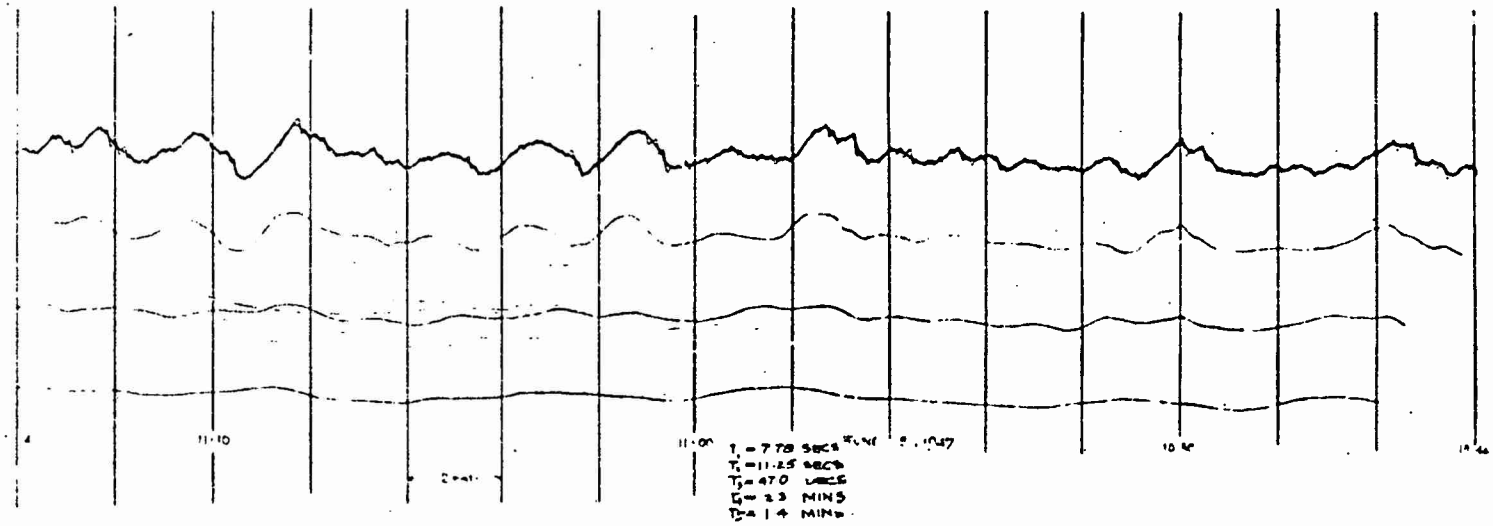

FIGURE 24 SUCCESSIVE RESIDUATIONS OF LONG WAVE SENSOR RECORD, MOSS LANDING, JUNE 2, 1947

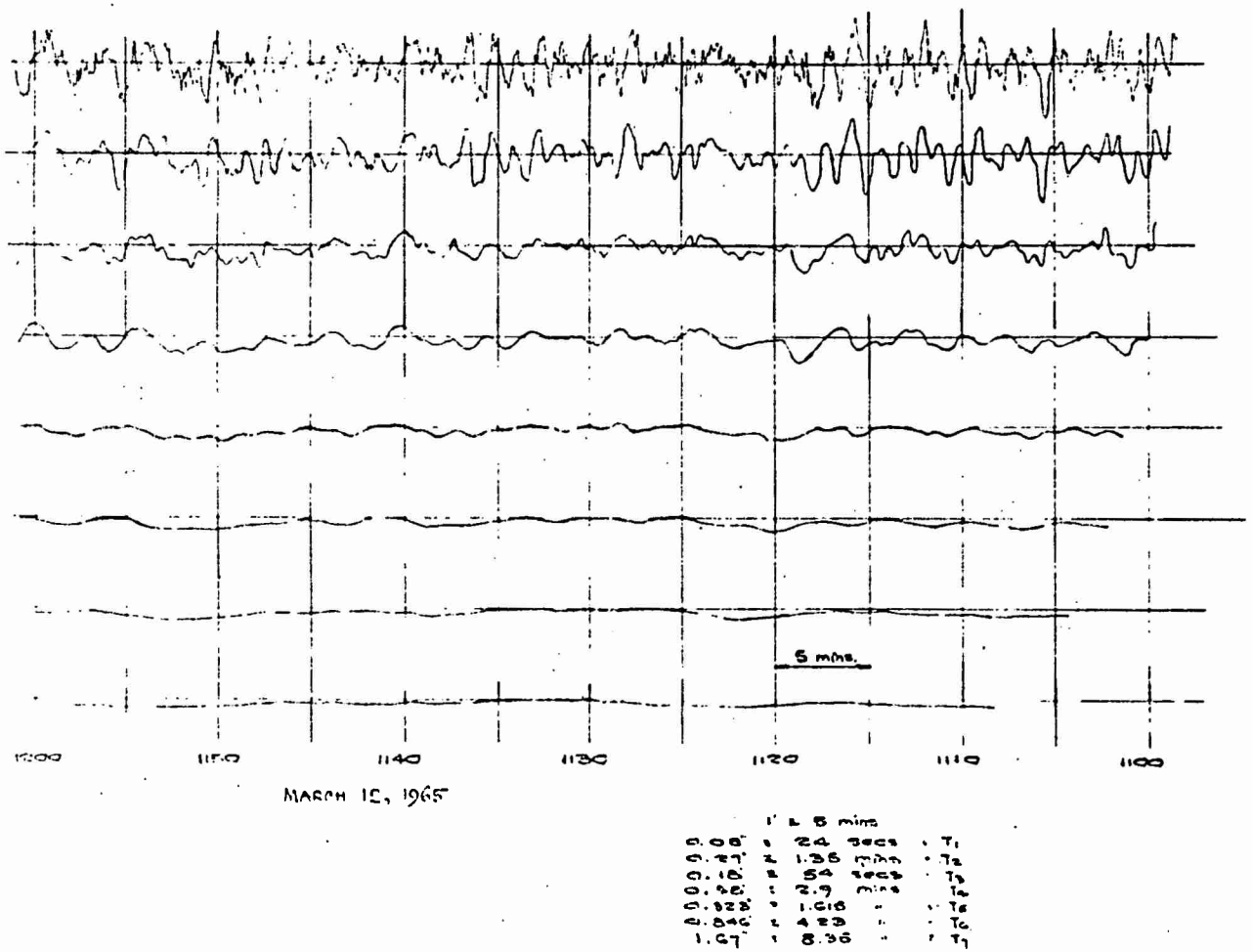

FIGURE 25 SUCCESSIVE RESIDUATIONS OF WAVE SENSOR RECORD AT LOCATION OUTSIDE MUNICIPAL WHARF NO. 2, MAR. 12, 1965

The results of the residuations are conveniently summarized in Table I. Somewhat arbitrary separation of apparent periodicities into column groupings has been made to allow of comparisons being made between analyses for Monterey Harbor, Moss Landing and Santa Cruz. The first two rows of Table I are obtained from the tide gage record at Monterey Harbor (see Fig. 20) on the occasion of the tsunami that originated from the Alaskan earthquake of March 28, 1964.

The residuation analyses do not specify the heights of the individual wave components although these could be obtained by a full application of the method. Table I thus gives no indication of relative heights in the manner of Fig. 19.

We shall not at this stage attempt a full correlation of our results with those of Marine Advisers or of the Corps of Engineers, but we may note in passing that some of the frequencies that evolve from the residuation are in good general agreement with period-bands in Fig. 19 which have the greatest average or maximum height. The prominences at 11, 8.5, 4.6, 3.3, 2.5, 1.3, 1.0, and 0.75 mins. in Fig. 18 are in good accord with several of the columns of Table I.

The residuation analysis of the sensor record obtained on March 12, 1965 (cf. Table I and Fig. 25) reflects conditions outside the Municipal Wharf No. 2. This is the location originally recommended for survey by the writer at the meeting of July, 1963, because of tendency that the area between Wharf No. 2 and the shore would have to develop the antinodes of seiches or standing waves.

The residuation analyses cover three periods on March 12, each approximately an hour. In general they show substantially the same periodicities continuously active over the 3-hour interval. During this time, to quote from the letter of Mr. G. P. Reilly (SPNGP of March 17, 1965), Chief of the Engineering Division, U. S. Army Engineer District, San Francisco:

> "... the sea conditions were generally calm. The weather was variable with intermittent light drizzle on 12 March. During the

TABLE 1

APPARENT PERIODS OF OSCILLATION IN TIDE GAGE
AND LONG WAVE SENSOR RECORDS (Residuation Analysis)

DATE & TIME	SENSOR LOCATION	SEQUENCE OF APPARENT PERIODS - mins. or secs. (s)																
1400, Mar. 29, 1964 -0400, Mar. 30, 1964	Monterey Tide Gage	60	36.3	22.6		13.0	9.8		5.9									
March 29, 1964 0000-0900	Monterey Tide Gage	60	35.7 32.3	19.6	17.3	11.1	9.3		5.5									
Feb. 10, 1964	Monterey Sensor No. 1				17.1 (?)		9.6 (?)			3.8	2.5			1.00	42-45s			
	Monterey Sensor No. 2				17.2				5.7	4.1		1.95	1.20					
	Monterey Sensor No. 3											1.7			44.8s	23.4s	15.0s	9.3s 6.9s
March 12, 1965 0850-1000 1000-1100 1100-1200	Outside Municipal Wharf No. 2					13.5 12.1	8.4 8.4	6.1		4.6 4.4 4.2	2.3 2.8 2.9	 1.6	1.30 1.32 1.35	0.98 1.00 0.90	42 s 36 s	 24.0s 24.0s		
May 27, 1947 1148-1214	Moss Landing									3.9 4.1	2.5 2.2	1.96	1.2		50.1s 32 s 31 s			
June 2, 1947	Moss Landing									4.6	2.3		1.4		47 s		11.3s	7.8s
Nov. 24, 1964	Santa Cruz (1)	66	30	23.2		13.6 11.0		6.3										
	Santa Cruz (2)	86 (?)	28.5			13.0				3.8								

measurement period no difficulties were observed in the small boat marina. However, at about 11:30 a.m. on March 12, relatively strong currents were observed at the entrance to the small craft marina. These currents were highly variable and reversing, and had apparent periods of between one and three minutes. The significant heights of wind waves at the beach adjacent to the landward (SE) side were less than one-half foot at the sensor and breakers on the adjacent beach were less than one and one-half feet."

The fact that strong reversible currents of a period between 1 and 3 mins. were observed around 11:30 a.m. provides, perhaps, an interesting clue to the cause of the disturbance. The residuations (Table I) show that in the period range mentioned there was active between 1100 and 1200 hours an oscillation of 1.6 mins. period, not evident during the preceding 2 hours. The implied evidence is that this particular periodicity was responsible for flushing the marina.

It is significant that the residuation analysis performed on the MA sensor records for Feb. 19, 1964, (Table I) show evidence of 1.7 and 1.95 min. oscillations at Sensors 2 and 3. According to Marine Advisers (1964 a), this was an occasion of the most extensive reported difficulties and damage to small craft in the 6-month period of observation from October, 1963 to April, 1964. Bearing in mind conclusion (c) of Section 9, the implication again is that harbor oscillations of about 1.6 to 1.7 mins. period provide the stimulus to pump the marina area. Further consideration of this possibilty will arise in the next section and at a later stage in this report.

11. Wave-Energy Spectra for Locations in Monterey and Santa Cruz Harbors (Marine Advisers' Data)

The sea-energy spectra derived by Marine Advisers (1946 a) from spectral analysis of particular samplings of their recorded wave data, help to shed further light on the responses of Monterey Harbor to the influences of long-period waves.

We tend in general to concur with the interpretations which Marine Advisers (1964 a) have placed upon the spectra obtained from the records of the three cases analyzed by them, namely:

A. February 11; 1964, (0000-1730 PST) - the occasion of most extensive reported difficulties and damage to small craft during the period of observation (winds to 35 knots from W and NW).

B. March 27, 1964 (1730) - March 28, 1964 (1100 PST) the occasion of the arrival of the tsunami from the Alaskan earthquake.

C. April 12, 1964 (0000-1400 PST) - an occasion of no reported damage or difficulties (winds less than 10 knots from NW).

For convenience of discussion here we reproduce the wave spectra derived by Marine Advisers for cases (A) and (C) in such a way as to facilitate comparison not only of the peculiarities of the cases but also of the features of the spectra from individual sensor locations. The composite Fig. 26 plots sea-energy against wave-frequency and it will be understood that ordinate-values applicable to each sensor in Figs. 26 a and 26 b are referred to the energy-values specified on the right-hand margin of each diagram.

It is perhaps a slight disadvantage of the form of calculation and presentation of the spectra that the entire period-band greater than about 4.5 mins. is compressed into the narrow frequency-band from 0 to 0.00375 cycles/sec., (covering only 1-1/2 ins. of chart space in the original published form). Nevertheless the period band-spread over the range of higher frequencies important to Monterey Harbor is otherwise very adequate.

The spectra of Figs. 26 show numerous teeth-like serrations which increase in number with increase of frequency. These serrations overlie broad humps and troughs (dash lines) which in a general way are similar for cases A and C for each sensor location. The humps and troughs, however, are not similar as between individual sensors. Marine

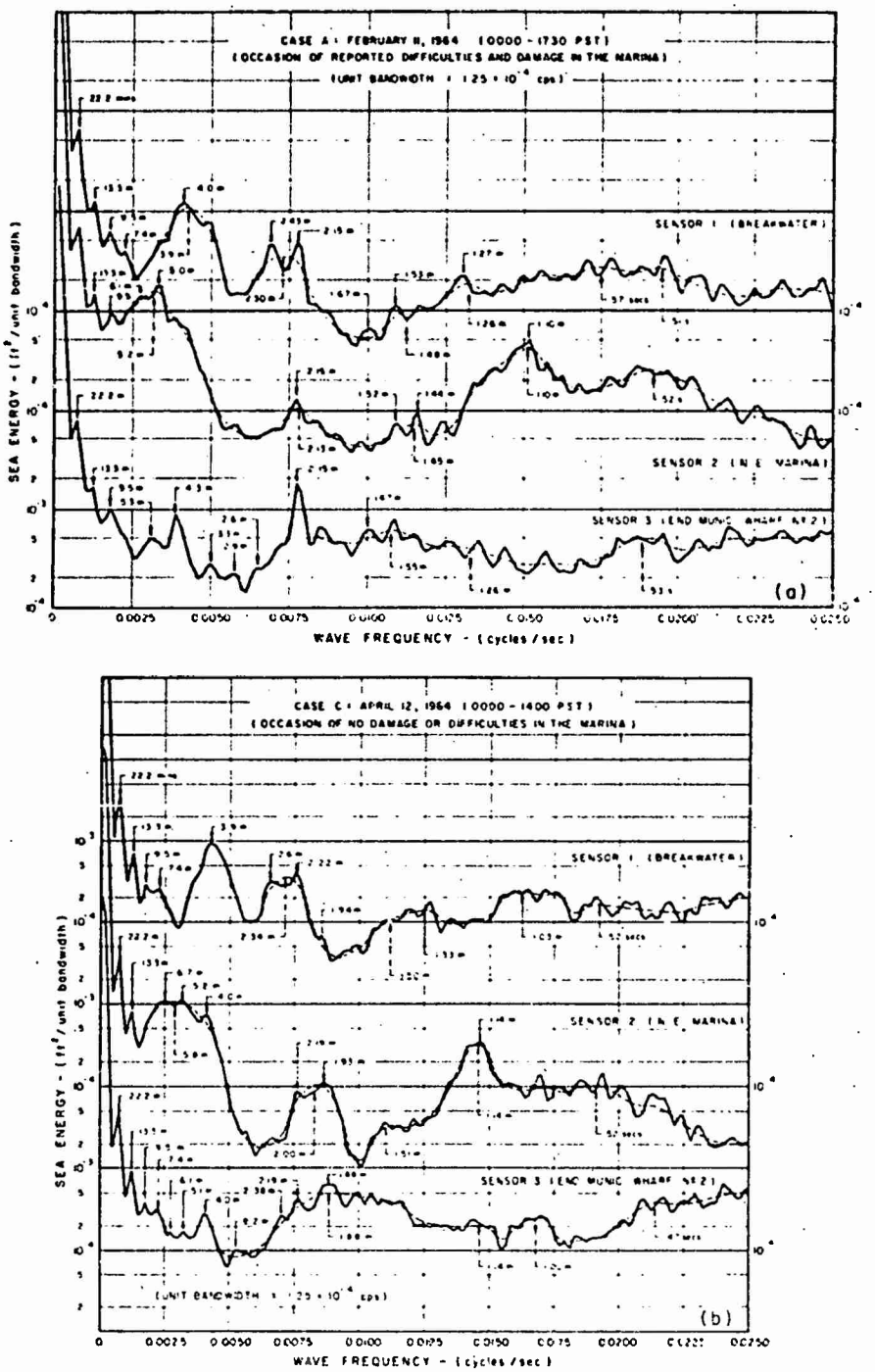

FIGURE 26 SEA-ENERGY SPECTRA FOR MA SENSOR LOCATIONS IN MONTEREY HARBOR: (a) FEB. 11, 1964 (CASE A); (b) APRIL 12, 1964 (CASE C)

Advisers (1964 a) have inferred that these broad humps are indicative of resonant responses of the harbor basins to wave frequencies within the band-spread of the humps; with this view we concur. Marine Advisers have also noted that at low frequencies, serrations occur at the same frequencies on all the spectra analyzed from which they infer that the peak frequencies are evidence of modes of oscillation in which the whole bay and near-harbor environment respond to external excitation. With this view we concur also, but must point out that the poor resolution of the wave spectrum at very low frequencies necessarily makes the peak-frequency, or period values, shown in Figs. 26, rather approximate for frequencies less than 0.0025 cycles/ sec.

Regarding the individual teeth of the serrations in the wave spectra, it is probable that these reflect high-order modes of resonance at which particular basins can oscillate. It is known for instance that a long narrow rectangular basin of uniform depth will have a large number of detectable modes of oscillations at periods diminishing in harmonic series. For a broad rectangular basin the number of possible detectable modes is very much greater. Since each mode has a frequency band-spread of response, the proximity of any two or more modes in terms of frequency tends to accumulate the response through overlapping, accounting for the development of a hump response.

As an example of this argument we may refer to the sea-energy humps at the periods 2.30 mins. (case A) and 2.34 mins. (case C) at the Sensor 1 location (Figs. 26). In both Fig. 26 a and 26 b this hump has two prominent teeth, marking resonances at about 2.5 and 2.2 mins. The external excitation in cases A and C was obviously such as to excite both these modes of response near the breakwater to about the same energy level. From this it is obvious that Sensor 1 must have recorded a beat oscillation resulting from the interaction of these two modes.

Either of these two modes could affect the interior of the harbor, separately or collectively. If one of the two modes of oscillation happened to be nodal at the other sensor positions, it would fail to register; if it were antinodal it would register as an individual peak. On referring to

Figs. 26 we find, indeed, that only the 2.15 min. peak is prominent in the Sensor 2 and Sensor 3 spectra (case A) and that it also shows at these sensors for case C. The inference then is that this period stimulates the interior of the marina, while the 2.5 min. period is relatively inactive (at least at the Sensor 2 location).

In both cases A and C (Figs. 26), Sensor 2 within the marina shows strong energy-level response to oscillations in the period range 5.2 to 5.8 mins. Correlating-information from Crops of Engineers drawings Nos. 6/17/19 showed that difficulties in the marina were apparently unrelated to the 3.9 min. sea-energy hump registered by Sensor 1 (see remark under b, Section 9). Since no trouble was reported on April 12, 1964 (case C), although energy-levels for the period range 3 to 6 mins. were comparable, we conclude that the deduction b of Section 9 (Corps of Engineers data) supports the spectral energy information (Fig. 26) in showing that trouble in the marina is not a function of periodicities in the band-spread 3-6 mins.

We have already made the tentative deduction in the last section (10) that excitation periods in the neighborhood of 1.6 mins. may be linked to the marina troubles. Comparison of the sea-energy spectra for cases A and C in Figs. 26 fails to reveal any very obvious resonance at this period, though there is definitely evidence of a minor energy hump in the period range 1.45 to 1.55 mins. Comparing cases A and C, energy-levels for Sensors 1 and 3 (external to the marina) are much the same. However, the energy level at Sensor 2 within the marina over the period range from about 50 secs. to 3 mins. (case A) is about twice that for case C and herein therefore definitely lies the source of the difficulties and damage.

It should be pointed out that the fact that a prominent resonance at about 1.6 mins. is not really evident in the spectra for Sensor 2 in the marina is not proof that it does not exist and is not critical. The Sensor 2 location in the marina could be nodal for a 1.6 min. oscillation and therefore would not register it. It was for this reason that the writer advocated a measuring location external to Municipal Wharf No. 2, where all exciting oscillations tend to be antinodal and therefore reveal themselves. The

minor energy peaks at 1.67 mins. in Fig. 26a could mean that a major resonance peak exists for some position in the marina other than that of the NE corner.

It would seem inappropriate to stress unduly the conclusion arrived at from the Residuation Analysis, because of paucity of information, but the general inference must be that model experimentation will have to concentrate a great deal on the period band of long-wave activity below say .3 mins.

Before leaving the subject of Marine Advisers sea-energy spectra, it is convenient to assemble the peak-energy periods (in the period-range greater than 1.7 mins.) for each sensor location and each case, including case B. This assembly of periods is compiled in Table II from which it will be noted that there is a surprising degree of similarity with the column figures of Table I. Indirectly this justifies the soundness of the Residuation Analysis, just as the latter clarifies the meaning of the peaks of the wave-energy spectra.

TABLE II

PERIOD OF OSCILLATION ACCORDING TO
PEAKS OF SEA ENERGY SPECTRA (Marine Advisers , 1964 a)

Date	Monterey Sensor No.	Sequence of Periods (mins.)												
Case A Feb. 11, 1964	1		22.2		13.3	9.5	7.4		4.9	4.0		2.5	2.2	1.7
	2		22.2		13.3	9.5		6.1	5.0				2.2 2.0	1.8
	3		22.2		13.3	9.5			5.3	4.3	3.3 2.9	2.6	2.1 2.0	
Case B March 28, 1964 (tsunami)	1	33.3					8.3	5.8		4.3	3.2	2.4	2.0	
	2	33.3		16.7			8.3		5.3	4.4	3.3	2.5	2.3	
	3	33.3		16.7		9.5		6.1		4.3	3.5	2.4	2.1	
Case C April 12, 1964	1		22.2		13.3	9.5	7.4			3.9		2.6	2.2 2.0	1.9
	2		22.2		13.3			6.7	5.1	4.0	3.0	2.5	2.2	1.9
	3		22.2		13.3	9.5	7.4	6.1	5.1	4.0	3.2	2.4	2.2	1.9

III A. ANALYSIS OF OSCILLATING CHARACTERISTICS OF MONTEREY BAY: APPROXIMATE ANALYTIC SOLUTIONS FOR SEICHES IN SEMI-ENCLOSED BASINS

1. Two-Dimensional Oscillations in Basins of Various Geometrical Shapes

The discussions in Part I already appear to focus on the main elements of the trouble at Monterey Harbor. However, the nature of the excitations is unknown and the possibility that any of them could be chain-type resonances remains to be explored. A chain-type resonance occurs when a resonator is inside another resonator, which may in turn be part of a still larger resonator. Chain-resonance results when resonant frequencies of the innermost resonator are also resonant frequencies of the outer resonators.

The subject of resonant oscillations or seiches in fully enclosed basins has been fairly thoroughly treated in the literature of hydrodynamics of which mention should be made of the important contributions of Chrystal (1904), Lamb (1932) and Defant (1960). A recent review of the subject has been compiled by Wilson (1965) from whose article Table III is conveniently reproduced. This table gives the first four modes of oscillation in the sequence of modes in which the various shapes of basins can oscillate.

It turns out that natural bodies of water that are long and narrow enough to qualify for two-dimensional treatment of theory often show oscillating characteristics that conform quite closely to the quartic profile, shown in the fourth row of Table III. The quartic profile is a reasonable mathematical approximation to the configuration of some lake beds, particularly that of Lake Garda, Italy. Evidence of this is shown in Table IV (Wilson, 1965) which compiles observed ratios of oscillating periods for typical lakes and seas around the world.

Merian's generalized formula (first row, Table III), is always a very useful first approximation to the periods of two-dimensional oscillation

TABLE III

MODES OF FREE OSCILLATION
IN BASINS OF SIMPLE GEOMETRICAL SHAPE (CONSTANT WIDTH)

BASIN TYPE		PROFILE EQUATION	PERIODS OF FREE OSCILLATION					
Description	Dimensions		Fundamental T_1*		Mode Ratios T_n/T_1			
					n = 1	2	3	4
Rectangular	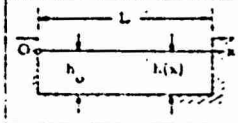	$h(x) = h_o$	$\frac{2L}{\sqrt{gh_o}}$		1.000	0.500	0.333	0.250
Triangular (Isoceles)	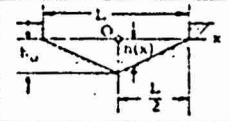	$h(x) = h_o\left(1 - \frac{2x}{L}\right)$	$1.305\ \frac{2L}{\sqrt{gh_o}}$		1.000	0.626	0.436	0.343
Parabolic	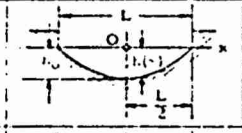	$h(x) = h_o\left(1 - \frac{4x^2}{L^2}\right)$	$1.110\ \frac{2L}{\sqrt{gh_o}}$		1.000	0.577	0.406	0.316
Quartic	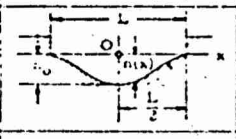	$h(x) = h_o\left(1 - \frac{4x^2}{L^2}\right)^2$	$1.242\ \frac{2L}{\sqrt{gh_o}}$		1.000	0.666	0.500	0.386
Triangular (Right-angled)	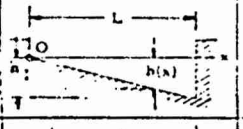	$h(x) = \frac{h_1 x}{L}$	$1.640\ \frac{2L}{\sqrt{gh_1}}$		1.000	0.546	0.377	0.288
Trapezoidal	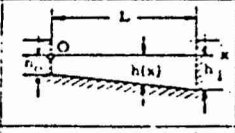	$h(x) = h_o + mx$ $m = \frac{(h_1 - h_o)}{L}$			1.000	0.546	0.377	0.288
Coupled, Rectangular	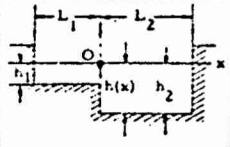	$h(x) = h_1\ (x < o)$ $h(x) = h_2\ (x > o)$ $\left(\frac{h_1}{h_2} = \frac{1}{4}\right)$	$\frac{L_1}{L_2} = \frac{1}{2}$	$\frac{4L_2}{\sqrt{gh_2}}$	1.000	0.500	0.250	0.125
			$\frac{L_1}{L_2} = \frac{1}{3}$	$\frac{3.13L_2}{\sqrt{gh_2}}$	1.000	0.559	0.344	0.217
			$\frac{L_1}{L_2} = \frac{1}{4}$	$\frac{2.73L_2}{\sqrt{gh_2}}$	1.000	0.579	0.367	0.252
			$\frac{L_1}{L_2} = \frac{1}{8}$	$\frac{2.31L_2}{\sqrt{gh_2}}$	1.000	0.525	0.371	0.279

* Formulae have not been given when too involved to state simply

TABLE IV

SEICHES IN TYPICAL LAKES; OBSERVED MODES OF OSCILLATION

NAME OF LAKE	COUNTRY	OBSERVED PERIODS OF OSCILLATION					
		Fundamental T_1 (mins)	Mode Ratios T_n/T_1				
			n = 2	3	4	5	6
Geneva	Switzerland	74.0	0.480				
Constance	German-Swiss Border	55.8	0.700	0.503			
Garda	Italy	42.9	0.666	0.507	0.348	0.281	0.230
Loch Earn	Scotland	14.5	0.557	0.414	0.275	0.244	0.198
Loch Treig	Scotland	9.2	0.560				
Loch Neagh	Ireland	96.0	0.718	0.468			
Ontario	U.S.A.	289.0					
Erie	U.S.A.	858.0	0.632	0.409	0.292	(0.262)	
Michigan-Huron	U.S.A.	2700.0					
Michigan	U.S.A.	543.0	0.535				
Superior	U.S.A.	480.0					
Tanganyika	Africa	4.5	0.511	0.378			
Chiemsee	S. Bavaria, Germany	41.0					
Vättern	Sweden	179.0	0.542				
Königsee	Germany	10.6					
Yamanaka	Japan	15.6	0.677	0.350			
Chiuzenji	Japan	7.7					
Baikal	U.S.S.R.	278.2					
Sea of Aral	U.S.S.R.	1368.0					
Sea of Azov	U.S.S.R.	1470.0	0.603	0.522			
George	Australia	131.0					
Baltic Sea - Gulf of Fin.		1636.0					

when a mean depth h is prescribed. The formula gives the period T_n of any n^{th} mode in terms of h and the mean basin length L, namely

$$T_n = \frac{2L}{n\sqrt{gh}} \qquad (2)$$

2. Oscillations in Three-Dimensional Basins of Various Geometrical Shapes

When the three-dimensionality of a basin must be taken into account, the results of Table III lose some of their applicability. The observed periods of oscillation of real bodies of water are of course a function of their plan form as well as their depth peculiarities.

For a limited number of cases where the three-dimensional nature of the basin shape conforms to a simple geometrical form, readily descriptive mathematically, the regime of oscillations can be exactly derived from hydrodynamical theory.

Since our interest is in open-mouth basins which qualify as bays, we shall confine attention to simple geometrical shapes of such semi-enclosed basins. Typical examples are illustrated in Table V (Wilson, 1965) and the results drawn from the publications of Lamb (1932) and Goldsbrough (1930).

Of special interest to this study are the cases of semi-elliptic and semi-circular basins of semi-paraboloidal bottom shape, because of the obvious similarity that Monterey Bay has to the semi-elliptic or part-circular plan-form. These are represented in the last two rows of Table V.

Gulfs, bays and inlets along the coastlines of the world oscillate with characteristic periods peculiar to their shape and bottom topography. Table VI (Wilson, 1965) records the observed periods of oscillation of typical bays and harbors around the world. These will tend to agree with the mathematical formulations of Table V, if the bay's shape is a reasonable approximation to one of the simple geometrical forms. Table Bay,

TABLE V

MODES OF FREE OSCILLATION
IN SEMI-ENCLOSED BASINS OF SIMPLE GEOMETRICAL SHAPE
[BASED ON LAMB, (1932) & GOLDSBROUGH, (1930)]

BASIN TYPE		PROFILE EQUATION	PERIODS OF FREE OSCILLATION				
Plan Form	Depth Profile		Fundamental T_1	Mode Ratios T_n/T_1 $\left(n = \frac{a+1}{2}\right)$			
				n = 1	2	3	4
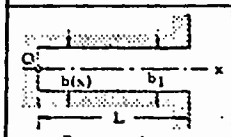 Rectangular	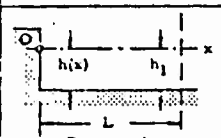 Rectangular	$h(x) = h_1$	$2.000 \frac{2L}{\sqrt{gh_1}}$	1.000	0.333	0.200	0.143
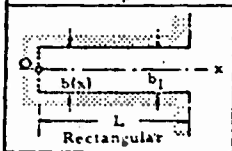 Rectangular	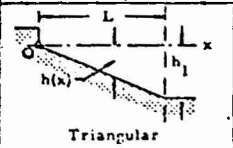 Triangular	$h(x) = \frac{h_1 x}{L}$	$2.618 \frac{2L}{\sqrt{gh_1}}$	1.000	0.435	0.278	0.203
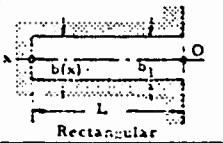 Rectangular	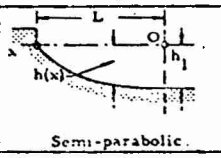 Semi-parabolic	$h(x) = h_1\left(1 - \frac{x^2}{L^2}\right)$	$2.220 \frac{2L}{\sqrt{gh_1}}$	1.000	0.409	0.259	0.189
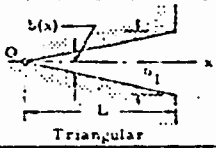 Triangular	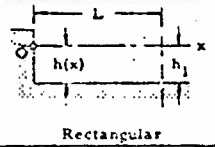 Rectangular	$b(x) = \frac{b_1 x}{L}$ $h(x) = h_1$	$1.309 \frac{2L}{\sqrt{gh_1}}$	1.000	0.435	0.278	0.203
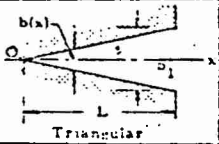 Triangular	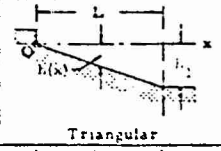 Triangular	$b(x) = \frac{b_1 x}{L}$ $h(x) = \frac{h_1 x}{L}$	$1.655 \frac{2L}{\sqrt{gh_1}}$	1.000	0.541	0.374	0.283
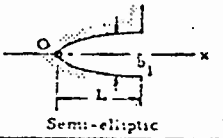 Semi-elliptic	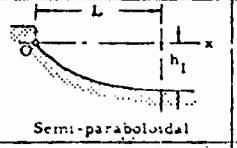 Semi-paraboloidal	$b_1/L = 2$ $b_1/L = 4/3$ $b_1/L = 1$ $b_1/L = 2/3$	$2.220 \frac{2L}{\sqrt{gh_1}}$	1.000	0.707 0.554 0.447 0.317	0.578 0.493 0.408 0.455	0.376 0.323 0.264 0.185
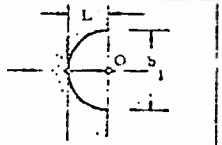 Semi-circular	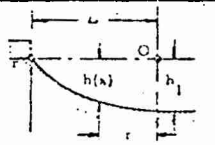 Semi-paraboloidal	$h(x) = h_1\left(1 - \frac{r^2}{L^2}\right)$	$2.220 \frac{2L}{\sqrt{gh_1}}$	1.000	0.707	0.578	0.500

TABLE VI

COASTAL SEICHES IN TYPICAL GULFS, BAYS & HARBORS
OBSERVED MODES OF OSCILLATION

NAME OF GULF, BAY OR HARBOR	COUNTRY	OBSERVED PERIODS OF OSCILLATION (approximate) (mins)					
St. Johns Harbor	Bay of Fundy, Canada	74	42				
Narragansett Bay	Rhode Is., USA	44	46				
Vermillion Bay	La., USA	180	120				
Galveston Bay	Texas, USA	75					
San Pedro Bay	Los Angeles, Calif., USA	55-60	27-30	15	9-11	2-5	
San Francisco Bay	Calif., USA	116	47	34-41	24-27	17-19	
Monterey Bay	Calif., USA	60-66	36-38	28-32	22-24	16-20	10-15
Hilo Bay	Hawaii, USA	20-25	10	7			
Guanica	Puerto Rico Caribbean	45					
Lerwick	Scotland	28-30					
Port of Leixoes	near Porto, Portugal	20-25	13-15	3-5			
Bay of Naples	Italy	48	17-18				
G.of Venice-G.of Trieste	N. Adriatic Sea	210-240	60	40	10	5	
Euripus, (G. of Talanta)	Greece, betw. Is. Euboe & mainland	105	60				
Algiers	Algeria, N. Africa	20-26					
Casablanca	Morocco, N. Africa	35-40	18-20				
Table Bay, Capetown	South Africa	58-62	38-43	25-30	18-21	14-17	10-11
Algoa Bay, Port Elizabeth	South Africa	69-75	57	42-52	35	20-25	16-17
Tamatave	Madagascar	15	8-10	1-2			
Tuticorin, G. of Mannar	India-Ceylon	180					
Bay of Hakodate	Hokkaido, Japan	45-57	21-24				
Bay of Aomori	Honshu, Japan	295	103	23-26			
Bay of Ofunato	Honshu, Japan	41-44	36-39	12-17	5-6		
Bay of Nagasaki	Kyushu, Japan	69-72	54	44-45	40	32-38	22-25
Wellington	New Zealand	28	?	?			
Lyttleton	New Zealand	156	?	?			

Cape Town, is found to be such a case (Wilson, 1953 b), and many others can be closely approximated by the mathematical forms. We shall now examine what information can be gained from fitting Monterey Bay to mathematical forms for which the solutions are known.

3. Circular Basin Analogy Applied to Monterey Bay

Fig. 27 is a working drawing showing Monterey Bay fitted into a circular basin as a full quadrant subtending an angle of 90°. The sea-bed of the bay, of course, is riven by the deep Monterey Canyon, but this is perhaps narrow enough to permit the assumption that its effect on the regime of oscillations throughout much of the bay will be quite small. Profiles of the sea-bed at various sections are shown which suggest that if the imaginary circular basin had a conical bottom, the fit could be relatively good. However we wish to make use of the known results for a circular basin of uniform depth and those also for a circular basin of paraboloidal bottom (Lamb, 1932 Ed.). If the bed be assumed of uniform depth h_1, in the first instance, it appears that a reasonable value for mean depth (ignoring the deep canyon) is about 240 feet. (If the bed be taken with a paraboloidal bottom, the central depth h_o that would yield the same volume of contained water would be 480 feet.)

We revert to Lamb's results (1932 Ed., Art. 191, p. 285) which show that a circular basin of uniform depth can perform free oscillations in symmetrical modes in which the nodes are all circles, and in unsymmetrical modes in which the nodes are combinations of diameters and circles. In the gravest mode of the symmetrical class the nodal circle has a radius $r = 0.628\,R$, where R is the radius of the basin. The period corresponding to this mode is given by the relationship

$$T = \frac{2\pi R}{3.832\sqrt{gh}} \qquad (3)$$

For the applicable values $R = 10^5$ ft., $h = 240$ ft., $g = 32.2$ ft/sec.^{2} we find $T = 31.1$ mins. The nature of this oscillation as it may be assumed

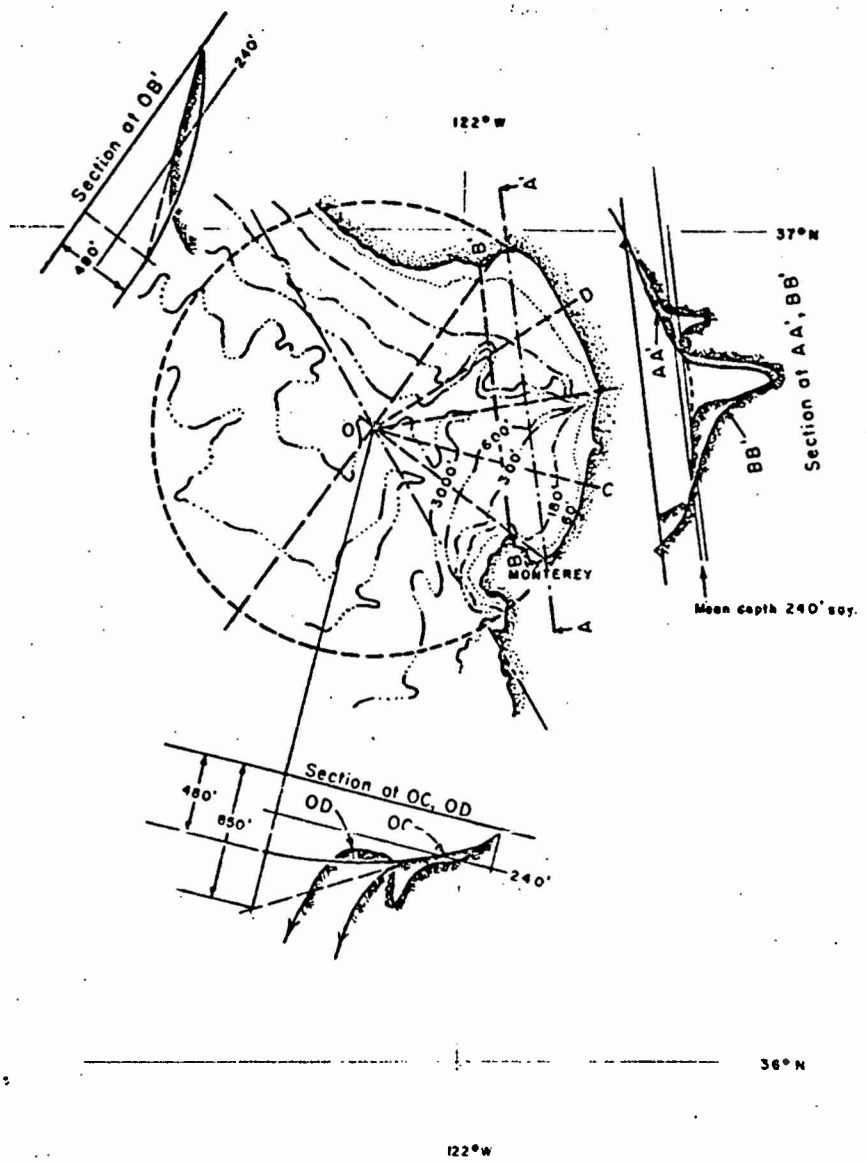

FIGURE 27 GEOMETRICAL ANALOGY OF MONTEREY BAY TO THE QUADRANT OF A CIRCULAR BASIN

to affect Monterey Bay is shown in Fig. 28 a . It appears that the position of the node is reasonably close to the edge of the continental shelf (h = 600 ft. contour) to give this mode some realism as a fundamental circular-shelf oscillation.

In general we may designate the mode of oscillation as of (m, n) type where m represents the number of nodal diameters and n the number of nodal circles. Eq. (3) thus gives the period $T_{m,n}$ for $m = 0$, $n = 1$. The succession of modes of oscillation of symmetrical ($m = 0$) types is shown in Figs. 28 a to 28 c . As to whether any of these modes has a chance of occuring in any of the forms shown is really dependent on whether the oscillating system accommodates itself with the topographical features of the bay. Already remarked is the fact that in Fig. 28 a the node is in rough agreement with the shelf edge. In Fig. 28 c , this fit is even better and the oscillation of period $T_{o,3} = 11.7$ mins. can be described as the second-mode circular-shelf oscillation. (This neglects the node closest to the center of the imaginary circular basin). In Fig. 28 b the oscillation of period $T_{o,2} = 17.0$ mins. corresponds to a fundamental bay oscillation in which the node at the mouth is a circle concentric with the shoreline joining the point of Monterey Peninsula and Santa Cruz. This is also a realistic free oscillation.

In the unsymmetrical class ($m \neq 0$) the free oscillations involve nodal diameters and nodal circles. A sequence of possible modes which fit the topography of Monterey Bay are shown in Figs. 28 d to 28 k. In general the oscillations have been indicated by sets of contour lines to designate simultaneous elevations above still water (full lines) and depressions below normal level (dash lines). These contours are made to fade out outside the immediate topographical area where they are likely to be sustained.

The lowest mode of the unsymmetrical class has a period $T_{1,o} = 64.7$ mins. and is shown in Fig. 28 d. This corresponds to a shelf oscillation. The shelf edge in this case is the more distant one, which is seen to correspond (canyon excepted) quite well with the nodal diameter.

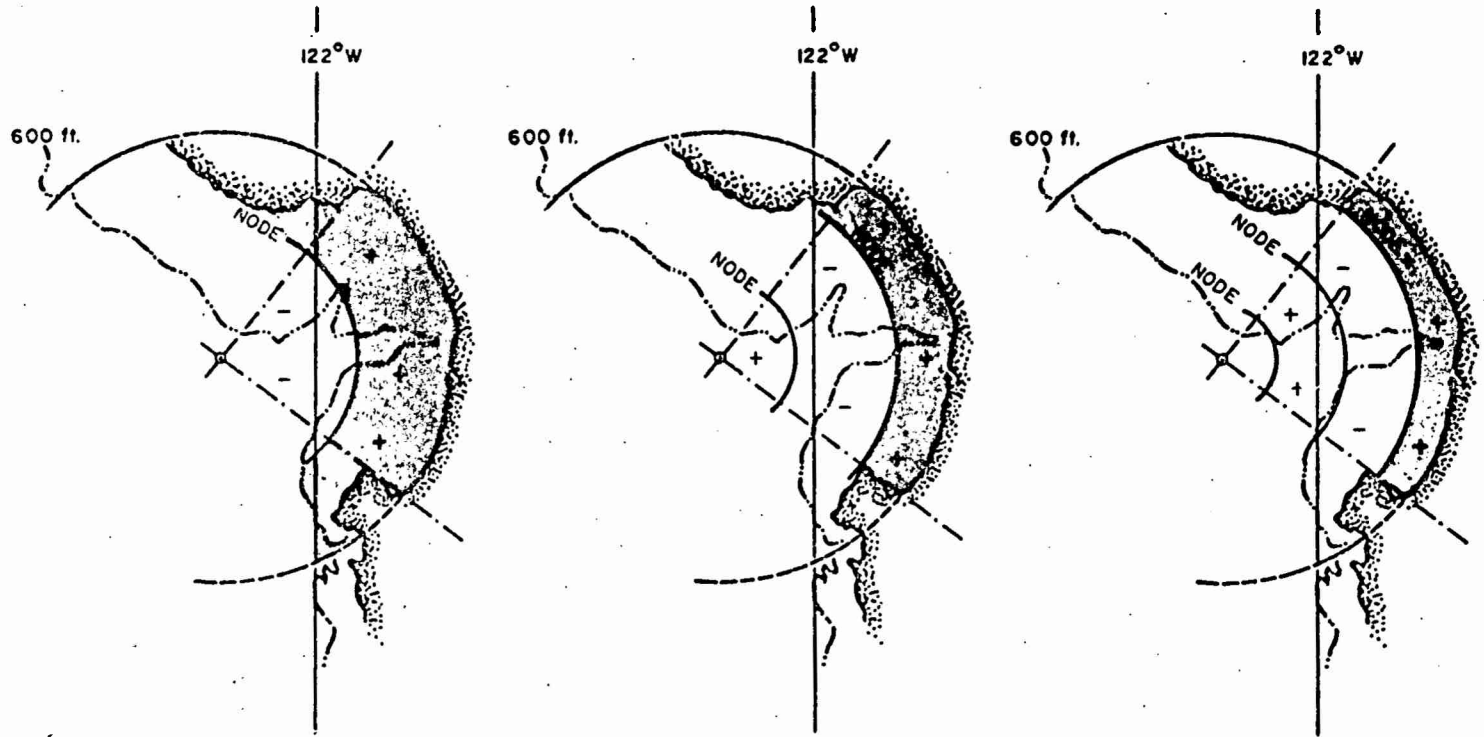

(a) Symmetrical Mode (0, 1)
$T_{0,1}$ = 31.1 mins.
(r/R = 0.628)

(b) Symmetrical Mode (0, 2)
$T_{0,2}$ = 17.0 mins.
(r/R = 0.343, 0.787)

(c) Symmetrical Mode (0, 3)
$T_{0,3}$ = 11.7 mins
(r/R = 0.236, 0.542, 0.850)

FIGURE 28 POSSIBLE MODES OF OSCILLATION FOR MONTEREY BAY ACCORDING TO CIRCULAR BASIN ANALOGY (ANALYTIC CALCULATIONS)

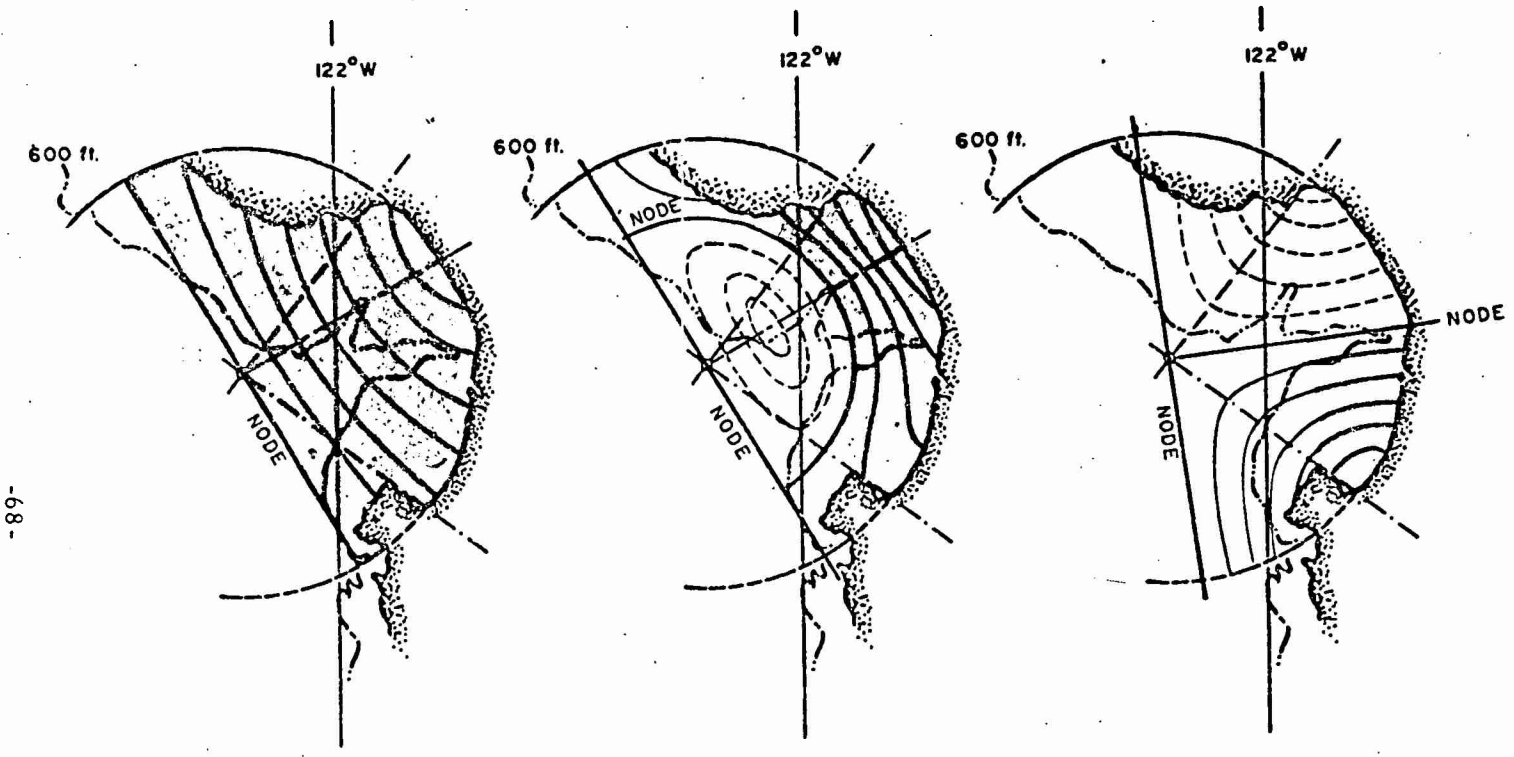

(d) Unsymmetrical Mode (1, 0)
$T_{1,0}$ = 64.7 mins.

(e) Unsymmetrical Mode (1, 1)
$T_{1,1}$ = 22.3 mins.
(r/R = 0.66)

(f) Unsymmetrical Mode (2, 0)
$T_{2,0}$ = 38.4 mins.

FIGURE 28 (cont.) POSSIBLE MODES OF OSCILLATION FOR MONTEREY BAY ACCORDING TO CIRCULAR BASIN ANALOGY (ANALYTIC CALCULATIONS)

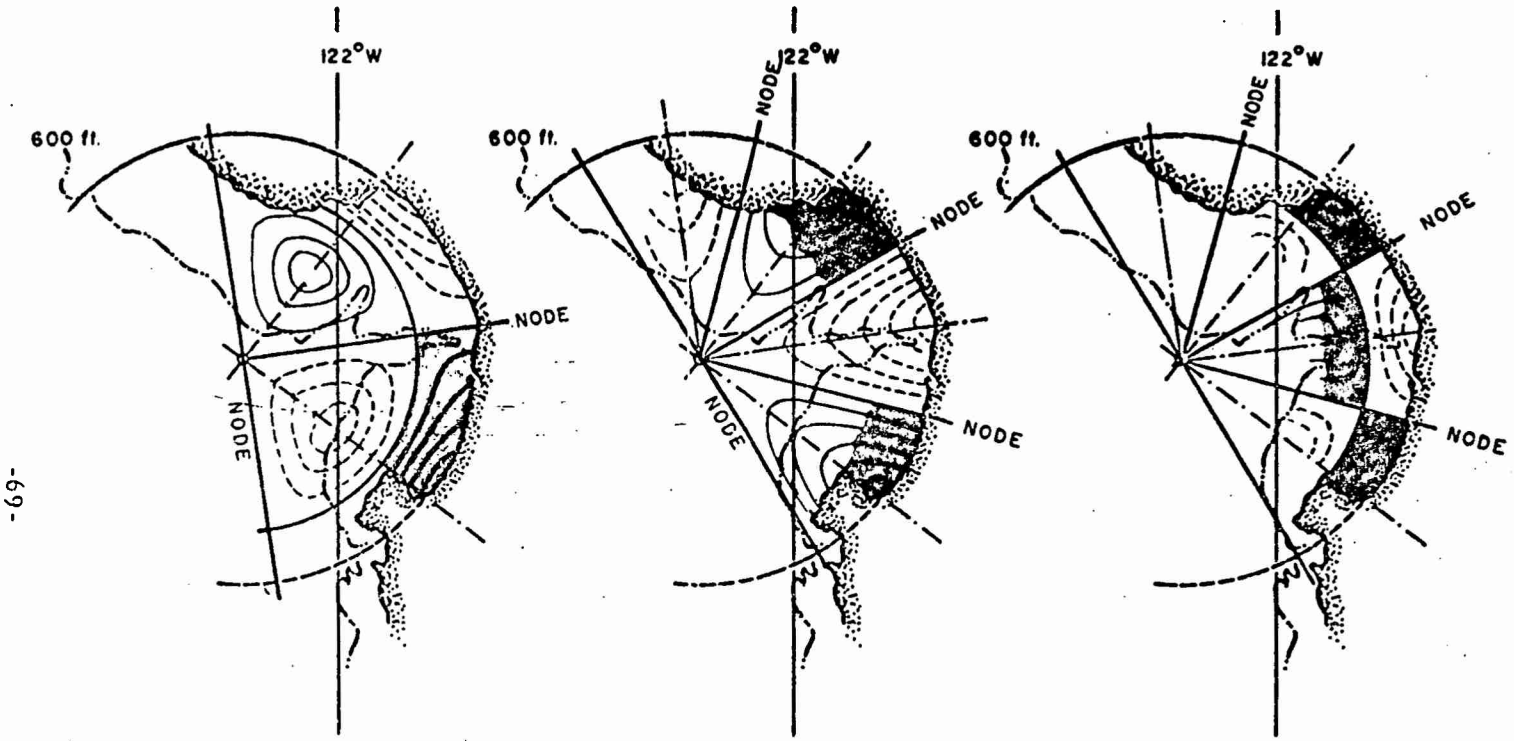

(g) Unsymmetrical Mode (2, 1)
$T_{2,1}$ = 17.8 mins.
(r/R = 0.78)

(h) Unsymmetrical Mode (4, 0)
$T_{4,0}$ = 22.5 mins

(i) Unsymmetrical Mode (4, 1)
$T_{4,1}$ = 12.8 mins.
(r/R = 0.83)

FIGURE 28 (cont.) POSSIBLE MODES OF OSCILLATION FOR MONTEREY BAY ACCORDING TO CIRCULAR BASIN ANALOGY (ANALYTIC CALCULATIONS)

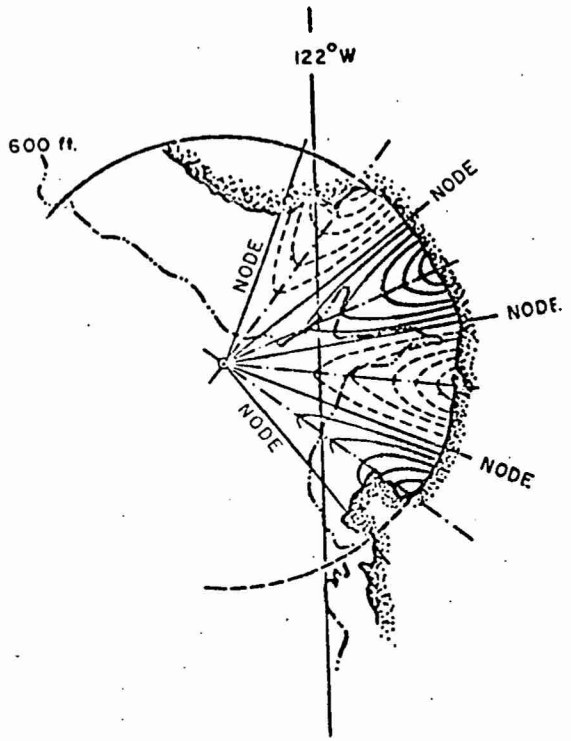

(j) Unsymmetrical Mode (6, 0)
$T_{6,0}$ = 15.9 mins.

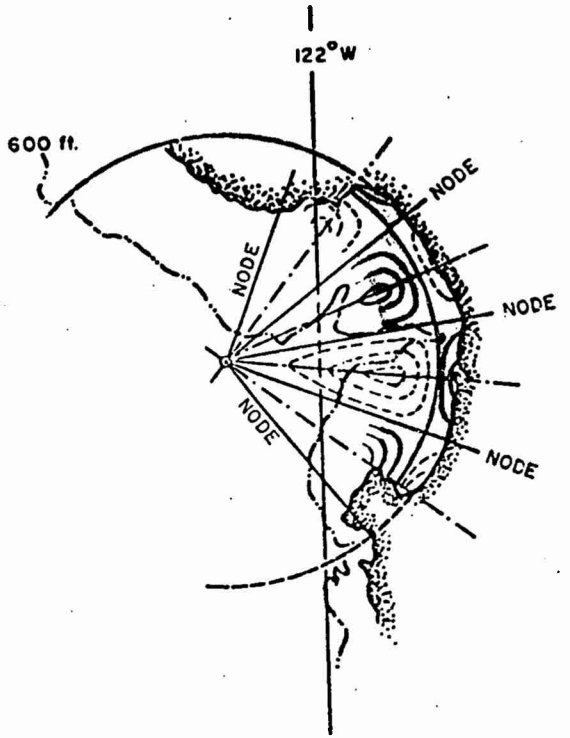

(k) Unsymmetrical Mode (6, 1)
$T_{6,1}$ = 10.1 mins.
(r/R = 0.93)

FIGURE 28 (cont) POSSIBLE MODES OF OSCILLATION FOR MONTEREY BAY ACCORDING TO CIRCULAR BASIN ANALOGY (ANALYTIC CALCULATION)

The next mode Fig. 28 e with $T_{1,1}$ = 22.3 mins. is determined by the agreement of the nodal diameter with the outer shelf edge. The node circle complements that of Fig. 3 a but the oscillation, unlike that of Fig. 28 d, is strongest in the northern part of the bay and weakest in the south.

In Figs. 28 f, g and h we have a succession of modes of oscillation which effectively are the uninodal, binodal and trinodal seiches for the bay in the longitudinal north-south direction. The periods found are respectively $T_{2,0}$ = 38.4 , $T_{4,0}$ = 22.5 and $T_{6,0}$ = 15.9 mins. Each of these modes is realizable and could be expected to be quite strongly in evidence in tide-gauge and other records for the bay.

In Figs. 28 i , j and k we have examples of two-dimensional (combined longitudinal and transverse) oscillations for the bay in which the transverse (EW) effect is uninodal and the longitudinal (NS) effect is respectively uninodal, binodal and trinodal. The periods for these combined oscillations are $T_{2,1}$ = 17.8 , $T_{4,1}$ = 12.8 and $T_{6,1}$ = 10.1 mins.

In summary the following Table VII gives the various periods $T_{m,n}$ for Monterey Bay as the quadrant of both a circular basin of uniform depth and a circular basin of paraboloidal bottom. It would seem that there is reasonable expectation that the periods listed in columns 3 and 4 of Table VII will represent approximate limits to the range of values of natural periods of Monterey Bay for the different oscillating modes. The listing of periods, of course, is incomplete. Higher-mode (shorter-period) oscillations exist, but it has not been considered worthwhile to pursue the circular basin analogy too far because of the increasing importance of local effects upon the oscillating behavior of parts of the bay. These effects are more satisfactorily analyzed by the wave-refraction technique, still to be discussed.

TABLE VII

PRINCIPAL OSCILLATIONS FOR MONTEREY BAY
CIRCULAR BASIN ANALOGY

TYPE OF OSCILLATION		PERIOD OF OSCILLATION $T_{m,n}$ (mins.)		Remarks on Oscillation Type
No. of Nodal Diameters m	No. of Nodal Circles n	Uniform Bed h_1 = 240'	Paraboloidal Bed h_o = 480'	
0	1	31.1	29.8	circular shelf
0	2	17.0	17.2	circular node at bay mouth
0	3	11.7	12.2	second mode, circular shelf
1	0	64.7	59.6	outer shelf
1	1	22.3	22.5	second mode, outer shelf
2	0	38.4	42.1	uninodal NS
2	1	17.8	18.8	uninodal NS, EW
4	0	22.5	29.8	binodal NS
4	1	12.8	14.9	binodal NS uninodal EW
6	0	15.9	24.3	trinodal NS
6	1	10.1	12.7	trinodal NS uninodal EW

III B. ANALYSIS OF OSCILLATING CHARACTERISTICS OF MONTEREY BAY: SEMI-EXACT NUMERICAL SOLUTIONS OF MODES OF TWO-DIMENSIONAL OSCILLATION

1. Defant's Method of Numerical Solution of Hydrodynamical Equations

The problem of the oscillating characteristics of an open-mouth bay of irregular shape and bottom topography can be approached by integrating the hydrodynamical equations by finite difference procedures using a number of different possible techniques such as those of Chrystal (1904), Defant (1925, 1963), Hidaka (1936), Ertel (1933), Caloi (1954), Stoker (1957), Raichlen (1964) and others. Defant's method (or adaptations of it) is perhaps that most widely used and depends upon the representation of the equations of motion and continuity in the form respectively

$$\frac{\delta^2 \xi(x,t)}{\delta t^2} = -g \frac{\delta \eta(x,t)}{\delta x} \tag{4}$$

$$\eta(x,t) = \frac{-1}{b(x)} \frac{\delta}{\delta x} \left[S(x)\, \xi(x,t) \right] \tag{5}$$

where η and ξ are respectively the vertical and horizontal displacements of a water particle at any distance x along the valley route ("talweg") of the bay from an origin taken in the still water surface at the mouth (or the closed end) of the bay. The quantities $b(x)$ and $S(x)$ are respectively the width of the bay and the cross sectional area of the water body at right angles to the valley route at any distance x and are both functions of x.

By assuming solutions to ξ and η of the form

$$\text{(i)} \quad \xi = \xi(x) \cos(\sigma t - \epsilon)$$

$$\text{(ii)} \quad \eta = \eta(x) \cos(\sigma t - \epsilon) \tag{6}$$

Eqs. (4) and (5) can be expressed in the form

$$\text{(i)} \qquad \xi(x) = \frac{1}{S(x)} \int_o^x \eta(x)\, b(x)\, dx$$

$$\text{(ii)} \qquad 4\eta(x) = \frac{\sigma^2}{g} \xi(x)\, \Delta x \tag{7}$$

where σ is the angular frequency of any particular mode of oscillation.

In finite difference form Eqs. (7) become

$$\xi_n = \frac{-1}{S_n} \left[q_{n-1} + a_n \frac{\eta_n + \eta_{n-1}}{2} \right]$$

$$\eta_n = \eta_{n-1} + \frac{\delta\sigma^2}{g} \frac{\xi_n + \xi_{n-1}}{2} \tag{8}$$

where n is an integer 0, 1, 2, 3.... representing stations along the valley route at an increment of distance δ apart, and $a_n(x)$ is the surface area between orthogonals to the valley route at any two stations n and $(n-1)$. These equations are now readily solved to give

$$\text{(i)} \qquad \xi_n = - \frac{1}{S_n(1 + \frac{2\beta}{S_n})} \left[q_{n-1} + a_n(\eta_{n-1} + \beta\xi_{n-1}) \right]$$

$$\text{(ii)} \qquad q_n = q_{n-1} + a_n \left(\frac{\eta_n + \eta_{n-1}}{2}\right) \tag{9}$$

$$\text{(iii)} \qquad \beta = \frac{\delta\sigma^2}{4g}$$

The procedure is now an iterative one which depends on knowing certain starting values for $n = 0$. Thus we require to know ξ_o, η_o,

q_o and β . In Defant's approach σ is assumed in the first instance by the application of Merian's formula for an open-mouth rectangular basin, namely

$$T = \frac{2\pi}{\sigma} = \frac{4L}{\sqrt{gh}} \tag{10}$$

where L is the overall distance along the valley route and h is the mean depth for the entire basin. By starting the iteration at the head of the bay where the usual assumption made is that

$$\begin{aligned} &\text{(i)} && \xi_o = 0 \\ &\text{(ii)} && q_o = 0 \\ &\text{(iii)} && \eta_o = 100 \text{ cms} \end{aligned} \tag{11}$$

application of the recursion formulas (8) and (9) will permit evaluation of q_n , ξ_n , η_n when $n = N$ at the mouth of the bay, the expected node position. Here we require $\eta_n = 0$. If this is not satisfied, the technique requires selection of a new value of σ in (9 iii) and further iterations until the requirement is met.

In a more sophisticated adaptation of this method which closely follows the procedure developed by Raichlen (1964) and has been further refined by Hendrickson (Appendix A) a series of N equations is derived for each n^{th} station of the total N stations along the valley route, of the general form:

$$a_{n,n+1}\ \eta_{n+1} + a_{n,n}\ \eta_n + a_{n,n-1}\ \eta_{n-1} = \beta_k\ \eta_n \tag{12}$$

where the a's are coefficients and β_k is defined by Eq. (9 iii) for any k where $k = 1, 2, \ldots . N$. The quantity β_k is termed an 'eigenvalue' of the solution and for the N-equations there exist N-values of β which satisfy the equations. From Eq. (9 iii) the k^{th} eigenvalue yields the k^{th}

eigen-period or modal period at which the system can oscillate, namely

$$T_k = \frac{2\pi}{\sigma} = \sqrt{\frac{\beta_k \delta}{g}} \qquad (13)$$

The N-equations of the type of Eq. (12) form an N x N matrix whose solution yields the desired eigenvalues and modal periods. The calculation of the matrix solution is readily programmed for high-speed computation.

The essential difference between Raichlen's (1964) method and that developed here concerns the terminal boundary condition adopted at the head of the bay. Raichlen's terminal condition is based on the assumption that the slope of the water surface at the head of the bay $\left(\frac{\delta \eta}{\delta x}\right)_L$ is zero. This is an approximation which tends to lose validity with the higher modes of oscillation. In our studies (cf. Appendix A) the assumption is avoided by merely asserting the true condition that the flow normal to the boundary of the bay (that is, the sea-bed or beach-slope) is zero.

In applying Eqs. (12) and (13) to Monterey Bay it was necessary to assume a suitable location for the node at the mouth (which governs all the analytic solutions given in Table V for bays of any shape). The node was assumed, 'a priori', to connect Pinos Point on the Monterey Peninsula with the spur of land just west of Santa Cruz.

The 'talweg' or valley-route was taken approximately along the axis of the submerged Monterey canyon and the x-distance along this route from the node to Moss Landing was conveniently divided into 18 equi-distant intervals of amount δ, thus making $N = 18$. The coefficients a of Eq. (12) are functions of $b(x)$ and $S(x)$ at each n^{th} point or cross-section along the talweg and must, of course, be predetermined from measurements taken off topographical maps of the bay.

2. Checking of the Program for Computer Solution of the Matrix Equations

By way of checking the computer program written for solving matrix equations of two-dimensional open-mouth bay oscillations, check calculations were performed on four geometrical analogies by which Monterey Bay can be roughly approximated and for which exact mathematical solutions are available. These analogies liken Monterey Bay to configurations specified in Table V, namely

(i) A triangular bay with uniformly sloping bed
($L = 67,500$ ft., $b_1 = 150,000$ ft., $h_1 = 560$ ft.)

(ii) A triangular bay with horizontal bed
($L = 67,500$ ft., $b_1 = 150,000$ ft., $h_1 = 560$ ft.)

(iii) A rectangular bay with uniformly sloping bed
($L = 45,000$ ft., $b_1 = 125,000$ ft., $h_1 = 560$ ft.)

(iv) A rectangular bay with semi-parabolic bed
($L = 45,000$ ft., $b_1 = 125,000$ ft., $h_1 = 560$ ft.)

The analogies are admittedly poor fits to the real shape of the bay. Nevertheless their solution by matrix methods should give orders of magnitude for the periods, approximating the results expected, and at the same time should meet the requirements of the known mathematical solutions available from Table V for the cases concerned. Thus besides checking the computer program, the results should yield the approximate oscillating characteristics of the bay.

For the numerical calculations of cases (i) to (iv), it was necessary to adopt a 'talweg' or axis of symmetry for each analogy and for the prescribed dimensions, compute the appropriate cross sectional areas and widths at each of $N(=18)$ stations along the valley route. The applicable values of the coefficients a were hereby determined for entry in the matrix equations.

Results of the check calculations, made for the above four cases after elaboration of the computer program, are shown in Table VIII.

TABLE VIII

EXACT AND NUMERICALLY DERIVED MODAL PERIODS FOR GEOMETRICAL ANALOGIES TO MONTEREY BAY

Basin Type	Method of Calculation	Fundamental Period (mins.)	Mode Ratios T_n/T_1			
			n = 1	2	3	4
(i)	Analytic	27.7	1.000	0.541	0.374	0.283
	Numerical	27.4	1.000	0.546	0.376	0.286
(ii)	Analytic	21.9	1.000	0.435	0.278	0.203
	Numerical	23.0	1.000	0.468	0.295	0.215
(iii)	Analytic	29.2	1.000	0.435	0.278	0.203
	Numerical	29.0	1.000	0.424	0.272	0.205
(iv)	Analytic	24.8	1.000	0.409	0.259	0.189
	Numerical	24.7	1.000	0.410	0.260	0.194

Within the limits of the 18-station division of the 'talweg' of the bay these results must be considered very good. They demonstrate that a reliable program has been developed, which can match results known to be correct from exact mathematical theory. The actual period values evolving in the third column are less important but show that the fundamental oscillation for the bay with a node at the mouth is expected to be of the order of 22 to 29 mins. (according to the crude analogies by which the bay has been modelled in cases (i) to (iv)).

3. Two-Dimensional Modes of Oscillation of Monterey Bay

Once the reliability of the computer program was demonstrated, as in the test-cases of the last section, it was possible to proceed to a more refined numerical solution of the real Monterey Bay.

The 18 x 18 matrix coefficients derived for the whole bay are recorded in Fig. 29. The inset shows the location of the assumed node and the 'talweg' together with the principal dimensions L and h_o, respectively the length along the talweg from node to bay-head and the mean depth of water at the nodal cross-section.

The results of the numerical computation for the first four modes of oscillation are illustrated in Fig. 30, and show the mode-shapes or profiles of the water surface in these (lowest) modes of oscillation.

The sequence of modal periods of oscillation, pursued to the eighth mode, evolve as follows:

$$T_n = 32.3,\ 14.3,\ 9.5,\ 7.0,\ 5.78,\ 5.14,\ 4.46,\ 4.08,\ \ldots\ldots\ldots\ldots\ldots\ \text{mins.} \qquad (14)$$

It is certainly unwise to exploit this series too far, even though the computer solution evolves 18 separate modes of oscillation. Beyond the first few modes the others become less meaningful and accurate in a bay that can support three-dimensional oscillations, because of the limitations of the matrix-order. Actually there has not been very strong evidence in the records for oscillations of periods other than the first. In Tables I and II of Part II (Sections 10, 11) 9.5 mins., 5.5 to 5.9, 4.9 to 5.3 min. oscillations appear to be significant at Monterey, but of these only the 9.5 min. period may be associated with the third-mode oscillation, transverse to the bay, as suggested by the series (14).

Raichlen's method for achieving results equivalent to sequence (14) was found to yield the series:

$$T_n = 32.5,\ 15.4,\ 12.0,\ 8.9,\ 6.7,\ \ldots\ \text{mins.} \qquad (15)$$

n

n	1	2	3	4	5	6	7	8	9	10	11	12	13	14	15	16	17	N = 18
1	1.5620	-0.7308																
2	-0.7188	1.3750	-0.6566															
3		-0.6083	1.1820	-0.5739														
4			-0.6016	1.1830	-0.5822													
5				-0.5898	1.1580	-0.5682												
6					-0.5687	1.1240	-0.5561											
7						-0.5842	1.1070	-0.5230										
8							-0.5012	0.5050	-0.4046									
9								-0.4164	0.7420	-0.3260								
10									-0.3240	0.5980	-0.2744							
11										-0.3025	0.5890	-0.2867						
12											-0.3294	0.5970	-0.2678					
13												-0.2820	0.4440	-0.1628				
14													-0.1464	0.2310	-0.0852			
15														-0.1743	0.3020	-0.1283		
16															-0.1634	0.2440	-0.0806	
17																-0.1790	0.1980	-0.0190
N = 18																0.0685	-0.2740	0.2055

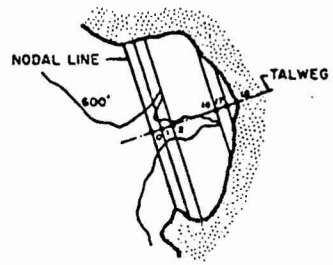

MONTEREY BAY
(COMPLETE)

L = 56,250 ft.
h_o = 567.663
N = 18

FIGURE 29 INPUT DATA FOR 18 x 18 MATRIX FOR TWO-DIMENSIONAL COMPUTER SOLUTION OF MODES OF OSCILLATION OF MONTEREY BAY

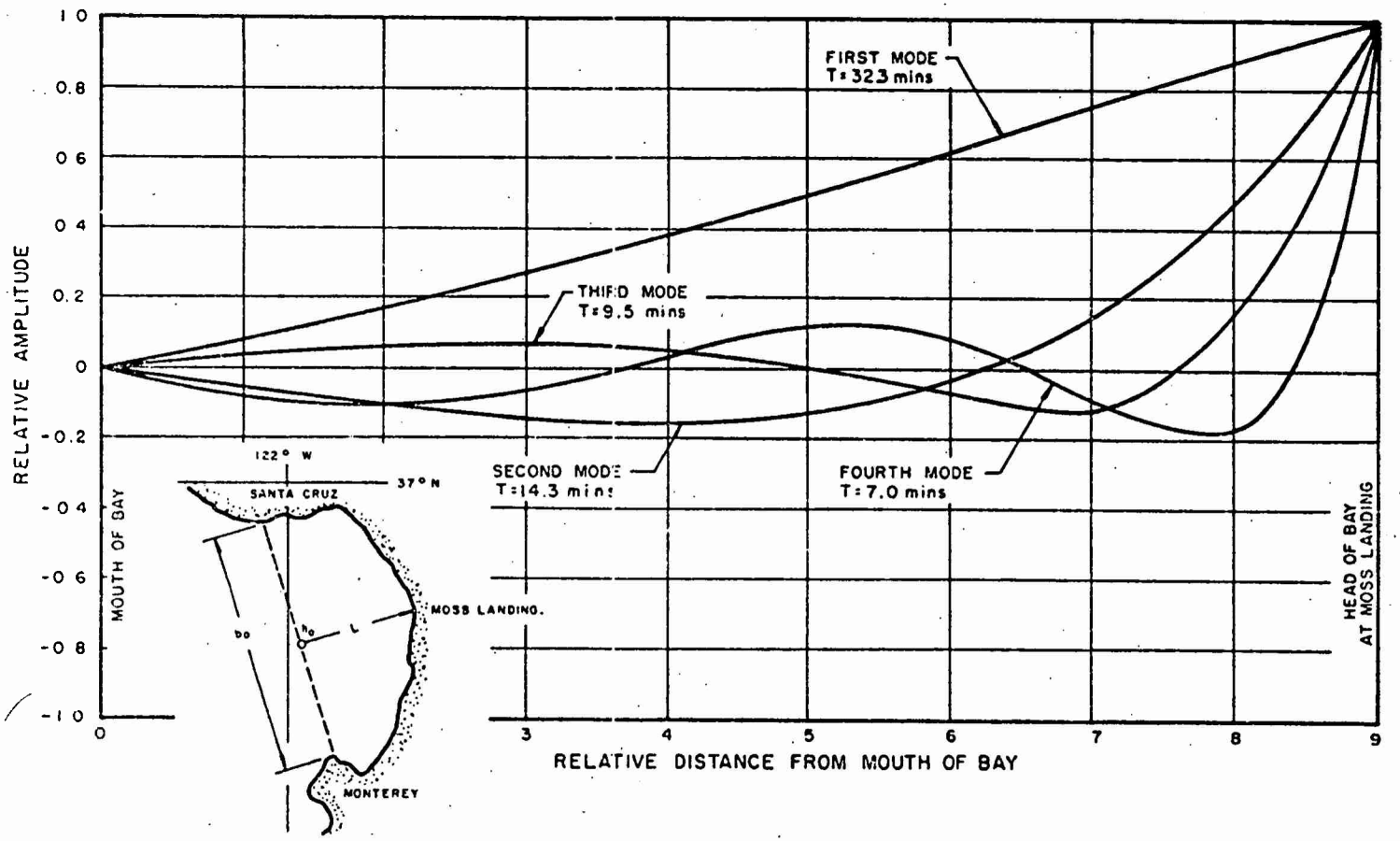

FIGURE 30 PROFILES OF WATER-SURFACE ELEVATION ALONG AXIS OF BAY FOR FOUR LOWEST MODES OF WHOLE OSCILLATION IN MONTEREY BAY (NUMERICAL CALCULATION)

though Raichlen himself, in applying it to Monterey Bay with data furnished to him by SEA, has come up with the sequence:

$$T_n = 32.7,\ 16.4,\ 10.3,\ 7.7,\ 6.1,\ \ldots\ldots \text{ mins.} \qquad (16)$$

Neither of these series (15) or (16) can be considered as accurate as (14) because of the defiency in the boundary assumption.

4. Two-Dimensional Modes of Oscillation of Southern Portion of Monterey Bay

It is probable that in the neighborhood of the harbor the portion of the bay between Point Pinos and Fort Ord behaves very much as a bay within a bay. To explore this possibility, a two-dimensional numerical 'talweg' solution was sought of the oscillating properties of this area on the assumption that a node could be inferred across the "mouth" of this inner bay.

The 16x16 matrix developed for this case is shown in Fig. 31 and the area of bay covered is illustrated in the inset. In this case the 'talweg' is a curved line following approximately the axis of greatest depth in this horn of the bay, and the nodal line has been selected to be normal to this axis and tangential to Pinos Point on the Monterey Peninsula.

The results that evolve are interesting. The various modal periods comprise the series:

$$T_n = 13.3,\ 6.8,\ 4.52,\ 3.56,\ 3.02,\ 2.58,\ 2.22,\ 1.94,\ 1.68,\ \ldots\ldots\ldots\ldots\ldots\ldots \text{mins.} \qquad (17)$$

Every one of these periods can be identified in the sea-energy spectra results tabulated in Table II and, to a fairly satisfactory extent also, in the Residuation Analyses of Table I. It would seem to be a valid conclusion that the southern portion of Monterey Bay does indeed oscillate in

n \	1	2	3	4	5	6	7	8	9	10	11	12	13	14	15	N = 16
1	2.0420	-0.9742														
2	-1.0242	1.9920	-0.9478													
3		-1.0227	1.9780	-0.9553												
4			-0.9880	1.9140	-0.9260											
5				-0.9330	1.7320	-0.7990										
6					-0.8520	1.5640	-0.7120									
7						-0.7711	1.4100	-0.6389								
8							-0.6891	1.2580	-0.5689							
9								-0.6892	1.2400	-0.5508						
10									-0.6391	1.1220	-0.4829					
11										-0.5479	0.9300	-0.3821				
12											-0.4736	0.7920	-0.3184			
13												-0.3764	0.5920	-0.2156		
14													-0.2650	0.3800	-0.1150	
15														-0.2307	0.2580	-0.0273
N = 16														0.0810	-0.3260	0.2440

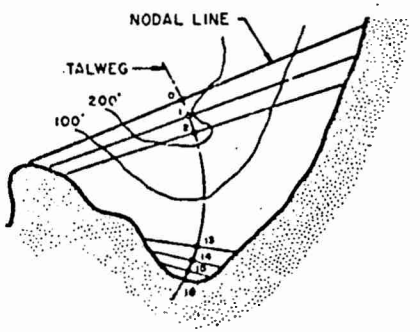

MONTEREY BAY
(PARTIAL)

L_x = 16,666 ft.

l_o = 133.443

N = 16

FIGURE 31 INPUT DATA FOR 16 x 16 MATRIX FOR TWO-DIMENSIONAL COMPUTER SOLUTION OF MODES OF OSCILLATION OF SOUTHERN EXTREMITY OF MONTEREY BAY

this manner and that the higher modes are prominent in the harbor area. The mode shapes corresponding to the first four periods T_n of the series (17) are shown in Fig. 32.

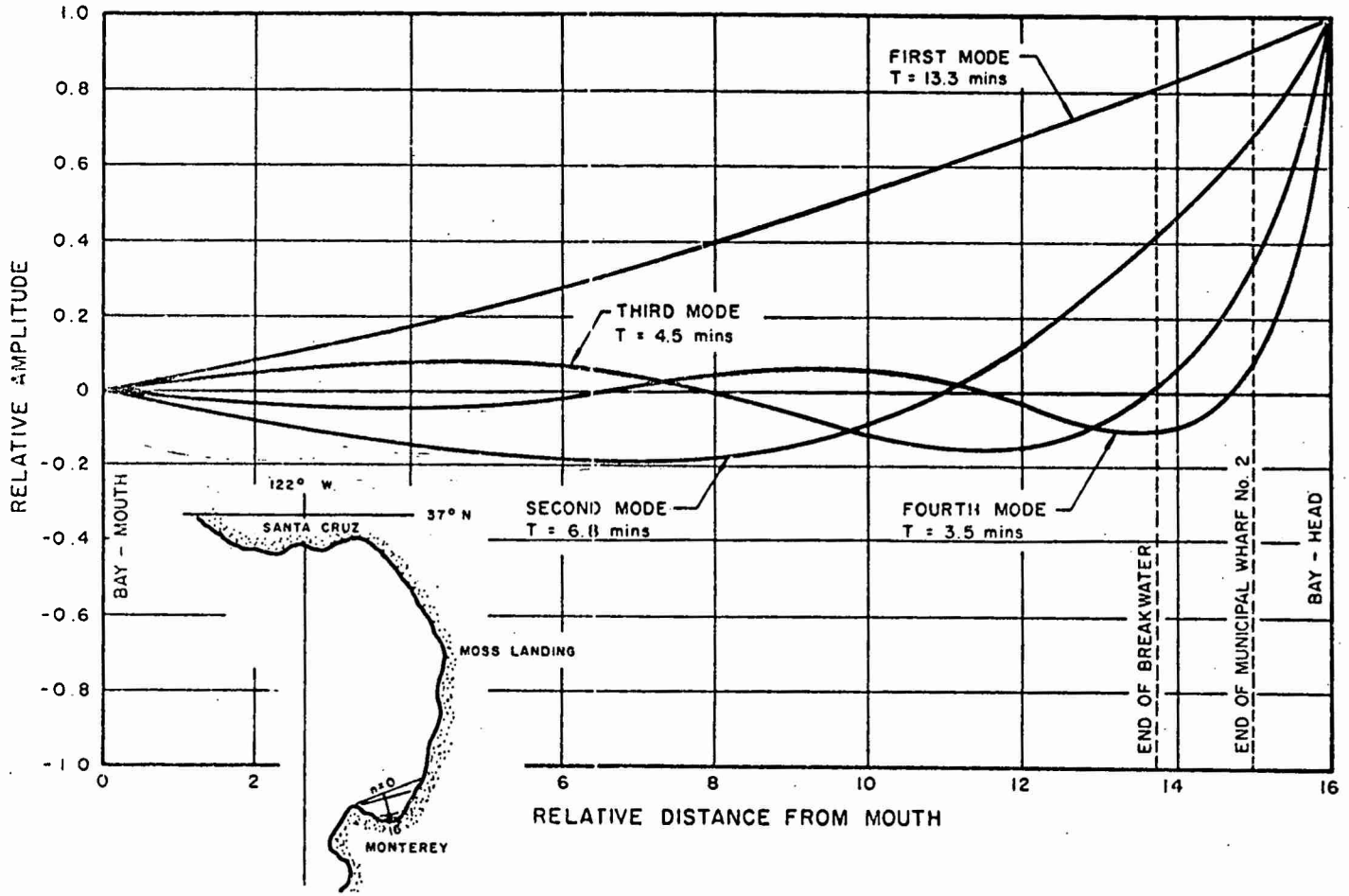

FIGURE 32 PROFILES OF WATER-SURFACE ELEVATION ALONG 'TALWEG' FOR FOUR LOWEST MODES OF OSCILLATION OF SOUTHERN PORTION OF MONTEREY BAY (NUMERICAL CALCULATION)

III C. ANALYSIS OF OSCILLATING CHARACTERISTICS OF MONTEREY BAY: SEMI-EXACT NUMERICAL SOLUTION OF MODES OF THREE-DIMENSIONAL OSCILLATION

1. Stoker's Method for Numerical Solution of Hydrodynamical Equations

Stoker (1957, p. 424) has shown that the problem of three-dimensional oscillations of water in lakes or basins is one of the classical eigenvalue problems of mathematical physics, amenable to solution by appropriate manipulation of the linearized long-wave theory and the use of finite difference procedures.

Hendrickson and Kilmer (Appendix B) have adapted the equations of Stoker and generalized them to curvilinear coordinates for finite-difference application to Monterey Bay. The work discussed in Part III A has already shown how satisfactorily a part-circular basin can be fitted to the boundary shape of Monterey Bay. This fact therefore led to the adoption of a polar-coordinate system for treating the three-dimensional eigenvalue problem.

The presumption is still that a node at the mouth of the bay governs the oscillating response of the area. The node is therefore taken in approximately the same location as that shown in the inset of Fig. 29.

The three-dimensional continuity equation for linear shallow-water waves of Stoker combined with the free surface condition (Bernoulli equation) and generalized to curvilinear coordinates (in particular, to polar coordinates, Appendix B), forms the field-equation governing the water-surface elevation η at any point in the bay.

The boundary conditions imposed on the field-equation (Eq. B-6, Appendix B) require that η be everywhere zero along the node and that at the coastline the field-equation be satisfied for the special condition of zero water-depth. Wherever a finite depth prevails at the coast, such as may arise in fitting a polar-coordinate network to Monterey Bay, the boundary condition requires that the velocity of flow normal to the vertical boundary be zero.

As described in Appendix B a computer program was developed for the finite-difference solution of the equations of an N x N matrix, where N is the number of grid points in the reticulation for describing the depth-distribution throughout the bay.

2. Test Application of Computer Procedures to Case of Semi-Circular Bay with Semi-Paraboloidal Bottom

In order to check the numerical procedures the computer program was applied to a case for which the exact mathematical solutions are available. Such a case is the semi-circular basin with semi-paraboloidal bottom topography, whose oscillating regime is explicitly known from hydrodynmical theory (of Lamb, 1932, pp. 291-293; also Table V).

The reticulation network adopted to specify the bottom topography is shown in Fig. 33a. After painstaking elimination of many troubles in the computer programming, success was finally achieved in a very satisfactory numerical check of the analytic solution. This is illustrated in Figs. 33a to 33d and Fig. 34, which present the first four and the tenth mode shapes, respectively, for the open-mouth basin. These are determined from an 85 x 85 matrix solution, on the assumption that a nodal-diameter exists across the mouth. The isolines define contours of water level, normalized to unit value at the antinodes.

It will be recognized that the first four modes of oscillation depicted in Figs. 33 are 'unsymmetrical' modes involving only nodal radii (equivalent to Figs. 28d, f, h and i), and that the 10th mode (Fig. 34), involving one nodal diameter and one nodal semi-circle, corresponds to Fig. 28e. The calculated mode-period ratios, T_n/T_1, where T_n is period of the n-th mode and T_1 that of the fundamental mode of oscillation, compare very well with the theoretical in Table IX.

The eigenvalues, which involve the squares of the frequencies or periods, are fairly close approximations to the true values, but deviate towards ever larger errors as the mode-number increases. The error is necessarily a reflection of the limitations of the grid system adopted;

TABLE IX

MODES OF FREE OSCILLATION IN OPEN-MOUTH SEMI-CIRCULAR BASIN: EXACT AND NUMERICAL SOLUTIONS

Mode Number	Mode-Period Ratio, T_n/T_1	
n	Numerical Solution	Analytic Solution*
1	1.000	1.000
2	0.708	0.707
3	0.581	0.578
4	0.509	0.500

* See also Table V

the finer the mesh the less will be the error. It follows that in any numerical solution of eigenvalue problems of this kind, only the first 20 percent, say, of the eigenvalues computed can be relied on to give a satisfactory rendering of the lowest modes of oscillation.

3. Three-Dimensional Modes of Oscillation of Monterey Bay

After confirmation of the computer program, in the manner described, it was applied to the difficult topography of Monterey Bay. It was found expedient to model the bay with a polar coordinate network of grid-points spaced at intervals of 6250 feet, radially, and 5° of angle, as shown in Fig. 35a. To cover the sharp depth changes in the submarine canyon the differential angular increment in the region was reduced from 5° to 2.5°. The angular increment was also taken at 2.5° in the region of Monterey Harbor in order to give somewhat better definition to the oscillations in this area. Besides the grid-point locations, Fig. 35a shows the values of water depth assigned to each point; (peripheral stations in the Santa Cruz and Monterey areas and along the node line are marked with the station numbers in larger figures).

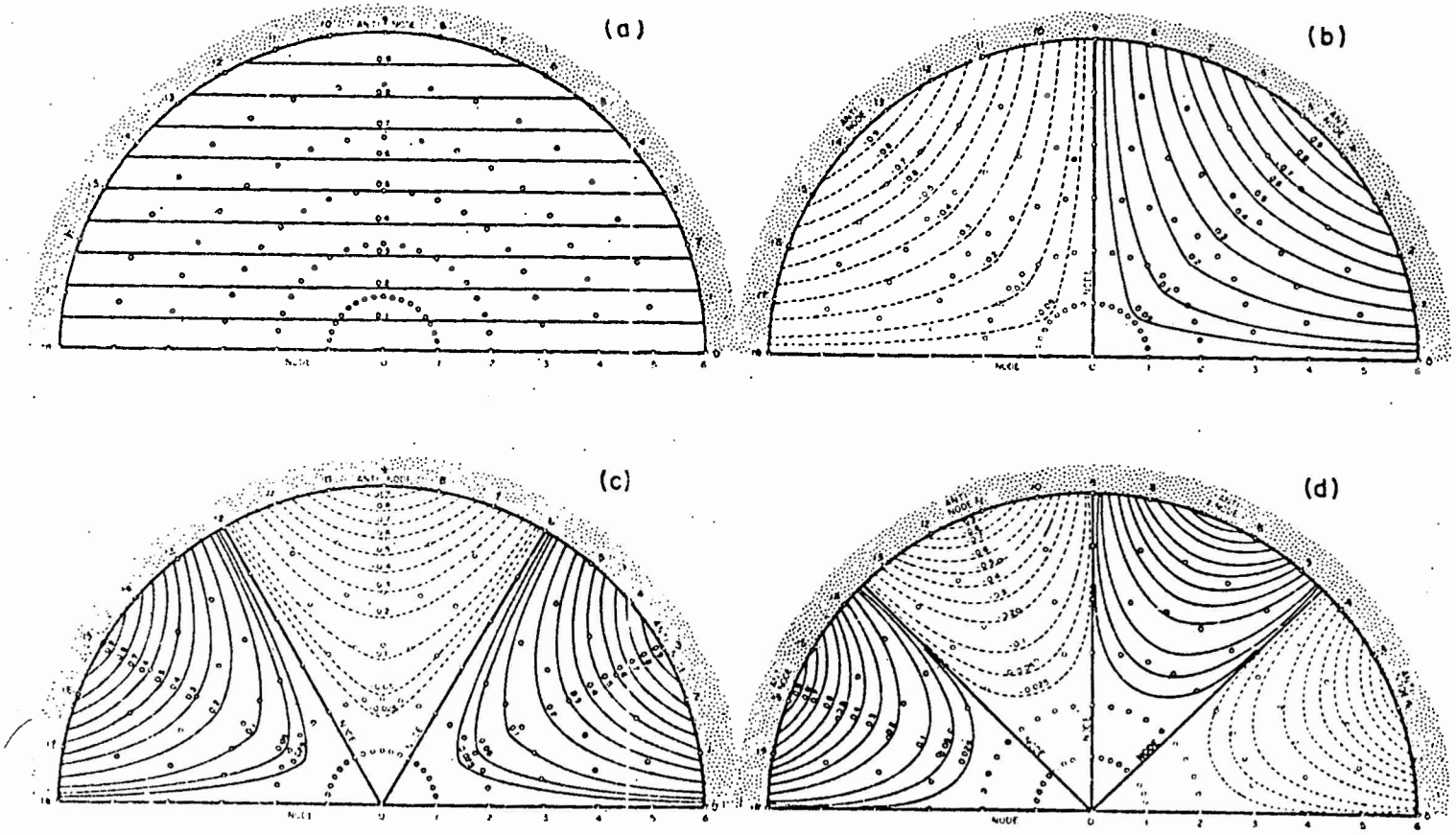

FIGURE 33 CONTOURS OF WATER-SURFACE ELEVATION FOR FOUR LOWEST MODES OF OSCILLATION IN A SEMI-CIRCULAR BASIN WITH SEMI-PARABOLOIDAL BOTTOM (NUMERICAL CALCULATION)

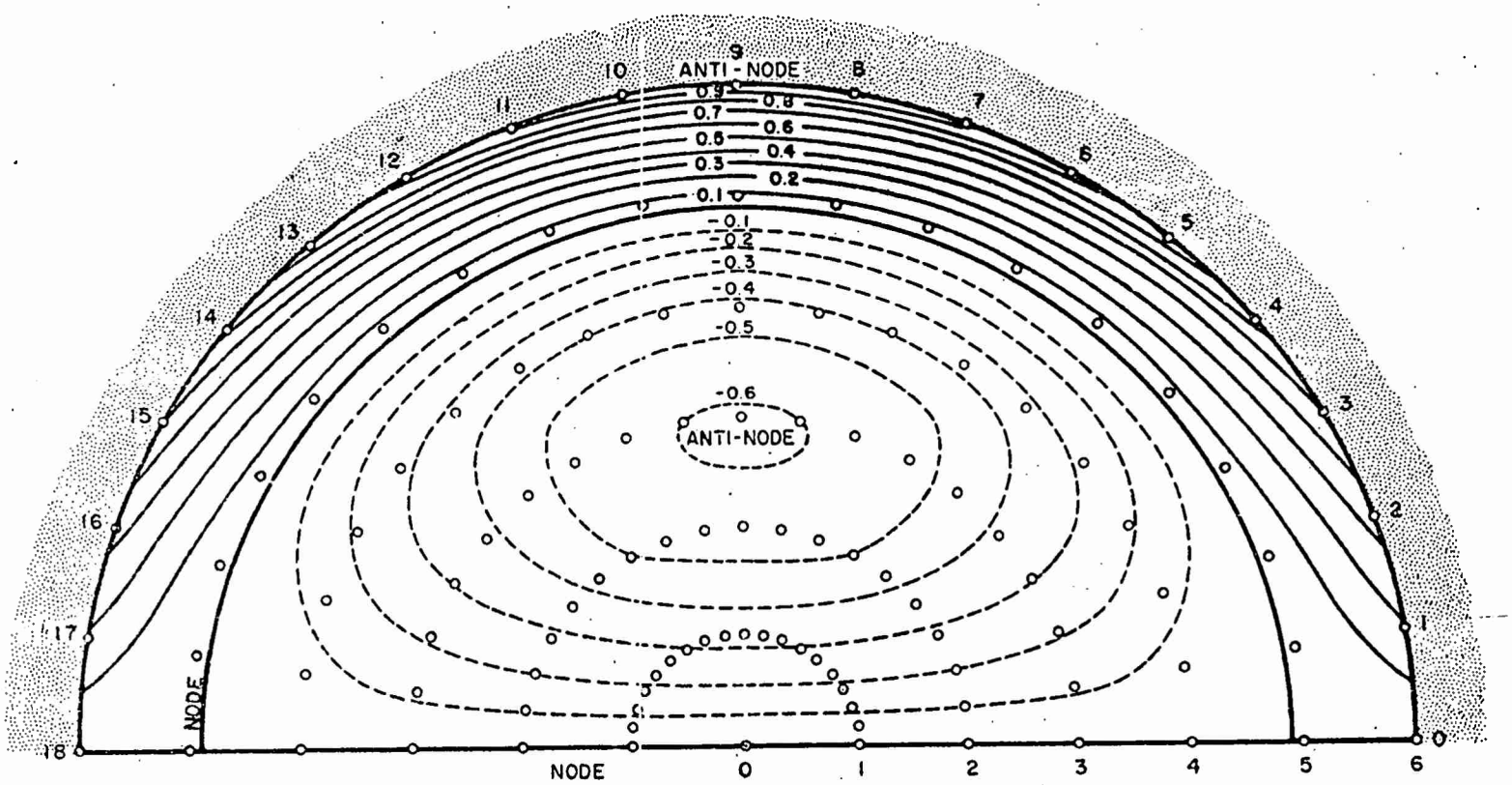

FIGURE 34 CONTOURS OF WATER-SURFACE ELEVATION FOR 10th MODE OF OSCILLATION IN A SEMI-CIRCULAR BASIN WITH SEMI-PARABOLOIDAL BOTTOM (NUMERICAL CALCULATION)

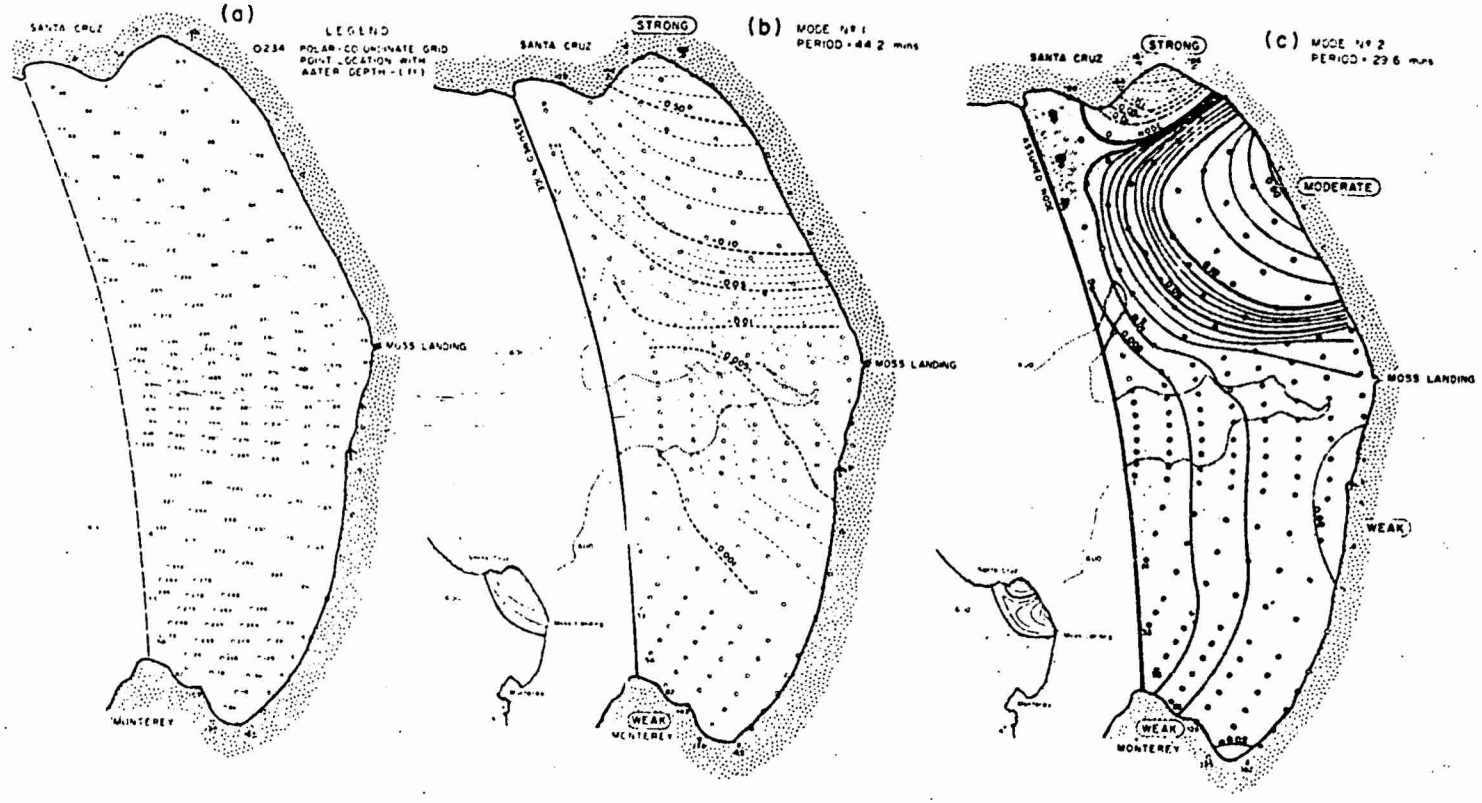

FIGURE 35 NUMERICAL CALCULATION OF MODES OF OSCILLATION OF MONTEREY BAY; (a) POLAR-COORDINATE GRID NETWORK (b) FUNDAMENTAL MODE; (c) 2nd MODE

It was decided to give the assumed node at the mouth of the bay a slight concavity seaward in deference to the results of Figs. 28. As before (in Figs. 29 and 30), however, the node was presumed to connect Pinos Point on the Monterey Peninsula and Point Santa Cruz (Fig. 35). At the outset it must be realized that the results of the three-dimensional study discussed herein are only as good as this assumption of a node will allow. If the assumption is a poor one the validity of results must necessarily suffer. There is, however, no alternative to this other than to extend the scope of the oscillating area clear to the continental shelf edge outside the bay. For an introduction to this kind of work, this would have been prohibitively expensive and complicated.

Figs. 35 b and 35 d through 38 show the normalized mode shapes evolving from the numerical calculations and the corresponding modal periods for the first nine modes of oscillation. The 20th and 22nd mode shapes are included in Fig. 38 as matter of interest. Contours are elevations of water level, above (plus) or below (minus) still water level, normalized to unit value at the highest antinode, marked 'strong'. Other antinodes (peaks or troughs of water level) are either 'moderate' or 'weak' according to their normalized values. A moderate antinode may have a peak value between 0.6 and 0.1; a 'weak' antinode a value less than 0.1 .

The small inset figures in Figs. 35 to 38 are rough simplifications of the type of oscillation occurring. Thus for the first mode, having a period of 44.2 mins., the oscillation effectively embraces the northern half of the bay only. The same is true of the second mode of oscillation (T_2 = 29.6 mins.), Fig. 35 c . These results appear to show no relation to those derived in Parts III A and III B of this report, for it is clear that the deep submarine canyon is having a most profound effect on the oscillating regime of the whole area. Rather than discuss the results further at this point, we shall await the findings of the long-period wave refraction analysis, and then attempt an ensemble of findings in Part IV of this report. The sequence of modal periods, however, up to the ninth,

is conveniently given here, namely

$$T_n = 44.2,\ 29.6,\ 28.2,\ 23.3,\ 21.6,\ 20.4,\ 19.4,\ 18.7,\ 17.6,\ \ldots\ldots\ldots\ldots \text{mins.} \quad (18)$$

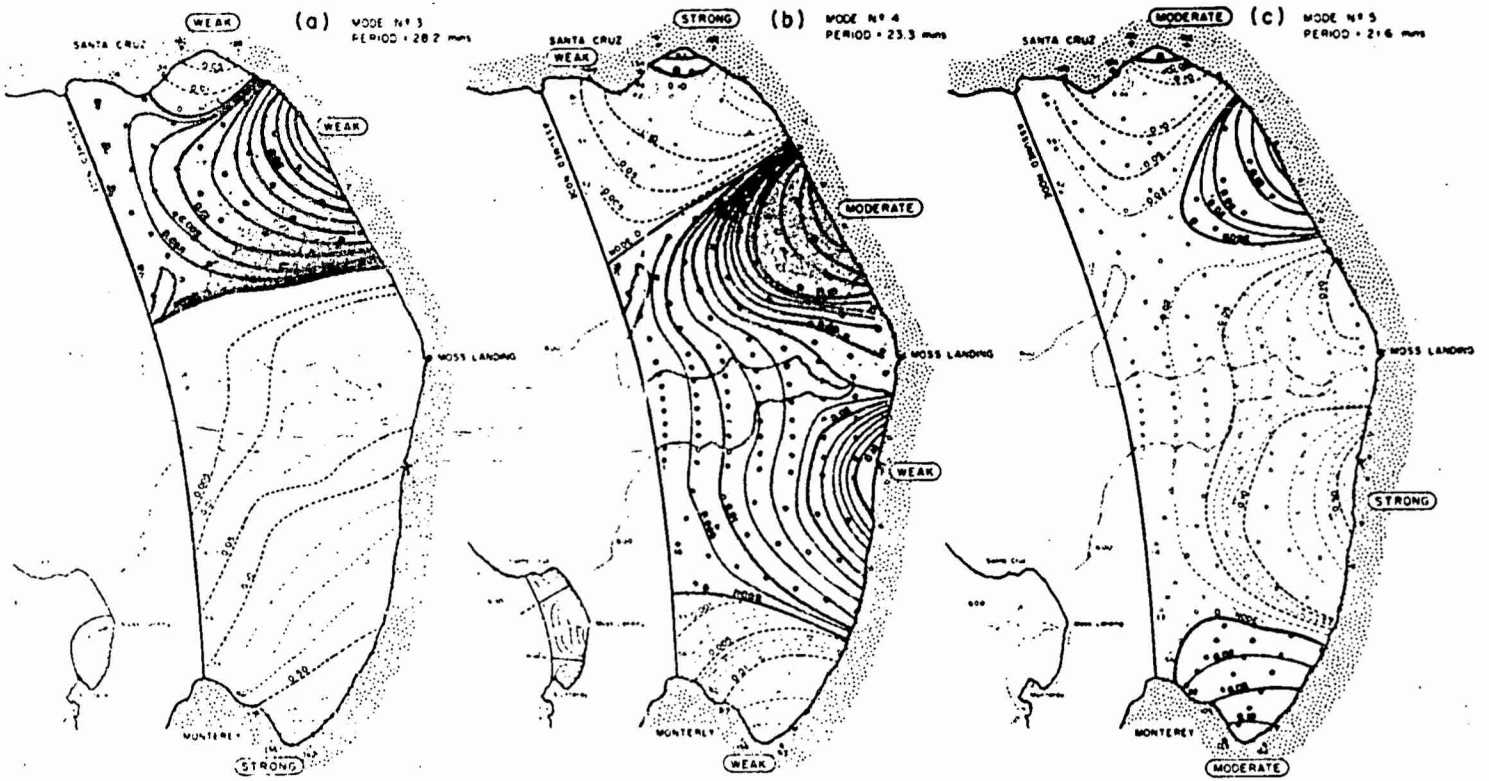

FIGURE 36 NUMERICAL CALCULATION OF MODES OF OSCILLATION OF MONTEREY BAY; MODES 3, 4 and 5

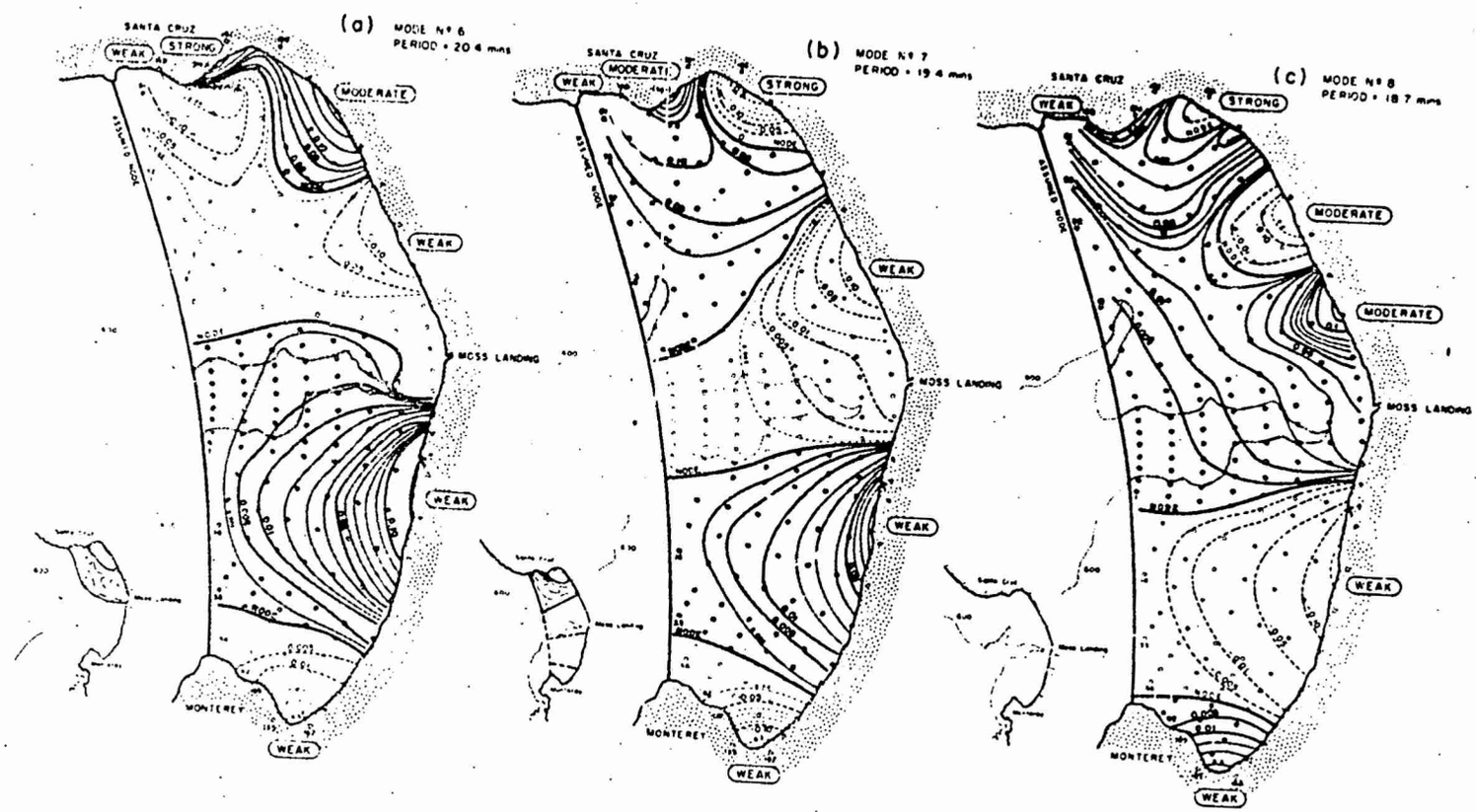

FIGURE 37 NUMERICAL CALCULATION OF MODES OF OSCILLATION OF MONTEREY BAY; MODES 6, 7, and 8

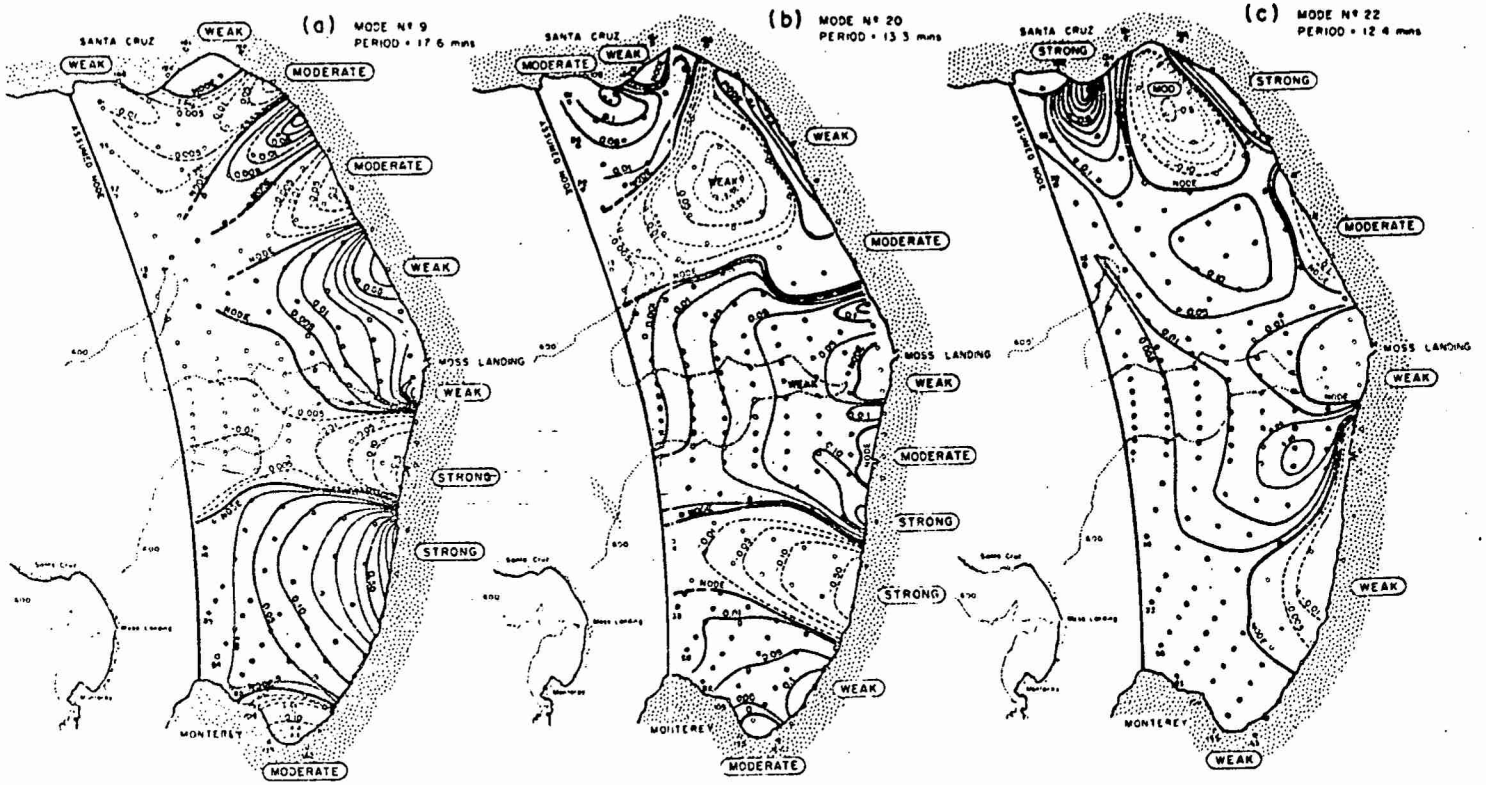

FIGURE 38 NUMERICAL CALCULATION OF MODES OF OSCILLATION OF MONTEREY BAY; MODES 9, 20 and 22

III D. ANALYSIS OF OSCILLATING CHARACTERISTICS OF MONTEREY BAY: WAVE REFRACTION DIAGRAM TECHNIQUES

1. Long-Period Wave Refraction-Diagram Techniques Utilized in this Study

For purposes of long-period wave refraction analysis, suitably contoured working charts were prepared, based on Coast and Geodetic Survey Maps Nos. 5402 and 5403, with scales respectively 1:210,666 and 1:50,000.

By way of aiding the graphical work of plotting wave fronts, auxiliary diagrams were prepared appropriate to the chart scales (Figs. 39 to 41). A typical auxiliary diagram comprises a curve which plots ordinates of distance (to the map scale) that a long wave will travel in a certain interval of time at the velocity $c(=\sqrt{gh})$, against abscissae of water depth h. Separate auxiliary diagrams for time intervals of 10, 20, 30, 60 and 90 secs. were included (see Fig. 40). The diagrams serve the purpose of permitting the intercept of distance (advanced by a long wave in a specific interval of time) to be picked off for any depth by means of thumb-screw dividers and pricked on to the working chart.

Because long waves are susceptible to refraction effects even in deep water, the technique followed at the outset was to assume that any long waves approaching Monterey Bay have an initially straight wave frontage in 10,000 feet of water. From Fig. 42 (Wilson, 1957) it will be seen that this is valid really for waves of only about 1 min. and less. Waves longer than this in period will already have been refracted in deeper water, but the curvature of the wave fronts that such long waves would actually have in 10,000 ft. depth is assumed to be relatively unimportant at a great distance from Monterey Bay, on the same principle that it has now clearly been demonstrated that the initial direction in deep water, of short period waves incident on a coastline, may be quite radical without producing too marked a directional change of the waves close to the coast. The object of initial refraction-diagram work was to propagate the waves from the water depth of 10,000 ft towards the coast and the mouth of the

Figure 39

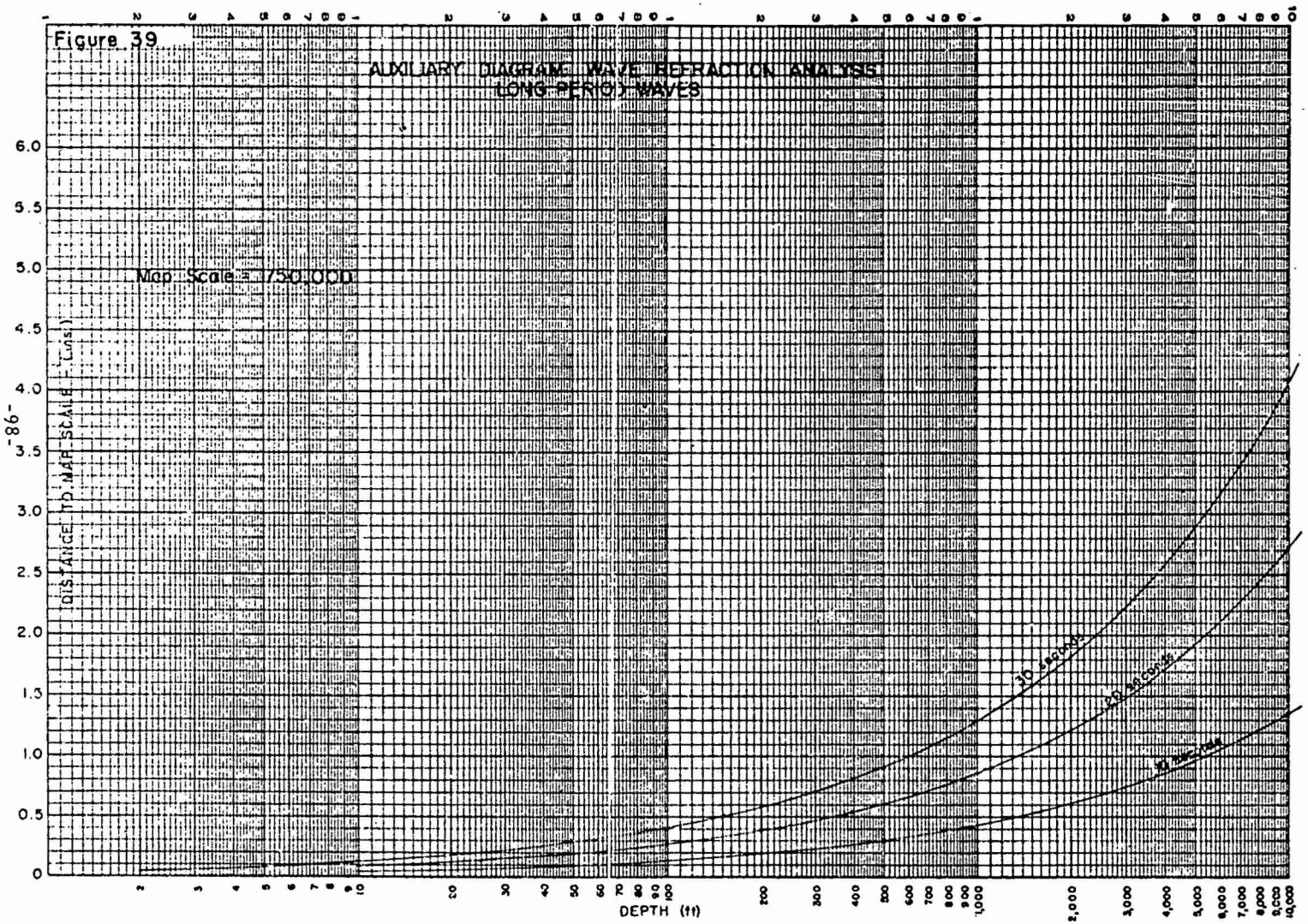
AUXILIARY DIAGRAM, WAVE REFRACTION ANALYSIS
(LONG PERIOD WAVES)
Map Scale = 1/50,000
DISTANCE TO MAP SCALE (Ins.)
DEPTH (ft)
30 Seconds
20 Seconds
10 Seconds

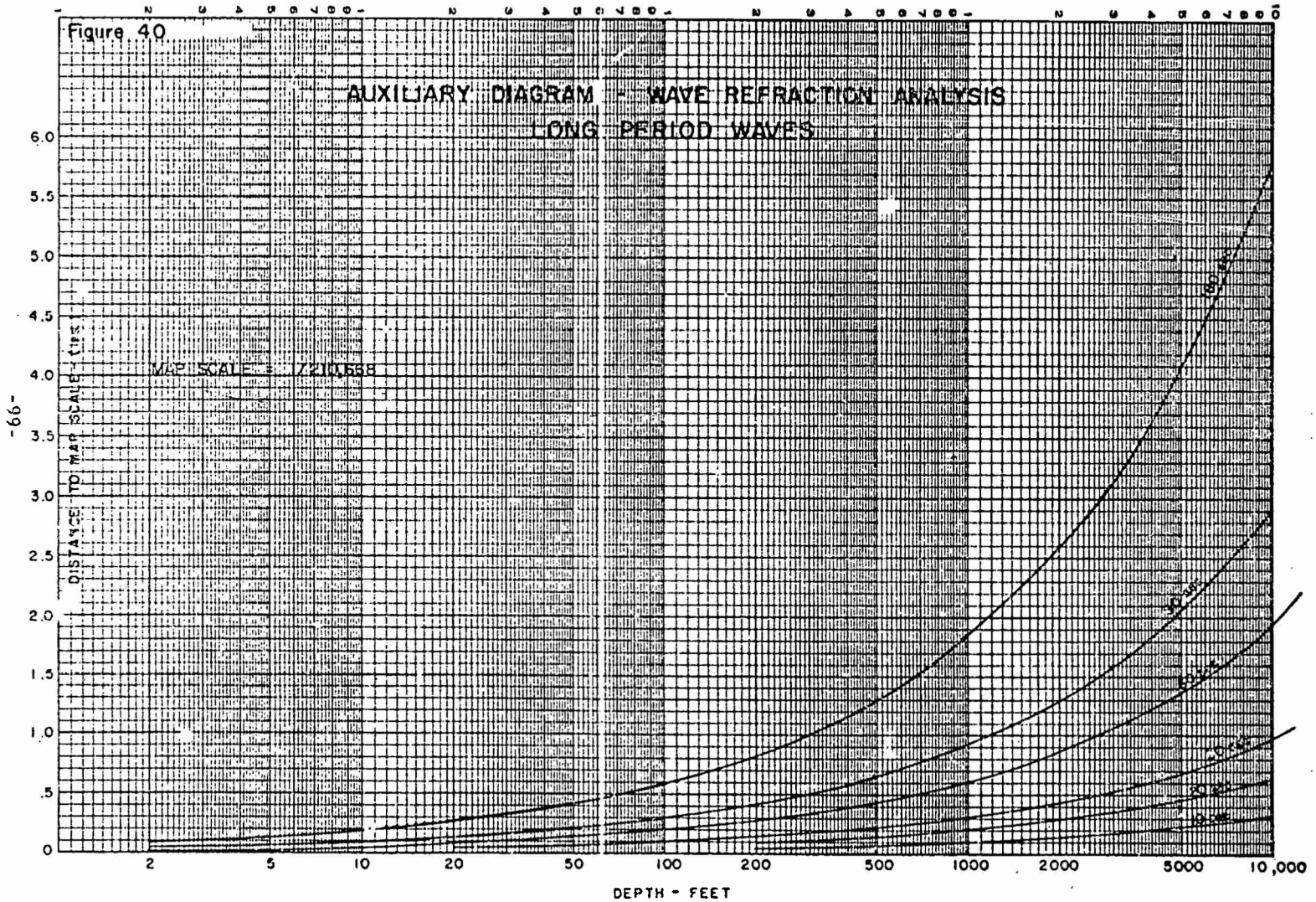
Figure 40
AUXILIARY DIAGRAM - WAVE REFRACTION ANALYSIS
LONG PERIOD WAVES
MAP SCALE = 1/2000
DISTANCE TO MAP SCALE (INS.)
DEPTH - FEET
6.0
5.5
5.0
4.5
4.0
3.5
3.0
2.5
2.0
1.5
1.0
.5
0
2
5
10
20
50
100
200
500
1000
2000
5000
10,000

Figure 41

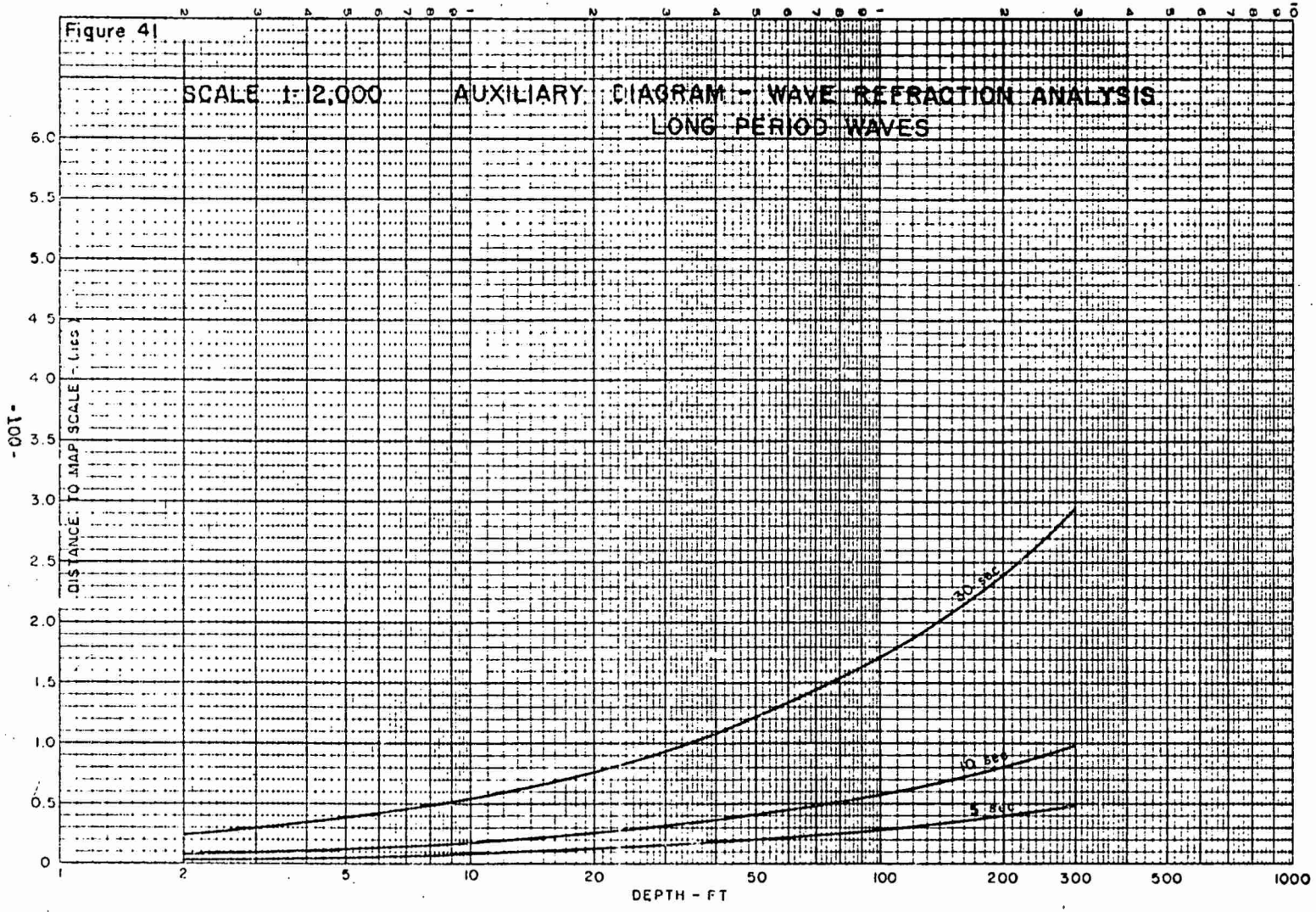
SCALE 1:2,000 AUXILIARY DIAGRAM - WAVE REFRACTION ANALYSIS
LONG PERIOD WAVES
DISTANCE TO MAP SCALE - Lies
-100-
6.0
5.5
5.0
4.5
4.0
3.5
3.0
2.5
2.0
1.5
1.0
0.5
0
30 sec
10 sec
5 sec
1
2
5
10
20
50
100
200
300
500
1000
DEPTH - FT

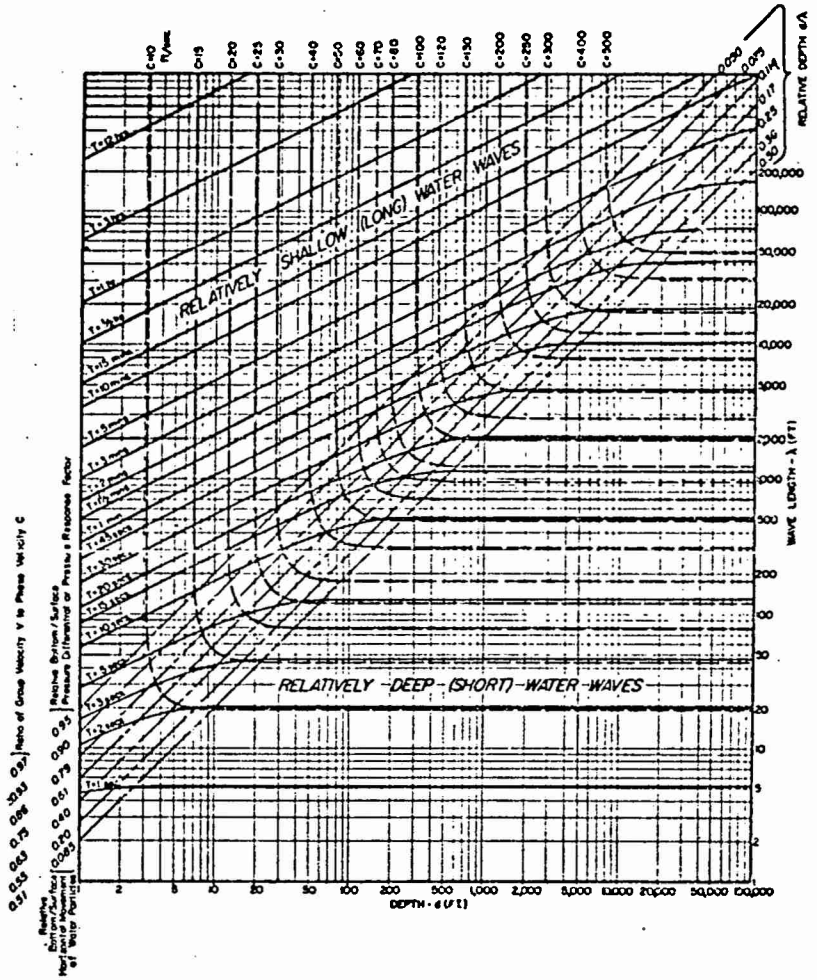

FIGURE 42 CHARACTERISTICS OF SMALL AMPLITUDE WATER WAVES, AIRY THEORY (from Wilson, 1957)

bay on the scale of 1: 210,666 and thence to transfer the curved wave fronts, so determined, to the larger scale charts of 1 : 50,000 on which the wave propagation into Monterey Bay could be followed in detail.

For a correct interpretation of long-wave behavior in the period-range from about 20 secs. to 3 mins., it will be seen from Fig. 42 that the intermediate velocity law, $c = \sqrt{(g/k \tanh kh}$, where $k = 2\pi/\lambda$ and λ is the wave length, really needs to be taken into account.

However, if we consider a long-wave of 45 secs. period as being about the lower limit of our interest, Fig. 42 tells us that, without appreciable error, the velocity law $c = \sqrt{gh}$, upon which the auxiliary diagrams, Figs. 40 to 41, are based, will be valid in depths of water less than about 700 feet. Between depths of 10,000 feet and 700 feet, then, waves of periods between 3 mins. and 45 secs. will not be refracted as much as longer waves. This will have to be borne in mind when we come to consider the effects of the Monterey Canyon on the propagation of long-waves into Monterey Bay.

2. Propagation of Long-Period Waves into Monterey Bay

Refraction diagrams were prepared for three initial directions of approach of long waves to Monterey Bay. Substantially these directions are WNW, WSW and SSW. Figs. 43, 44 and 45 show the first phase of wave propagation from these directions towards the bay mouth -- effectively up to the edge of the continental shelf (h = 600 ft.) in the region of Monterey.

Comparison of Figs. 43 and 45 shows that the initial 90°-of-angle disparity in approach-direction of the long waves at 10,000 ft. depth has been narrowed to a mere 30° at the shelf edge.

It will be seen that the wave fronts are greatly influenced by the deep submarine canyon that virtually divides the bay in two parts. The canyon and its forks and the numerous chines on the continental slope have the effect of causing the waves to form frequent caustics, or

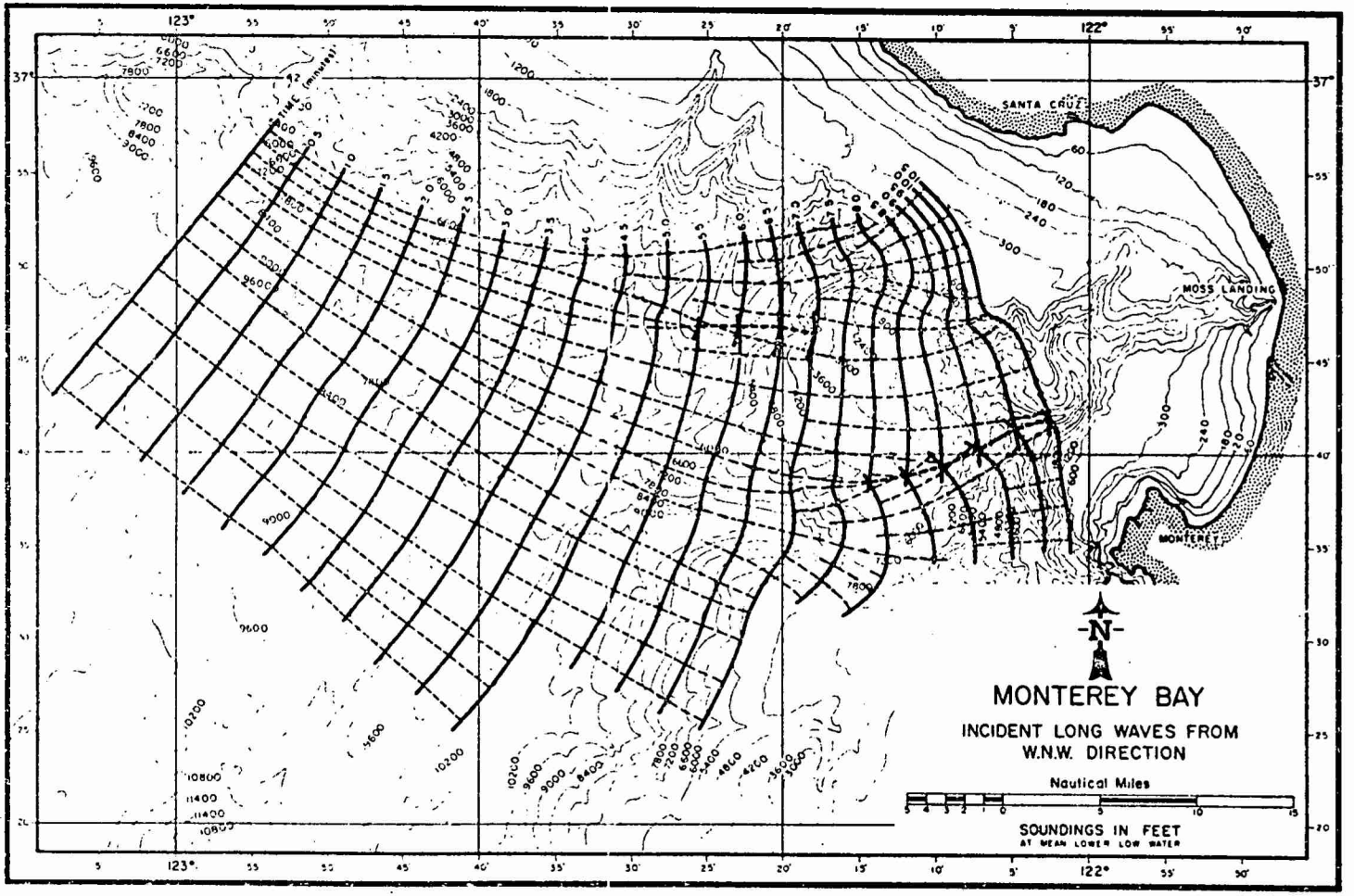

FIGURE 43 APPROACH OF LONG-PERIOD WAVES TO MONTEREY BAY FROM WNW

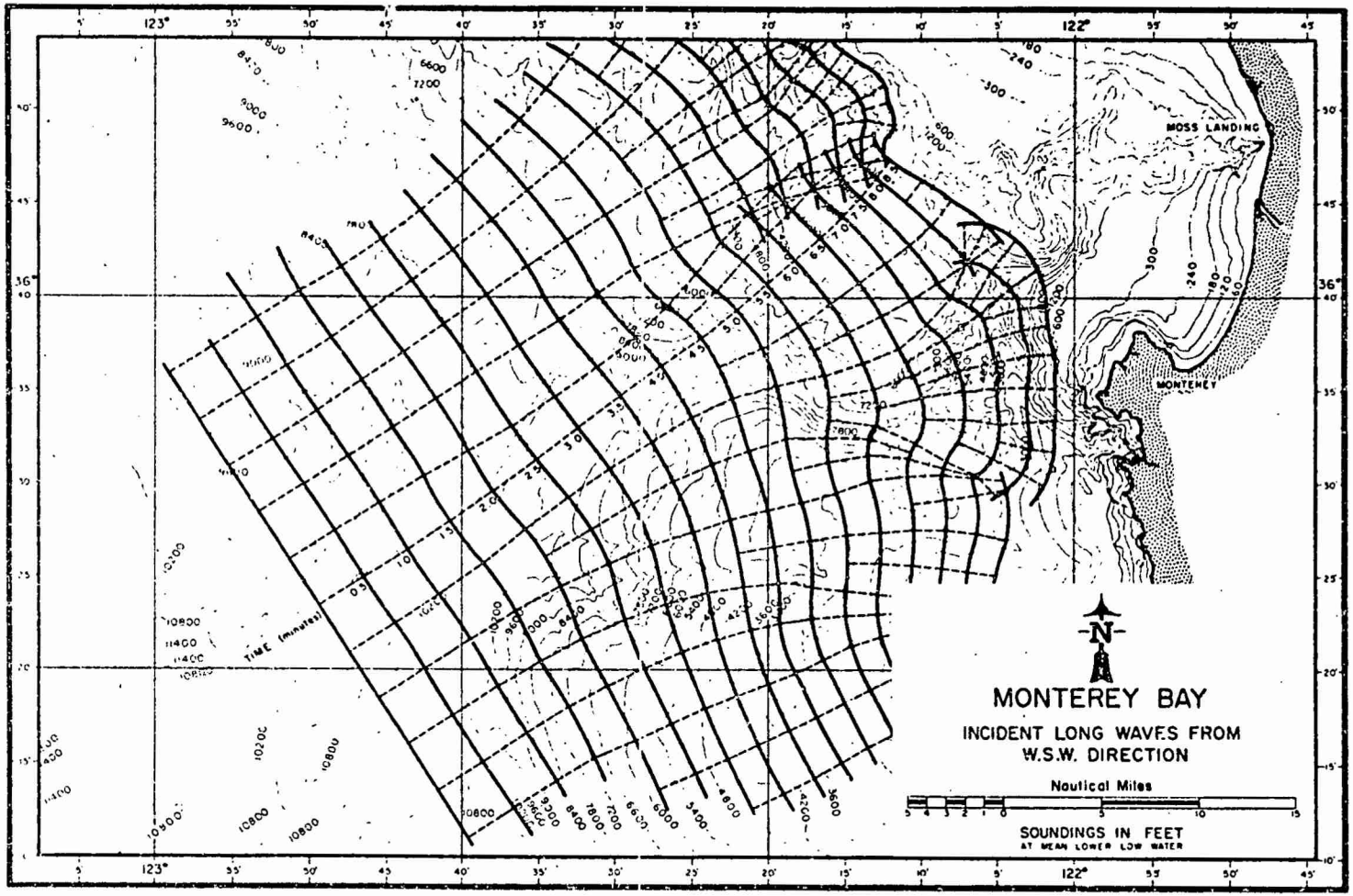

FIGURE 44 APPROACH OF LONG-PERIOD WAVES TO MONTEREY BAY FROM WSW

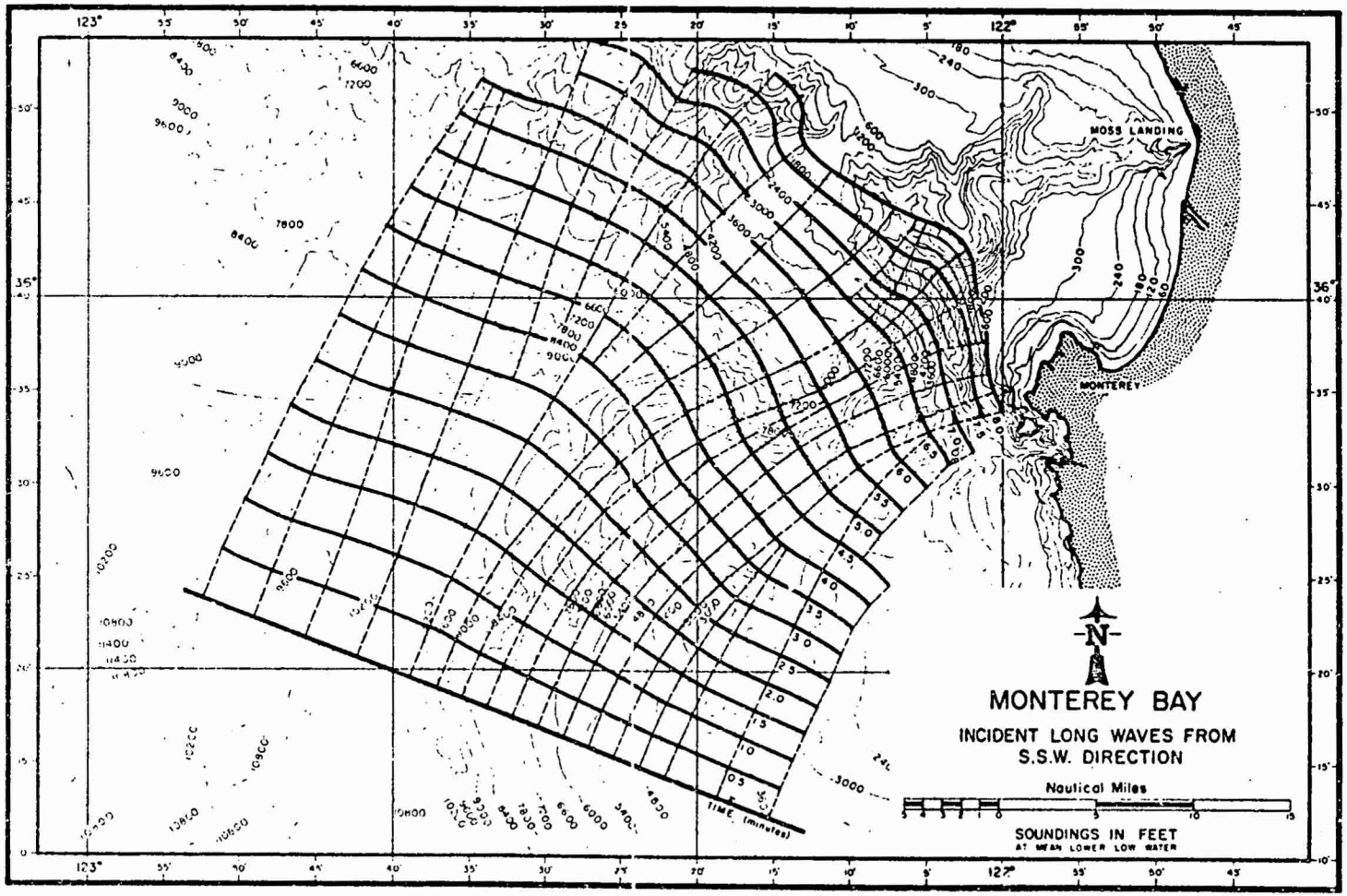

FIGURE 45 APPROACH OF LONG-PERIOD WAVES TO MONTEREY BAY FROM SSW

overlapping waves where orthogonals (or wave rays) intersect each other. This becomes a great deal more obvious in Figs. 46, 47 and 48 which continue the wave propagation from the shelf edge into the bay.

It will be noted in particular from these figures that the effect of the deep Monterey Canyon is to refract the long waves to north and south so drastically, that those refracted southwards, for instance, tend to cross over the waves that continue eastward (from further south) at a sharp angle approaching almost 90°. At the same time the refraction from the canyon is so great that only very small amounts of long wave energy converge southward in this manner. For all intents and purposes, then, the main sweep of long wave energy into the bay comes from waves that pass clear (north or south) of the submerged canyon.

It is evident from Figs. 46, 47 and 48 that long waves reaching the coast in the vicinity of Monterey Harbor have only very small differences of direction; the original 90° disparity of direction angle has now been reduced almost to nil. This fact is further exemplified in Fig. 49, which shows the wave fronts from the original three directions superimposed upon each other. A main difference here, of course, will reside in the relative amounts of incident long wave energy coming from the original three directions.

For greater accuracy in the plotting of wave fronts near the harbor, an enlarged chart of the area to a scale of 1: 12,000 was developed. Wave fronts introduced on to this from the smaller scale charts (Fig. 49) near Pinos Point, on the Monterey Peninsula, were refracted forward again to the coast. These refraction diagrams are illustrated in Figs. 50 and 51. It was found expedient to combine the wave fronts from the WNW and WSW directions at this stage, as shown in Fig. 50.

It is of interest to compare Figs. 50 and 51 with the aerial photograph (Fig. 9) showing wave fronts of short-period waves.

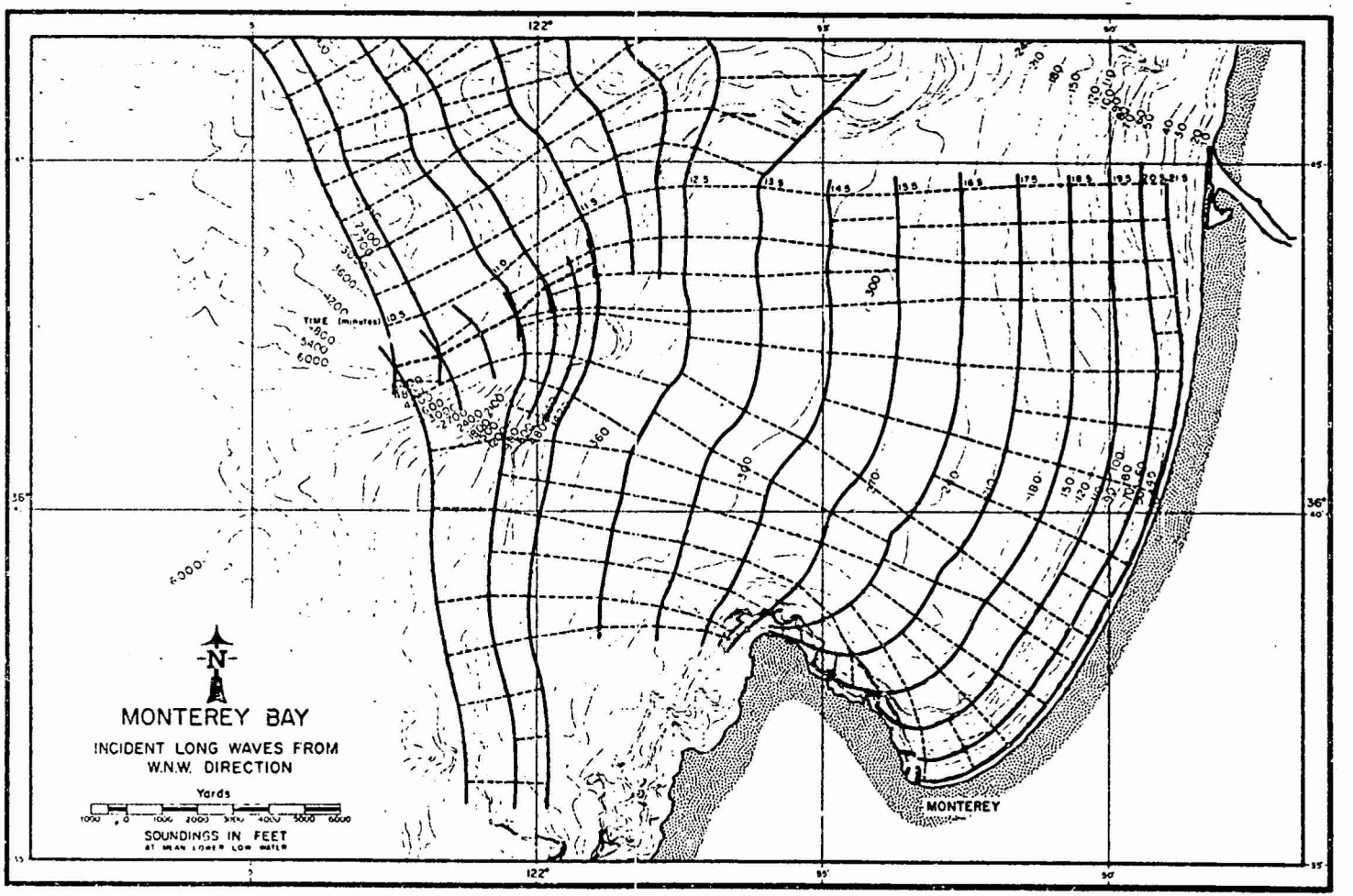

FIGURE 46 ENTRY OF LONG-PERIOD WAVES INTO MONTEREY BAY FROM WNW

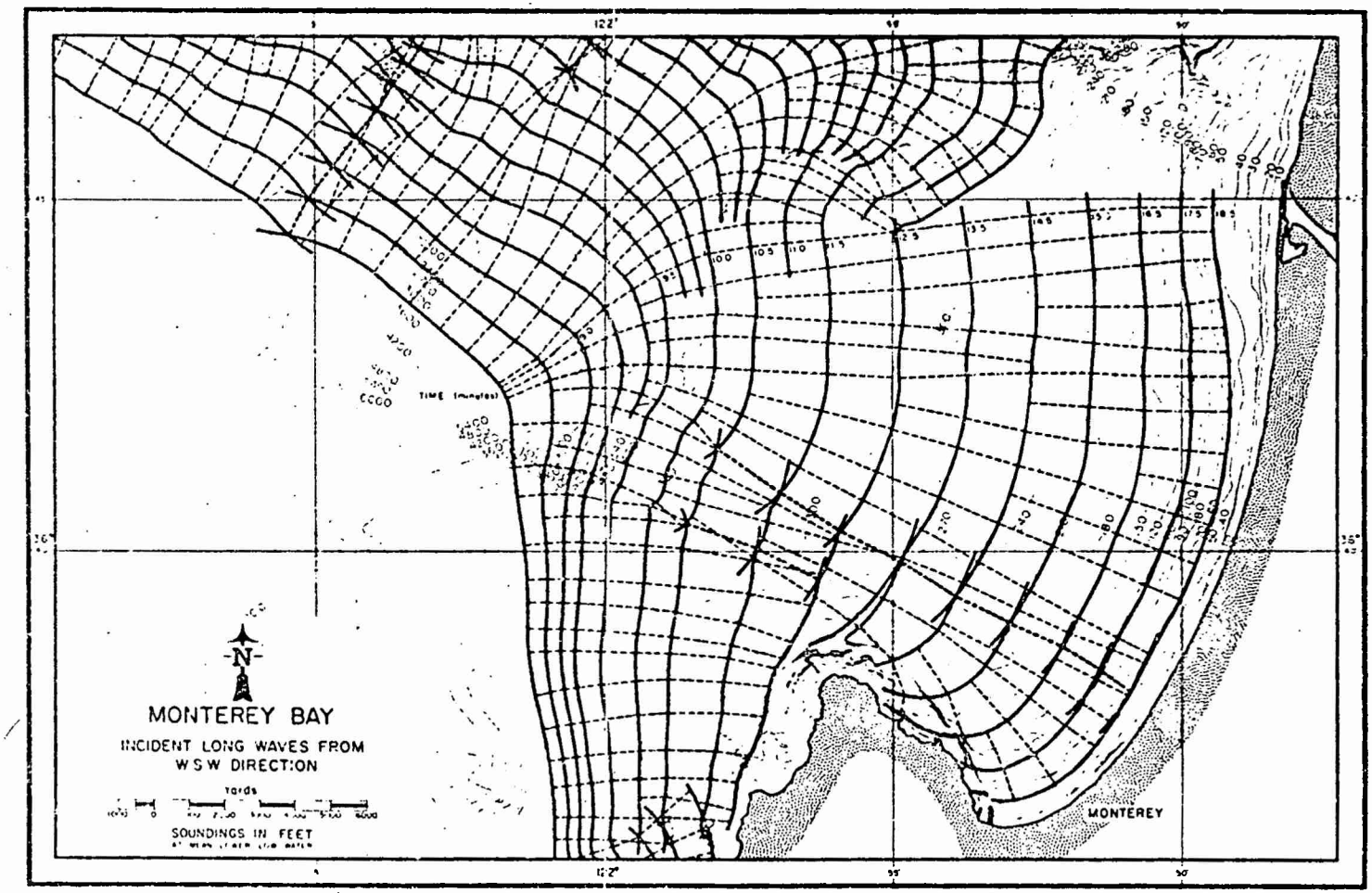

FIGURE 47 ENTRY OF LONG-PERIOD WAVES INTO MONTEREY BAY FROM WSW

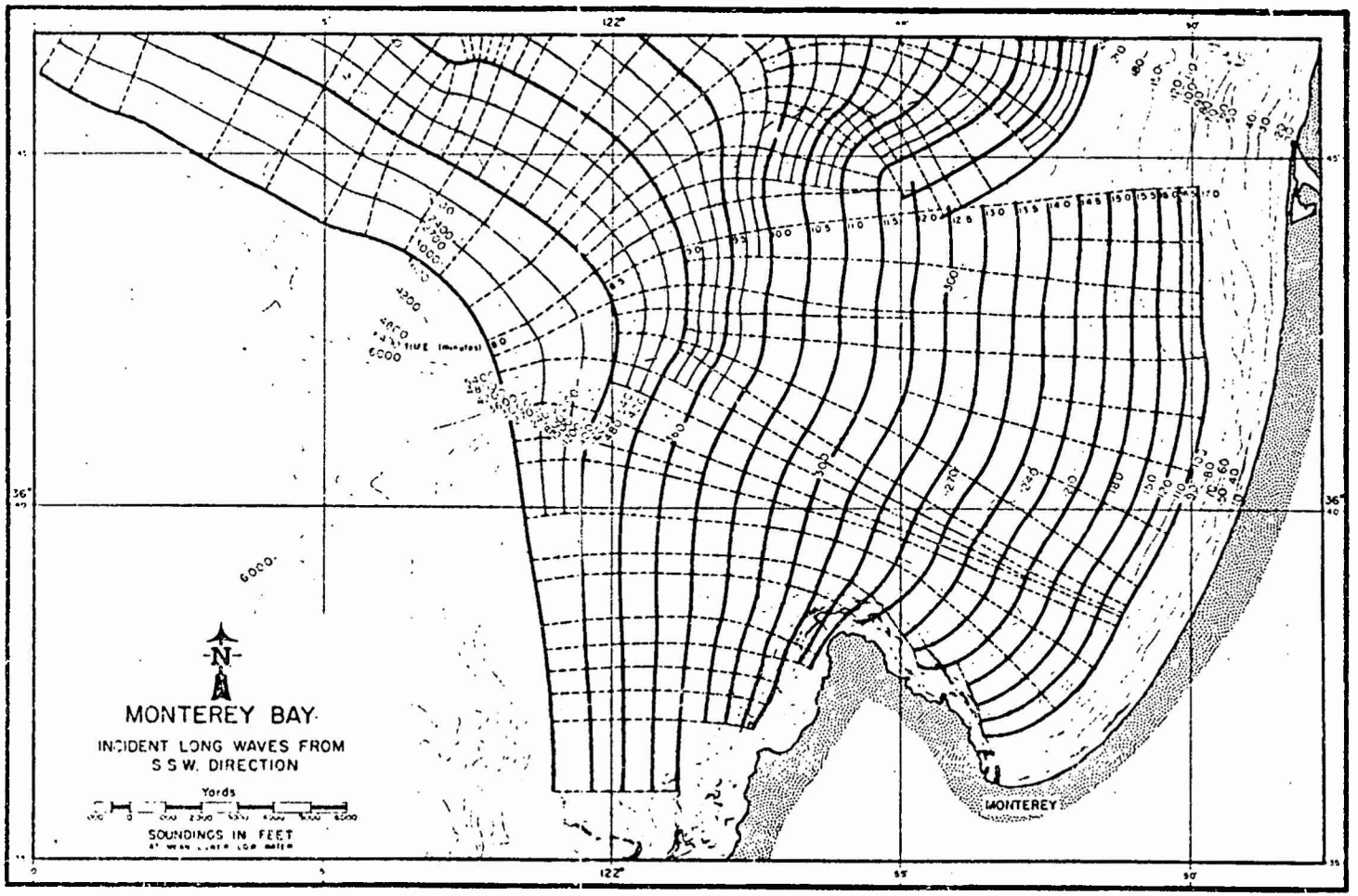

FIGURE 48 ENTRY OF LONG-PERIOD WAVES INTO MONTEREY BAY FROM SSW

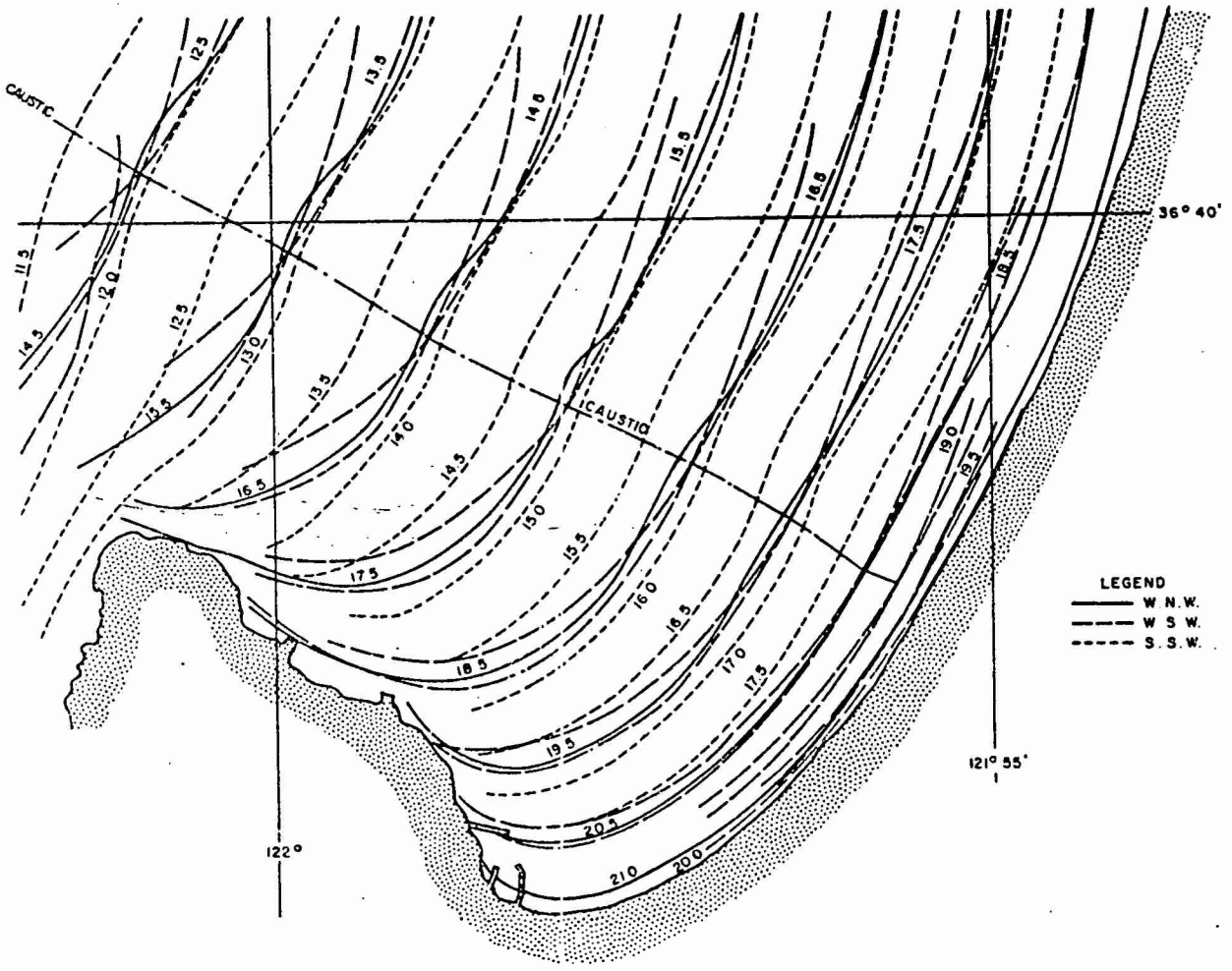

FIGURE 49 LONG-PERIOD WAVE REFRACTION IN THE SOUTHERN PORTION OF MONTEREY BAY

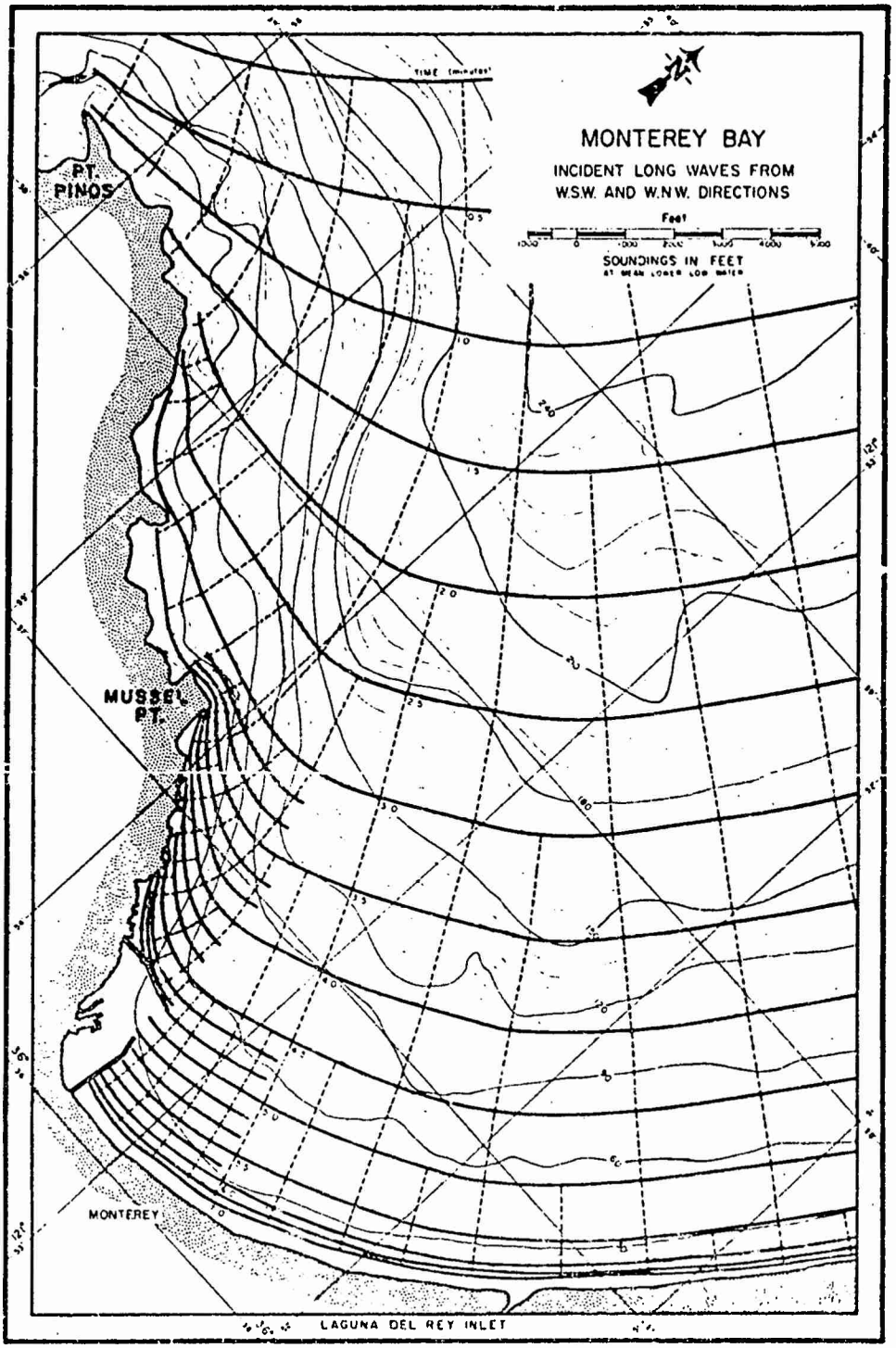

FIGURE 50 LONG PERIOD WAVE APPROACH TO MONTEREY HARBOR FROM WSW AND WNW

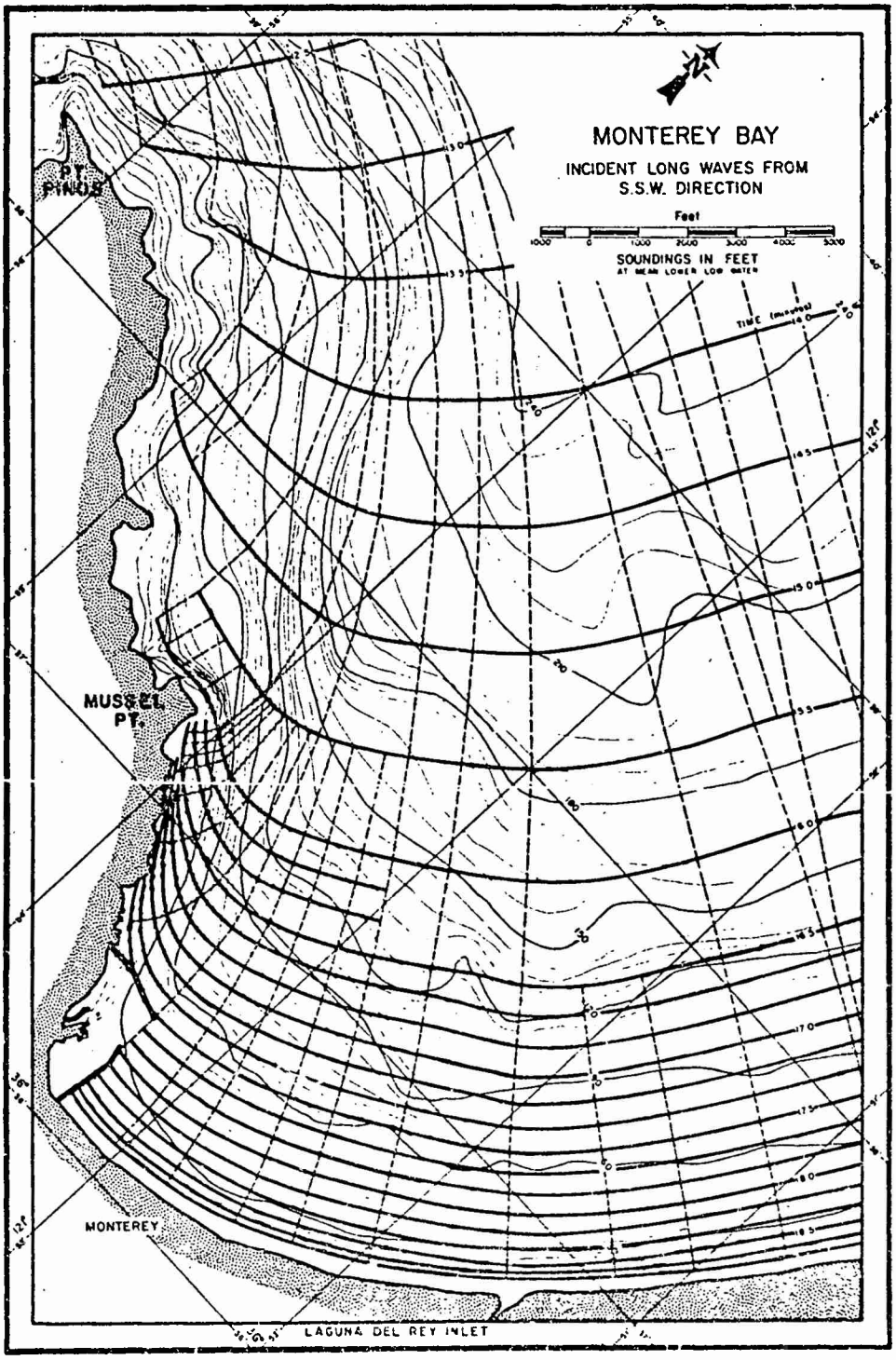

FIGURE 51 LONG-PERIOD WAVE APPROACH TO MONTEREY HARBOR FROM SSW

3. Long-Period Wave Refraction Coefficients for Monterey Bay

A remarkable feature of the submarine canyon effect is that it provides considerable overall protection to the bay from the ingress and worst effects of long period waves.

For example, waves approaching from the WNW direction affect the bay from an energy front of about 33,000 feet (5.4 n. mi.), width, reckoned at a distance of about 350,000 feet (57.5 n. mi.) from the coastline. The average refraction coefficient for the whole bay is thus about 0.50 on the basis that the coastline of the bay is approximately 131,000 feet (21.4 n. mi.) long between extreme north and south portions. In particular, however, the refraction coefficient for the southern half of the bay is about 0.45. The Santa Cruz Harbor area appears to have a refraction coefficient of about 0.35 from this approach direction.

From the WSW direction, the submarine canyon provides remarkable protection. The refraction coefficient for the bay as a whole is only about 0.09. The northern and southern halves, in particular, each absorb about half the incident energy and consequently also have refraction coefficients approximating 0.09. On the other hand the northern coastline of the bay tends to receive most of the brunt of wave attack and long wave energy is concentrated by caustic effects on the Santa Cruz Harbor embayment which tends to have a refraction coefficient as high as 1.90.

From the SSW direction more energy is capable of reaching the southern half of the bay than seems possible from the other directions of wave approach. The refraction coefficient for the southern part approximates 0.60. In contrast, the northern half of the bay almost completely protected and has a refraction coefficient of as little as 0.09. The Santa Cruz Harbor area again receives a major share of long-wave energy and a refraction coefficient value of 0.80 is indicated for its small embayment.

In summary, Table X gives approximate results for the ingress of long period wave energy to Monterey Bay.

In comparison with refraction coefficients for short-period waves

(8 to 20 secs.), discussed in Part II(5), it seems evident that long period waves convey relatively much less energy to the southern half of Monterey Bay from the WNW approach direction than do short waves. Table X shows that more long-period wave energy reaches the southern part of the bay when the wave approach direction is from SSW; however, from this direction it is evident from the discussions of Part II that very little short-period wave activity reaches the bay. This conclusion, considered in conjunction with the tentative conclusion that long and short-period wave activity are uncoupled, suggests that the southern Pacific Ocean may be a prime source for the disturbances experienced in Monterey Bay.

TABLE X

REFRACTION COEFFICIENTS
FOR LONG-PERIOD WAVES

Approach Direction	Whole Bay	Southern Half	Northern Half	Santa Cruz Bay
WNW	0.50	0.50	0.45	0.35
WSW	0.09	0.09	0.09	1.90
SSW	0.60	0.60	0.09	0.80

4. Travel Times of Long-Period Waves

Figs. 43 to 51 show the travel times of the wave fronts related to their initial starting positions. In general, wave fronts are shown at every half-minute of their progress shoreward or at every 10 secs. in the more detailed work.

From adaptation of the generalized Merian formula for the periods of free oscillation in an open-mouth rectangular bay of uniform depth (see Table V, row 1), namely

$$T_n = \frac{4L}{n\sqrt{gh}} \qquad (19)$$

where $n(= 1, 3, 5, \ldots)$ is an integer, we infer for the case of $n = 1$ that

$$T_1 = 4(t)_L \tag{20}$$

where $(t)_L$ is the travel time of the waves to propagate over the distance L from from the baymouth to the head of the bay, since by definition

$$c = \sqrt{gh} = \frac{L}{(t)_L} \tag{21}$$

From Eq. (20), then, we have a rough means of determining the fundamental period of oscillation of the bay on the assumption that a node forms at the mouth.

If the node at the mouth of Monterey Bay were considered to be in line with the long wave fronts that are parallel to the coast and at the same time tangential to Pinos Point, when extended in a straight line (Fig. 49), the travel time $(t)_L$ involved is seen to be from 6 to 7 mins. From Eq. (20), the fundamental period would thus tend to be of the order

$$T_1 = 24 \text{ to } 28 \text{ mins.} \tag{22}$$

5. Refraction Coefficients for Area Proximate to Monterey Harbor

By use of Eq. (1) (Part II (5)), long-wave refraction coefficients, referred to wave heights at the initial starting points of the wave refraction, in 10,000 ft. water depth, have been evaluated in Figs. 52 to 54. Contours of K_r-values define their distribution over the area in the neighborhood of Monterey Harbor.

From the initial WNW direction, it is seen from Fig. 52 that the long waves attain only very low heights near the harbor. The refraction coefficient values in general are low, being less than 0.18 throughout the area shown.

Fig. 53 represents the equivalent result for long-waves from the

WSW direction, external to the bay. The contour form is generally similar but the refraction coefficient values are considerably smaller and generally less than 0.05 throughout the area.

Fig. 54 presents the case for long waves entering the bay from the SSW direction. The contour form, though generally similar, differs in detail from the other cases, and shows refraction coefficients at higher levels. These are generally less than 0.37.

The relative maximum refraction coefficient values from Figs. 52 to 54 may be compared with figures quoted in Section 3 as follows:

TABLE XI

REFRACTION COEFFICIENTS
FOR LONG-PERIOD WAVES

Approach Direction	Southern Half Monterey Bay	Vicinity Monterey Harbor
WNW	0.45	0.18
WSW	0.09	0.05
SSW	0.60	0.37

The K_r-values, of course, are not expected to agree as between the half-bay and the Monterey Harbor area, but they should, and do, reflect the same relative trend.

It is now of interest to compare refraction coefficient values along the coast as between long and short waves. Reverting back to Fig. 11 it will be noticed that heavy full-line curves (marked T > 1 min.) are inserted in the region of Monterey (covering a distance of about 2-1/2 n. mi.) for the SSW, WSW and WNW directions. These depict the comparable effects of long waves. A noticeable feature here is the relative strength of the long-wave effect from the SSW direction, already remarked on in Section 3.

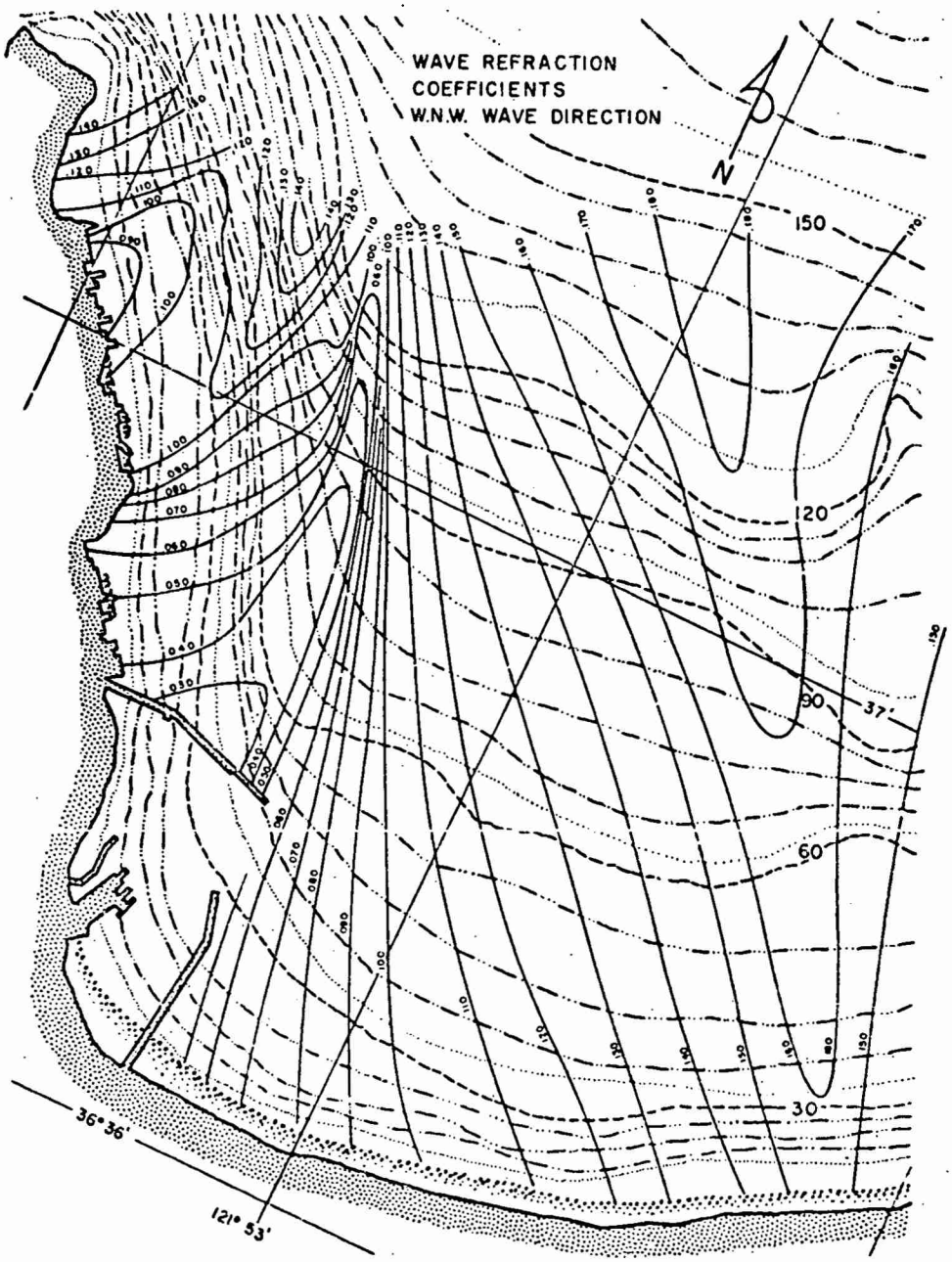

FIGURE 52 LONG-PERIOD WAVE REFRACTION COEFFICIENTS IN THE AREA OF MONTEREY HARBOR REFERRED TO WNW APPROACH DIRECTION IN 10,000 FT. WATER DEPTH

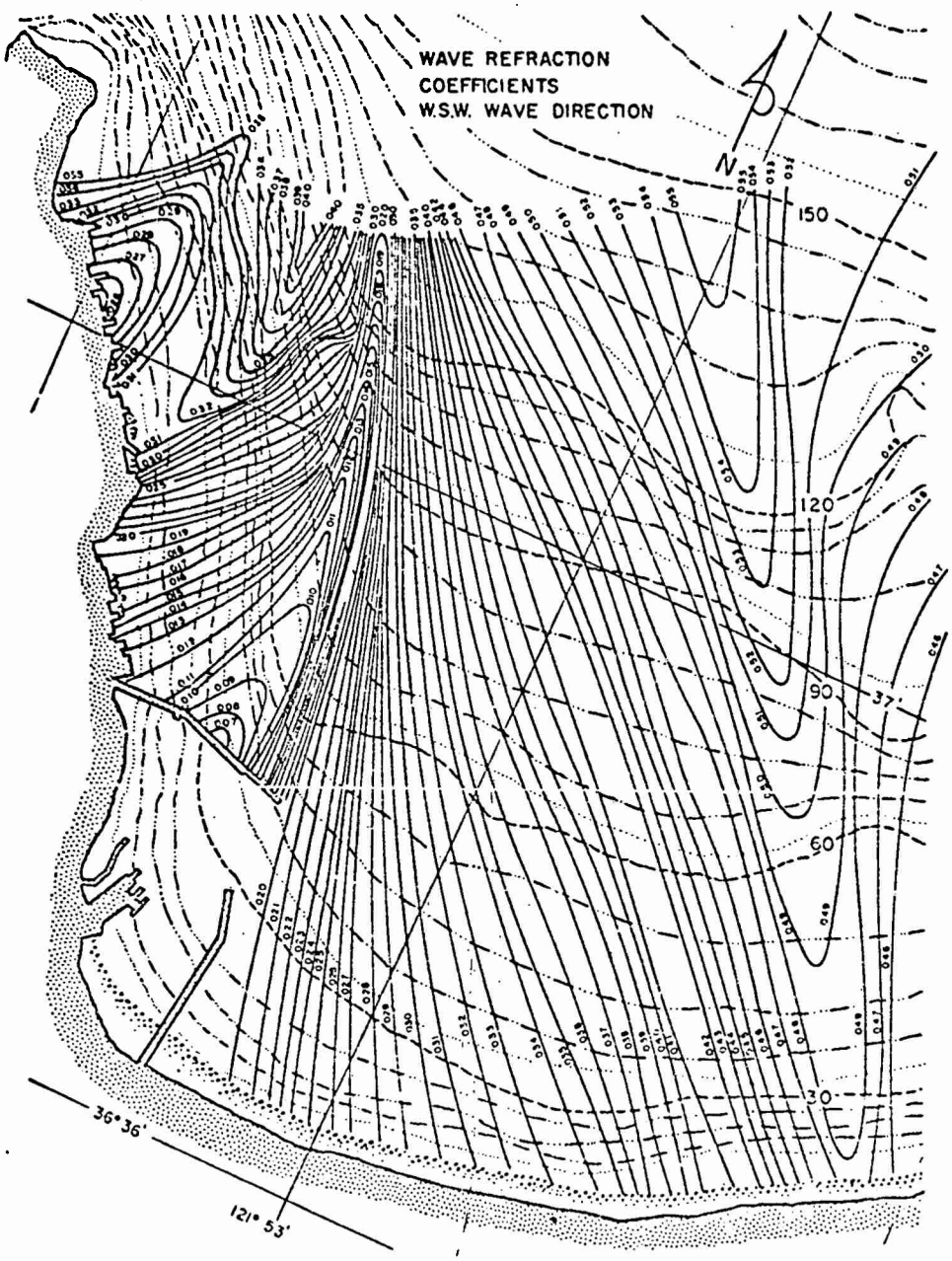

FIGURE 53 LONG-PERIOD WAVE REFRACTION COEFFICIENTS IN THE AREA OF MONTEREY HARBOR REFERRED TO WSW APPROACH DIRECTION IN 10,000 FT. WATER DEPTH

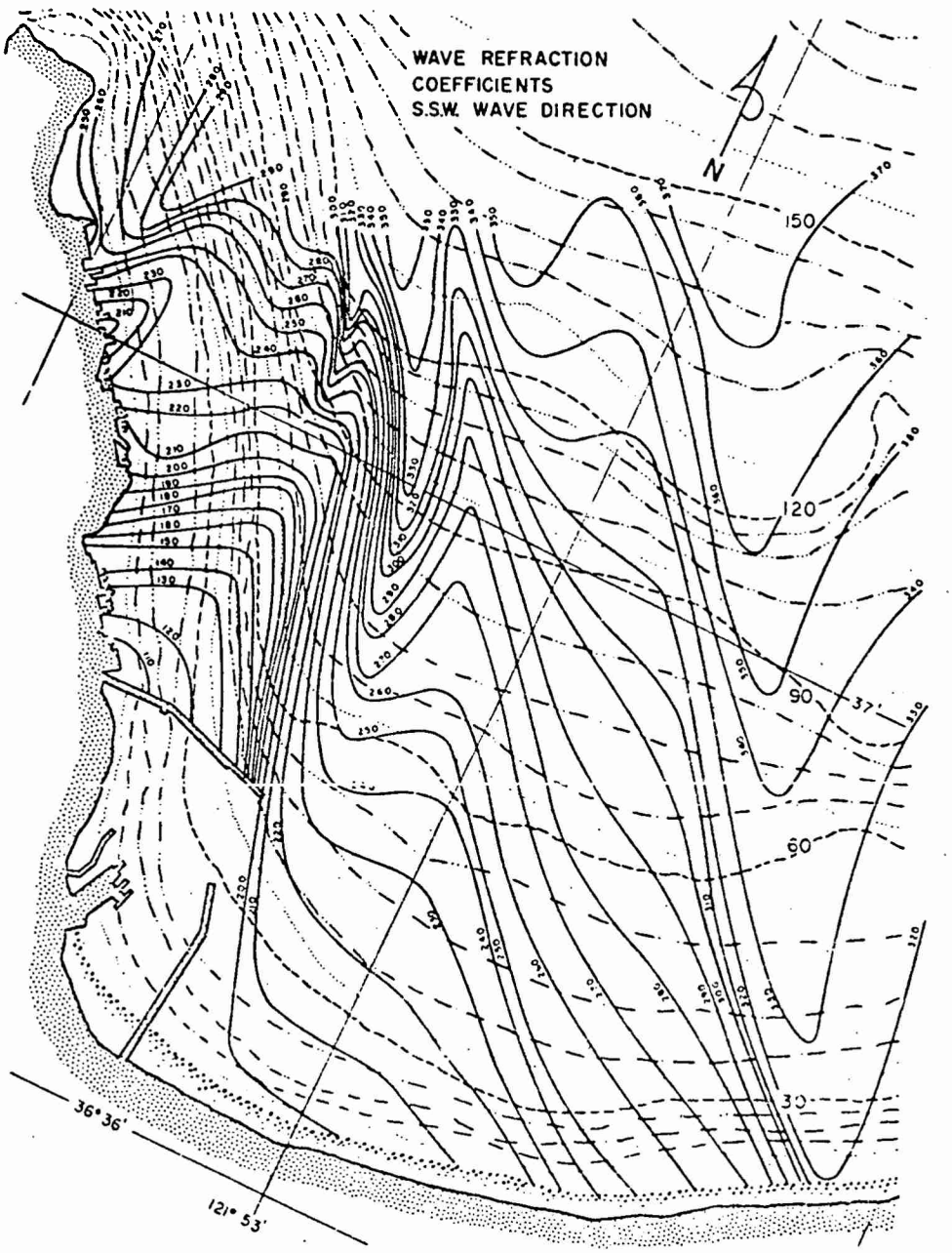

FIGURE 54 LONG-PERIOD WAVE REFRACTION COEFFICIENTS IN THE AREA OF MONTEREY HARBOR REFERRED TO SSW APPROACH DIRECTION IN 10,000 FT. WATER DEPTH

6. Refraction and Further Refraction of Long-Period Waves

Figs. 50 and 51 have shown that long-period wave fronts will vary effectively parallel the coastline on reaching the shore, particularly in the region of Fort Ord. Along the rocky coastline of the Monterey Peninsula there is some obliquity of incidence.

The smooth beaches of the bay will obviously reflect the long waves almost directly backward along their approach orthogonals, until, of course, refraction effects begin to play their part in spreading the reflected energy.

The general principle for constructing reflected waves along a boundary to which the waves are oblique is the same as that governing the reflection of light. The angle of reflection of the outgoing wave ray is taken equal to the angle of incidence of the incoming wave ray.

On this basis the primary reflections shown in Fig. 55 have been developed graphically and refracted seawards from the coast north and east of the harbor and from the breakwater of the harbor itself. The inherent tendency for the long wave energy of reflection to radiate outwards and diffuse itself along coast is patently apparent from the diverging wave rays. Numerous caustics are rapidly formed and the reflection pattern in places tends to become quite complex.

For the same area as shown in Fig. 55, Fig. 56 gives the pattern of Refraction Coefficients for the reflected waves. The contour-values refer to the reflected wave system coming off the coast and harbor from incident long waves originally from the SSW. The effect of the reflected waves in spreading and forming frequent caustics is to cause pinnacles of relatively high refraction-coefficient values at certain points in the near-harbor area. The highest of these values is 0.60 referred to the original incoming waves outside the bay.

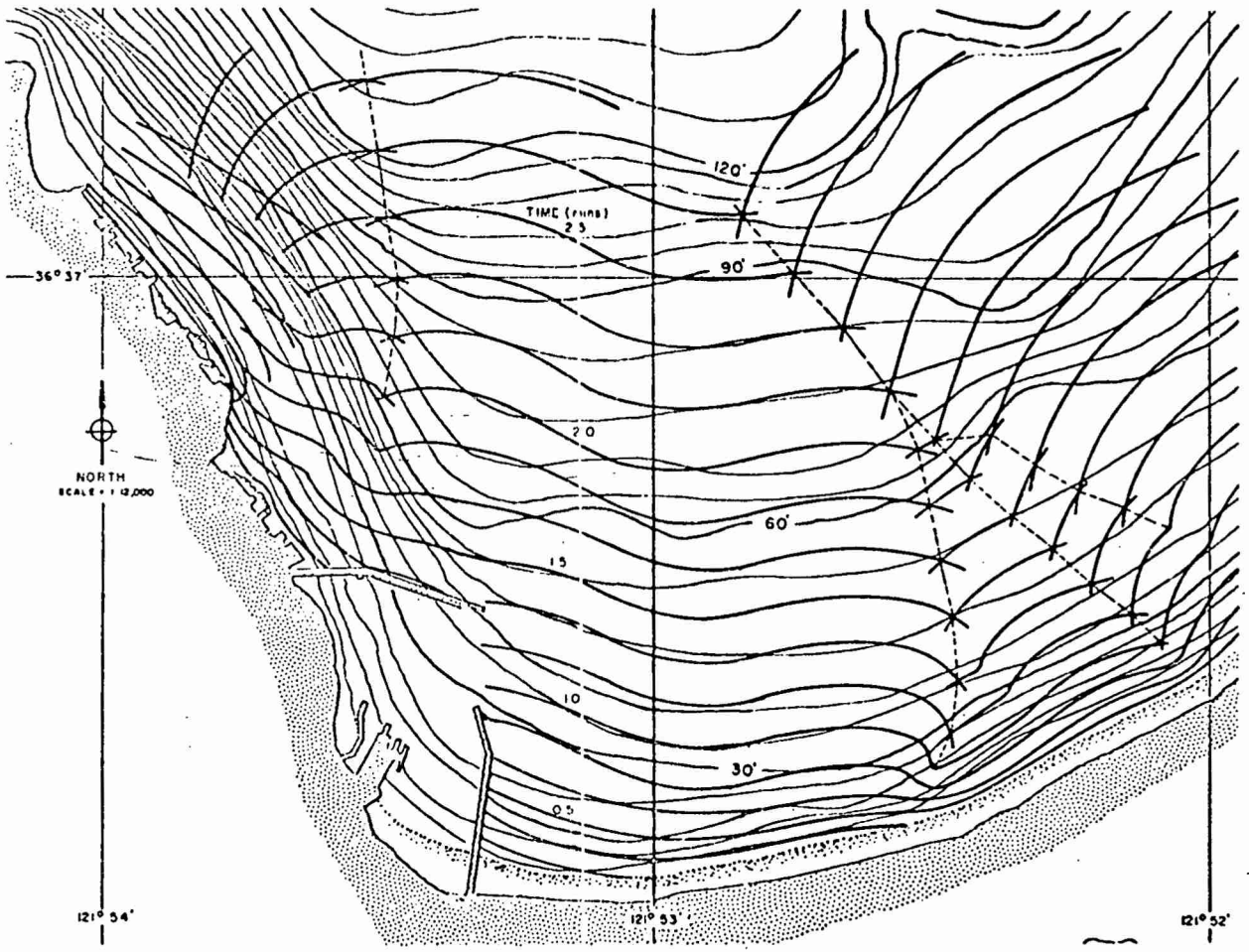

FIGURE 55 REFRACTION OF PRIMARY REFLECTED LONG WAVES IN NEIGHBORHOOD OF MONTEREY HARBOR

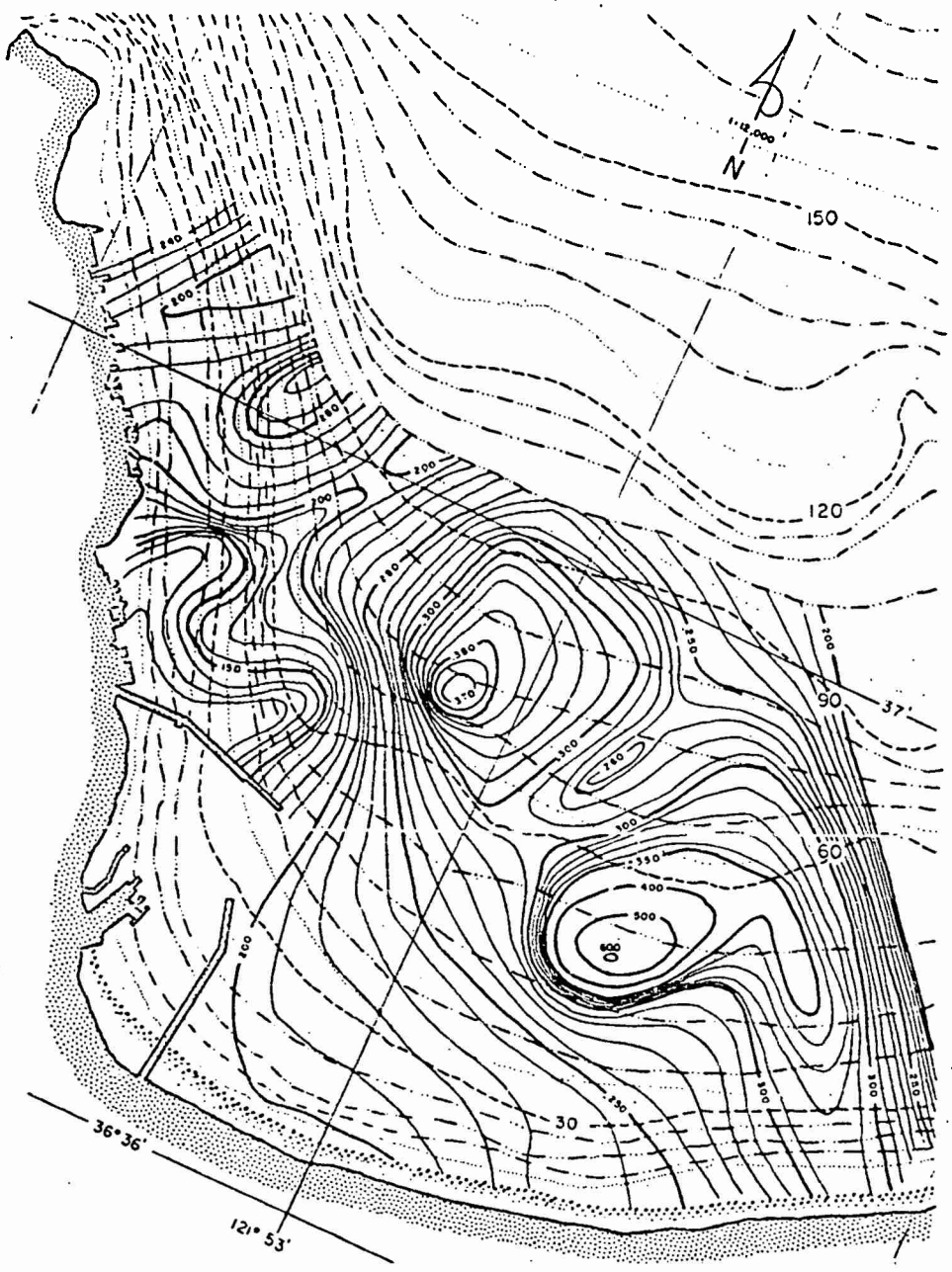

FIGURE 56 REFRACTION COEFFICIENTS FOR PRIMARY LONG-PERIOD WAVE REFLECTIONS NEAR MONTEREY HARBOR, REFERRED TO SSW APPROACH DIRECTION IN 10,000 FT. WATER DEPTH

7. Standing Waves from Incident Waves and Primary Reflections

The methods for accomplishing a graphical synthesis of standing waves from the refraction diagrams of incident and reflected waves have been outlined previously (Wilson, 1951 and 1959). The necessary condition for existence of a standing wave is that it shall have an antinode along the boundary normal to the approach direction of the waves. In evolving the oscillation pattern from wave-refraction diagrams, only the primary reflections of the incident waves are taken into account. Secondary reflections are inevitable but because they are evanescent in the overall distance of the waves travelled they may not always obscure the primary standing-wave formations.

As an example of method we show in Fig. 57 incident long waves reaching the coast in the area of Monterey Harbor from the SSW direction. By regarding these frontal positions of the waves at every 10 secs. as being part of a long wave system of 2.5 mins. (or 150 secs.), it is clear that every 10 secs. between fronts represents $10/150 \times 360^{\circ}$ (or 24°) of angular distance in the long wave.

If by normalizing the wave amplitude to unity we then assign unit amplitude for the incident wave at the coast at the point where the incident long wave reaches the root of Municipal Wharf No. 2, then 10 secs. seaward of this position at the next wave front, the amplitude will be $\cos 24^{\circ}$ or 0.914. The next wave front seaward of that will have an amplitude $\cos 48^{\circ}$ or 0.669, and so on.

By overlaying a grid on Fig. 57 as shown in Fig. 58, the values of normalized amplitude can be interpolated readily for each grid point. The same grid, overlaid on the corresponding diagram of refraction coefficient values, shown in Fig. 59, permits the values of applicable refraction coefficients at grid points to be interpolated. For each grid point the product of the normalized amplitude A_i and the refraction coefficient $(K_r)_i$ of the incident long wave finally establishes the true relative amplitude $A_i(K_r)_i$ at the point.

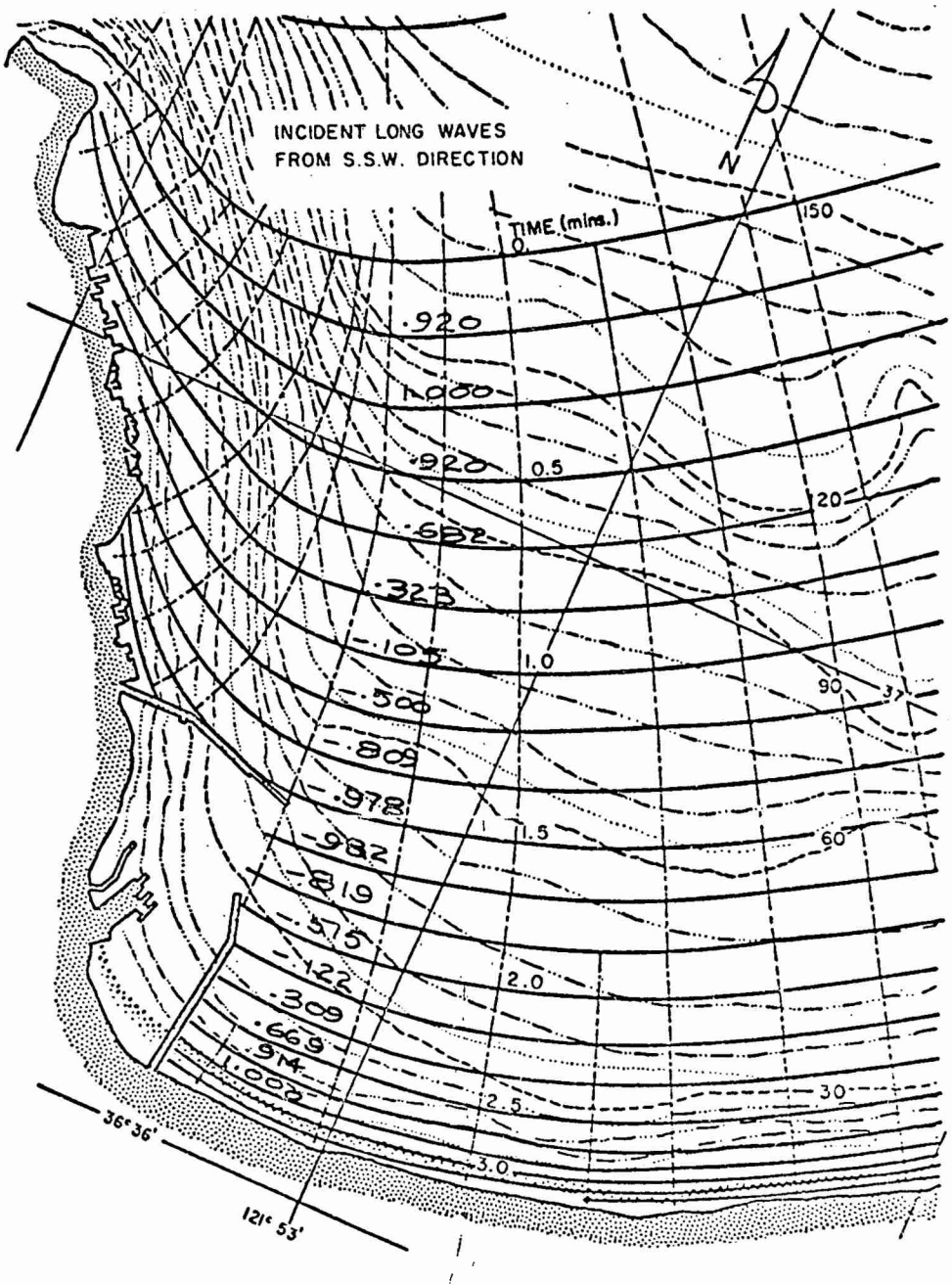

FIGURE 57 NORMALIZED AMPLITUDES OF 2.5 MIN. LONG-PERIOD WAVE INCIDENT AT MONTEREY HARBOR FROM SSW

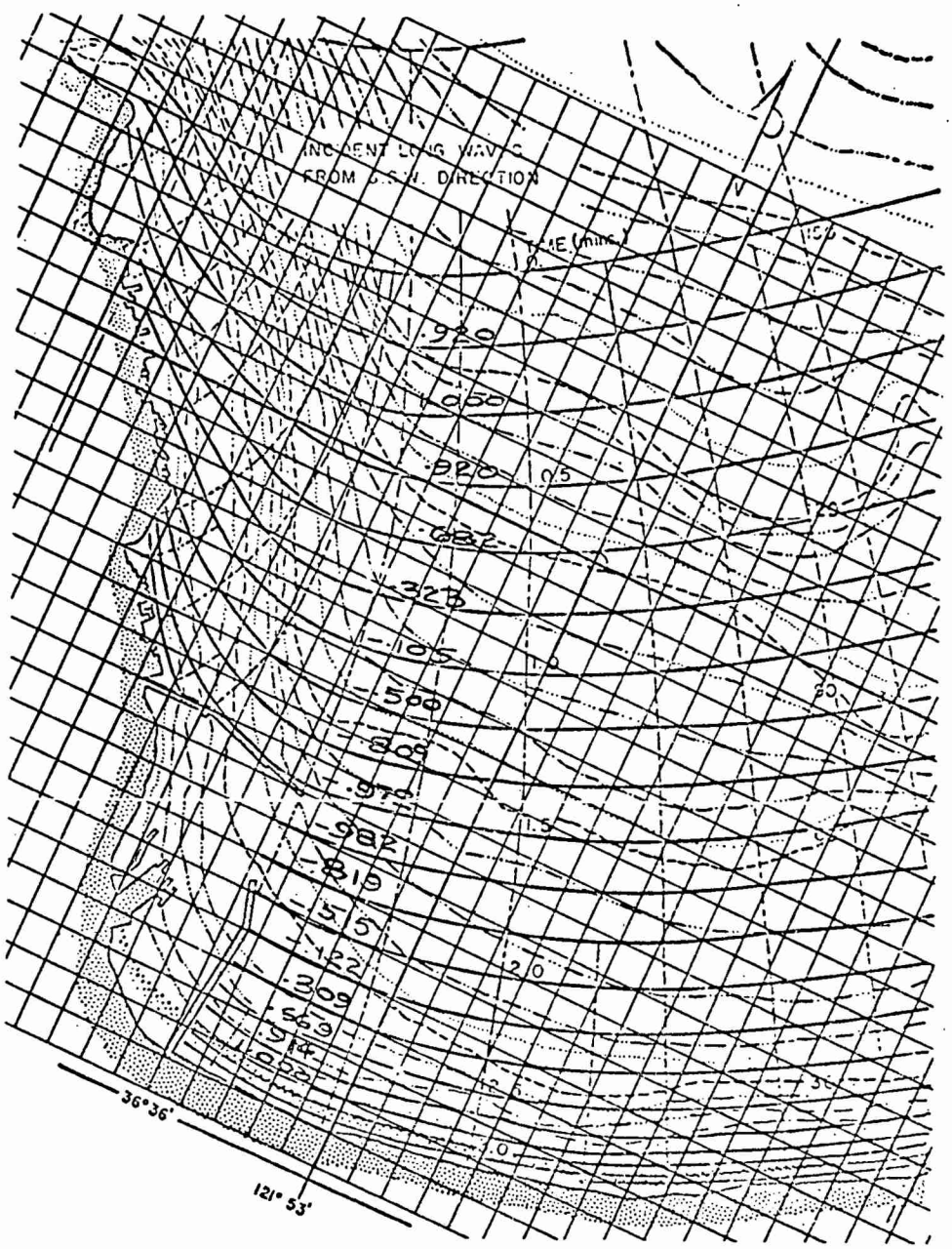

FIGURE 58 COORDINATE NETWORK SUPERIMPOSED ON FIG. 57

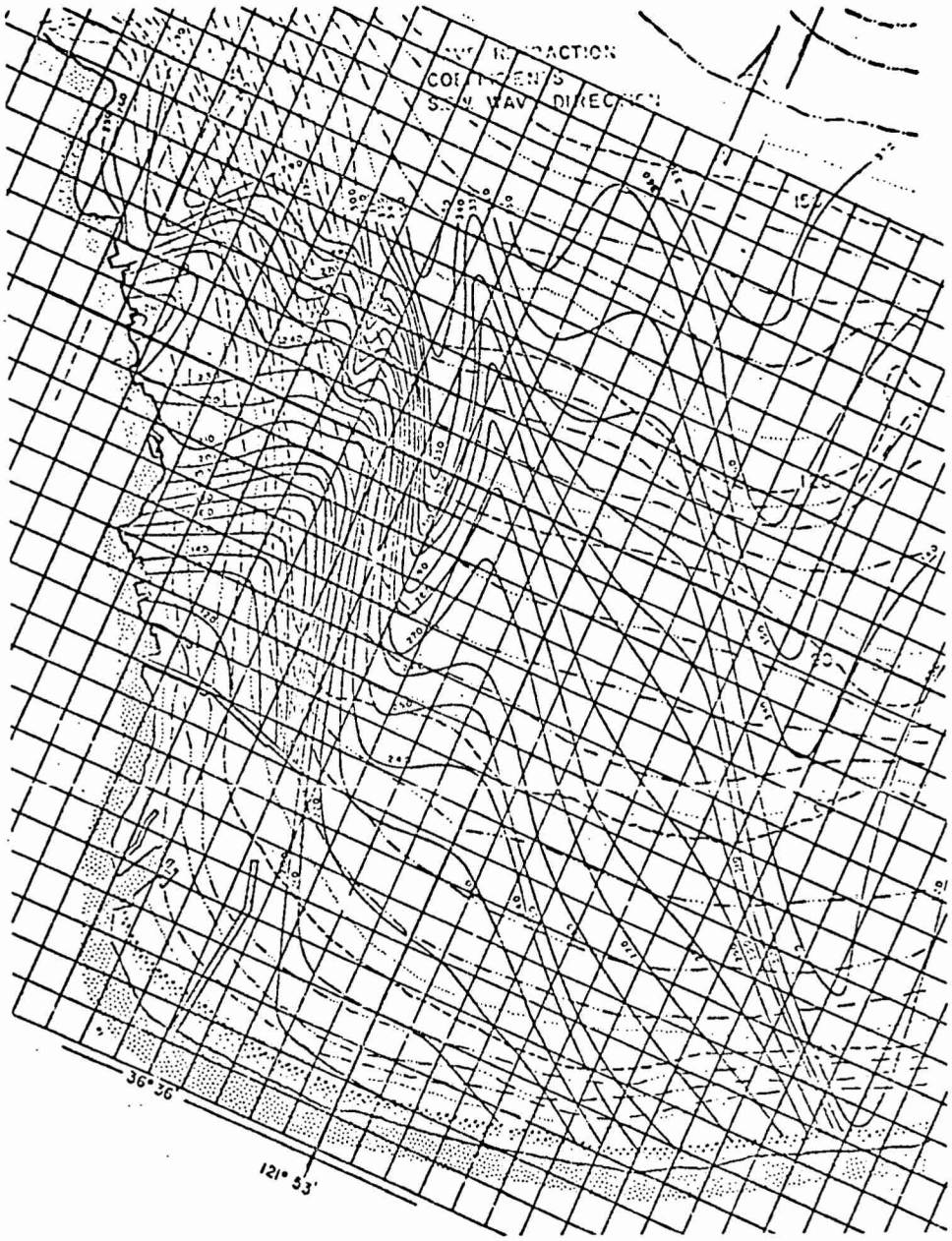

FIGURE 59 COORDINATE NETWORK SUPERIMPOSED ON FIG.. 54

The procedure for the primary reflected waves is similar and is illustrated in Fig. 60. Since the incident wave was taken to have unit amplitude at the root of the Municipal Wharf No. 2, the reflected wave must also have unit amplitude at that point. The amplitudes A_r for the primary reflection follow out from the coast in the same way as for the incident wave.

The reflection off the north breakwater of the harbor and the east coast of the Monterey Peninsula requires special consideration. Reference to Fig. 57 and comparison with Fig. 60 show that the particular reflected wave front which is in actual contact with the breakwater in Fig. 60 is the same wave front in Fig. 57 which carries the amplitude -0.978. Accordingly the amplitude of the next reflected wave front seaward of this has to be -0.982, or the same amplitude as the incident wave front in Fig. 57 which precedes that having amplitude -0.978. In this way, by continuing the same reasoning, amplitude values are assigned to all primary reflections off the breakwater as shown in Fig. 60.

At the coast adjoining the breakwater it is seen from Figs. 57 and 60 that the first reflection front is also the last incident front and can therefore be assigned the normalized amplitude -0.982. Reflected fronts seaward from this particular part of the coast then carry the amplitudes A_r shown in Fig. 4.

In Fig. 61 the grid network is overlaid on Fig. 60 and A_r values interpolated at grid points, while in Fig. 62 the grid-point values of wave refraction coefficients $(K_r)_r$ for the reflected waves are obtained. The product $A_r(K_r)_r$ finally gives the true relative amplitudes of the primary reflections.

On the assumption that no long-wave energy is lost during the primary reflection, the products $A_i(K_r)_i$ and $A_r(K_r)_r$ for the incident and reflected waves are directly additive to yield the relative amplitudes of the long waves outside the approaches to the bay.

We give finally in this section the results of applying this synthetic

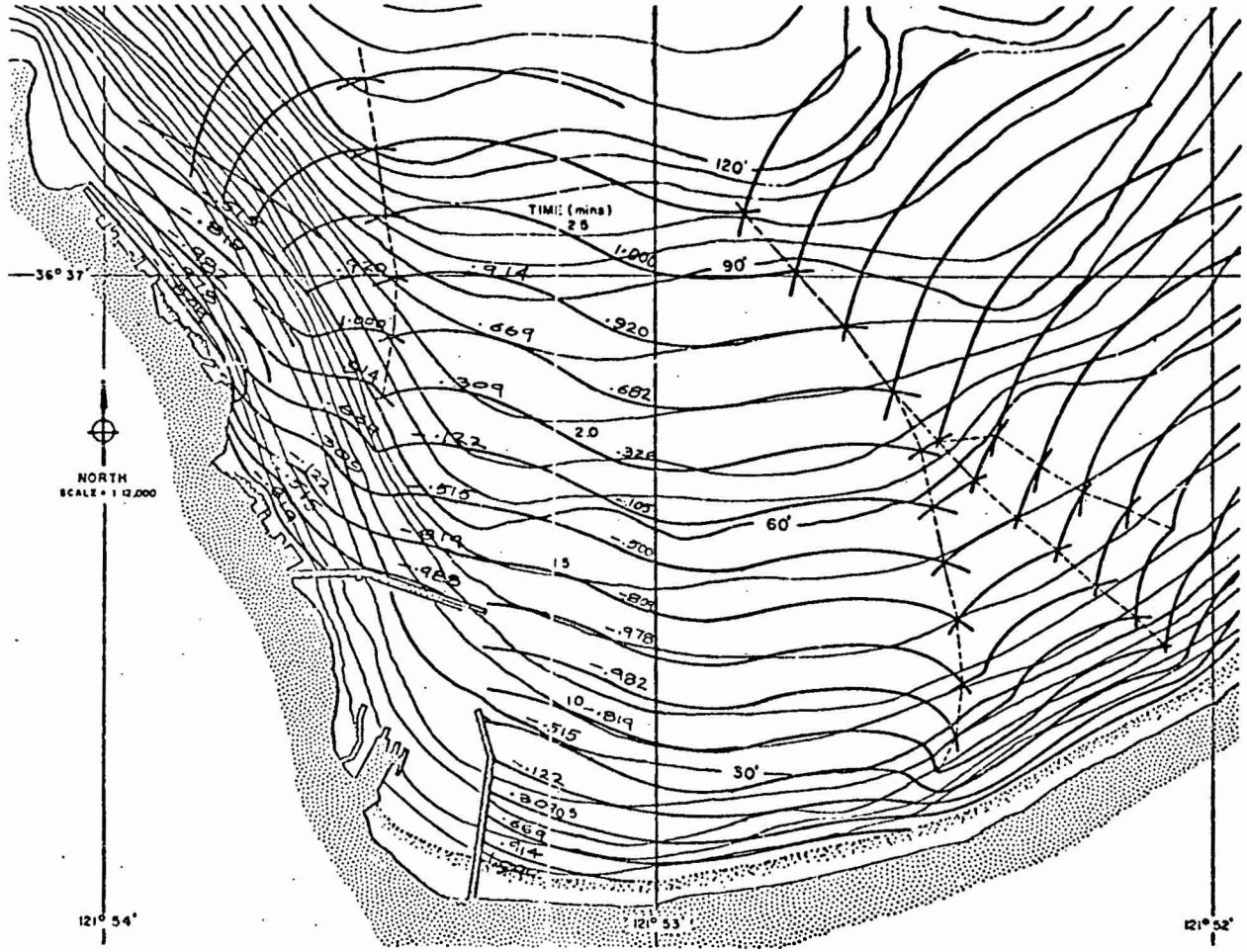

FIGURE 60 NORMALIZED AMPLITUDES OF 2.5 MIN. PRIMARY LONG-PERIOD WAVE REFLECTIONS NEAR MONTEREY HARBOR

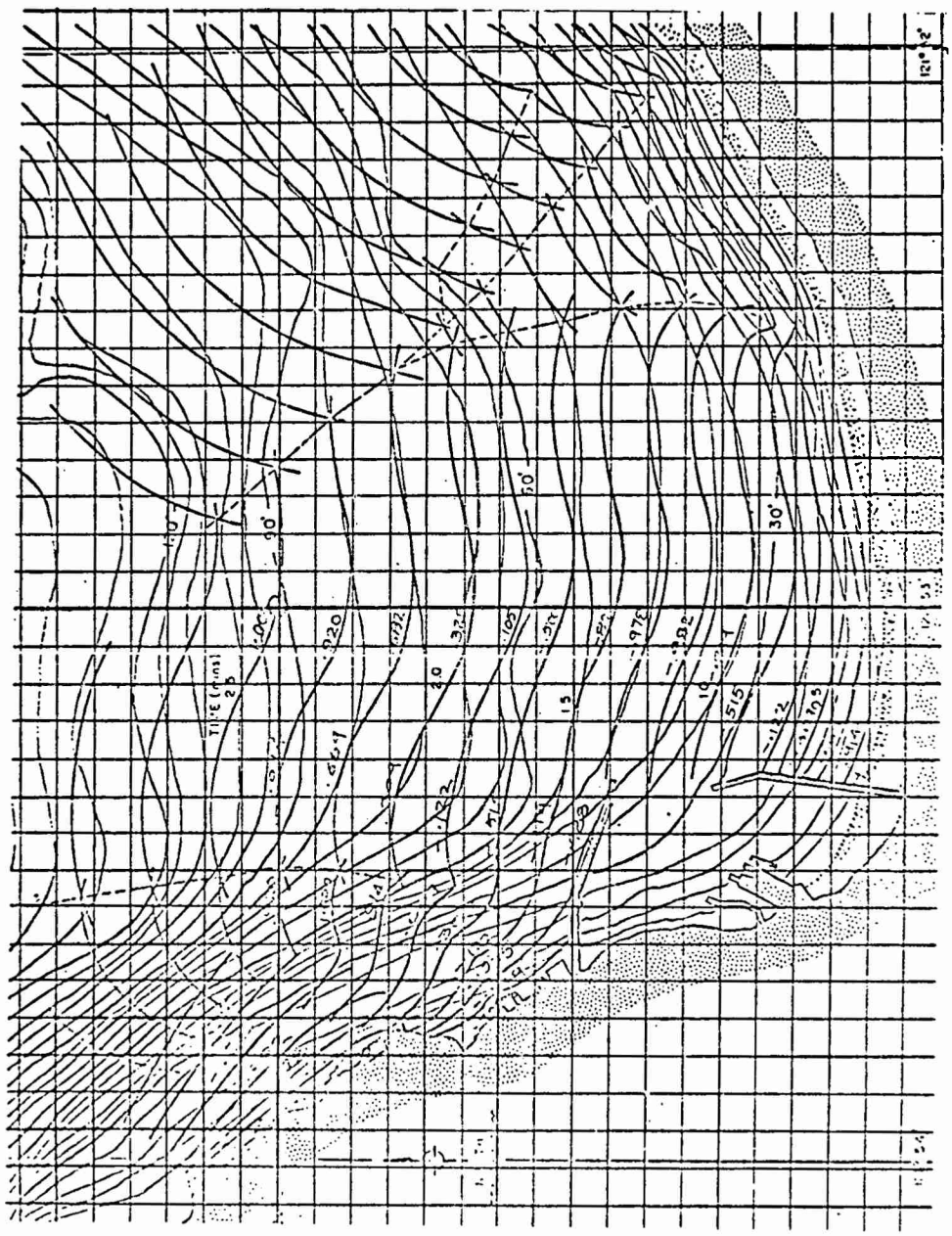

FIGURE 61 COORDINATE NETWORK SUPERIMPOSED OF FIG. 60

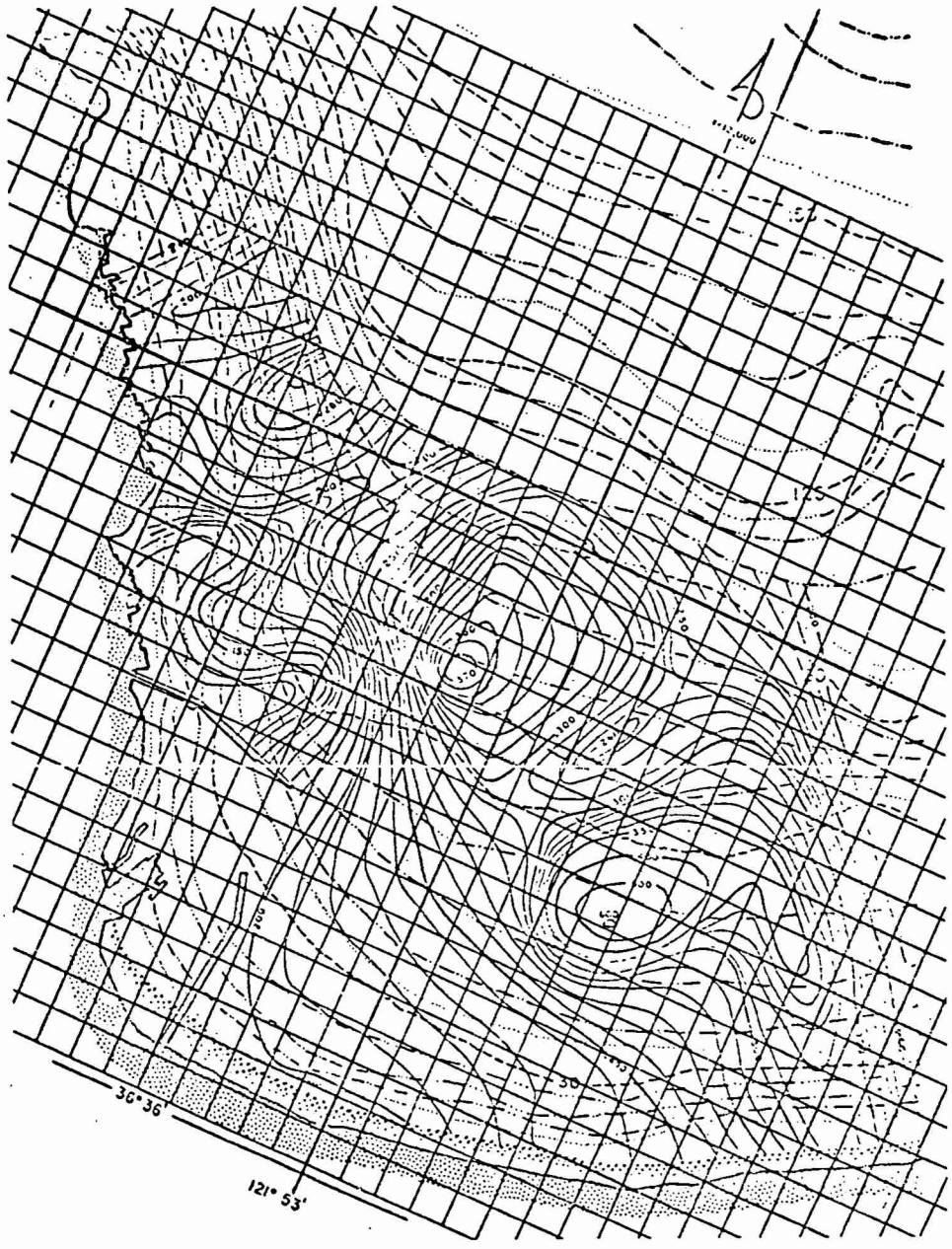

FIGURE 62 COORDINATE NETWORK SUPERIMPOSED ON FIG. 56

technique to long waves of specific periods. Thus the standing wave formed by 2.5 mins. waves is shown in Fig. 63, normalized to unit amplitude for the incoming wave in 10,000 ft. of water. The largest amplitude of an antinode in the area covered by Fig. 63 is only 0.75, which, of course, hardly supports the idea that this particular frequency can be resonant.

There is, however, an important additional aspect that remains to be taken into account. The height of a long wave propagating into shallow water is influenced by shoaling as well as refraction, and the modification of Eq. (1), taking this into account, is

$$\frac{H}{H_o} = K_r K_s = \sqrt{\frac{b_o}{b}} \sqrt[4]{\frac{h_o}{h}} \tag{23}$$

where K_s, the shoaling coefficient, in accord with Green's Law (Lamb, 1932, p. 275), is

$$K_s = \sqrt[4]{\frac{h_o}{h}} \tag{24}$$

and h and h_o are respectively the water depths for which the wave heights are (H/K_r) and H_o.

Eq. (24) would appear to be trivial when h tends to zero at the shore and K_s becomes infinite, but we can avoid this dilemma by noting from Eq. (23) that

$$H = (H_o K_r) K_s \tag{25}$$

and that when the depth h is zero there is still the wave amplitude $H/2$ to make the depth finite. Thus, by writing h in Eq. (24) as

$$h = h + \frac{H}{2} \tag{26}$$

and by combining this with Eqs. (24) and (25), the appropriate value of K_s to be used at any depth h is the root of the equation

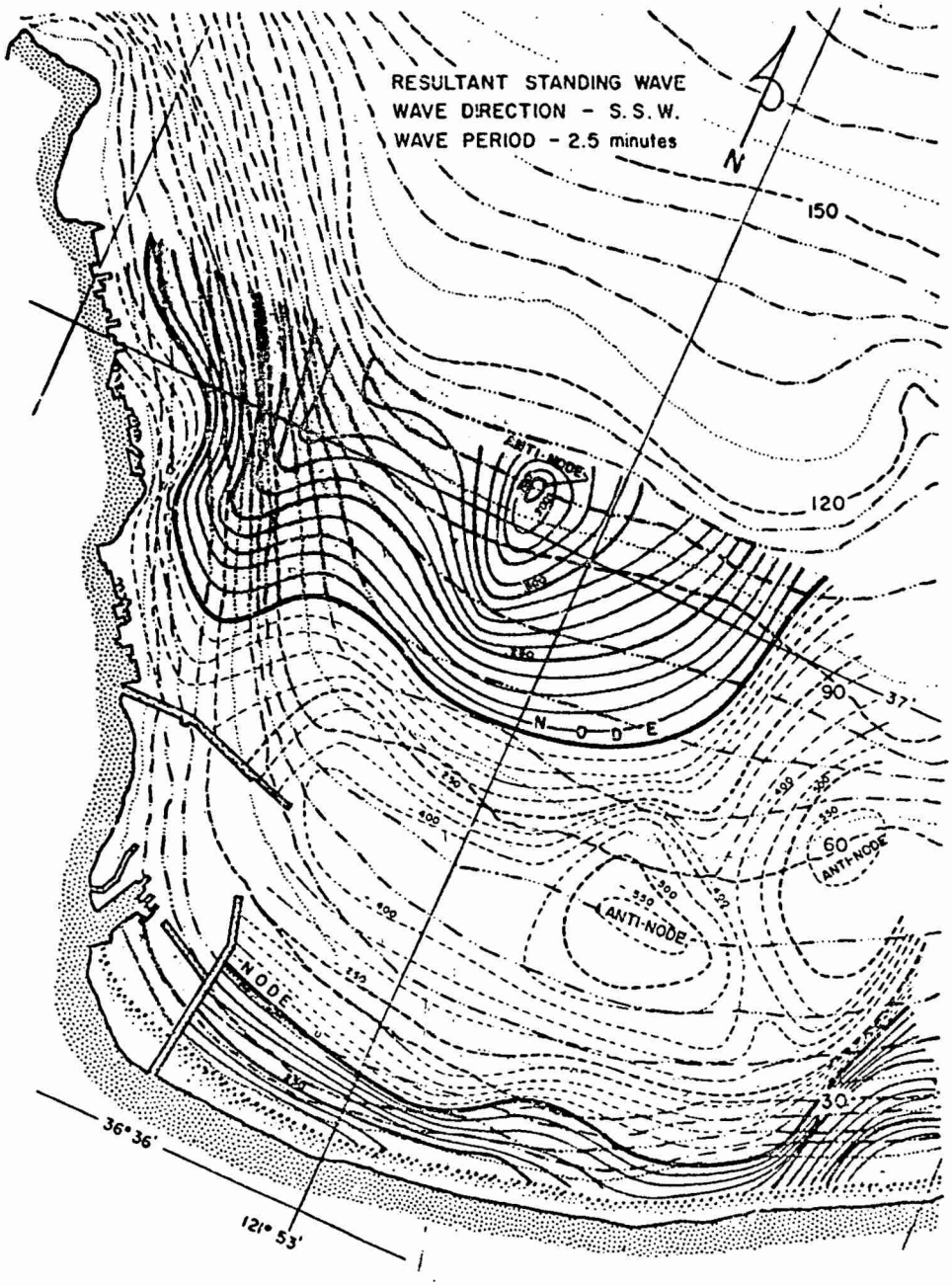

FIGURE 63 STANDING WAVE NEAR MONTEREY HARBOR RESULTING FROM 2.5 MIN LONG-PERIOD WAVES FROM SSW, NORMALIZED TO UNIT AMPLITUDE AT 10,000 FT. WATER DEPTH

$$K_s^5 + \frac{h}{A} K_s^4 - \frac{h_o}{A} = 0 \qquad (27)$$

where A now defines the amplitude $(H_o K_r)/2$ at any depth h as given by a standing-wave pattern such as Fig. 63.

At the coastal boundary for which h = 0 this leads to the result

$$K_s = \sqrt[5]{\frac{h_o}{A}} \qquad (28)$$

Consequently for h_o = 10,000 ft. and A = 0.400 (for H_o = 2.0 ft. in deep water) we find K_s = 7.578. For a 2 ft. high tsunami wave of 2.5 mins. period in 10,000 ft. of water, then, the indicated amplitude of the standing wave at the antinode near the root of Municipal Wharf No. 2 at the shore is 0.400 x 7.578 ft. or about 3 ft. The amplification factor would then be about 3 on a deep-water amplitude of 1 ft.

At the mouth of Monterey Harbor, Fig. 63 suggests that A will have a value of about 0.4 in a water depth h = 45 ft. Using Eq. (24) to calculate K_s for $h_o = 10^4$ ft. and h = 45 ft. we find K_s = 3.86. The standing wave amplitude then at the harbor entrance would be 0.4 x 3.86 or 1.55 for a 1 ft. amplitude wave in deep water (an amplification of 1.6).

The omission of the factor K_s in Fig. 63 does not greatly affect the basic pattern of the standing wave. For lack of time, therefore, the standing wave patterns for 2.5, 4.3, 6.1 and 13.3 min. long waves in Figs. 63 to 66 were not converted by the process of multiplication by K_s and this must be kept in mind.

The period of long waves selected for evaluating the standing wave formations near the harbor, shown in Figs. 63 to 66, are all periods that seem to have significance for the harbor according to information already gleaned in Parts II (10, 14) and III B (4) (cf. Tables I and II and Eq. (17)). Further discussion of this will appear in the next part.

It must be noted in passing that the results of this part can be

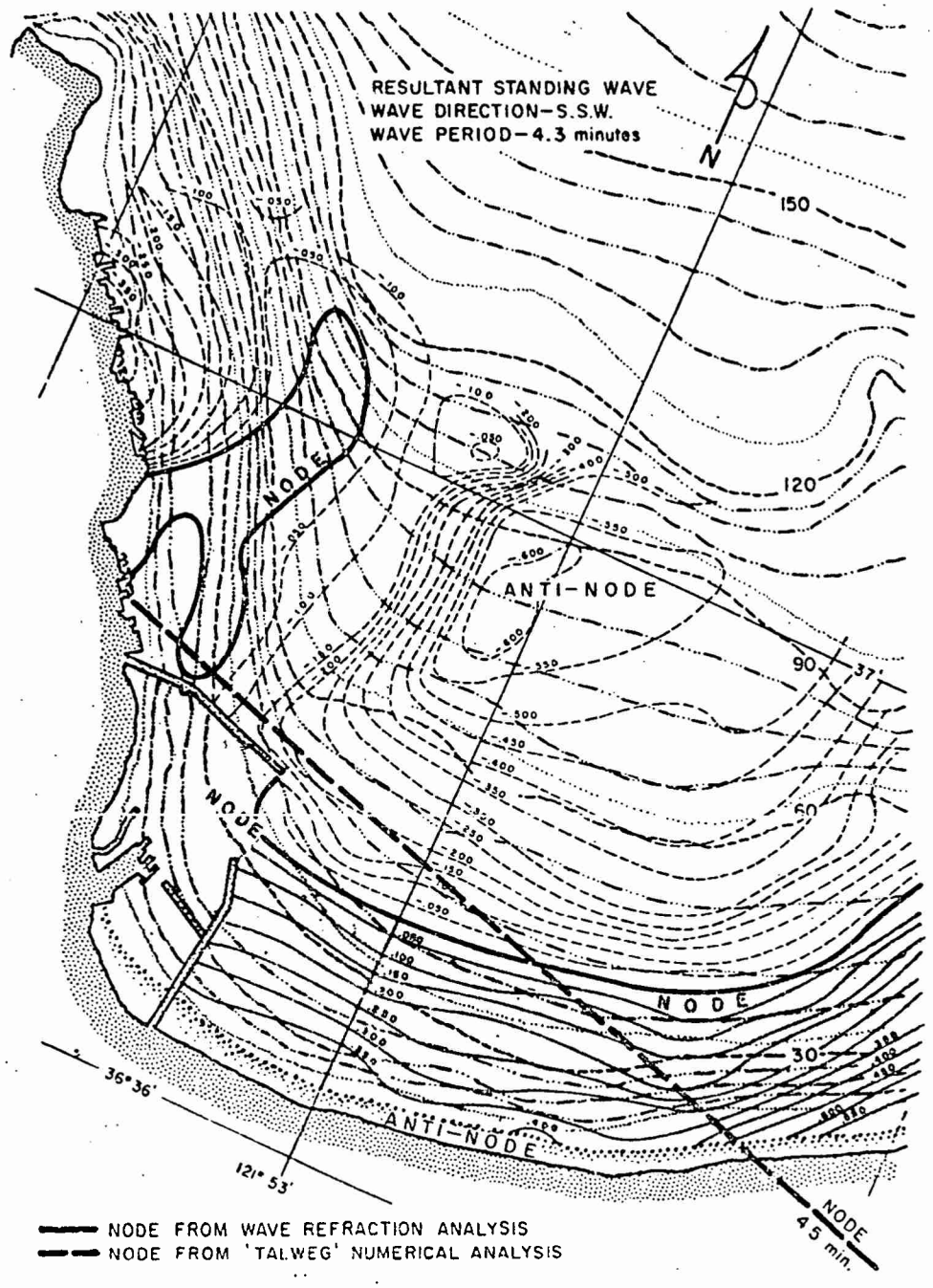

FIGURE 64 STANDING WAVE NEAR MONTEREY HARBOR RESULTING FROM 4.3 MIN. LONG-PERIOD WAVES FROM SSW, NORMALIZED TO UNIT AMPLITUDE AT 10,000 FT. WATER DEPTH

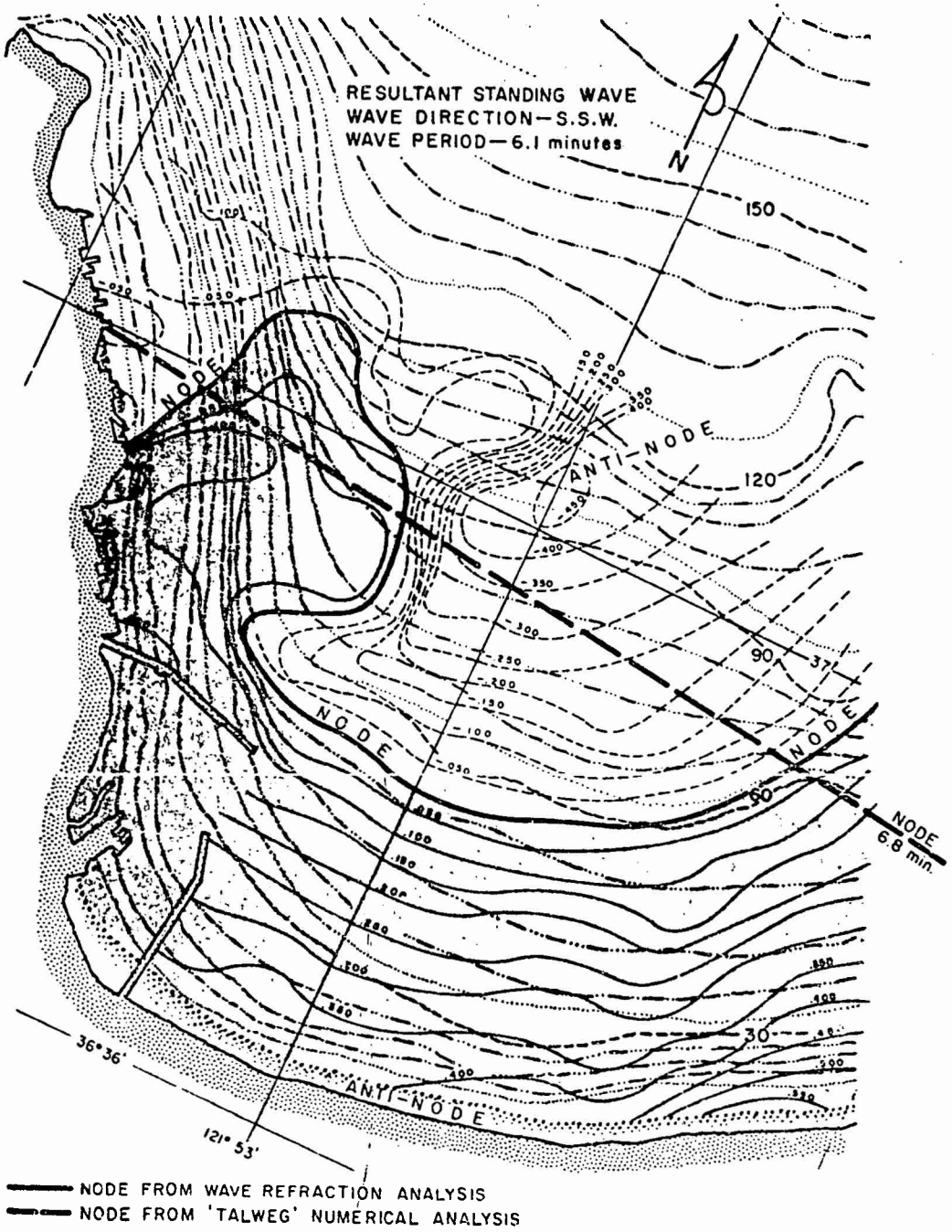

FIGURE 65 STANDING WAVE NEAR MONTEREY HARBOR RESULTING FROM 6.1 MIN. LONG-PERIOD WAVES FROM SSW, NORMALIZED TO UNIT AMPLITUDE AT 10,000 FT. WATER DEPTH

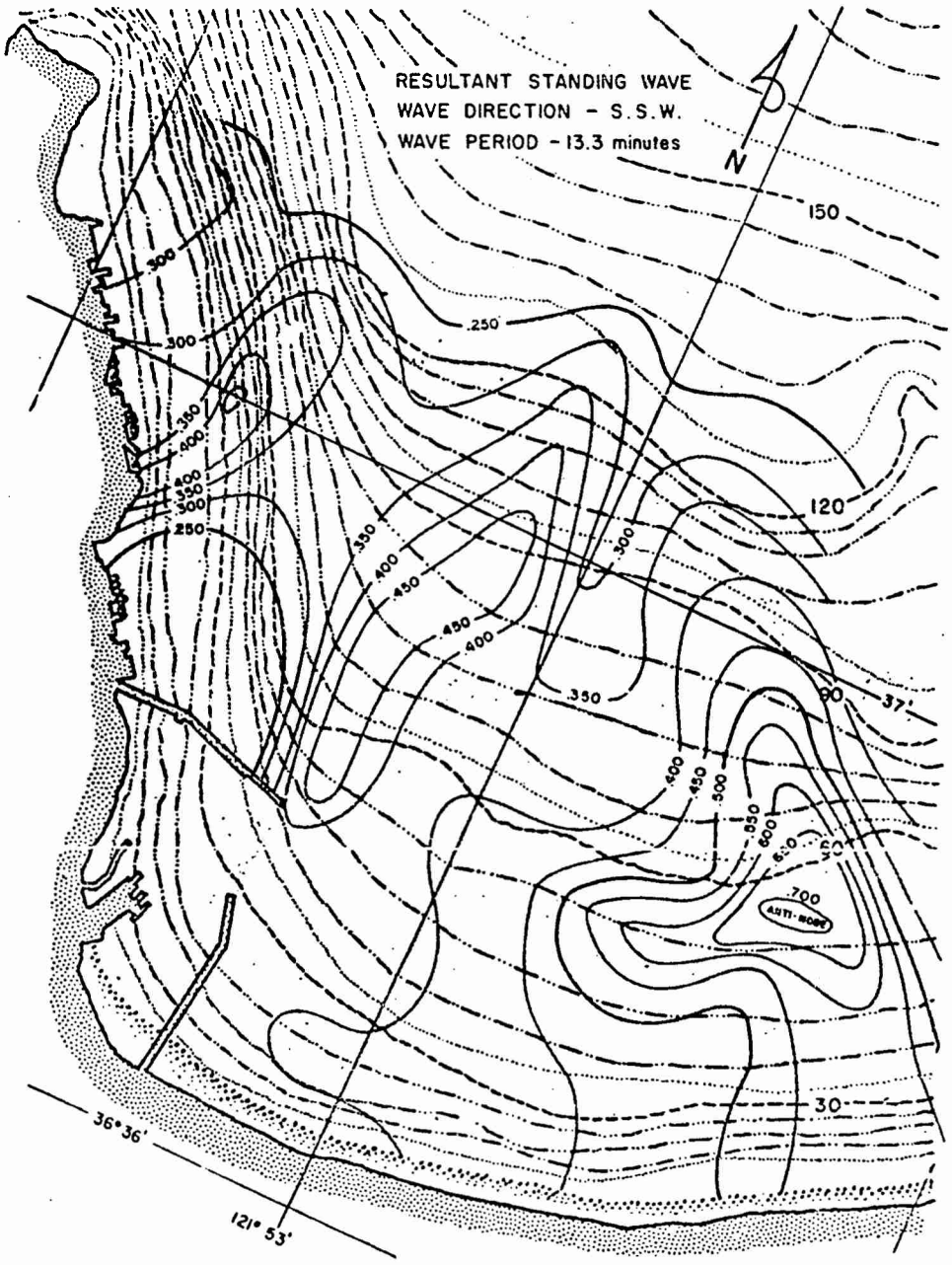

FIGURE 66 STANDING WAVE NEAR MONTEREY HARBOR RESULTING FROM 13.3 MIN. LONG-PERIOD WAVES FROM SSW, NORMALIZED TO UNIT AMPLITUDE AT 10,000 FT. WATER DEPTH

considered as being no more than guide lines to the nature of the oscillations near Monterey Harbor. Neglected have been both the reflected energy lost to the long waves in propagating into shallow water and the fact that Green's Law itself (Eq. (24)) no longer holds accurately in very shallow water (cf. Wilson, 1964), because of the changing nature of the wave form.

IV. INTERPRETATION AND CORRELATION OF FIELD MEASUREMENTS AND THEORETICAL (GRAPHICAL) ANALYSES

1. Long-Period Waves or Surf-Beats in Monterey Bay?

A question of considerable importance to surge-action modelling is whether the surging phenomenon is the result of genuine long waves originating from the open sea or whether it is merely the result of the ingress of beats of high and low waves of short period which induce the development of surf beat first drawn attention to by Munk (1949) and Tucker (1950).

The mechanism of surf-beat formation has been studied by Longuett-Higgins and Stewart (1962) and can be accounted for on the basis of a momentum flux or radiation stress of the shoreward moving waves. Lundgren (1963) has defined it in a somewhat different way as 'wave-thrust'. Although correlation has been established between beats of high waves and induced long-period surf-beats, several anomalies remain unexplained, one of which is that the expected dependence of surf-beat amplitude on the square of the wave height is not found in practice, Tucker having found the relationship to be more nearly linear.

Munk (1962) concluded that surf-beat consists of some nonlinear action between ordinary waves and their low frequency grouping, but points out that it has now been demonstrated that they are shoreward-moving long waves that are not evident in deep water. Tucker (1963), in commenting on this considers that the surf-beat waves would have to be forced waves which at some stage become released as free waves. Inconsistencies of correlation remain to be explained.

The problem before us is not so much whether surf-beats exist (which is not denied) but whether they are the sole cause of the surge phenomenon, or whether the amplitude of long-wave they generate is sufficient to account for the troubles commonly experienced in so many ports of the world and in Monterey Harbor in particular.

We have already seen that the evidence of Part II of this study favors a dissociation between severe long-period wave activity in Monterey Bay

and ordinary sea and swell waves. Much of this evidence, however, is indirect and therefore difficult to prove. It is nevertheless to be noted that both Munk, et al (1959) and Tucker (1963) now agree that surf-beats are unable to account for the whole spectrum of long-period wave activity that derives from distant storms. Furthermore, Donn and McGuinness (1960) attribute long-waves of 4 to 10 mins. period, measured at the former Texas Tower No. 4 (off New York), to air-water coupling from atmospheric waves, rather similar to that demonstrated for longer-period seiches in Table Bay by Wilson (1953a). Tucker (1963) now believes that atmospheric pressure and surf-beat probably both contribute and overlap in generating the spectrum of long wave activity.

That long-waves accompanying storms are a physical reality has been shown quite positively by Wemelsfelder (1957). Proof of this is shown in Figs. 67a and 67b which are reproduced from Wemelsfelder's paper. Fig. 67a, for instance, shows oscillations accompanying a storm tide of December 30-31, 1943 in the North Sea. The storm surge was measured at four points as it traversed the Rotterdam Waterway from the Hoek of Holland to Rotterdam and, as clearly evident, long-waves of about 40 mins. period are identifiable riding the crest and trough of the much larger storm surges. Fig. 67b, which is another example of a storm tide in the North Sea (December 29-30, 1942), shows much shorter period wave effects with identifiable periods as small as 6 mins. Still shorter periods are probably effaced by the damping in the tide gauges and the compression of the time scale.

Because of their nature long-period waves are difficult to detect by eye unless the circumstances are specially favorable. Such an occasion seems to have arisen under storm conditions on October 28, 1947, at Depoe Bay, Oregon (Bascom, 1950), when at intervals of 10 to 20 mins. a series of from 3 to 5 waves of a period of 40 secs. could be observed traversing the outer bay and coming through the narrow entrance of Depoe Bay. These long-waves are said to have had spilling fronts and to have been surfboarding flotsam on their crests. The waves caused considerable damage to small craft within the shelter of Depoe Bay. It appears that

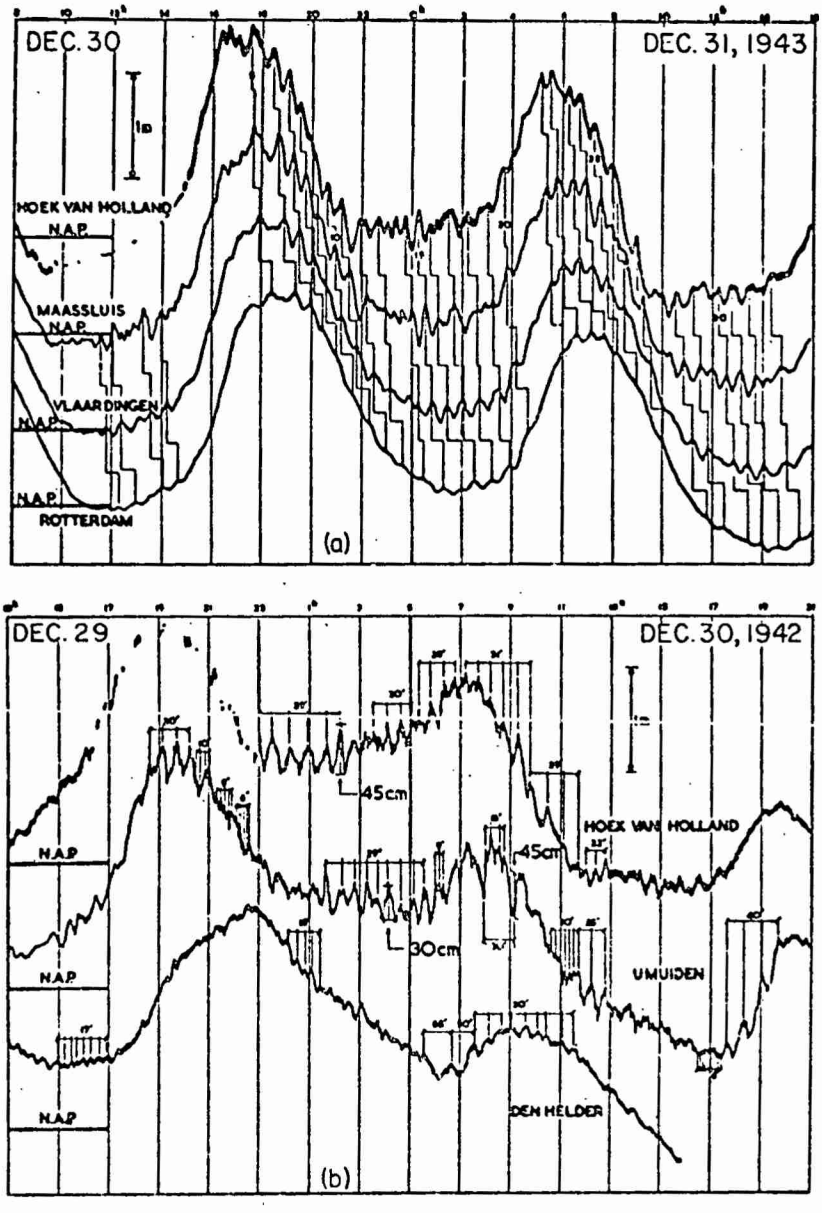

FIGURE 67 LONG-PERIOD WAVES ACCOMPANYING STORM TIDES IN THE NORTH SEA: (a) PROPAGATION OF LONG WAVES UP ROTTERDAM WATERWAY, DEC. 30-31, 1943; LONG WAVES ALONG THE COAST OF HOLLAND, DEC. 29-30, 1942 (from Wemelsfelder, 1957)

the long-waves became visible in this way because of the breaking of the ordinary waves on the outer reef.

With respect to Monterey Bay, the evidence of those wave recordings that are available, which show both ordinary short-period waves and long-period waves, seems to support the view that the dominant long-wave activity is not geared to beats of ordinary waves even when allowance is made for out-of-phasing as found in the original correlation work of Munk and Tucker.

An example of this is shown in two records (Fig. 68) obtained at Moss Landing on June 2, 1947 (11.20-12.08). These records, analyzed by Residuation procedures (see Fig. 24 and Table I) show evidence of 4.6, 2.3 and 1.4 min. waves, or oscillations, along with 47, 11 and 8 sec. waves. The short period 8 and 11 sec. waves or swells obviously occur in beats (Fig. 68) but there is no obvious correlation between the beats and the very prominent long period undulation in the record. Moreover, it is seen that the height of the long period activity at 11.58 is far greater than at 11.30 although at the latter time the swells were considerably higher than at 11.58.

Another example (Fig. 69) is drawn from data supplied to this project and is taken from MA Sensor 3 off the end of the Municipal Wharf No. 2 at the mouth of Monterey Harbor. This shows the wave trace at low (1 in. = 7.5 mins.) and high speed (1 in. = 30 sec.) operation. It is obvious that the large long-period waves found in this record (periods 1.7 mins. and 45 secs., cf. Table I and Fig. 22) are not easily linked with the small short-period swells in evidence.

Yet another case of this kind is to be seen in Fig. 25 where large amplitude long-period waves were accompanied by low wind waves under almost calm sea conditions (cf. report of Mr. G. P. Reilly quoted in Part II (10)).

The evidence that could be mounted to show directly or indirectly that harbor surging is much more than a phenomenon of surf-beats could be massive if recourse were had to data from Table Bay Harbor, Cape

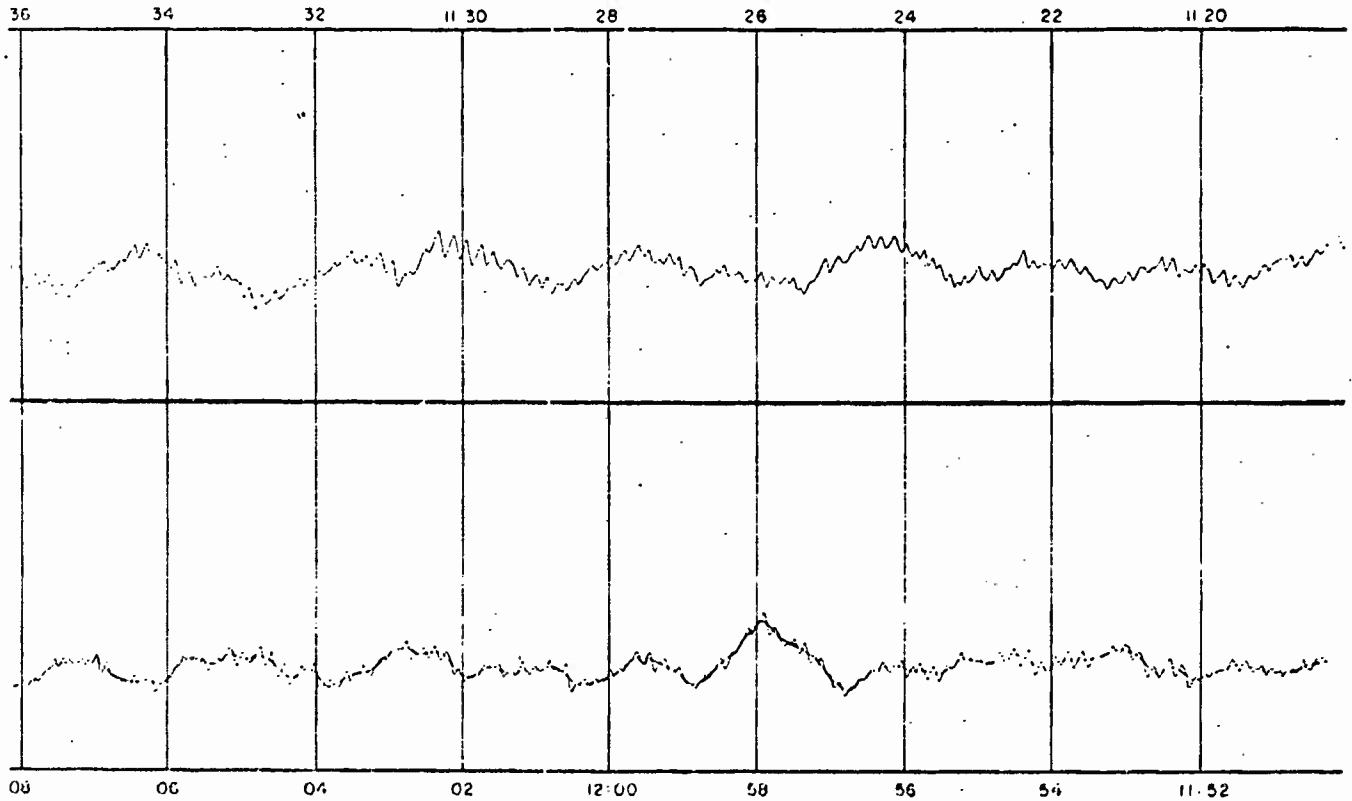

FIGURE 68 ORDINARY SWELLS AND LONG-PERIOD WAVES AT MOSS LANDING MONTEREY BAY, JUNE 2, 1947

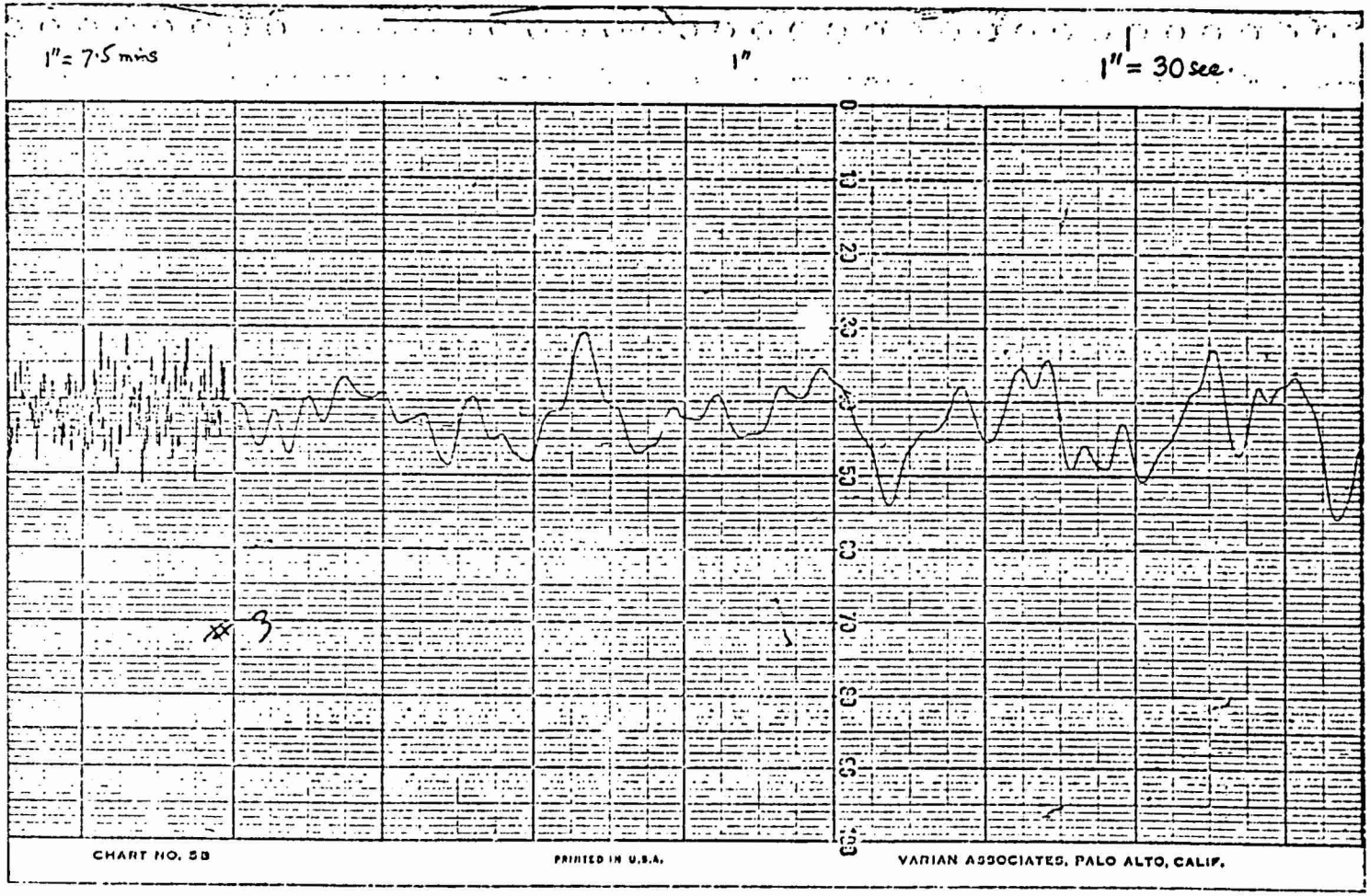

FIGURE 69 FACSIMILE OF WAVE RECORD FROM MA SENSOR 3, OFF END OF MUNICIPAL WHARF NO. 2, FEB. 10, 1964

Town (Wilson, 1951, 1957, 1959). In lieu of this it seems pertinent to point out one important observation. Although beats of waves pound all the coastlines of the world, there is singularly little evidence of serious harbor surging along any of the coastlines that lie in the lee of the land, relative to the movements of the large cyclonic storms of the temperate regions. On the other hand, one finds without exception that the coastlines that directly face the paths of extra-tropical and tropical cyclonic storms suffer acutely from long-period surging.

The association of the surging with cyclonic storms is now undeniable (Wilson, 1951, 1957, 1959; PIANC, 1957). At Cape Town, South Africa, the frequency of occurrance of surge troubles (mild, medium, severe or very severe), is shown on a monthly and annual basis (Fig. 70) from data given by Joosting (1959). From this it is clear that frequency of surging is related to the stormy winter months of May to August in the Southern Hemisphere (Fig. 70 a). There is also evidence to show (Fig. 70 b) that the surge phenomenon has a long-period secular fluctuation in intensity which appears to be related (with a phase and inverse-amplitude difference, Fig. 70 c) to the sunspot cycle. Attention to this was drawn by Wilson (1951, 1959 b) and by Joosting (1963). The explanation offered for this connection is that the sunspot cycle, through its known influence on solar radiation received by earth, causes a slow oscillation north and south, at 11-year intervals, of the atmospheric high pressure belts that overlie the oceans. This oscillation affects the dominant paths of the cyclonic storms correspondingly, and hence their proximity, or otherwise, to ports afflicted by surging.

On the basis of evidence available at present, then, we conclude that the surging in Monterey Bay is more likely to be a result of genuine long-period waves from the open ocean than from surf-beats generated locally by swells.

2. Oscillations Occurring in and Critical to Monterey Harbor

From the considerations of Part II (10) and (11) it was concluded tentatively that long-period waves in the period-band less than 3 mins.

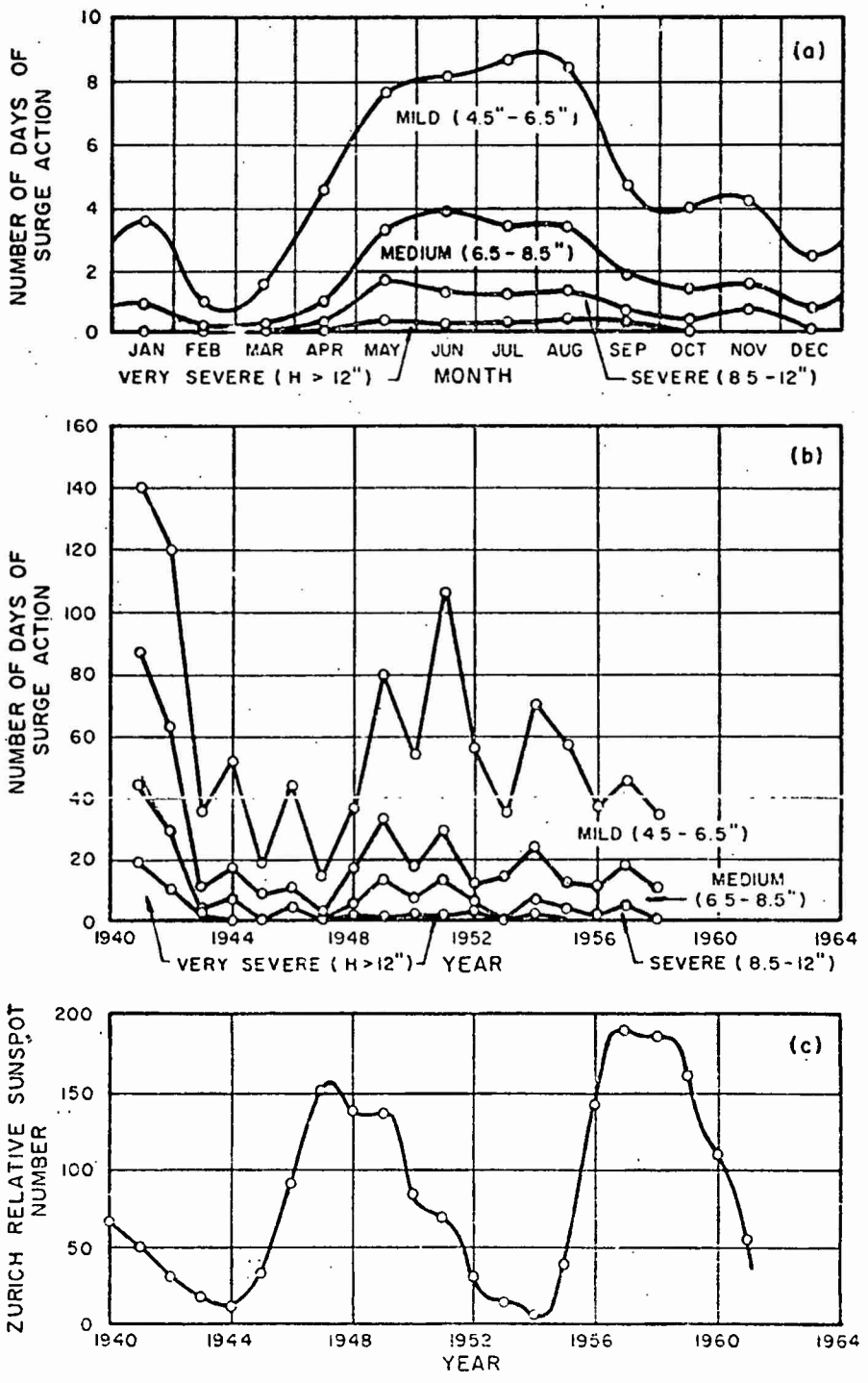

FIGURE 70 FREQUENCY OF OCCURRENCE OF SURGING IN TABLE BAY HARBOR, CAPE TOWN

were likely to be most critical for Monterey Harbor and its marina in particular and that a periodicity of about 1.7 mins. might be particularly important for the latter.

We may examine this question further, if approximately, by making rough estimates of the fundamental modes of oscillation in which Monterey Harbor is likely to resonate.

By utilizing the result of the second row of Table V and likening the outer basin of the harbor to a rectangular open-mouth basin with sloping bed for which the length $L \simeq 1400$ ft. and the maximum depth $h_1 \simeq 32$ ft., we find for the fundamental period

$$T_1 = 230 \text{ secs.} = 3.8 \text{ mins.}$$

Its second-modal period T_2 would be $0.435\ T_1$ (Table V) or

$$T_2 = 1.7 \text{ mins.}$$

The first of these periods would seem to explain the great prominence of the 3.9 min. sea-energy hump at Sensor 1 location in the wave spectra of Figs. 26. It could also explain the minor hump at 1.67 mins. period seen in Fig. 26a.

Utilizing the same equation from Table V with application to the marina, which also approximates a basin with sloping bed, the relevant dimensions now are $L \simeq 700$ ft., $h_1 \simeq 16$ ft. From this we find

$$T_1 = 162 \text{ secs.} = 2.7 \text{ mins.}$$

$$T_2 = 100 \text{ secs.} = 1.7 \text{ mins.}$$

The results are for an open-mouth basin.

Since the marina has only a very narrow entrance and is virtually sealed off, though able to absorb external excitation, it may also oscillate

or show response in the manner of a closed basin with sloping bed, in conformity with row 5 of Table III. In this case its fundamental and second-mode periods would be

$$T_1 = 101 \text{ secs.} = 1.7 \text{ mins.}$$

$$T_2 = 55.4 \text{ secs.}$$

These results are of considerable interest for they seem to explain, nominally at least, both the importance of the 2.3 min. sea-energy humps in Fig. 26 and also the significance of a 1.7 min. periodicity as a possible cause of trouble in the marina. In this respect it should be noted that these oscillations would require strong movements of water through the marina entrance in keeping with the observations.

The prominence of the 2.3 min. periodicity outside the marina, particularly in the breakwater bight is unexplained but could easily arise through the external basin resonating in some other mode to that presumed above.

We may conclude and confirm then that the troubles of the marina and harbor are definitely related to the incidence of long wave energy in the period range below 3 mins.

3. Oscillating Behavior of Monterey Bay

The numerous methods of approach which have been used in Part III to study the oscillating characteristics of Monterey Bay shows both interesting similarities and disturbing inconsistencies.

If we were to ignore the three-dimensional numerical work of Part III C we should have theoretical results apparently in reasonable agreement. The following comparisons evolve:

A. Theoretical (Analytic) Models - (Two-Dimensional Modes)

(a) Circular Bay (Semi-Paraboloidal Bed) Analogy (cf. Table VII)

$$T_n = 29.8,\ 17.2,\ 12.2,\ \ldots\ldots \text{mins.} \quad (29)$$

(b) Circular Bay (Horizontal Bed) Analogy (cf. Table VII)

$$T_n = 31.1,\ 17.0,\ 11.7,\ \ldots\ldots \text{mins.} \quad (30)$$

(c) Triangular Bay (Sloping Bed) Analogy (cf. Table VIII)

$$T_n = 27.7,\ 15.0,\ 10.4,\ 7.8,\ \ldots\ldots \text{mins.} \quad (31)$$

(d) Triangular Bay (Horizontal Bed) Analogy (cf. Table VIII)

$$T_n = 21.9,\ 9.6,\ 6.1,\ 4.5,\ \ldots\ldots \text{mins.} \quad (32)$$

(e) Rectangular Bay (Sloping Bed) Analogy (cf. Table VIII)

$$T_n = 29.2,\ 12.7,\ 8.1,\ 5.9,\ \ldots\ldots \text{mins.} \quad (33)$$

(f) Rectangular Bay (Semi-Parabolic Bed) Analogy (cf. Table VIII)

$$T_n = 24.8,\ 10.2,\ 6.4,\ 4.7,\ \ldots\ldots \text{mins.} \quad (34)$$

B. Theoretical (Numerical) Models - (Two-Dimensional Modes)

(a) 'Talweg' Approximation (cf. Eq. (14))

$$T_n = 32.3,\ 14.3,\ 9.5,\ 7.0,\ 5.8,\ 5.1,\ 4.5,\ 4.1,\ \ldots\ldots\ldots\ldots \text{mins.} \quad (35)$$

C. Theoretical (Graphical) Model - (Two-Dimensional Mode)

(a) Long-Wave Travel-Time Approximation

$$T_n = 28, \ldots\ldots\ldots\ldots\ldots \text{mins.} \qquad (36)$$

The most accurate of these theoretical models is obviously likely to be B (a) with the sequence of periods (35). However, the only periods in the field measurements of Table I and II that can approximately match the sequence (35) are T_n = 28.5 to 36.3 mins. (Table I) or T_n = 33.3 mins. (Table II); T_n = 8.4 to 9.3 mins. (Table I) or T_n = 9.5 mins. (Table II), so that we are not really assured that the meaning of these latter periods found in the field data conforms to the two-dimensional modes of oscillation of the whole bay as suggested by the period sequences (29) to (36).

When we compare three-dimensional modes of oscillation, the following results may be cited from Parts III A and III C:

D. Theoretical (Analytic) Models - (Three-Dimensional Modes)

(a) Circular Bay (Semi-Paraboloidal Bed) Analogy (cf. Table VII)

$$T_n = 60, 42, 30, 24.3, 22.5, 18.8, 17.2, 14.9, 12.7, 12.2, \ldots\ldots \text{mins.} \qquad (37)$$

(b) Circular Bay (Horizontal Bed) Analogy (cf. Table VII)

$$T_n = 65, 38, 31, 22.5\text{-}22.3, 17.8, 17.0, 15.9, 12.8, 11.7, 10.1, \ldots\ldots \text{mins.} \qquad (38)$$

E. Theoretical (Numerical) Models - (Three-Dimensional Modes)

(a) Polar Coordinate Network Approximation (cf. Figs. 35 to 38)

$$T_n = 44.2,\ 29.6,\ 28.2,\ 23.3,\ 21.6,\ 20.4,\ 19.4,\ 18.7,\ 17.6, \ldots . 13.3, \ldots . \quad 12.4, \ldots \ldots \text{mins.} \tag{39}$$

From Parts II (10) and II (11), the combined sequence of periods from field observations and analysis is

F. Measured Observations (Residuation and Spectral Analyses)

(a) Residuation Analyses (Monterey, Moss Landing and Santa Cruz) (cf. Table.I)

$$T_n = 86\,(?),\ 60\text{-}66,\ 28.5\text{-}36.3,\ 19.6\text{-}23.2,\ 17.1\text{-}17.3,\ 11.0\text{-}13.6,\ 8.4\text{-}9.3,\ 6.1\text{-}6.3,\ 5.5\text{-}5.9, \ldots . \text{mins.} \tag{40}$$

(b) Spectral Analyses (Monterey) (cf. Table II)

$$T_n = 33.3,\ 22.2,\ 16.7,\ 13.3,\ 9.5,\ 7.4\text{-}8.3,\ 5.8\text{-}6.1,\ 4.9\text{-}5.3, \ldots . \text{mins.} \tag{41}$$

The sequences (37) to (41) show resemblance here and there but no very great overall consistency. That there should be is perhaps expecting too much, for the obvious reason that all the periods in the sequence (39) could not be expected to register at Monterey for comparison with the sequence (41).

Of the theoretical results D and E for three-dimensional modes of oscillation of Monterey Bay, E (a) must be considered most accurate. This being so, we must attempt to align the sequence (39) with such

observations as are applicable. First it must be noted, on reverting back to Figs. 35 to 38, that the deep canyon in Monterey Bay functions very much as a divider between the north and south portions of the bay, whose free oscillations therefore are to a large extent uncoupled. Perhaps this is really not surprising since the effect of any sharp discontinuity in submarine topography, equivalent to the edge of a continental shelf, is to serve as a nodal position for any shelf oscillation to which the shelf is susceptible. The fundamental-mode oscillation shown in Fig. 35 b is uninodal for the north (Santa Cruz) end of the bay with the node effectively lying at the bay mouth and along the northern edge of the submarine canyon (see inset). The southern part of the bay is largely unaffected by the period of 44.2 mins.

Reference to Table I (or period-sequence (40)) and Table II (or period-sequence (41)) shows no evidence for a 44 min. oscillation in the wave spectra and Residuation analyses of the long wave records. This lack of evidence is not necessarily a disqualification for the numerical study. It probably means no more than that the assumption of a node-line at the bay-mouth in the position of Fig. 35 is in practice not too valid. The node should perhaps lie somewhat intermediate between the bay-mouth and the 600 ft. depth contour as a likely conflict of the bay-mouth constriction on the shelf oscillation. With some allowance for this conclusion we may proceed to compare calculated periods of higher modes with those encountered in the records.

Mode No. 2 (Fig. 35 c) with a period of 29.6 mins. shows up virtually as a binodal oscillation for the northern half of the bay. In the Residuation analyses for Santa Cruz (cf. Table I or sequence (40)) we find evidence for 28.5 and 30 min. oscillations which support this mode.

Fig. 35 c shows very weak response in the Monterey area, yet in both Table I (sequence (40)) and Table II (sequence (41)) Monterey shows strong evidence for oscillations in the period range of 32-36 mins. This nonagreement must again be ascribed to the probability that the assumed node position is not too good an approximation.

Mode No. 3 (Fig. 36 a), which exhibits the first strong oscillation in the southern part of the bay, is, however, obviously the counterpart of Fig. 35 b for the north, and its period of 28.2 mins. could be expected to lengthen and more closely approach 32-36 mins. if the node had been taken further seaward in the first instance. This mode again shows the marked effect of the canyon. The oscillation to the north is weak and the oscillation to the south is thus effectively a uninodal shelf-oscillation (see Fig. 36 a, inset).

Fig. 36 b shows a mode of period 23.3 mins. which is again weak in the south and strong in the north. At Santa Cruz, however, it tends to be weak. The next mode of period 21.6 mins. (Fig. 36 c) exhibits moderately strong antinodes in the north and south portions of the bay. Near Santa Cruz it could probably explain the 19.6 to 23.2 min. oscillations near Monterey evident in Table I (sequence (40)). Even though this mode exhibits coupling over the bay (see Fig. 36 b, inset) the amplitudes are so small over the submarine canyon as to imply that the effect of the latter is still largely nodal.

Proceeding in this wise we note that of the next four mode-shapes (Figs. 37 and 38 a) only the last with a period of 17.6 mins. is moderately strong in the Monterey area. Tables I and II (or sequences (40) and (41)) show evidence for period prominence in the neighborhood of 16.7-17.3 mins. which could be confirmation of this oscillation. At the northern end of the bay in the Santa Cruz region all the responses are weak and, in fact, we find no evidence for these periods in the Santa Cruz records.

Qualitatively, then, as far as this study has gone, it can be said that Monterey Bay functions virtually as two independent open-mouth bays whose mouth-boundaries lie approximately at the real mouth of the bay and along the center-line of the submarine canyon. This conclusion is important and justifies the effort made in solution of this problem since it means that the modelling of Monterey Harbor in relation to its long wave problem can be confined to the southern half of the bay.

On this premise, then, the fundamental modal period for the southern

half of Monterey Bay could be expected to be of the order of 28 to 33 mins. and would tally quite well with the graphical result (sequence (36)).

It is almost certain that the numerical calculations epitomized in Figs. 35 to 38 cannot be considered acceptable for high-order modes. The basic assumption of the establishment of a node across the mouth of such a broad-mouth, short-length bay as Monterey is undoubtedly being overstrained beyond the third mode (Fig. 36.a). Consequently the 'talweg' solution of Part III (4) for the southern portion of Monterey Bay takes on a measure of much greater importance.

In this case the 'talweg' numerical solution can be expected to apply reasonably accurately (within the limits of the assumed node position), because there are no violent changes of depth in the area covered (see inset to Fig. 31).

4. Conclusions Regarding Excitation and Response of Monterey Harbor

For comparative purposes we now review the results of Eq. (17), and of Tables I and II as follows. Recapitulated, Eq. (17) suggests that the periods

$$T_n = 13.3,\ 6.8,\ 4.52,\ 3.56,\ 3.02,\ 2.58$$
$$2.22,\ 1.94,\ 1.68 \ldots\ldots \text{mins.} \tag{42}$$

are apparently representative of modes of oscillation in which the southern part of Monterey Bay responds readily to stimulation.

Peaks on the sea-energy spectra (Figs. 26, Table II) show the following congruencies with some of the above figures

$$T_n = \ldots 13.3,\ \ldots 5.8\text{-}6.7,\ \ldots 3.9\text{-}4.4,\ 2.9\text{-}3.5$$
$$2.4\text{-}2.6,\ 2.0\text{-}2.2,\ 1.7\text{-}1.9,\ \ldots\ldots \text{mins.} \tag{43}$$

In addition the Residuation analyses of long-wave records (Table I)

yield the following similarities:

$$T_n = \ldots 11.0\text{-}13.6, \ \ldots 6.1\text{-}6.3, \ \ldots 3.8\text{-}4.6, \ \ldots 2.2\text{-}2.9, \ 1.7\text{-}1.96, \ \ldots\ldots \text{mins.} \tag{44}$$

Because of these indications that several of the periods in the sequence (42) are important to the regime of oscillations affecting Monterey Harbor, it was decided to explore the nature of some of these in the immediate harbor vicinity. Periods which seems to be consistently strong in the records are

$$T_n = 13.3, \ \ldots 6.1, \ 4.3, \ 2.5, \ \ldots\ldots \text{mins.} \tag{45}$$

These periods accordingly were those selected for study with the aid of the wave-refraction diagrams.

From the above we conclude that periods at or near those given in sequence (45) will be resonant for the near-harbor area. We have already noted (Section 2) that a periodicity of about 2.5 mins. will excite an open-mouth fundamental oscillation in the marina.

On consulting Fig. 63 it is also apparent that the 2.5 min. oscillation external to the harbor has a node directly in line with the mouth of the marina. This ensures that the chain-resonance sequence is established as between bay and harbor and the marina forms a perfect echo-chamber for this frequency.

Fig. 64 suggests that the node of the 4.3 min. external resonant oscillation will penetrate the entrance of the harbor quite close to the end of the Municipal Wharf No. 2. MA Sensor 3 near this position would thus tend to show rather minor response to this period, a fact confirmed by Figs. 26, while MA Sensor 1 in the breakwater bight would register very strong response because of the fact, shown in Section 2, that the outer harbor basin tends to have a fundamental period of oscillation of its own of precisely this period. Fig. 26 shows that at the MA Sensor 1 location the response at 4.3 mins. period is indeed very strong. The periodicity

is not otherwise crucial to the marina.

The next oscillation of 6.1 mins. (Fig. 65) has a node somewhat seaward of the breakwater. The harbor will therefore be in the antinodal area and response will be moderate. If the external oscillation has a slight off-resonance period of 5 to 6 mins., the node would probably be moved shoreward from the position shown in Fig. 65, to a position approximately in line with the breakwater.

For this situation the external basin of the harbor would be antinodal at this period, but since the period is approximately twice that of the fundamental open-mouth period for the marina, it would tend to 'pump' the harbor, and some degree of strong flushing of the marina entrance could be expected. Figs. 26 show that Sensor 2 response to 5.2 to 5.8 min. frequencies in the marina is very pronounced as might be expected.

Figs. 66 for the 13.3 min. standing wave shows the whole region near the harbor to be antinodal. The harbor itself does not have any tendency to echo this frequency and so the response registered on all sensors will be nominal as shown in Fig. 26.

It is of interest to compare the nodal positions prescribed by the numerical 'talweg' solution of Fig. 32 with the nodes found by graphical refraction techniques in Figs. 64 and 65. Thus in Figs. 64 and 65 heavy dash-lines represent the nodes for the 4.5 and 6.8 min. oscillations respectively, as defined by Fig. 32. For the area involved the comparisons are reasonably good, bearing in mind that the periods being compared are not identical.

The straight-line nodes of the 'talweg' solutions are obviously very great simplifications of the oscillating regime. Their positions, however, accord reasonably well with the positions derived graphically and each method is therefore a confirmation of the other in a general sort of way.

V. FEASIBILITY OF MODEL (OR MODELS) FOR SIMULATING OBSERVED AND DEDUCED CHARACTERISTICS

1. Type of Model (or Models) to Reproduce Surging in Monterey Harbor

The evidence of Part IV tends to show the following:

(a) That the influence of the deep canyon on the oscillating characteristics of the bay is so profound that the bay functions as two independent halves.

(b) That the 'open-mouth' 'talweg' numerical calculation, applied to the bight within the lee of the Monterey Peninsula, appears to give a reasonable indication of the oscillating properties of the area.

(c) That the wave periods of concern to Monterey Harbor are likely to be less than 3 mins. and certainly less than 7 mins.

(d) That the oscillations found from graphical synthesis of wave refraction procedures are realistic models of those prescribed by the 'talweg' numerical solution and serve to explain the peculiarities of the wave-energy spectra at all three sensor locations.

Having regard to our discussions of Part IV (1), it would appear then that the oscillating regime in the neighborhood of Monterey Harbor can be successfully reproduced by long waves of the appropriate periods bearing upon the harbor from the directions shown in Figs. 50 and 51.

Since our concern is with long-wave periods of less than 7 mins., say, it would be appropriate to consider Mussel Point (about half-way between Pinos Point and Monterey, Fig. 50) as being about the outer boundary limit of a surge-action model. If the seaward boundary were taken closer to the harbor than this the longer-period oscillations (near 7 mins.) would have to be generated in tidal fashion by introducing and withdrawing water from the model. It would be desirable to avoid this

unless pneumatic wave generators of the type used for the Hilo Harbor tsunami model were employed.

Because it has been clearly established that the long-wave energy coming across the rim of the deep submerged canyon on the northern edge of the continental shelf (for the southern part of the bay) is very insignificant, it appears that it would be uncessary to worry about long-period wave generation from a flanking direction. A side boundary for the model, normal to the coast from near the inlet to the Laguna del Ray, would thus not seriously interfere with the oscillating regime, provided it were suitably equipped with energy-absorbing filters.

The recommended limits for a surge-action model of Monterey Harbor may then be prescribed in Fig. 71 with two wave-generator units to reproduce the correct directions of approach of the long waves south of Mussel Point.

Such a model would cover a prototype area of about 4 sq. mi. and would be adequate to accommodate the proposed extensions to the harbor, and whatever other modifications in the area might be considered. There seems no need for a second model.

2. Design of Model to Achieve its Purpose

A surge-action model can usually tolerate a much greater degree of scale distortion than is permissible with ordinary wave-action models. Nevertheless, since it will probably be necessary to operate the model down to wave periods of 20 secs., or even 15 secs., the amount of distortion should be as little as possible.

The model proposed is about four times as large area-wise as that originally built at Vicksburg in 1947 (Hudson, 1949). The need for incorporating so much water area may perhaps be questioned. Here the writer would point out the special peculiarities of the contours of refraction coefficient for reflected waves, shown in Fig. 56. These very largely determine the features of the standing-wave regime in the near harbor

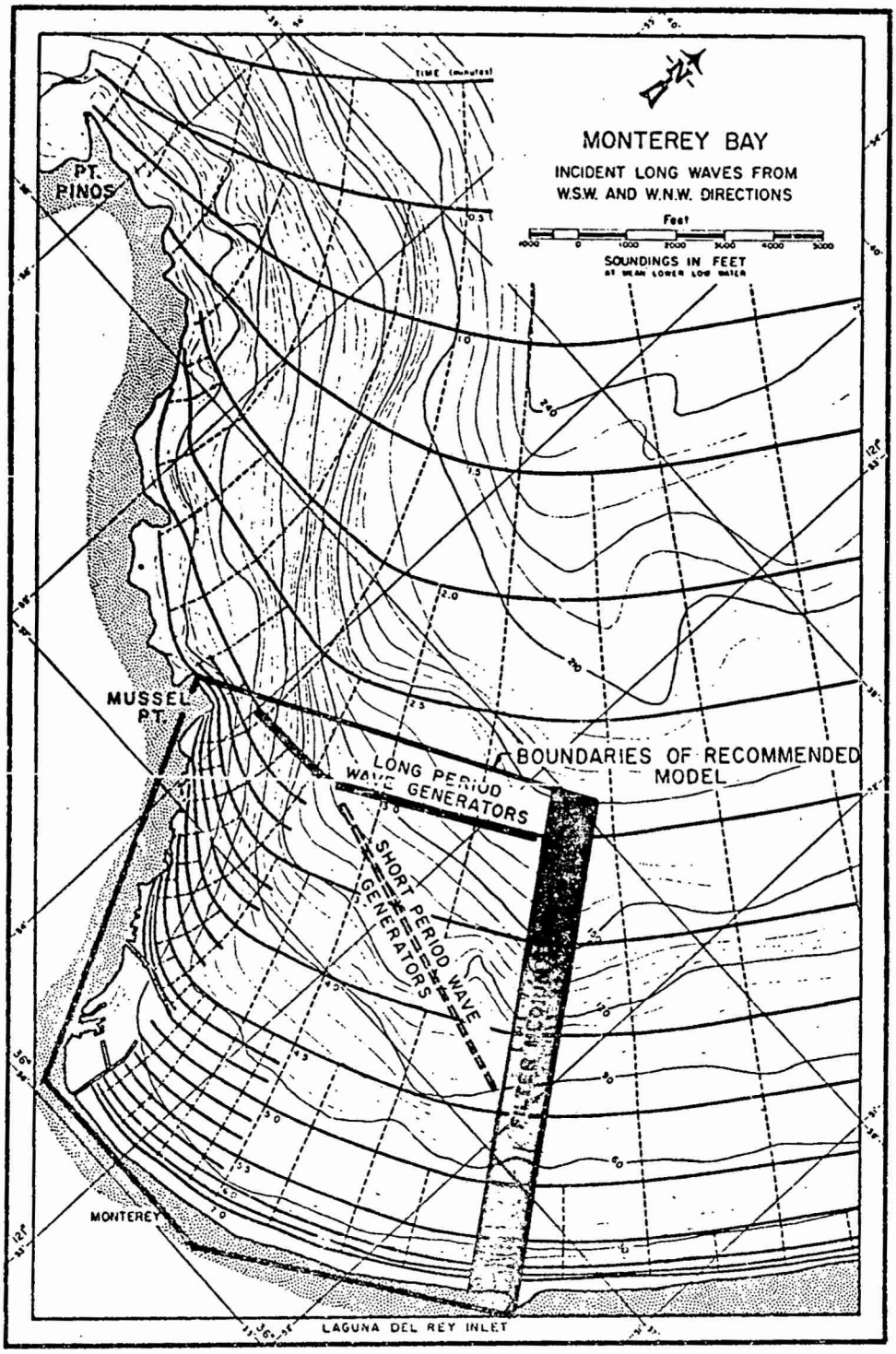

FIGURE 71 RECOMMENDED BOUNDARIES OF SURGE-ACTION MODEL FOR MONTEREY HARBOR

area. Too great a restriction on the water area outside the harbor in the model will interfere with this regime, particularly insofar as it is affected by reflected energy from the coastline near Fort Ord and the inlet to the Laguna del Ray. Further the proposed harbor extensions will alter the standing-wave regime outside the harbor, and here again adequate water space is needed for a correct regime to be simulated.

On the basis that the harbor area is $10^4 \times 10^4$ sq. ft. as prescribed in Fig. 71, we may adopt a horizontal linear scale for the model of 1 : 200 in order to bring it to a convenient size of 50 x 50 ft. If in addition we adopt a vertical scale of 1 : 120 we shall have a distortion factor for the model of 200/120 or 1.67, and the maximum water depth in the marina (about 16 ft.) will be scaled in the model to 16 x 12/120, or 1.6 ins., which is considered an adequate working depth in that inner basin.

The low distortion factor of 1.67 is considered quite satisfactory for reliable reproduction of long-wave effects down to 30 secs. period. As a test of this we may determine the true time-distortion for 30 sec. waves from the formula (Wilson, 1959):

$$\frac{T_m}{T_n} = 1 + \sqrt{\frac{\alpha^2}{3}\,(\phi^2 - 1)} \qquad (46)$$

where

$$\text{(i)} \quad \alpha = KD \qquad \text{(ii)} \quad \phi = \frac{\delta}{\lambda} \qquad (47)$$

and T_m , T_n are respectively the prototype times in the model and in nature, while K is the prototype wave number ($= 2\pi/L$, L = wave length), D the prototype depth and δ , λ are respectively the vertical and horizontal scales.

For 30 sec. (prototype) waves in a water depth $D = 15$ ft.,

$L \cong 470$ ft., making $\alpha = 0.2$. For $\phi = 1.67$ we then have

$$\frac{T_m}{T_n} = \sqrt{1 + \frac{0.04}{3} \times 1.78}$$

$$= 1.012$$

which represents an error of just over 1 percent.

The actual time scale τ for the model with $\delta = 1/120$ and $\lambda = 1/200$ will be given by

$$\tau = \frac{\lambda}{\sqrt{\delta}} \tag{48}$$

from which we find $\tau = 0.055$. For convenience of calculation it might be desirable to adjust the vertical scale to 1/144 so as to make $\tau = 0.06$, a more convenient figure for rapid conversion of model and prototype times.

As regards the details of model design it does not seem appropriate at this time to enter upon these. The writer envisions a fixed-bed model accurately contoured out to the wave-generator locations shown in Fig. 71. The provision of filter material in front of the wave generators, and particularly along the east wall of the model, are problems of design which also are best left to a later stage in the model development.

It would seem to be desirable that the model be tested out for fairly short-period waves, for which the directions of approach may well differ from those shown in Fig. 71. The latter figure therefore shows short-period wave generators moved to a more angular position.

3. Use of Field Data In Formulating Model Test Program

The sea-energy spectra of Figs. 26 can be used directly for determining the adjustments needed on the wave generator for different frequencies of input to the model.

The surge-action model should be used as its own wave-spectrum analyzer. That is to say, by generating a succession of long waves of a given frequency in the model it should be possible to measure the $(\text{height})^2$ of the resulting oscillations at each of the three locations of the MA sensors in the prototype harbor. The succession of $(\text{height})^2$ - values plotted against frequency or period for each frequency test should correspond to the sea-energy spectra of Figs. 26. They can be made to correspond by suitably adjusting the wave amplitude at the generator for each frequency.

For the operation of the model, then, a preliminary phase of testing will be necessary merely to establish generator control-settings that will simulate as far as possible the known prototype sea-energy spectra at the three stations.

Once this phase is completed the model will be ready to perform its functions as a general spectrum analyzer at any point within the model area. The necessary requirement here would be that the model be operated at a particular frequency-setting and height measurements made at points of interest, and the frequency setting then adjusted by a small increment and the height measurements repeated. Substantially this is the technique that has commonly been adopted in surge-action models before (cf. Hudson, 1949; Wilson, 1951, 1959, etc.) but the measurements are now precisely quantitative to match the controlling field spectra.

4. Analysis and Interpretation of Model Results

Once it has been confirmed that the model can reasonably well simulate the observed field data, model wave-energy spectra can be obtained for any location whatever inside or outside the harbor.

For a comparison of the effects on the harbor of any new structure (breakwater, etc.) it is necessary only to remeasure the wave-energy spectra at points of interest, resulting from introduction of the new structure, in order to determine its effect on the oscillating regime. The extent to which the wave-energy level is lowered by a harbor improve-

ment scheme will be the measure of success of the scheme.

There would, however, be an outstanding problem to be resolved. The threshold limit below which the wave-energy spectra would have to be depressed in order to render a location in the harbor immune, or reasonably immune, to surging troubles would have to be established. This could be achieved by more field measurements of the type of Figs. 26, which would establish the precise energy-levels at which difficulties are encountered in the marina or elsewhere.

Once the model wave-energy spectra have been compiled from tests for points of interest, these can be analyzed according to the methods of this report for any proper understanding of the phenomena involved.

REFERENCES

Abecasis, F. M. (1964); Resonance conditions in No. 1 dock of Luanda Harbour; Proc. IXth Coastal Eng. Conf., Lisbon (June 1964); Coastal Eng. Research Council, ASCE, New York, N.Y. 1965, pp. 800-831.

Bascom, W. (1950); Surging in Depoe Bay, Oregon; Bulln. Beach Erosion Board, Corps of Engrs., U.S.Army, v. 4 (4), Oct. 1950, pp. 32-39.

Biesel, F. and Lé Mehauté, B., (1955); Notes on the similitude of small scale models for studying seiches in harbors; La Houille Blanche, v. 10(3), 1955, pp. 392-407.

Caloi, P. (1954; Gezeiten Problems des Meeres in Landnahe, Problems der kos mischen physik VI (Hamburg, Germany), 1925, 80 pp.

Carr, J.H. (1953); Long period waves or surges in harbors; Trans ASCE v. 188, 1953, pp. 588-616.

Chrystal, G. (1904-05); On the hydrodynamical theory of seiches (with bibliography on seiches); Trans Roy. Soc. Edinb., v. 41(III), 1906, pp. 599-649.

Chrystal, G. (1906); Investigation of seiches off Loch Earn by the Scottish Loch Survey; Trans. Roy. Soc. Edinb., v. 45(II), pp, 382-387.

Defant, A. (1925); Gezeiten Problems des Meeres in Landnahe, Problems der kos mischen physik VI, (Hamburg, Germany) 1925, 80 pp.

Defant, A. (1960); Physical Oceanography; v. II (Pergamon Press, Oxford, England), 1960, Chaps. VI, XVI.

Ertel, H. (1933); Eine neue Methode zur Berechnung der Eigen-Schwingungen von Wassenmassen in Seen, Unregelmassiger Gestalt, S. B. Preuss. Akad., Wifs. (Berlin), v. 24, 1933.

Goldsbrough, G. R. (1930); The tidal oscillations of an elliptic basin of variable depth; Proc. Roy. Soc., London, v.130(A), 1930, pp. 157-167.

Hidaka (1936); Application of Ritz Variation Method to the Determination of Seiches in a Lake, Mem. Imp. Mar. Obs. Kobe, v. 6(2), 1936.

Hudson, R. Y. (1949); Wave and surge action, Monterey Harbor, Monterey California; Tech. Memo. No. 2-301, Waterways Experiment Station, Corps. of Engrs., U.S.Army, Sept. 1949, 24 pp. and 45 plates.

Hydrographic Office (1944); Atlas of sea and swell charts, North Eastern Pacific Ocean, H.O. Pub. No. 799D, U.S. Navy Hydrographic Office, Wash., D.C., 1944 (reprinted U.S. Navy Oceanographic Office, 1964).

Johnson, J. W. (1953); Engineering aspects of diffraction and refraction; Trans. ASCE, v. 118, 1953, pp. 617-652.

Joosting, W. C. Q. (1959); The troubled waters of Table Bay Harbor; Trans. S.A. Inst. C. E. v.1, 1959, pp. 211-222.

Joosting, W. C. Q. (1963); Sea waves and the harbors of South Africa; Proc. Diamond Jubilee, S. A. Inst. C.E., 1963, pp. 93-95.

Knapp, R. T. and Vanoni, V. A. (1945); Wave and surge study for the Naval Operating Base, Terminal Island, California; Tech. Report, Hydraul. Structures Lab., Calif. Inst. Tech, Jan. 1945, 241 pp.

Knapp, R. T. (1949); Model studies of Apra Harbor, Guam, Midway Islands; Report No. N-63, Hydrodynamics Laboratories, Calif. Inst. Tech, June 1949, 207 pp.

Lamb, H. (1932 Edn.); Hydrodynamics (Cambridge, Eng., 1932, Dover Public. Inc., N.Y., 1946).

Longuett-Higgins, M.S. and Stewart, R. W. (1962); Radiation stress and mass transport in gravity waves with application to 'surf-beats'

Lundgren, H. (1963); Wave thrust and wave energy level; Proc. Xth Congr. Int'l. Assoc. Hydraul. Res., (London) v. 1, July 1963, pp. 147-151.

Marine Advisers (1964a); A broad-frequency-band wave study at Monterey Harbor, Calif.; Tech. Report to U.S. Army Engr. Dist., San Francisco, Marine Advisers, La Jolla, Calif., July 1964.

Marine Advisers (1964b); Wave recording at Santa Cruz Harbor, Calif.; Letter Report to Division of Small Craft Harbors, Dept. of National Resources, Sacramento, Calif. from Marine Advisers, La Jolla, Calif., April 1964.

Marine Advisers (1964c); A long-wave and wind recording study at Half Moon Bay, Calif.; Tech. Report to U.S. Army Engineer District, San Francisco; Marine Advisers, La Jolla, Calif., Mar. 1964.

Munk, W. H. (1949); Surf beats; Trans Am. Geophys. Union, v. 30, 1949, pp. 849-854.

Munk, W. H., Snodgrass, F. E. and Tucker, M. J. (1959); Spectra of low frequency ocean waves; Bulln. Scripps Inst. Oceanography, Univ. Calif., La Jolla, 1959, 361 pp.

Munk, W. H. (1962); Long ocean waves; The Sea (Interscience Publishers, New York), v. 1, 1962, pp. 647-663.

National Marine Consultants (1960); Wave statistics for seven deep water stations along the California coast; Tech. Report National Marine Consultants, Santa Barbara, Calif., Dec. 1960 (unpublished).

O'Connor, P. (1964); Short-term sea-level anomalies at Monterey, Calif.; M.S. Thesis, U.S. Naval Postgraduate School, Monterey, Calif., 1964, 56 pp.

Raichlen, F. (1964); Two-Dimensional shallow water oscillations in basins of arbitrary shape; Tech. Memo 64-3, Keck Lab. Hydraul. and Water Resources, Calif. Inst. Tech., May 1964, 23 pp.

Reed, R. J. and Rogers, D. G. (1962); The circulation of the tropical stratosphere in the years 1954-1960; Journ. Atmos. Sci., v. 19, Mar. 1962, pp. 127-135.

Reid, W. J. and Wade, J. B. (1963); Surf beats at Taranaki, New Zealand; Paper 1.13, Proc. Xth Congr. Int'l. Assoc. Hydraul. Research, London, July 1963, v. 1, pp. 93-100.

Shapiro, R. and Ward, F. (1962); A neglected cycle in sunspot numbers; Jour. Atmos. Sci., v. 19, Nov. 1962, pp. 506-508.

Stoker, J. J. (1957); Water waves; (Interscience Publishers, Inc., New York), 1957, Chap. 10.

Tucker, M. J. (1950); Surf beats: sea waves of 1 to 5 min. period; Proc. Roy. Soc. London, v. 202(A), 1950, pp. 565-573.

Tucker, M. J. (1963); Long waves in the sea; Science Progress, v. LI (203), July 1963, pp. 413-424.

Wemelsfelder, P. J. (1957); Origin and effects of long period waves in ports; Communication 1, Sec. II, Proc. XIXth Int'l. Navig. Cong. (London), July 1957, pp. 167-176.

Wilson, B. W. (1951); Research and model studies of range action in Table Bay Harbor, Cape Town; D.Sc. Thesis, Univ. Cape Town, South Africa, 1951, 468 pp.

Wilson, B. W. (1953a); Generation of long-period seiches in Table Bay, Cape Town, by barometric oscillations; Trans. Am. Geophys. Union, v. 35(5), Oct. 1954, pp. 733-746.

Wilson, B. W. (1953b); Table Bay as an oscillating basin; Proc. Minnesota Int'l. Hydraul. Conv., Sept. 1953, Minneapolis, Minn. (Int'l. Assoc. Hydraul. Research), pp. 201-212.

Wilson, B. W. (1957); Origins and effects of long-period waves in ports; Communication 1, Sec. II, XIXth Int'l. Navig. Congr., London, July 1947, pp. 13-61.

Wilson, B. W. (1959); Research and model studies on wave action in Table Bay Harbour, Cape Town; Trans. S.A. Inst. C.E., v.1(6,7), June-July, 1959; v.2(5), May 1960.

Wilson, B. W. (1964); Long wave modification by linear transitions (discussion); Proc. ASCE, v. 90 (ww4), Nov. 1964, pp. 161-165.

Wilson, B. W. (1965); Seiche; Encyclopedia of Marine Geophysics (Rheinhold Public. Inc.), 1965 (publication pending).

APPENDIX A

TWO-DIMENSIONAL OSCILLATIONS IN OPEN BASIN OF VARIABLE DEPTH

by

J. A. Hendrickson

TWO-DIMENSIONAL OSCILLATIONS IN OPEN BASIN OF VARIABLE DEPTH

The analysis of two-dimensional oscillations in open basins is based on the assumption that the wave lengths of the surface waves are long with respect to the water depths. With this premise and the assumption of linear wave theory, Stoker (1957, pp. 414-425) has shown that the continuity equation of hydrodynamics may be written in terms of the free surface variation of the potential function and the local depth. If we consider only two-dimensional flow (i.e., time and one-coordinate variation of the potential function), we may write the continuity equation as

$$\left(A(x)\phi_x\right)_x = \frac{b(x)}{g}\phi_{tt} \qquad \text{(A-1)}$$

where

$A(x)$ is the cross-sectional area of flow as a function of the surface coordinate x,

ϕ = potential function,

$b(x)$ = width of basin as a function of surface coordinate x,

g = acceleration due to gravity,

and subscripts denote differentiation with respect to time or space.

In addition to Eq. (A-1), the linearized free-surface condition must be satisfied. This condition may be written as

$$\phi_t = -g\eta(x) , \qquad \text{(A-2)}$$

where

$\eta(x)$ = perturbed surface elevation measured with respect to the mean-surface elevation.

Eq. (A-1) may be differentiated with respect to time and Eq. (A-2)

substituted with the result

$$\left(A(x)\eta_x\right)_x = \frac{b(x)}{g}\eta_{tt} \quad . \tag{A-3}$$

Finally, we assume that $\eta(x,t)$ possesses the separable form

$$\eta(x,t) = \eta(x)e^{i\sigma t} \quad , \tag{A-4}$$

where $\sigma = \frac{2\pi}{T}$,

and T = the period of the surface wave.

Hence, if Eq. (A-4) is substituted into Eq. (A-3), we obtain the field equation describing the surface elevation behavior

$$\frac{d}{dx}\left[A(x)\frac{d\eta}{dx}\right] + \frac{\sigma^2 b(x)\eta}{g} = 0 \quad . \tag{A-5}$$

If we let $A(x) = b(x)\,h(x)$, where $h(x)$ = mean water depth, then Eq. (A-5) may be equivalently written as

$$bh\frac{d^2\eta}{dx^2} + \left[b\frac{dh}{dx} + h\frac{db}{dx}\right]\frac{d\eta}{dx} + \frac{\sigma^2 b\eta}{g} = 0 \quad . \tag{A-6}$$

In general, the numerical solution of Eq. (A-6) is sufficient for the solution to two-dimensional oscillations in open basins, provided certain boundary conditions are satisfied. Fig. A-1 shows a typical basin of the type herein considered. At point "0" the existence of a node line is assumed. Hence η_o is taken to be zero. The conditions holding at point N are taken to be one of two types.

(a) Depth at N approaches zero. If the depth, h_n, approaches zero the field equation, Eq. (A-6), simply becomes

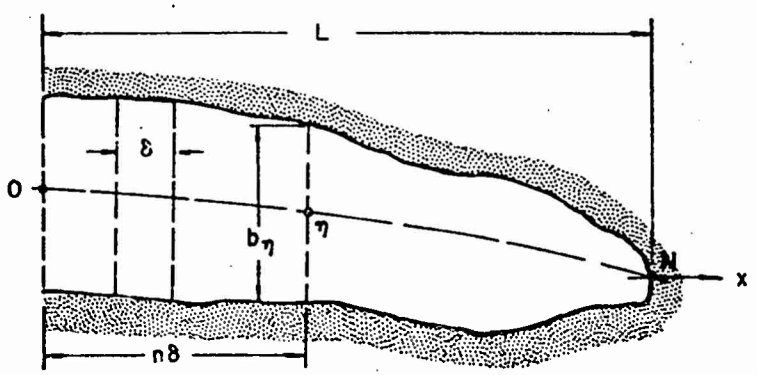

FIGURE A-1 TYPICAL OPEN MOUTHED BAY AND COORDINATE SYSTEM USED IN TWO-DIMENSIONAL OSCILLATION STUDY

$$\frac{dh}{dx}\left.\frac{d\eta}{dx}\right|_N + \frac{\sigma^2 \eta_N}{g} = 0. \qquad \text{(A-7)}$$

(b) Finite Depth at Point N. If the depth, h_n, is finite, there can be no normal velocity to the boundary at point N. Hence, $d\eta/dx\big|_N = 0$, and Eq. (A-6) becomes

$$h\left.\frac{d^2\eta}{dx^2}\right|_N + \frac{\sigma^2 \eta_N}{g} = 0. \qquad \text{(A-8)}$$

Eq. (A-6) may be converted into numerical form in the usual manner, employing three point central differences. Hence, if we let

$$h_\eta = \frac{h_\eta}{h_o}; \quad b_n = \frac{bn}{L}, \quad \text{and } x = \frac{\eta L}{N},$$

where h_o = depth at point 0

L = length of basin,

and N = number of points considered in numerical solution between points 0 and N,

it may be shown that Eq. (A-6) becomes

$$\eta_n\left[2\hat{h}_n - \lambda^2\right] - \eta_{n+1}\left\{\hat{h}_n + \frac{1}{4}\left[\hat{h}_{n+1} - \hat{h}_{n-1} + \left(\frac{\hat{h}_n}{\hat{b}_n}\right)\left(\hat{b}_{n+1} - \hat{b}_{n-1}\right)\right]\right\} \tag{A-9}$$
$$- \eta_{n-1}\left\{\hat{h} - \frac{1}{4}\left[\hat{h}_{n+1} - \hat{h}_{n-1} + \left(\frac{\hat{h}_n}{\hat{b}_n}\right)\left(\hat{b}_{n+1} - \hat{b}_{n-1}\right)\right]\right\} = 0$$

where $\lambda^2 = \dfrac{\sigma^2 L^2}{N^2 g\hat{h}_o}$.

Eq. (A-9) holds to $n = N - 1$. At point N, either Eq. (A-7) or (A-8) must be applied. Hence, for instance, if the depth, h_N, approaches zero Eq. (A-7) will apply. Approximating the derivatives in Eq. (A-7) on the basis of three-point backward differences, it may be shown that the numerical equivalent of Eq. (A-7) becomes

$$\eta_N\left\{\frac{3}{4}\left[4\hat{h}_{N-1} - \hat{h}_{N-2}\right] - \lambda^2\right\} - \eta_{N-1}\left(4\hat{h}_{N-1} + \hat{h}_{N-2}\right) + \frac{1}{4}\eta_{N-2}\left(4\hat{h}_{N-2} - \hat{h}_{N-2}\right) = 0 \tag{A-10}$$

Finally, for numerical solutions to the problem for N points, N-1 equations of the type of Eq (A-9) are formed and one equation of the type of Eq. (A-10) is formed. The resulting N x N eigenvalue matrix is then solved to obtain the eigenvalue (and hence the periods of oscillation), the eigenvector and hence the mode shapes corresponding to each eigenvalue.

APPENDIX B

THE NUMERICAL CALCULATION OF THE THREE-DIMENSIONAL OSCILLATING CHARACTERISTICS OF BAYS AND HARBORS UNDER THE INFLUENCE OF GRAVITY

by

J. A. Hendrickson and R. E. Kilmer

THE NUMERICAL CALCULATION OF THE THREE-DIMENSIONAL OSCILLATING CHARACTERISTICS OF BAYS AND HARBORS UNDER THE INFLUENCE OF GRAVITY

As a basis for the study of the three-dimensional oscillating characteristics of bays and harbors certain equations developed by Stoker* will be used. Utilizing the linearized theory of harmonic water waves, where the water depth is small compared to the wave length, Stoker shows that the general field equation of the potential function in rectilinear coordinates may be reduced to the following free-surface wave equation

$$(h\bar{\phi}_x)_x + (h\bar{\phi}_z)_z - (\frac{1}{g}\bar{\phi}_t)_t = 0 \qquad \text{(B-1)}$$

where

$\bar{\phi}$ = the potential function evaluated at the equilibrium position of the free-surface

h = $h(x, z)$ = the value of the water depth

g = acceleration due to gravity

x, z = rectilinear space coordinates

t = time

and subscripts denote differentiation with respect to space or time variable.

The linearized Bernoulli's equation for the free surface may be written as

$$\eta = -\frac{1}{g}\bar{\phi}_t \qquad \text{(B-2)}$$

where η = the surface displacement from its equilibrium position.

---

* J. J. Stoker, "Water Waves," Interscience Publishers, Inc., New York, 1957, pp. 414-419.

Further, for harmonic motion, we may use the relation

$$\eta = \eta(x,z)\exp^{(i\sigma t)} \quad , \tag{B-3}$$

where σ = the circular frequency of oscillation.
Hence, combining Eqs. (B-1), (B-2) and (B-3) yields the following differential equation governing the displacement of the free surface.

$$(\hbar\eta_x)_x + (\hbar\eta_z)_z + \frac{\sigma^2}{g}\eta = 0 \tag{B-4}$$

Eq. (B-4) may be generalized to a curvilinear coordinate system with the result

$$\frac{1}{h_1 h_2}\left[\frac{\delta}{\delta q_1}\left(\frac{h_2}{h_1}\hbar\frac{\delta\eta}{\delta q_1}\right) + \frac{\delta}{\delta q_2}\left(\frac{h_1}{h_2}\hbar\frac{\delta\eta}{\delta q_2}\right)\right] + \frac{\sigma^2}{g}\eta = 0 \quad , \tag{B-5}$$

where h_1, h_2 are the curvilinear distortion factors, and q_1, q_2 are the curvilinear coordinates. Hence, in polar coordinates, for example, Eq. (B-5) becomes

$$\frac{1}{r}\frac{\delta}{\delta r}\left(r\hbar\frac{\delta\eta}{\delta r}\right) + \frac{1}{r^2}\frac{\delta}{\delta\theta}\left(\hbar\frac{\delta\eta}{\delta\theta}\right) + \frac{\sigma^2}{g}\eta = 0 \quad . \tag{B-6}$$

For the purpose of the present study of Monterey Bay, it is convenient to work in polar coordinates. Hence Eq. (B-6) will be utilized in conjunction with the appropriate boundary conditions.

BOUNDARY CONDITIONS

We will be concerned with three types of boundary conditions: (a) fixed vertical boundary where the water depth is finite, (b) a solid-liquid interface of negligible water depth, and (c) a node line in the fluid where the surface elevation η is zero. These cases are treated as follows:

(a) Fixed Vertical Boundary. For this case, assuming finite water depth, the velocity of fluid flow across the boundary is zero. Hence, if the normal to the boundary be denoted by n

$$\phi_n = 0$$

Hence, from Eq. (B-2) we obtain the surface condition

$$\eta_n = 0 \qquad \text{(B-7)}$$

(b) Solid-Liquid Interface of Zero Water Depth. We will assume that at such boundaries the fluid oscillations do not materially alter the geometrical location of the boundary. Moreover, we will allow finite surface deformation at such boundaries. This assumption is valid for cases where the bottom slope is of a reasonable value such that surface deformations do not result in major water "run-up." Hence at such boundaries, the field equation must be satisfied with the restriction that the depth h be set to zero.

(c) Node Line in Fluid Media. Unlike physical boundaries, whose location is known, the exact location of the node line which is found to exist in the vicinity of the open entrance to Bays and Harbors is not a priori known. Moreover, we cannot proceed with the solution to the oscillation problem without first defining the boundaries of the region of interest. In the case of physically enclosed basins, of course, we may easily define the boundaries of the region and in most cases the boundary conditions (a) and (b) will adequately apply. In the case of the open bay, however, we must enclose our boundary with the assumption of the existence and location of a node line in the fluid itself, where the surface elevation η is taken to be zero. Often, physical observation may be used to set the location of such a node line. However, in many cases experience and intuition must be used to set the node-line location. In the case of Monterey Bay, however, the geometrical topography of the area greatly simplifies the problem of the node line location. In this case it is adequate to assume that the node line runs between Point Pinos and Point Santa Cruz or Point Pinos and Soquel Point. For our calculations, the former location was chosen.

Finally, having the region of interest defined along with the appropriate boundary conditions, the field equation must be satisfied at the

boundary and in the interior of the region. Since the only forcing function is due to gravity, it is recognized that we are dealing with an eigenvalue problem. The procedure to be used for the solution of this problem will be numerical in nature. The remainder of this section will be devoted to a description of the numerical procedure used to describe the problem as well as a description of the computer program used to solve the attendant numerical equation.

NUMERICAL PROCEDURE

General Star Field Equation

Carrying out the indicated differentiation in Eq. (B-6) we obtain

$$h\frac{\partial^2\eta}{\partial r^2}+\frac{\partial\eta}{\partial r}\left(\frac{h}{r}+\frac{\partial h}{\partial r}\right)+\frac{1}{r^2}\frac{\partial\eta}{\partial\theta}\frac{\partial h}{\partial\theta}+\frac{h}{r^2}\frac{\partial^2\eta}{\partial\theta^2}+\frac{\sigma^2}{g}\eta=0 \qquad \text{(B-8)}$$

Eq. (B-8) can be written for a general star in finite difference form using three-point central difference for unequal spacing shown in Fig. B-1 as

$$\begin{aligned}
&2h_{n,j}\left(\frac{N^2}{a^2}\right)\left[\frac{\alpha\eta_{n-1,j}-(\alpha+\beta)\eta_{n,j}+\beta\eta_{n+1,j}}{\alpha\beta(\alpha+\beta)}\right]\\
&+\frac{N^2}{a^2}\left[\frac{\beta^2\eta_{n+1,j}+(\alpha^2-\beta^2)\eta_{n,j}-\alpha^2\eta_{n-1,j}}{\alpha\beta(\alpha+\beta)}\right]\left\{\frac{h_{n,j}}{n}+\left[\frac{\beta^2h_{n+1,j}+(\alpha^2-\beta^2)h_{n,j}-\alpha^2h_{n-1,j}}{\alpha\beta(\alpha+\beta)}\right]\right\}\\
&+\frac{N^2}{a^2}\left(\frac{1}{n\Delta\theta}\right)^2\left[\frac{\delta^2\eta_{n,j+1}+(\gamma^2-\delta^2)\eta_{n,j}-\gamma^2\eta_{n,j-1}}{\gamma\delta(\gamma+\delta)}\right]\left[\frac{\delta^2h_{n,j+1}+(\gamma^2-\delta^2)h_{n,j}-\gamma^2h_{n,j-1}}{\gamma\delta(\gamma+\delta)}\right]\\
&+\frac{2h_{n,j}N^2}{a^2}\left(\frac{1}{n\Delta\theta}\right)^2\left[\frac{\gamma\eta_{n,j-1}-(\gamma+\delta)\eta_{n,j}+\delta\eta_{n,j+1}}{\gamma\delta(\gamma+\delta)}\right]+\frac{\sigma^2}{g}\eta_{n,j}=0
\end{aligned} \qquad \text{(B-9)}$$

where

$n=\frac{N}{a}r$ = denotes the arcs of equal radius which range from 0 to N

$j=\frac{J}{\theta_T}\theta$ = denotes the radii of equal angle which range from 0 to J

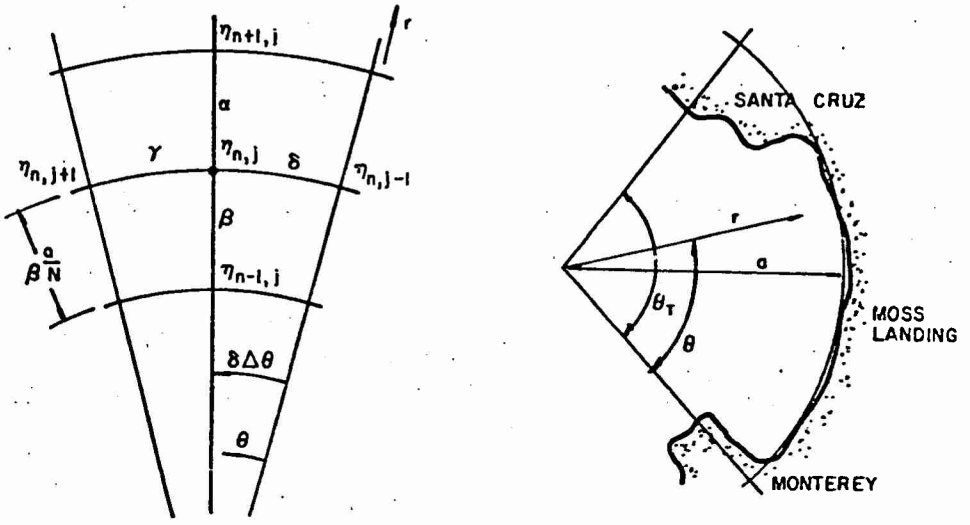

FIGURE B-1
POLAR COORDINATE GRID FOR A GENERAL STAR FIELD EQUATION

a = the radius of the basin

θ_T = the angular width of the basin

$\frac{a}{N}$ = the reference radius difference between equal angular arcs

$\Delta\theta = \frac{\theta_T}{J}$ = the reference angular difference between the radii

α , β = the ratios of actual radius difference to reference radius difference

δ , γ = the ratios of actual angular difference to reference radius difference

Unequal spacing between certain points were required for introducing a finer mesh over the submarine canyon and certain other critical areas or in regions near boundaries nonconformant to one of the orthogonal coordinates.

Let

$$\lambda^2 = \frac{\sigma^2 a^2}{N^2 g h_o} \tag{B-10}$$

and

$$h_{n,j} = \frac{\hat{h}_{n,j}}{h_o} \tag{B-11}$$

where h_o = a reference depth.

Then Eq. (B-9) can be written as

$$\eta_{n,j}\left\{\frac{1}{\alpha\beta}\left[2h_{n,j} - (\alpha-\beta)a(h)\right] - \left(\frac{1}{\gamma\delta}\right)\left(\frac{1}{n\Delta\theta}\right)^2\left[2h_{n,j} - (\gamma-\delta)b(h)\right] - \lambda^2\right\}$$

$$- \frac{\eta_{n+1,j}}{\alpha(\alpha+\delta)}\left[2h_{n,j} + \beta a(h)\right] - \frac{\eta_{n-1,j}}{\beta(\alpha+\beta)}\left[2h_{n,j} - \alpha a(h)\right] \tag{B-12}$$

$$- \frac{\eta_{n,j+1}}{\gamma(\gamma+\delta)}\left(\frac{1}{n\Delta\theta}\right)^2\left[2h_{n,j} + \delta b(h)\right] - \frac{\eta_{n,j-1}}{\delta(\gamma+\delta)}\left(\frac{1}{n\Delta\theta}\right)^2\left[2h_{n,j} - \gamma b(h)\right] = 0$$

where

$$a(h) = \frac{h_{n,j}}{n} + \left[\frac{\beta^2 h_{n+1,j} + (\alpha^2 - \beta^2) h_{n,j} - \alpha^2 h_{n-1,j}}{\alpha\beta(\alpha+\beta)} \right]$$

and

$$b(h) = \frac{\delta^2 h_{n,j-1} + (\gamma^2 - \delta^2) h_{n,j} - \gamma^2 h_{n,j-1}}{\gamma\delta(\gamma+\delta)}$$

Eq. (B-12) will be recognized as the general field equation for an eigenvalue problem where λ^2 is the eigenvalue and $\eta_{n,j}$ are elements of the eigenvector. For the case where $\alpha = \beta = \delta = \gamma = 1$, Eq. (B-12) reduces to

$$\begin{aligned}
&\eta_{n,j}\left[2h_{n,j}\left(\frac{1+n^2\Delta\theta^2}{n^2\Delta\theta^2}\right) - \lambda^2\right] \\
&- \eta_{n+1,j}\left[h_{n,j}\left(\frac{2n+1}{2n}\right) + \frac{1}{4}(h_{n+1,j} - h_{n-1,j})\right] \\
&- \eta_{n-1,j}\left[h_{n,j}\left(\frac{2n-1}{2n}\right) - \frac{1}{4}(h_{n+1,j} - h_{n-1,j})\right] \\
&- \eta_{n,j+1}\left(\frac{1}{n\Delta\theta}\right)^2\left[h_{n,j} + \frac{1}{4}(h_{n,j+1} - h_{n,j-1})\right] \\
&- \eta_{n,j-1}\left(\frac{1}{n\Delta\theta}\right)^2\left[h_{n,j} - \frac{1}{4}(h_{n,j+1} - h_{n,j-1})\right] = 0
\end{aligned} \qquad \text{(B-13)}$$

Boundary Conditions

a. Fixed Vertical Boundary. A fixed vertical boundary is not present in Monterey Bay so the corresponding finite difference equations

were not derived.

b. Solid-Liquid Interface of Zero Water Depth. The solid-liquid interface of zero water depth boundary condition is satisfied by using a three-point backward difference equation along the radius for n = N (at the head of the bay) and three-point forward or backward difference equation along the arc at the sides of the bay. In the event that the depth rapidly varied along the radii or arcs at the boundaries, a two-point forward or backward difference equation was sometimes used for the depth derivatives.

Hence, for n = N where three-point backward differences are used Eq. (B-12) becomes

$$\eta_{N,j}\left\{-h_{N,j}-\frac{3}{2}\left[\frac{h_{N,i}}{N}+(h_{N,i}-h_{N-1,i})\right]+\frac{2h_{N,i}}{N^2\Delta\theta^2}-\lambda^2\right\}$$

$$-\eta_{N,j+1}\left(\frac{1}{N\Delta\theta}\right)^2\left[h_{N,i}+\frac{1}{4}(h_{N,j+1}-h_{N,j-1})\right]$$

$$-\eta_{N,j-1}\left(\frac{1}{N\Delta\theta}\right)^2\left[h_{N,i}-\frac{1}{4}(h_{N,j+1}-h_{N,j-1})\right] \qquad \text{(B-14)}$$

$$+\eta_{N-1,j}\left\{2h_{N,i}+2\left[\frac{h_{N,j}}{N}+(h_{N,i}-h_{N-1,j})\right]\right\}$$

$$-\eta_{N-2,j}\left\{h_{N,i}+\frac{1}{2}\left[\frac{h_{N,j}}{N}+(h_{N,i}-h_{N-1,j})\right]\right\}$$

The inclusion of $h_{N,j}$ was required in Eq. (B-14) due to the large depths in the vicinity of Moss Landing. All other points along the arc n = N had a depth of zero.

For the right side of the bay where forward differences are used and $h_{n,j} = 0$, Eq. (B-13) becomes

$$\eta_{n,j}\left\{\frac{3}{2}\left(\frac{1}{n\Delta\theta}\right)^2 h_{n,j+1} - \lambda^2\right\}$$

$$-\eta_{n+1,j}\left[\frac{1}{4}(h_{n+1,j} - h_{n-1,j})\right]$$

$$+\eta_{n-1,j}\left[\frac{1}{4}(h_{n+1,j} - h_{n-1,j})\right] \qquad \text{(B-15)}$$

$$-2\eta_{n,j+1} h_{n,j+1} + \frac{1}{2}\eta_{n,j+2} h_{n,j+1} = 0$$

For the left side of the bay where backward differences are used and $h_{n,j} = 0$, Eq. (B-13) becomes

$$\eta_{n,j}\left\{\frac{3}{2}\left(\frac{1}{n\Delta\theta}\right)^2 h_{n,j-1} - \lambda^2\right\}$$

$$-\eta_{n+1,j}\left[\frac{1}{4}(h_{n+1,j} - h_{n-1,j})\right]$$

$$+\eta_{n-1,j}\left[\frac{1}{4}(h_{n+1,j} - h_{n-1,j})\right] \qquad \text{(B-16)}$$

$$+2\eta_{n,j-1} h_{n,j-1} - \frac{1}{2}\eta_{n,j-2} h_{n,j+1} = 0$$

c. Node Line in Fluid Media. The node line boundary condition is satisfied by

$$\eta_{n,j} = 0 \qquad \text{(B-17)}$$

COMPUTER PROGRAM

The computer program used to solve the eigenvalue problem is based on the Hessenberg Algorithm*. This method uses triangular

---

* S. H. Crandall, "Engineering Analysis," McGraw-Hill Book Co., Inc., New York, 1956, pp. 86-91.

decomposition to generate lower and upper triangular matrices from the matrix of field equations. A characteristic equation is then obtained from the lower triangular matrix whose roots are the eigenvalues. As each root λ^2 is found in order of increasing magnitude, the value of the root is substituted into the lower triangular matrix to obtain an intermediate vector y. The vector y is multiplied times the upper triangular matrix to obtain the corresponding mode vector.

The flow diagram of the complete computer program is shown in Fig. B-2.

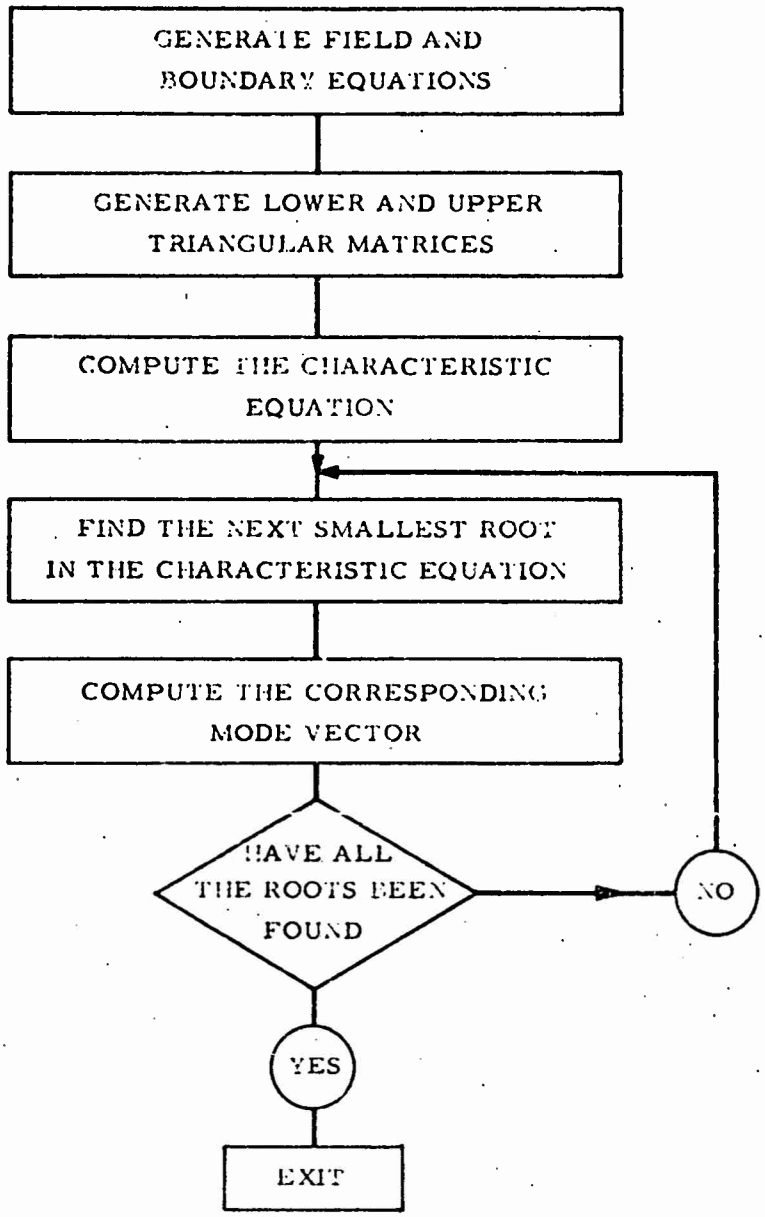

FIGURE B-2
FLOW DIAGRAM FOR COMPUTER PROGRAM TO COMPUTE THE MODE VECTORS

Unclassified
Security Classification

DOCUMENT CONTROL DATA - R&D

(Security classification of title, body of abstract and indexing annotation must be entered when the overall report is classified)

1. ORIGINATING ACTIVITY (Corporate author)

Science Engineering Associates
San Marino, California

2a. REPORT SECURITY CLASSIFICATION

Unclassified

2b. GROUP

3. REPORT TITLE

FEASIBILITY STUDY FOR A SURGE-ACTION MODEL OF MONTEREY HARBOR, CALIFORNIA

4. DESCRIPTIVE NOTES (Type of report and inclusive dates)

5. AUTHOR(S) (Last name, first name, initial)

Wilson, Basil W. Hendrickson, James A.

Kilmer, Robert E.

6. REPORT DATE	7a. TOTAL NO. OF PAGES	7b. NO OF REFS
October 1965	201	45

8a. CONTRACT OR GRANT NO.	9a. ORIGINATOR'S REPORT NUMBER(S)
DA-22-079-CIVENG-65-10 b. PROJECT NO.	U. S. Army Engineer Waterways Experiment Station, Contract Report No. 2-136
c.	9b. OTHER REPORT NO(S) (Any other numbers that may be assigned this report)
d.	

10. AVAILABILITY/LIMITATION NOTICES

Distribution of this document is unlimited.

11. SUPPLEMENTARY NOTES	12. SPONSORING MILITARY ACTIVITY
Conducted for U. S. Army Engineer Waterways Experiment Station, Corps of Engineers, Vicksburg, Miss.	

13. ABSTRACT

This report attempts to answer basic questions regarding the feasibility of reproducing in an engineering model the surge phenomenon that at various times occurs in Monterey Harbor, California. A fairly extensive discussion is devoted to wind and wave climate prevailing in and near Monterey Bay. Sea and swell data are summarized for the deep-water vicinity-area and for Monterey Bay itself. Monterey Harbor tends to be quite well protected from the longer period swells. Statistical data for the occurrence of long-period waves at three sensor positions are examined and compared with similar-type data for Santa Cruz Harbor and for Half Moon Bay Harbor. The oscillating characteristics of Monterey Bay are examined from several points of view. A detailed study is made of the manner of propagation of long period waves into Monterey Bay. Attention is given to the question whether the surge phenomenon in Monterey Harbor is the consequence of surf-beats or of genuine long-period waves. It is concluded the latter are most probably the cause, and their relationship to cyclonic storms is indicated. The final section of the report discusses the feasibility of a model to reproduce the surge phenomenon and draws upon all the information gained in the preceding parts of the report for this purpose. It is concluded that the conditions can be modeled with reasonable chance of success, and suggestions are made for the calibration of the model and for the analysis and interpretation of the results it may yield.

DD FORM 1 JAN 64 1473

Unclassified
Security Classification

Unclassified

Security Classification

14 KEY WORDS	LINK A		LINK B		LINK C	
	ROLE	WT	ROLE	WT	ROLE	WT
Hydraulic models						
Monterey Harbor, Calif.						
Surge						
Waves						

INSTRUCTIONS

1. ORIGINATING ACTIVITY: Enter the name and address of the contractor, subcontractor, grantee, Department of Defense activity or other organization *(corporate author)* issuing the report.

2a. REPORT SECURITY CLASSIFICATION: Enter the overall security classification of the report. Indicate whether "Restricted Data" is included. Marking is to be in accordance with appropriate security regulations.

2b. GROUP: Automatic downgrading is specified in DoD Directive 5200.10 and Armed Forces Industrial Manual. Enter the group number. Also, when applicable, show that optional markings have been used for Group 3 and Group 4 as authorized.

3. REPORT TITLE: Enter the complete report title in all capital letters. Titles in all cases should be unclassified. If a meaningful title cannot be selected without classification, show title classification in all capitals in parenthesis immediately following the title.

4. DESCRIPTIVE NOTES: If appropriate, enter the type of report, e.g., interim, progress, summary, annual, or final. Give the inclusive dates when a specific reporting period is covered.

5. AUTHOR(S): Enter the name(s) of author(s) as shown on or in the report. Enter last name, first name, middle initial. If military, show rank and branch of service. The name of the principal author is an absolute minimum requirement.

6. REPORT DATE: Enter the date of the report as day, month, year, or month, year. If more than one date appears on the report, use date of publication.

7a. TOTAL NUMBER OF PAGES: The total page count should follow normal pagination procedures, i.e., enter the number of pages containing information.

7b. NUMBER OF REFERENCES: Enter the total number of references cited in the report.

8a. CONTRACT OR GRANT NUMBER: If appropriate, enter the applicable number of the contract or grant under which the report was written.

8b, 8c, & 8d. PROJECT NUMBER: Enter the appropriate military department identification, such as project number, subproject number, system numbers, task number, etc.

9a. ORIGINATOR'S REPORT NUMBER(S): Enter the official report number by which the document will be identified and controlled by the originating activity. This number must be unique to this report.

9b. OTHER REPORT NUMBER(S): If the report has been assigned any other report numbers *(either by the originator or by the sponsor)*, also enter this number(s).

10. AVAILABILITY/LIMITATION NOTICES: Enter any limitations on further dissemination of the report, other than those imposed by security classification, using standard statements such as:

(1) "Qualified requesters may obtain copies of this report from DDC."

(2) "Foreign announcement and dissemination of this report by DDC is not authorized."

(3) "U. S. Government agencies may obtain copies of this report directly from DDC. Other qualified DDC users shall request through _____."

(4) "U. S. military agencies may obtain copies of this report directly from DDC. Other qualified users shall request through _____."

(5) "All distribution of this report is controlled. Qualified DDC users shall request through _____."

If the report has been furnished to the Office of Technical Services, Department of Commerce, for sale to the public, indicate this fact and enter the price, if known.

11. SUPPLEMENTARY NOTES: Use for additional explanatory notes.

12. SPONSORING MILITARY ACTIVITY: Enter the name of the departmental project office or laboratory sponsoring *(paying for)* the research and development. Include address.

13. ABSTRACT: Enter an abstract giving a brief and factual summary of the document indicative of the report, even though it may also appear elsewhere in the body of the technical report. If additional space is required, a continuation sheet shall be attached.

It is highly desirable that the abstract of classified reports be unclassified. Each paragraph of the abstract shall end with an indication of the military security classification of the information in the paragraph, represented as *(TS), (S), (C), or (U)*.

There is no limitation on the length of the abstract. However, the suggested length is from 150 to 225 words.

14. KEY WORDS: Key words are technically meaningful terms or short phrases that characterize a report and may be used as index entries for cataloging the report. Key words must be selected so that no security classification is required. Identifiers, such as equipment model designation, trade name, military project code name, geographic location, may be used as key words but will be followed by an indication of technical context. The assignment of links, rules, and weights is optional.

Unclassified

Security Classification